PASTE DEPOSITION MODELLING, DECONSTRUCTING THE ADDITIVE MANUFACTURING PROCESS: DEVELOPMENT OF NOVEL MULTI-MATERIAL TOOLS AND TECHNIQUES FOR CRAFT PRACTITIONERS

A thesis submitted for the degree of Doctor of Philosophy

by

Esteban Schunemann

Department of Engineering and Design, Brunel University London

2015

I. Abstract

A novel paste deposition process was developed to widen the range of possible materials and applications. This experimental process developed an increasingly complex series of additive manufacturing machines, resulting in new combinations of novel materials and deposition paths without sacrificing many of the design freedoms inherit in the craft process. The investigation made use of open-source software together with an approach to programming user originated infill geometries to form structural parts, differing from the somewhat automated processing by 'closed' commercial RP systems.

A series of experimental trials were conducted to test a range of candidate materials and machines which might be suitable for the PDM process. The combination of process and materials were trailed and validated using a series of themed case studies including medical, food industry and jewellery. Some of the object created great interest and even, in the case of the jewellery items, won awards. Further evidence of the commercial validity was evidenced through a collaborative partnership resulting in the development of a commercial version of the experimental system called Newton3D. A number of exciting potential future directions having been opened up by this project including silicone fabrics, bio material deposition and inclusive software development for user originated infills and structures.

II. Acknowledgments

First and foremost I would like to extend my deepest gratitude to both my supervisors, Dr. Sarah Silve and Dr. Richard Bateman, without whom this project would have been impossible, the advice, guidance, critique and assistance in report writing was instrumental in the success of this research project.

I would like to thank Dr. Atanas Ivanov, Prof. Kai Cheng and Prof Tony Anson whose enthusiasm, support, provision of facilities and equipment were pivotal for the research.

I must acknowledge Brunel University and the School of Engineering and Design, including academic and technical staff, in particular Dr. Richard Rakowski for his words of encouragement and for allowing me to teach alongside him, giving me a positive change in routine. Paul Barrett, for his patience in my endless requests for laser cutting, and Paul Yates for his knowledge and expertise in CNC machining.

I also recognise the input by MSc students Efthimios Drakos and Jonathan Oxley for collaborating with me during the research project and bringing in valuable enthusiasm, feedback and companionship.

I would also like to extend my gratitude to the following people whose advice and enthusiasm were of great benefit during the metal clay study development and validation: Helen O'Neal from the PMC studio whose vast knowledge in PMC and the provision of materials were of great help for the feasibility study and the latter applications of AM in metal clay; Frank Cooper from the Jewellery Innovation Centre in Birmingham City University for his support of the project as a judge in the Goldsmiths' 2013 awards; Ann Marie Shillito for including my work in her book; Digital Crafts. And last but not least Silvain Promount from IMakr for his valuable support, patience and faith in the project which has led to a partnership and a start-up that will allow to project to remain alive for years to come.

I recognise that this research project would have been impossible without the funding provided by the Doctoral Training Grant scheme by the EPSRC, (ET/P504848/1) for which I am very thankful.

III. Declaration

Author's declaration

I declare that the work in this dissertation was carried out in accordance with the requirements of the University's Regulations and Code of Practice for Taught Programmes and that it has not been submitted for any other academic award. Except where indicated by specific reference in the text, this work is my own work. Work done in collaboration with, or with the assistance of others, is indicated as such. I have identified all material in this dissertation which is not my own work through appropriate referencing and acknowledgement. Where I have quoted or otherwise incorporated material which is the work of others, I have included the source in the references. Any views expressed in the dissertation, other than referenced material, are those of the author.

SIGNED: …… DATE: ……..

(Signature of student)

IV. Publication And Awards Arising From This Work

Making futures 2013, paper and presentation, peer-reviewed

Paste Deposition Modelling (PDM) A hybrid ALM/Craft process

Praxis & Poetics 2013, paper and presentation

Additive Manufacturing with Precious Metal Clay (PMC);
Aesthetic Opportunities that Bridge Digital and Traditional Craft

ResCon 2013 Brunel University, Research Student Conference, Abstract and presentation

Books

Some research outputs have also been published in Digital Crafts; industrial technologies for applied artists and designer makers. By Ann Marie Shillito. pages 114 and 124.

Awards

Silver and Joint winner of the 3D technological Innovation award at the Goldsmiths' Craft and Design Council 2013 awards.

Inclusion of silver piece "Seashell" in the curated Ganoksin online gallery.

3rd place in the EPSRC science photo competition 2013, equipment category.

V. Table of contents

VI. List of Figures

VII. List of Tables

VIII. List of equations

IX. Nomenclature

There is an abundance of AM systems, with such diversity there is also a large range of technologies being used, below is a brief overview of the terms and acronyms used in these technologies and throughout this document.

Terms and Acronyms	Definition
3D studio Max	3D CAD design software.
ABS	Acrylonitrile butadiene styrene, polymer used in FDM/FFF and common in injection moulded parts. (Smyth, 2013, p.25).
Alloy	Material composed of two or more elements, i.e. sterling silver- 92.5% silver, 7.5% copper.
Angle of Incidence	Angle at which light hits a surface.
Anisotropy	Mechanical property where a material is weak in one direction but not in another.
Build Plate, Platform, Chamber	The area or surface on to which a part is built.
CAD	Computer Aided Design, software solutions for virtual design in both 2D and 3D
CamBam	Software used to generate G-code for subtractive milling or engraving machining operations.

Terms and Acronyms	Definition
Code	Program instructions.
CorelDraw	Vector drawing CAD software.
Dilatant fluid	Shear thickening fluid; viscosity is increased when stress is applied. Related to non-Newtonian fluids.
DLP	Digital Light Processing. Digital projection technology used in some SLA systems.
DMLS: Direct Metal Laser Sintering	Virtually identical to SLS with the difference that metal powder is used instead of plastic, due to the weight of the part, this process requires some support.
EMC2	Motion control software used to operate a CNC machine, G-code is loaded into this software for this purpose.
Encoder	Device used to track the rotational position of a motor, or the linear position of a machine axis.
Envelope/Build Volume	The working area of the machine.
Extruder	Generally specific to FDM/FFF, the print head used to extrude plasticised polymers to build a part.
FDM: Fused Deposition Modeling FFF: Fused Filament Fabrication	A heated nozzle is used to soften and extrude a plastic filament to build the part, the extrusion head moves in the X and Y axes depositing the filament to build each layer, the heated plastic then fuses to the previous layers creating the object. Support using this method is either the same plastic as the part or as a separate material in the form of a soluble filament. -see also 'support'-

Terms and Acronyms	Definition
Feed-Rate	The speed at which the print head moves when creating the object.
Firmware	Internal software built into an electronic device.
Galvanometer	Related to laser and mirror galvanometer, a device to control the angle of a mirror used to direct a laser beam.
G-code	Program containing build parameters and machine instructions to create a part.
Green State	Term referring to a ceramic or clay object in a dry pre-firing state. Related to green strength.
Green Strength	Term referring to the strength of a dry ceramic or clay object before firing.
Infill	The infill is the build strategy used to create the inside infrastructure of a part and may be solid or low density.
Inkjet 3DP (Three Dimensional Printing)	An inkjet head is used to deposit droplets of binder over a bed of powder. Parts made with this process can feature full colour as seen in the Z-Corp machines.
Inkjet Metal 3DP	Similar in method to Inkjet 3dp, but works with metal powders and a jetted binder.
Investment Casting	Aka Lost-wax casting: a casting method where a positive wax pattern is coated in refractory material to create a mould for metal casting based on the shape of the original wax pattern.
Isotropy	Mechanical property were a material is strong in all directions
Lasercusing	Proprietary name for direct metal laser melting by Concept Laser.

Terms and Acronyms	Definition
Layer Height	The vertical thickness of each layer in an object build with AM.
Library	A file containing an arbitrary list of commands and macros used in a programming language.
LOM: Laminated Object Manufacture	Sheets of material are cut and adhered together to create the object. Materials can range from paper to ceramic tape, cutting methods include computer controlled knives or lasers.
Luer-Lok	Interface coupling usually used to connect syringe barrels to needles.
Mach3	Motion control software used to operate a CNC machine, G-code is loaded into this software for this purpose.
Macro	A custom subroutine contained in a library. In a program it can be called using a single command.
Monolithic material	Material composed of a single element, i.e. titanium
Parallel port	Data transfer computer interface port, used in some CNC machines.
PLA	Polylactic acid, polymer used in FDM/FFF (Smyth, 2013, p.27).
PMC	Precious Metal Clay, a malleable clay with a high metal particle content, when fired in a kiln the metal particles sinter and the mass becomes solid metal.
Polyjet And Multijet Modeling (MJM)	An inkjet head is used to deposit drops of photo-curing resin onto the printer bed, the types of resin used can vary in shore hardness to produce parts with both rigid and elastic features, the system also deposits a support material which is dissolved by warm water.

Terms and Acronyms	Definition
Rapid Move Feed-Rate	The speed at which the print head moves between machining/depositing operations, this is usually higher that the feed-rate.
Real-Time	Referring to computer systems, the immediate response to data sent.
Refractory	Heat resistant material, usually a ceramic or combination of.
SDL	Selective Deposition Lamination. Sheets of paper are cut and adhered together to create the object, parts can feature full colour.
Shore Hardness	Standardised hardness measurement for polymers, elastomers and rubbers.
Sintering	Process by which small particles of material are heated to a fraction below the melting point of the material which causes the particles to join to the surrounding particles to form a solid object. The final density depending on the particle size, shape, material and temperature.
SLA: Stereolithography	A UV light source is used to cure a liquid photo polymer resin, the model or part is made from the layers of the cured resin, these systems use the same resin for support.
Slic3r	Slicing software for FDM/FFF AM machines.
SLM: Selective Laser Melting	Similar to SLS and DMLS, but done at a much higher temperature where the material melts leaving a small pool, this process creates parts of greater strength and density.

Terms and Acronyms	Definition
SLS: Selective Laser Sintering	A laser is scanned across a bed of plastic powder. The heat from the laser sinters the particles together creating individual layers. After each layer is complete the bed moves down the Z axis and a 'recoater' distributes more powder over the whole bed in preparation for the next layer. The bed of powder acts as support for the part.
STL	STL stands for Standard Tessellation Language, since its inception it has become the industry standard file format for transferring CAD files for AM technologies. The file format STL was developed for 3D systems by the Albert-Battaglin Consulting Group in 1987 for use in moving 3D CAD models to SLA (RapidToday, n.d.).
Striation	Horizontal lines usually seen in sedimentary rock, also used to refer to the stair-stepping texture seen in AM parts/models.
Subroutine	A self contained section of code in a written program that is only executed when called, it can also be made to loop or use variables contained in the main program.
Support	Material used as scaffold to support overhangs and hollow builds, depending on process this can be powder, the same material as the rest of the build or a different material which may be soluble to ease in removal.
Variable	A user defined container that holds a specific value, may it be numerical or Boolean (true or false) in a program.

Chapter 1 Introduction

1.1 Introduction

Additive Manufacturing (AM) in recent years has become a common method for creating detailed parts or models from 3D CAD data; it is synonymous with 3D printing (3DP) or Rapid prototyping (RP). It relies on software to process the CAD data into thin layers that are then used to manufacture the object from the bottom up in successive layers.

There are many closed systems on the market and a limited spectrum of materials, most of which are suitable for prototyping purposes but often require a step-change with other processes to translate them into the correct material for purpose.

The current trend in the development of commercial systems is to lock down parameters to a narrow operational window where the user cannot make mistakes, to increase the perceived reliability of the technology, however in doing so the scope for creative exploration becomes limited.

However with the emergent open-design culture we see "*technophilic crafters 'hack' machines, reverse engineer them and apply craft thinking on them to make them into open tools that can do new crafty things*" (Von Busch 2010, p.119).

This way of thinking has led many practitioners to steer away from the conventions of commercial systems and develop their own methods which allows them to take ownership of the artefacts made with the process and engage in a creative enquiry where the practitioner can to take control of the AM process and make active decisions that are pertinent to the craft process and visual identity.

"*Contemporary craft is about making things. It is an intellectual and physical activity where the maker explores the infinite possibilities of materials and processes to produce unique objects*."
(Greenlees n.d)

Materiality is essential to craft thinking, what materials are selected and how they are treated is of great relevance. In some ways current AM processes have inadvertently through delivering design freedom, limited this creative enquiry by reducing the palette of materials available to the designer-maker. By the necessity of tuning these

limited materials to a small operational envelope the possible experimentation is discouraged.

The concept of Paste Deposition Modelling has the potential to increase this palette and open AM to experimentation and encourage a creative enquiry not only into the process but also into the materials.

The direction of this project is to de-construct the additive manufacturing process but with specific goals of restoring craft design freedoms and if possible introducing new possibilities of creating and using novel materials.

1.2 Aim

The aim of the project is to explore additive manufacturing in an unconstrained environment through a practical and design oriented methodology, were the process is not dependant on the software/firmware developed by manufacturers.

To open up AM to a range of tools where there is control on how an artefact is built and what material is used and not just limited to the prescribed material the system was designed for.

Integrate these into a craft based exploration where the designer maker has the opportunity of developing a visual identity outside the conventional 3D CAD environment,

To allow the designer maker to take responsibility for the outcome of the process, shift AM from craftsmanship of certainty to craftsmanship of risk.

To engage with the AM process not just as a manufacturing process but as a craft enquiry dialogue as well.

1.3 Objectives

- Review the current literature and practitioner work to determine state of the art.
- Investigate the constraints in existing systems and develop a solution for unconstrained AM.
- Create or modify an existing system to develop and explore the process.
- Validate the process through a series of case studies and demonstrator artefacts.

1.4 Structure Of Thesis

Chapter 1 Introduction

This chapter contains an overview of the field of additive manufacturing and introduces some of the issues of creative freedom, constrains and materials limitations along with the formal statement of aims and objectives.

Chapter 2 Literature Review

A survey of the current state of the art, published literature, cross section of the craft and practitioner work.

Chapter 3 Methodology

This chapter contains the experimental methods, equipment and processes developed throughout the research project.

Chapter 4 Case Studies

This chapter contains the outcomes from the research and presents them in the form of a series of process validation case studies.

Chapter 5 Commercial Validation

Here further validation of the process though a commercial venture is shown.

Chapter 6 Conclusions

Conclusions based on the outcomes of the project are drawn, along with the discussion of the contribution to knowledge

Chapter7 Recommendations/Future Work

Here a number of recommendation for potential future work are presented

Chapter 2 Literature Review

2.1 Chapter Introduction

Stereo lithography (SLA) is widely considered to be the first additive manufacturing system developed and released to the market, with fused deposition modelling (FDM) following soon after. However the process of adding layers of material has existed since the dawn of civilization, a good example of this process is the Coil Pot; the technique dating back to 3000 BC used rolled out lengths of clay which were layered together to form a ceramic vessel (Cooper, 1981)- not very different from the FDM process.

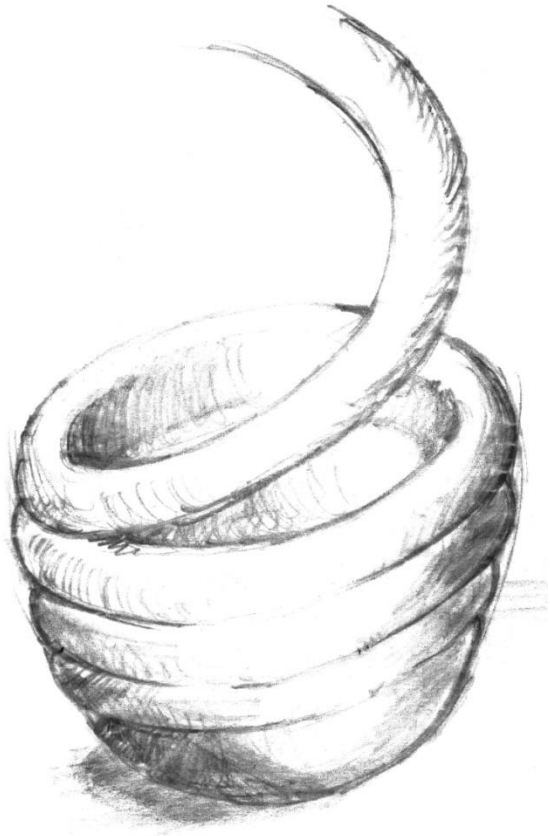

Figure 2.1, Coil pot build method example. figure by author

What is new however is the automation of this process and its link to a virtual environment that allows the designer to create an infinite amount of design permutations that can contain extravagant details and patterns that would be impossible or very difficult to make by any other means.

Manufacturing processes can be divided into three categories **(**Groover, 2012):

Subtractive

Material is removed from a block of material until the desired shape is reached.

Formative

Using mechanical force and or heat a ductile sheet of material is given shape, this also includes casting methods were the material is given shape whilst in a liquid state.

Additive

Material is manipulated and selectively worked to form successive layers to 'grow' a part.

This chapter introduces the principles of AM, the different technologies and materials used, and where information was available how the parts are processed for finishing. It also includes work done in the field of research in both technical and craft contexts.

2.2 Introduction to Additive Manufacturing

Rapid prototyping (RP), 3D printing (3DP), Additive Layer Manufacture (ALM) are widely used terms to describe the technology for building 3D artefacts from a 3D CAD file (*.stl) using a computer controlled system by adding material in layers. The steps are that the *.stl file is imported into the machine's software which slices the model into layers and processes the build orientation and any support required for the part to cope with overhangs. The model is then built by the machine 'bottom up' in successive additive layers.

These terms; RP, 3DP are either inaccurate or ambiguous. RP for example can be used to describe CNC machined prototypes, but this is a completely different method being subtractive instead of additive. Alternatively the additive layer build strategy can also be used to create products and not just prototypes. 3D printing is perhaps a less ambiguous term but one which is perhaps best reserved for systems that use inkjet heads to build up the material (more on this method in the Inkjet 3D printing section) as it is the most similar to document printers. Additive Layer Manufacturing (ALM), Additive Manufacturing (AM) are more accurate terms as they do not refer to a single

method or system but encompass the whole additive build method without leading to confusion with other manufacturing methods or specific applications such as prototyping.

The wide use of RP and 3DP terms has perhaps become confused due to media coverage of such systems; where these terms have been used interchangeably as they require less explanation to layman readers as they combine terms they are accustomed to. Whereas AM might be seen as an industrial manufacturing method and beyond reach of non specialists and would therefore be ignored by a wider audience.

There are many closed systems on the market and a limited spectrum of materials, most of which are suitable for prototyping purposes but often require a step-change with other processes to translate them into the correct material for purpose. In the jewellery sector an example would be the printing of wax masters for investment casting.

2.2.1 File processing

To create a physical representation of the virtual 3D model, the machine needs instructions for each layer of the build and this is done using slicing software. The software takes a 3D model, usually in *.stl format and slices it into thin layers, the thickness of each layer can be set by the user but it is also dependant on the capabilities of the system. At this stage if required, the software will generate the infill and support for the part. This slicing stage is critical for the success of the part. Decisions here can affect the structural integrity of the part as well as build time. Once the slicing operation is complete, some software packages allow the user to preview the tool path to inspect how the model will be built before generating the G-code. The user then has the option to save the G-code or send it straight to the machine if it is connected directly to the computer. Some software packages create the G-code in a form that is editable in standard word processing software. There are some language variations from system to system but most commands are the same, but other systems may use an encrypted form of G-code that is not editable by the user.

It is important to note that not all AM systems use G-code; it is more common in FDM style systems with three or more axes due to the similarities with CNC milling machines which also use G-code. Other technologies might use proprietary languages tailored to the individual system and technology, but the basic method of slicing the part into thin layers is common to all.

2.2.2 Build Times in ALM

The time is takes to build a part using an AM process depends on several factors such as infill density and complexity, vertical resolution (layer height) , support structures, part size and orientation.

However there is also the volume of the part to be considered, Carl Bass (2013) has suggested the notion that there is a kind of "Moore's law" which governs the amount of material and time it takes to build a part. He calls this law "The 3rd Power Law of 3D Printing", in it he claims that to build a part twice as big it takes 8 times more material and time, an increase to the 3rd power.

2.3 Computer Numerical Control (CNC)

CNC is a very broad term, but it is mainly used to describe milling machines and lathes that are controlled by a computer, terms such as CNC aluminium implies that the part was made with a CNC machine. Simpler CNC machines use stepper motors and lead screws to move the bed ways and tools as instructed by the CNC program (Figure 2.2).

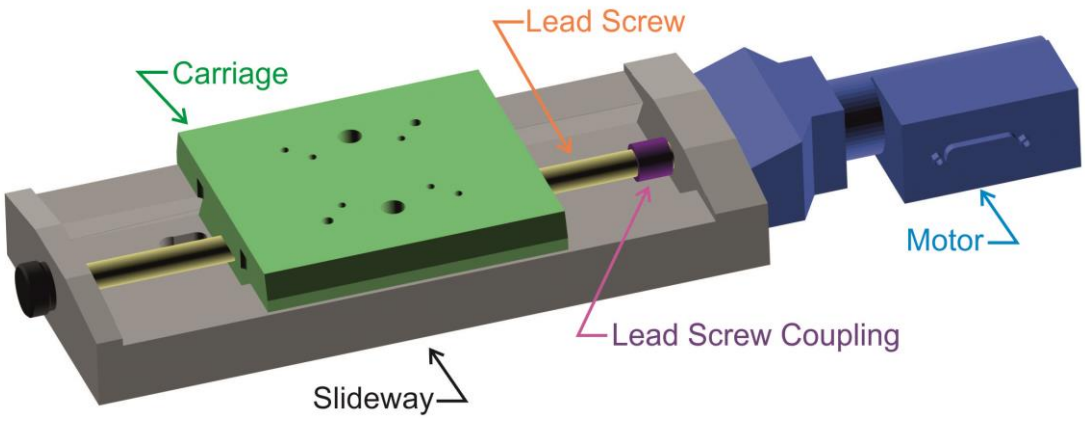

Figure 2.2, CNC axis parts, figure by author

In its most basic form, a CNC machine would be comprised of two or more axes driven by stepper motors and no feedback system in place; this is known as open-loop. The

main issue with this type of CNC is the lack of encoders to report the position of the axes (Stenerson & Curran, 2007, pp.11-14). Systems with encoders are referred to as closed-loop. There are two strategies for using encoders in CNC and they differ greatly in terms of cost and precision, the most basic and therefore cheapest is a rotary optical encoder, working the same way as the encoders in a ball type computer mouse. These encoders track the rotation of the stepper motors. This can then be used to determine how far the axis has moved by multiplying the number of revolutions by the pitch of the lead screw. This strategy however can be problematic as it doesn't take into account the backlash of the axis which can lead to inaccuracies. The backlash can however be accounted for in the software. The second strategy is to use linear encoders; these can be fixed in line with the axis and only measure the movement of the axis itself and not that of the stepper motor. With this, backlash compensation is no longer necessary.

The translation of rotary movement from a stepper motor to linear displacement can be done with a variety of methods:

Belt drive

Here the carriage is linked directly to a pulley; the belt can then be linked directly to the stepper motor or to a reduction gearbox to increase resolution. This type of drive is more common in 3D printers due to the lack of cutting forces.

Lead screws

Here the carriage is linked to the lead screw with a backlash nut, as the lead screw rotates the carriage moves, there are two main types of screw threads used in lead screws; trapezoidal (aka ACME) and ball screws, there is a third type called roller screw, but is very similar to the ball screw.

Trapezoidal screws can offer the highest pitch of the two but at the cost of efficiency, due to the sliding motion, because of the contact area between the threads these types of screw have a small amount of backlash (Stenerson & Curran, 2007, pp.15-16), this can be alleviated by preloading two threads on the same lead screw.

Ball screws have a much larger pitch but the threads work in a different way, here the ball screw nut is filled with ball bearings that act as the thread with the lead screw

having circular threads, so it is a rolling motion instead of sliding. The ball bearings increase the contact patch with the thread leading to reduced backlash, this type of screw is also much more efficient at translating linear movement (Stenerson & Curran, 2007, pp.15-16).

2.3.1 Motion control

For the CNC machine to accurately create a part all axes must be synchronised so the tool can be positioned and moved in 3D space. This requires each of the axis to be addressed independently and at the same time. This, in most hobby grade CNC machines is done using the parallel port on a pc with the actual motion control and synchronisation being managed by CNC software such as Mach3 (Newfangled, n.d.) or EMC2 (EMC2, n.d.) and run in real time. Typically if using standard stepper motors, the instructions sent out from the parallel port to each axis uses two pins from the parallel port, one direction pin; which is either on or off to indicate movement direction and one step pin; which controls the movement of the stepper motor by individual steps and is therefore turned on and off at a frequency that matches the required rotational speed of the motor as instructed by the motion control software (Stenerson & Curran, 2007, p.12).

Due to the possible variation in motor sizes and power consumption; the parallel port is usually protected by an opto-isolated breakout board, as shown in Figure 2.3. The board is connected to a power supply suitable for the number of motors being driven and to motor drivers for each axis.

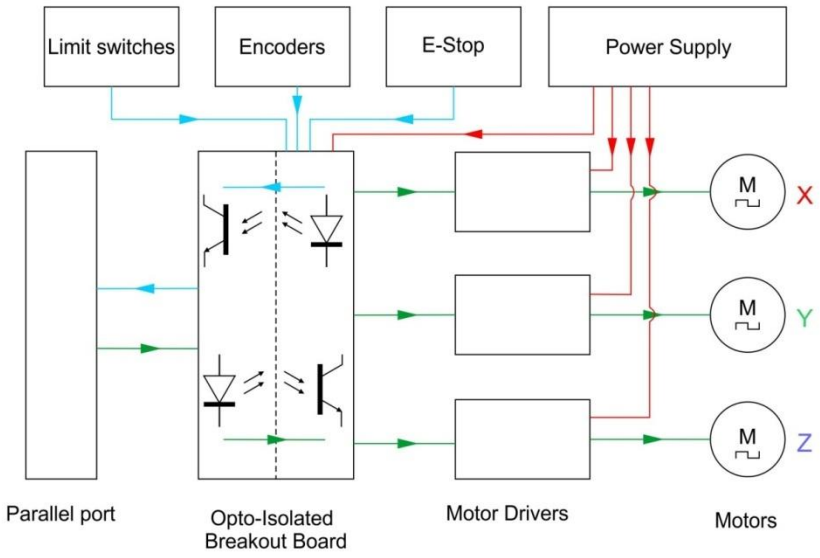

Figure 2.3, basic CNC controller block diagram, figure by: Author

Industrial CNC machines generally use custom made controllers with software tailored to the application the machine is designed for and typically use a tailor-made hardware solution. An example of this would be the motion controllers designed by Fanuc or Siemens.

Interface

The parallel port on a pc was originally designed to interface with dot matrix printers and plotter, which require several instructions to be sent at the same time. This quality makes the parallel port a viable option for interfacing with CNC machines and especially useful for building laboratory or prototype AM machines.

With the parallel port falling out of use in recent years, manufacturers have shifted towards using more modern USB or Ethernet interfaces. Yet the issue with USB is that data is transmitted in series, as mentioned earlier all axes in a CNC must be addressed at the same time to maintain synchronisation. Manufactures solved this by adding a data cache that can either drive the CNC axes as commands are sent, albeit with a small time delay or the whole set of instructions are sent and the machine works from the internal memory (Stenerson, Curran & Stenerson, 2007, p.10). With these systems motion control is done by the control board with internal firmware and not by software in the computer. Converting the parallel port to USB by using an adaptor is not possible unless it has been specifically designed for CNC. Generic adaptors would simply send the data in series and the system would not function.

Alternately some manufacturers do away with the computer interface and simply add a removable storage port such as SD memory cards and control the whole system internally. This is more common in consumer grade FDM machines, as it bypasses computer hardware compatibility issues that might arise and allows the manufacturer to control how the system is used, simplify calibration operations and make the system user friendly.

2.3.2 G-code, machine programming

Whilst there are many programming languages used in machine automation, G-code is the current industry standard for CNC machines and some AM machines. The code can be generated with several different methods; the most common being G-code generators. This type of program uses a CAD drawing, may it be 2D or 3D and generates a tool paths to produce the desired part, the tool paths are then converted to G-code for the target system. The generator may use a bespoke command library or macros if the CNC system needs any other commands.

The G-code may also be written by hand. The language was originally designed so that it could be read and understood by operators (Stenerson & Curran, 2007, p.60) and as such includes commands to machine pockets, drill hole arrays, create arcs, etc. The language also supports subroutines and variables allowing for more compact code.

Commands are split into two categories: G codes are preparatory functions that set the mode for the rest of the commands to come and M codes are machine specific miscellaneous functions such as machine coolant on/off. Below is a list of basic commands used in G-code (Stenerson & Curran, 2007, p.62 and Machmotion, n.d.):

Table 2.1, List of G-code commands. table by author

Command	Function
G01	Linear motion at set feed-rate
G00	Rapid move (normally used for positioning axes)

Command	Function
G61, G64	G61: Exact stop mode. G64: Constant velocity mode.
X, Y, Z	Address to an individual axis.
F (n)	Sets feed-rate to a user defined value.
M98, M99	M98: call subroutine. M99: End of subroutine

Designing for am

When designing objects and components the designer has to be familiar with the process that will be used to make the part, for example, when designing for the Fused Deposition Modelling (FDM) process several parameters must be kept in mind (more information on FDM can be found in the next section).

If the part is to feature thin walls then the number of perimeters and the nozzle size of the machine must be considered (Smyth, 2013, p.89), there is a common problem seen in many parts made with the process, where thin walls end up with small air gaps in between the perimeters that make the outside surfaces of the wall. The slicing software is sometimes not capable of adding infill if the gap between perimeters is too small. In order to make strong walls, the design wall thickness must take into consideration the number of perimeters the part will feature to allow for enough space for infill to be generated. For thin solid walls the thickness of the wall must be a multiple of the nozzle size. e.g.: for a 0.4mm nozzle, the minimum wall thickness is 0.8mm if it is made with one perimeter per outside surface, or 1.6mm if the wall features a more common two perimeters per outside surface. An example of the issue discussed can be seen in Figure 2.4, note the gap in the wall to the right of the figure, this gap is too small to fill with material so it is left hollow by the slicing software, this would produce a weak wall.

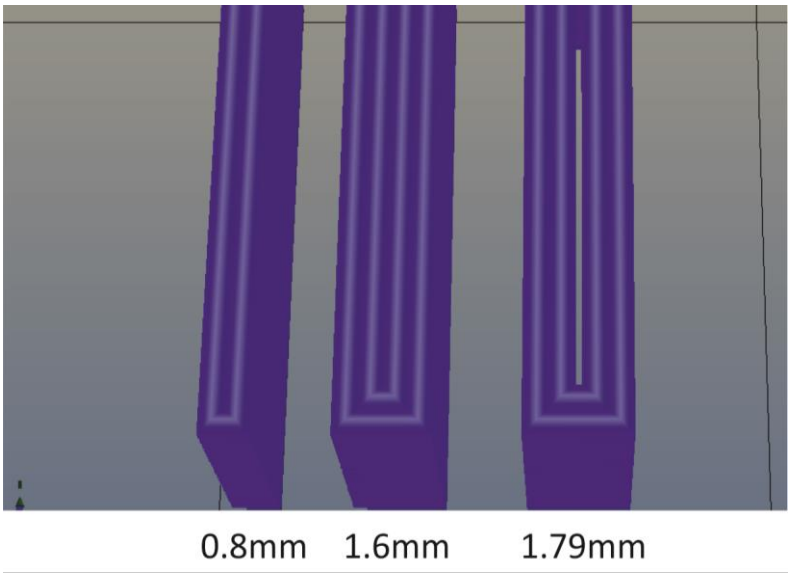

Figure 2.4, Screen shot from Repetier slicing software. Perimeter gap issue when nozzle size is not considered into design, wall width at 1.79mm produces this error, the gap is too small for infill. print parameters: nozzle size: 0.4mm, layer height: 0.15mm, perimeters: 2, infill density: 15%. figure by author

The perimeter gap issue can be resolved by considering the number of perimeters the part will have and the nozzle size of the machine that will make the part, this relationship can be expressed with Equation 2.1, where *'P'* is the number of perimeters, *'N'* is the nozzle size and *'W'* is the calculated wall width:

$$(2P) \times N = W$$

Equation 2.1, Relationship between number of perimeters and nozzle size to calculate design wall width. Equation by Smyth (2013, p.89)

This is but one example of the many considerations that much be taken to produce accurate parts in the FDM process, whilst most simple designs can be produced without this knowledge, more complex designs featuring parts that move or mesh mechanically require a deeper comprehension of the process.

The different technologies used in AM have their own idiosyncrasies and design requirements that the designer must know in order to successfully design for a specific process. As most CAD software packages are not designed specifically for AM the requirements are not reflected in the methods used to create objects in the specific CAD package used by the designer, issues only become evident in the slicing stage or once the part is made.

2.4 Additive Manufacture Systems

2.4.1 Fused Deposition Modelling and Fused Filament Fabrication

History of the technology

S. Scott Crump (1994) was the original inventor of Fused Deposition Modelling (FDM) and co-founder of Stratasys, FDM is a trademark name owned by Stratasys. Fused Filament Fabrication (FFF) is a trademark free name predominantly used for the RepRap project to avoid infringing on Stratasys (Reprap.org, n.d.). Both processes are virtually identical (Smyth, 2013, p.8). The RepRap project was developed by Adrian Bowyer (Reprappro.com, 2011) with the aim of creating a self replicating AM system. The project started the mass development of open source and entry level AM systems seen today based around the fused deposition modelling technique, this was due to the lapse of the original patent on FDM in 2009.

Introduction

Fused Deposition Modelling is a process in which a spool of plastic filament is drawn into a heated nozzle which respectively softens the filament enabling it to be extruded and deposited in layers according to the CAD data. The build is indexed down with every complete layer to form the 3D object.

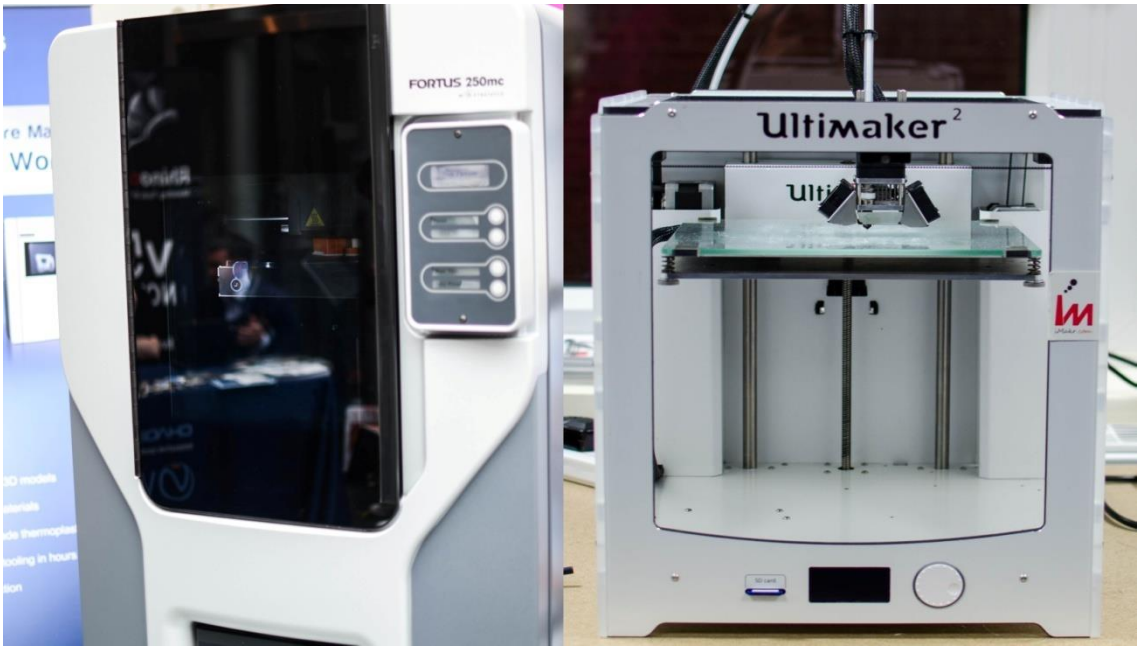

Figure 2.5, left: Industrial FDM system, Fortus 250mc Stratasys. Right: Hobby grade FFF system by Ultimaker. figure by author

Figure 2.6, Delta FFF system manufactured by WASP, figure by author

The machine layout in most FDM/FFF systems is similar to that of 3 Axis CNC machines. Some systems like the FDM machine shown in Figure 2.5 (left) have a full cabinet enclosure to maintain working temperature inside the chamber. Smaller systems typically feature an open frame and feature a desktop form factor. Some systems use a Delta configuration where all three slides are upright (Figure 2.6). The combination of the movement from all three slides resolves into X-Y-Z movement. The advantage of this configuration is that the build volume can be large while maintaining a small footprint. There are other axis configurations such as Polar (3ders, 2013), Hbot (Sollmann, Jouaneh & Lavender, 2010) and CoreXY (Moyer, 2012), however at this time they are under development and will not be covered in this document.

Whilst objects built with this process can be made solid, it is far more common to make the object either hollow or to a low internal density (infill), this saves both time

and material. Spanning structures such as overhangs or bridges require the structure be supported, for this the system builds a support structure that acts as a scaffold while the part is being built.

FDM structures

There are three types of structures systems need to builds to successfully complete a part:

Perimeters

Perimeters, shown in blue in Figure 2.7, form the outside surface or 'shell' of the part. The user can control the number of perimeters, two perimeters is the default on most systems. For parts that require more strength increasing this number might be necessary. (Smyth, 2013, p.88) The perimeters are organised in a concentric arrangement towards the centre of the part being built.

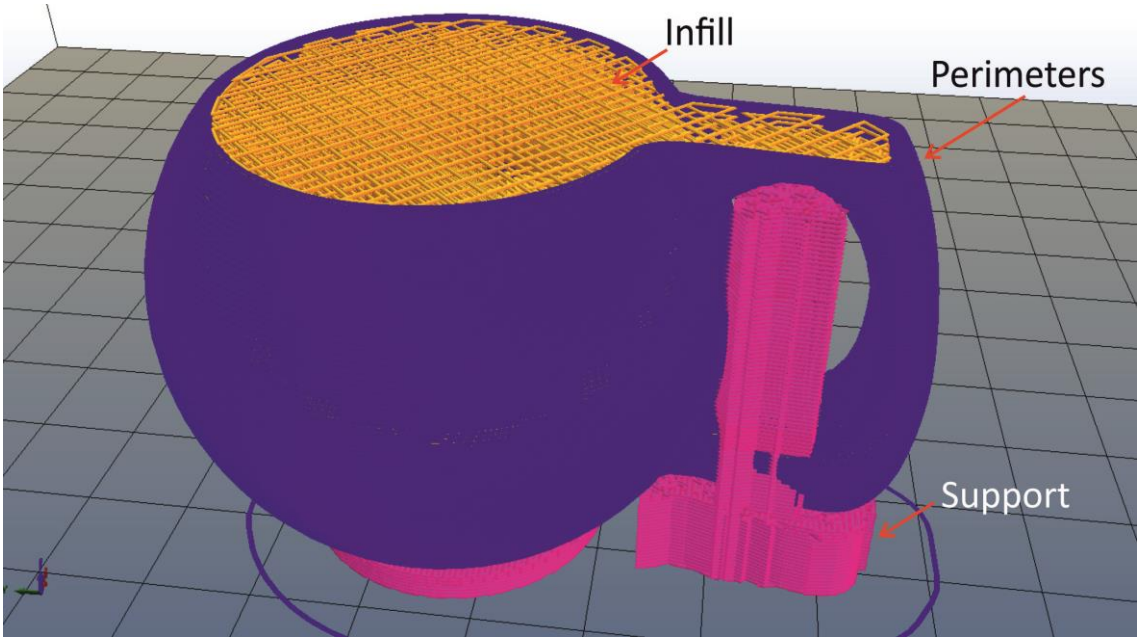

Figure 2.7, screenshot from Repetier slicing software, Infill in orange, perimeters in blue and raft/support in pink. figure by author

Infill

The infill (orange in Figure 2.7) forms the inside of the model and the user has some control over the density of the infill and choice of patterns (Figure 2.8). The main purpose of the infill is to give an infrastructure to the part and it can be made to a specific density from 0 to 100%, the lower the density the less material and time it takes to build. However, the density of the infill can have an impact on the strength of

the part, so the user must balance build time, material usage and part strength as appropriate.

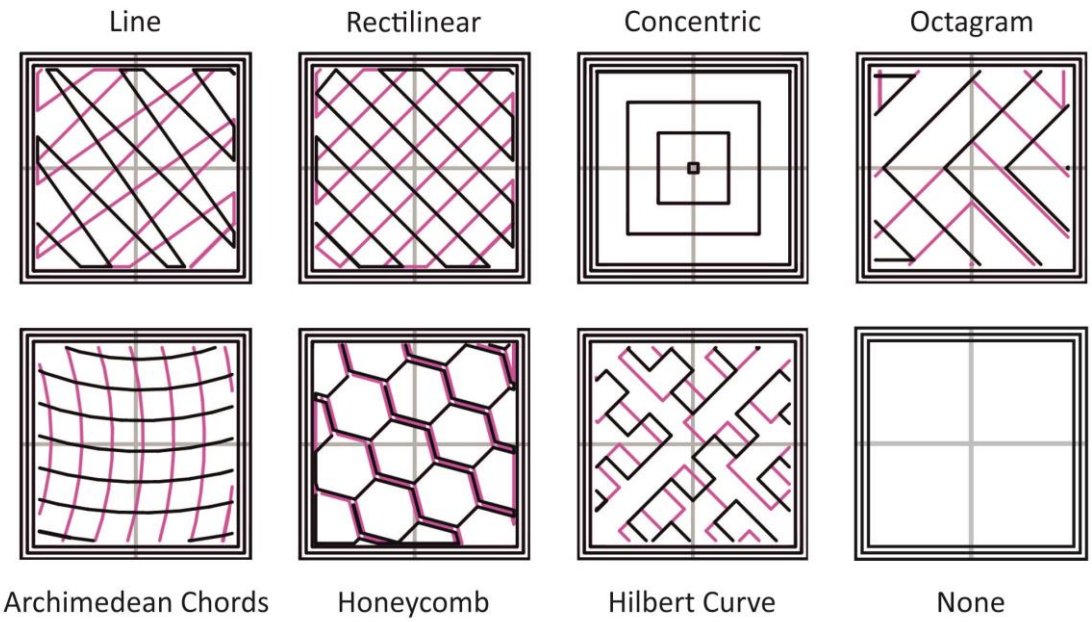

Figure 2.8, Infill patterns offered by Slic3r slicing software, original infill diagrams by Hodgson (n.d), figure by author

Support

The support (pink in Figure 2.7) acts as a scaffold to bear overhangs in the part being built, this structure is optional and only used when required. The user can control at what angle of the surface the supports are build, a setting of 45° would build supports on any surface below the set angle as shown in Figure 2.9. For troublesome parts it is possible to design support beams directly into the 3D CAD file, giving the user more control over how the part is built (Smyth, 2013, p.13).

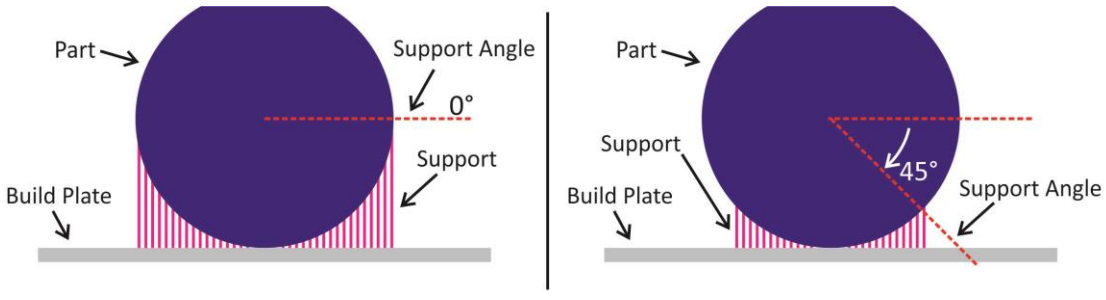

Figure 2.9, support angle diagram, left 90°support, right 45° support, pink lines represent support structure. figure by author

The platform where the part is built is not always level or completely flat so a 'raft' is needed. This is built under the part and is used to provide a level surface for the part. Some systems use a second head to deposit support material, this material is soluble in

water to simplify removal. Other systems however, use the same material as the rest of the build, and in these instances the support is designed to break away easily either by hand or using pliers.

Extruder

The extruder works by forcing a filament of material through a heated nozzle, with the filament driven by a gear connected directly to a stepper motor. A ball bearing under tension (see tension arm in Figure 2.10) is used to ensure the filament does not slip from the drive gear, as this would cause an interruption in the extrusion.

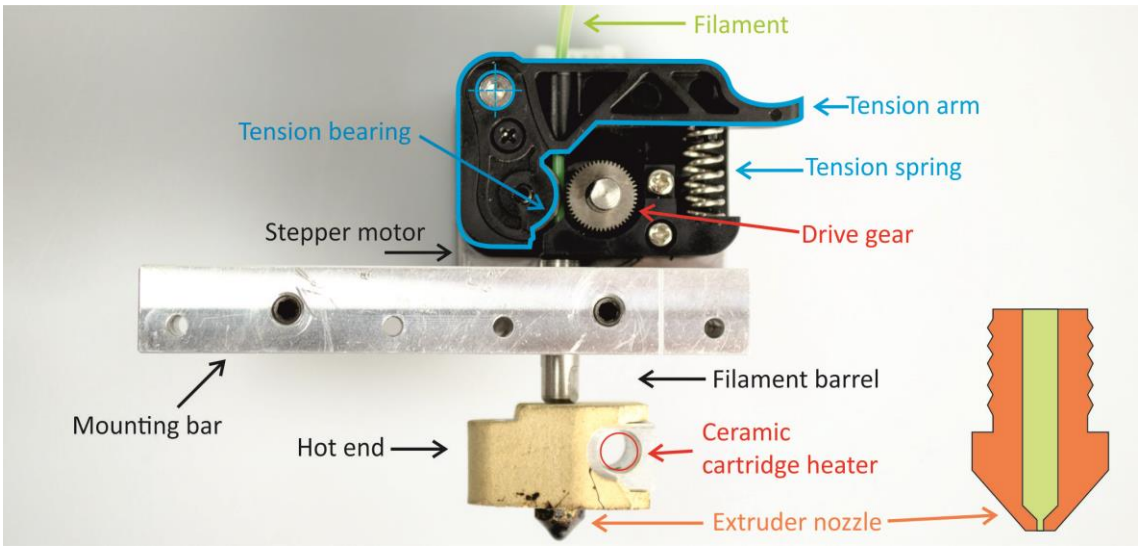

Figure 2.10, Filament extruder and components, figure by author

The filament is pushed into the hot end by the drive gear, the hot end is heated by a ceramic cartridge heater. A thermistor is also mounted on the hot end to provide temperature feedback.

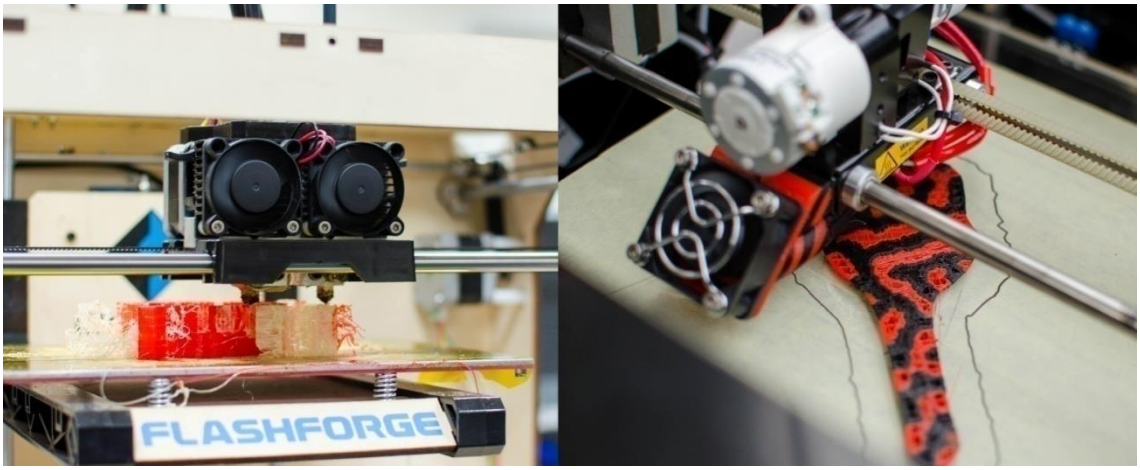

Figure 2.11, Dual material FFF systems. Left: flashforge system with two deposition heads. Right: Builder system, single head dual material system. figure by author

Some systems such as the *'Flashforge'* shown in Figure 2.11 (left) feature two extrusion heads, this enables the deposition of two materials in one build.

Other systems use a single extrusion head to deposit two materials; as implemented on the *'Builder'* system (3DPrinter4U, 2013) in Figure 2.11 (right) , the advantage here is that there is no offset between two deposition heads, and the extrusion head can also mix the materials for combination colours.

Resolution

The blunt shape of the nozzle is used to press the heat softened filament onto the rest of the build, this helps the layers adhere to each other. This is known as the 'width over height ratio' (JUSTPRINT3D, 2014), it maintains a proportional filament cross section across different layer heights. Naturally there is a limit as the layer height cannot be higher than the nozzle diameter. As the layer height gets smaller (higher Z resolution) the extruder might not be able to cope with the small volume of material being deposited. Using a 0.4mm nozzle the Ultimaker 2 is able to produce layer heights of 0.02mm (Ultimaker, n.d.), creating objects that look very smooth. However to increase the resolution on the X and Y axis the nozzle diameter needs to be smaller, but this increases the extrusion pressure and so the feed rate must be reduced so the extruder can cope. The heater temperature might also need to be increased to reduce the viscosity of the material.

Materials

The most common materials used in FDM are ABS and PLA, but due to the recent popularity of low cost FDM systems the material range has increased dramatically. It would be impossible to catalogue every single material available because new ones are being launched all the time however there are some categories that can be covered:

- Alloy materials blend a plastic with an additive, like metal powder, ceramic, carbon fibre, wood dust. Such as LayWood created by Kai Parthy (3ders., 2012).

- Elastomeric materials, these rubber-like materials show excellent strength and elasticity sold under the brand name NinjaFLex (NinjaFlex, 2014).

- Fun materials such as glow in the dark and thermochromic.

- Dedicated support materials, such as PVA filament, which dissolves in water (Formfutura, n.d.).

- High strength materials such as Polycarbonate and Nylon PET filaments for the food industry (Smyth, 2013, pp.23-31).

- Companies like Faberdashery (Faberdashery, n.d.) that manufacture PLA filament focus on vibrant colours.

This is just a small cross section of the scope of materials available; it is a market that is growing fast and is indirect evidence of the take up that FFF has received in recent years. In fact the Hobbyist market has grown by 346% from 2008 to 2011 (Copeland, 2013).

Finishing

How a part is finished depends on the materials it is made from, for example: the bronze filled alloy filament, BronzeFill (Colorfabb, n.d.) requires burnishing and polishing with metal polishing chemicals to bring out a bright finish. However most plastic parts can be sanded and painted as required and can also be drilled and tapped as long as the perimeter thickness supports it.

ABS materials can also be treated with acetone to make the surface smooth, this can either be applied by brush, repeatedly dipping in acetone (3dprintsexpress, 2013) or left in an atmosphere saturated with acetone vapour (Underwood, 2013).

Metal casting

Later in this chapter, AM of wax patterns for investment casting will be discussed as this uses a different technology to FDM, however investment casting is also possible using FDM technology.

In the past ALM has been used to create master patterns that are used to create moulds for casting in wax, the wax patterns are then used in investment casting (Owen_W, 2012), alternately the moulds for wax can also be build directly and injected with wax to create the wax form.

Although it is difficult to ascertain exactly when Lost PLA casting was first developed, one early example is by Rob Bryan (2012), where he made a casting of the famous Yoda bust found on Thingyverse (Thingiverse, 2011) in aluminium. The Yoda Bust was made in PLA with a 10% hexagon infill pattern and this light infill greatly reduced the amount of material that needed to be burned out. He embedded the PLA Yoda upside down in sand and added a cone shaped sprue, then using traditional sand casting equipment and setup; he proceeded to pour molten aluminium into the mould. The casting did not flow all the way into the cavity, -it is thought that the sprue was not big enough to allow the gas from the burning PLA to escape as the shoulders on the bust did not fill,- he also reflected on the need for more gates and vents to allow gas to escape from the smaller regions of the Yoda bust such as the ears. However the experiment was deemed successful, the partial casting of the Yoda bust featured high detail including the striations from the original AM part (Figure 2.12).

Figure 2.12, Rob Bryan's Lost PLA cast aluminium Yoda bust, partial casting. (Bryan, 2012)

The methodology of the experiment had one flaw; the amount of gas the PLA produced inhibited the flow of the molten aluminium. This could have been alleviated by burning out the PLA in a furnace; this of course would have been impossible due to the particular sand casting equipment used. It is evident that this experiment was

limited to the equipment available and its purpose was as proof of concept of the technique.

The work by Jeshua Lacock (2013) shows practical uses for the Lost PLA technique, where he cast an aluminium part for the Z axis of a CNC machine he was building. He initially printed the part at 100% scale to test fit into the CNC machine, once he was happy with the fit he reprinted the part 3% larger to account for the shrinkage of the cast aluminium. His casting was successful showing good dimensional stability as the part required no milling to fit the CNC machine. His casting technique was different from Rob Bryan's as he used a more traditional approach to investment casting by using investment powder to form the mould and then burning out the PLA using a furnace.

Figure 2.13 Colossal bust of Ramesses II, 1/20th scale By Cosmo Wenman in patinated bronze, figure by author, more information on piece (Wenman, 2013, B)

Cosmo Wenman (2013) demonstrated in his work that it is possible to use this technique in large scales. His work, involves 3D scanning famous works such as busts from museums using 123d catch - an image base 3D scanning application for mobile devices - then 3D printing them in PLA and casting them (Figure 2.13). He claims the process from 3D scanning to finished bronze cast can take as little as seven days.

2.4.2 StereoLithography Apparatus (SLA)

Introduction

First invented in the mid 1980s By Chuck Hull (Warnier, Verbruggen & Ehmann et al., 2014, p.11), SLA uses a UV light source, to selectively polymerise a photo-curing resin (Reeves, 2008), typical resolution for this technology is 0.01 to 0.1mm.

System layout

The layout of SLA type systems has changed over the years since its inception. The original layout by 3D systems used a large vat of resin at the bottom of the machine (Figure 2.14 A), the build plate is the lowered into this vat, a laser galvanometer positioned at the top of the machine then selectively polymerises the resin on top of the build plate. The build plate is then moved down, a recoater wiped across the top to redistribute the resin and the process is repeated. This layout was used on several models made by 3D systems including the SLA5000 (3Dsystems, 2003). However, the issue with this layout is that the full volume of the vat must be filled in order to build a part; this can be very costly on a system with a large build envelope.

In other variations of the design the layout was reversed, with the light source at the bottom and the resin vat at the top such as that used in the *'form1'* (Formlabs, n.d). This method also builds the part upside down with the build plate moving up rather than down (Figure 2.14 B). The resin that is in contact with the bottom of the resin vat is the resin that is cured by the laser, the layers bind to the resin vat. In order for the build to progress the fresh layer must be detached from the resin vat, in the *'Form1'* system, this is done mechanically by lowering one side of the resin vat peeling the cured resin from the vat (Figure 2.14 C).

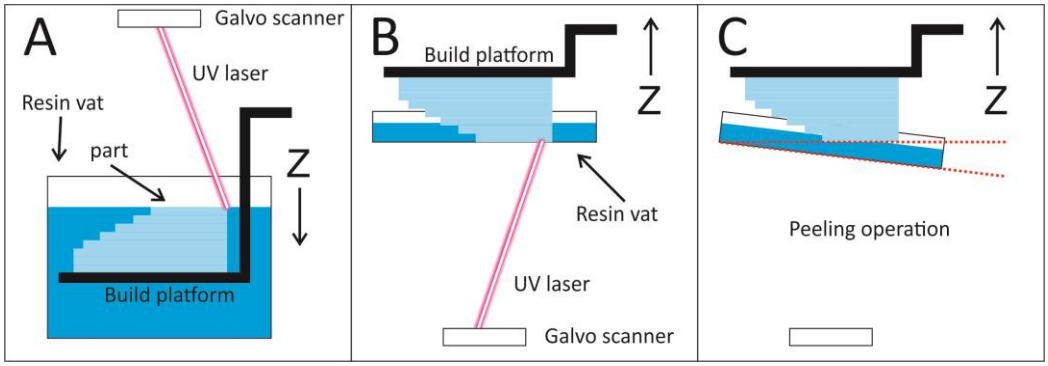

Figure 2.14 SLA system comparison, A: original layout, B: upside down layout, C: peeling operation. figure by author

There are two types of light sources which can be used in SLA systems: Laser and DLP projection. With a laser (Figure 2.16 A), it scans over the resin creating each individual feature of the layers, this can become time consuming when several parts are made at the same time or for large objects. The precision of the laser makes it possible to produce 0.08mm features in a large build chamber (DWS LAB, 2014). However for this type of system to produce accurate parts, the distance between the laser and the build plate needs to be large enough to reduce the angle of incidence between the build plate and the laser as the laser is projected from a single origin (Figure 2.15). This issue was demonstrated by user "damienideas" in the explore ideas daily blog (damienideas, 2013) where he established in the *'Form1'* the dimensional inaccuracy of the parts made when at the extremes of the build plate, due to the shape of the spot size of the laser becoming elongated owing to the angle of incidence, this could be corrected in software and it is most likely only a trait of that particular model of SLA system.

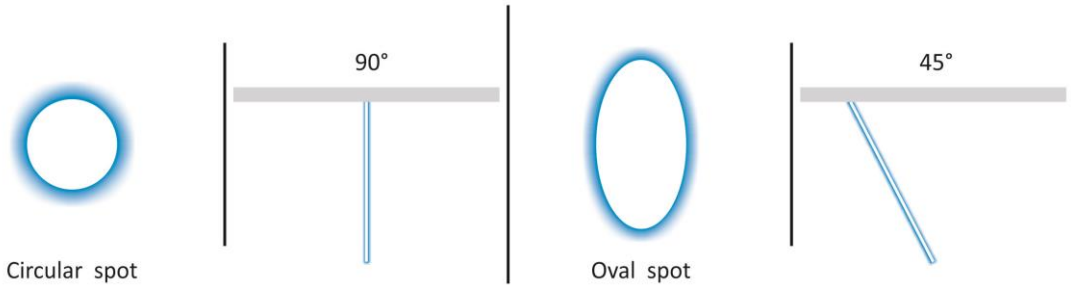

Figure 2.15, Laser beam spot shape at 90° and 45° angle of incidence, figure by author

Other systems such as *'DigitalWax'* (DWSSYSTEMS, n.d.), do not use a galvanometer to direct the laser but opt for an X and Y stage (Figure 2.16 B), which keep the laser perpendicular to the build plate and thus guaranty a consistent spot shape over the whole build plate.

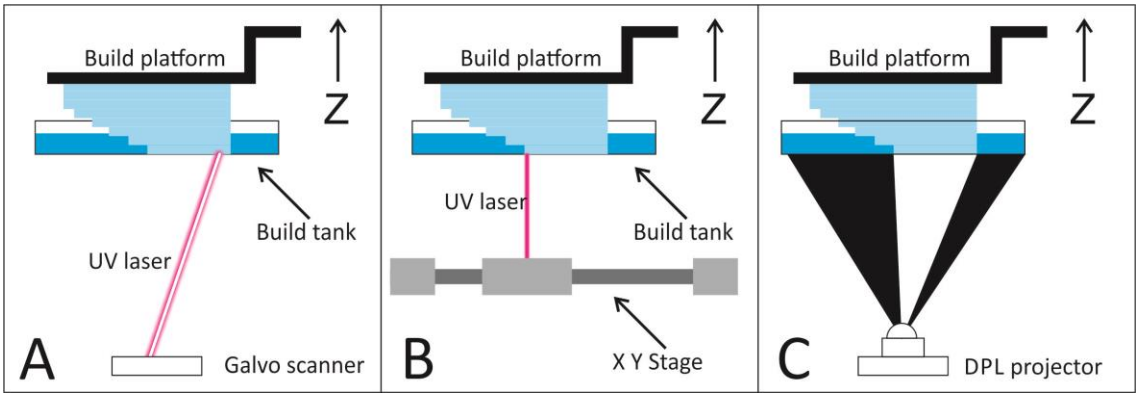

Figure 2.16 UV light source diagram, A: UV laser Galvanometer, B: X-Y stage for laser positioning, C: DLP projector. figure by author.

Systems that use DLP projection (Figure 2.16 C) do not sufferer the aforementioned issue as there are no moving parts changing the angle of the light source. These systems are capable of producing parts very fast as the projector illuminates the whole layer at once. This means that the time taken to produce a layer for a small part is the same as that for a large or multiple parts. Conversely the X and Y resolution can be problematic as it depends on the resolution of the DLP projector. In order to produce high resolution parts the projector must be positioned close to the build plate and this limits the size of the build envelope in the X and Y dimensions and as such this type of systems generally feature small build envelopes such as those seen in the *'Asiga'* product line (Asiga, 2014) and the *'MiiCraft'* system (MiiCraft, 2012).

Support

Due to the manner in which SLA works, the support for SLA is made from the same material as the rest of the build. Supports generally take the form of thin vertical struts that support areas such as overhangs and allow consecutive layers to be made. To aid in support removal, these support struts end in a cone shape, this makes them easy to break off and keeps the contact area with the build at a minimum and reduces the evidence of the support on the surface of the build; cutting down on post processing and finishing. Figure 2.17 shows how these supports are used, notice the cone shape at the end of the support struts and the spiked surface left by the removal of the support.

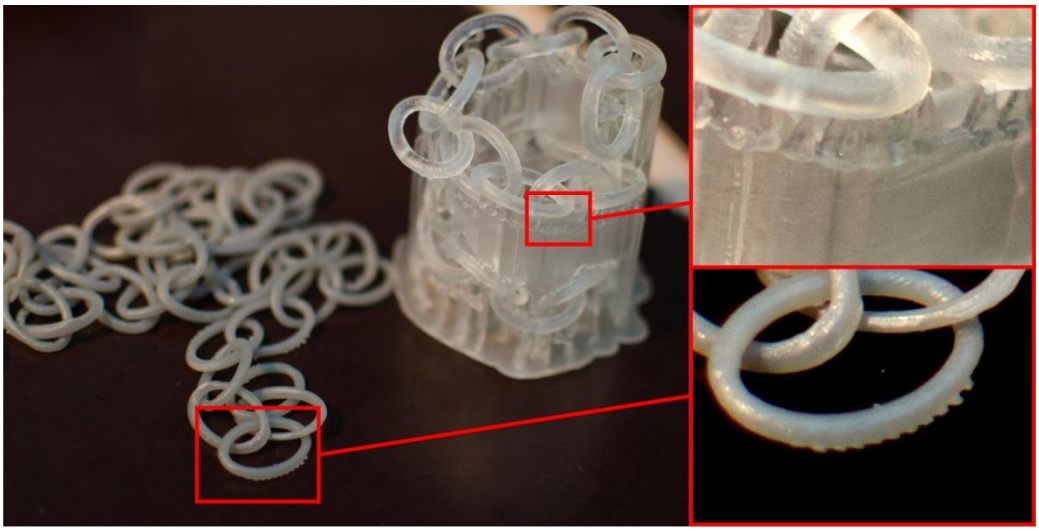

Figure 2.17 Chain built with Form1, details of support structure and removal of support, figure by author.

Materials

Materials for SLA are not as diverse as those seen in FDM on account of the chemistry involved. However there are several formulations for varying flexibility and rigidity, replicating common materials such as ABS, Polycarbonate and rubber. These materials are also supplied opaque and transparent in a range of colours. There are also ceramic filled materials for enhanced rigidity (DWS LAB, 2014) and materials for investment casting; (DWSSYSTEMS, n.d.) such as those used by the DigitalWax system.

The cost of SLA resins has been falling as more consumer systems come to market but at the moment it is still expensive at £100 per litre (Formlabs, 2014). With companies like *'Maker Juice'* manufacturing third party compatible resins this cost has been considerably lowered to £32 per litre (Makerjuice, 2014).

Finishing

Figure 2.18, finishing grades on SLA parts, made by Malcom Nicholls, figure by author.

Parts made in SLA show very little striation due to the layer heights of 0.01mm that the process is capable of. On account of this, the surface quality is very high and only requires light sanding to make the surface smooth and further polishing to reach near optical quality, Figure 2.18 shows a range of finishes produced by the service provider Malcom Nicholls, the resin can also be painted or vacuum metalized (Mnl, n.d.).

2.4.3 Laser Additive Manufacturing

The arena in laser AM technology can be confusing due to a lack of distinction between the different technologies but there are however five main technologies:

- Selective Laser Sintering (SLS)
- Direct Metal Laser Sintering (DMLS)
- Indirect Metal Laser Sintering
- Selective Laser Melting (SLM)
- LaserCusing.

All these systems work in a similar fashion where, by means of a laser, powdered material is selectively fused together. The distinctions lie with the type of materials that can be processed and the mechanics of fusing the powdered material.

The term SLS is usually reserved for the processing of plastics, such as Nylon, glass filled Nylon (3DSystems, n.d.).

DMLS is aimed towards processing metal alloys and as the name suggests it sinters the metal particles. Indirect Metal laser sintering does not sinter the metal in the build platform but rather it uses polymer coated metal powders to form the part, the polymer acts as a binder when heated by the laser. This process then requires a sintering post process in a kiln and infiltration with another metal to reduce porosity (Dewidar, Dalgarno ,et al, 2008, p.227).

SLM however fully melts the metal powder (Sinirlioglu, 2009, p.89) and as such is targeted towards monolithic metals such as titanium. This distinction between DMLS and SLM is not brought on by the technical limitations of either system but rather an issue of patent. LaserCusing developed by Concept Laser is virtually the same as SLM with particles achieving a full melt; however the laser is not directed by a galvanometer in this system but by means of an X and Y stage, keeping the laser perpendicular to the powder bed (Bujis and Leewen, 2005, p.35).

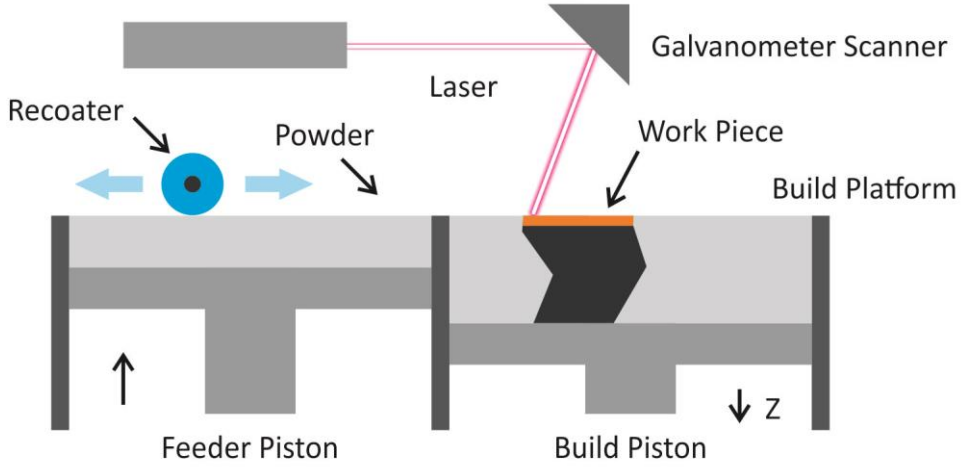

Figure 2.19, general system layout schematic for SLS, DMLS, SLM, LaserCusing. figure by author.

The diagram in Figure 2.19 shows the basic layout of the apparatus used; there are variations between the different technologies but the arrangement is similar. The process starts by spreading a layer of powder over the build platform using the recoater, the laser then fuses the powder layer according to the CAD data binding it to the build plate, the build piston then moves the plate down to the predetermined layer height for the next layer and the recoater lays a new layer of powder. This layer is then fused by the laser to the previous layer and the process repeats these steps until the work piece is complete (Figure 2.20). Materials that oxidise when heated require a reduction atmosphere, which is achieved by filling the chamber with either Argon or Nitrogen (Campanelli et al., 2010, p.238).

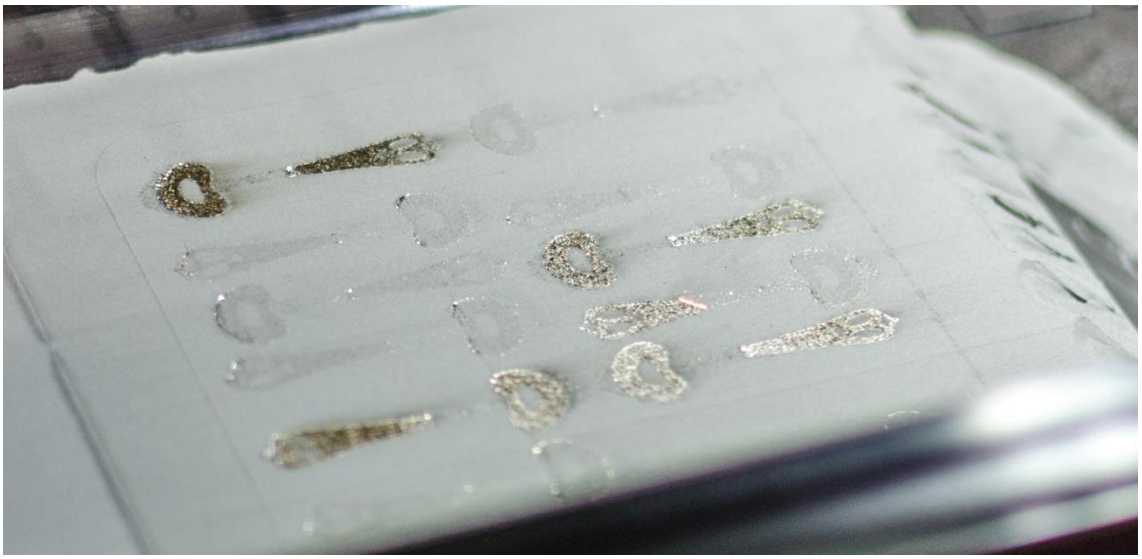

Figure 2.20, LaserCusing process building small spoons in silver, note the laser beam in the middle/right section of the image. figure by author.

Some DMLS and SLM systems heat the build chamber and the powder to a high temperature to improve the absorption of the laser, reduce the temperature gradients

and improve the wetting between layers. This also has the effect of preventing warping of the work piece due to non-uniform thermal expansion and contraction brought on by the localised heat of the laser (Campanelli et al., 2010, p.236).

Support strategy

While most non metal powder based systems don't require support, such as the Z-corp inkjet systems, with metal powder this is not the case. As the build progresses the metal powder surrounding the work piece is insufficient to support it and therefore supports are required to hold the part in position during the build stage. However that is not to say that some structures cannot be self supporting, according to the CPM EOS design guidelines (CPM, EOS, n.d. p3) draft angles above 30° are self supporting. Figure 2.21 shows an example of a draft angle below 30° that requires support, shown in red on the image to the right.

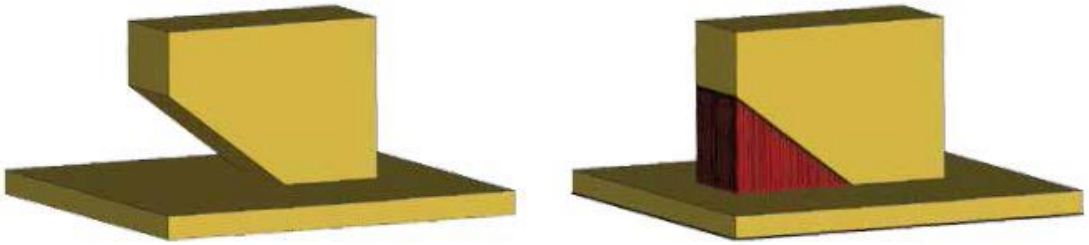

Figure 2.21, EOS CooksonGold draft angle design guideline, showing the support structure for angles below 30° (CPM, EOS, n.d. p3) Creator: CPM, EOS

Support structures must be considered when designing parts for AM in order to reduce the amount of post processing required to finish the part, in Figure 2.22, extracted from Jacobson's report (Jacobson and Bennett, 2006. p.736) an example can be seen where a design from a client was modified to reduce the amount of support required. The left of Figure 2.22 shows the support that would have been required to produce the stepped surface of the original design and on the right of Figure 2.22 (highlighted in red) is the modified surface, now a smooth 45° draft that requires no support. This modification had no impact on the function of the part but it increased production yield and reduced post processing work (Jacobson and Bennett, 2006.p.734-736).

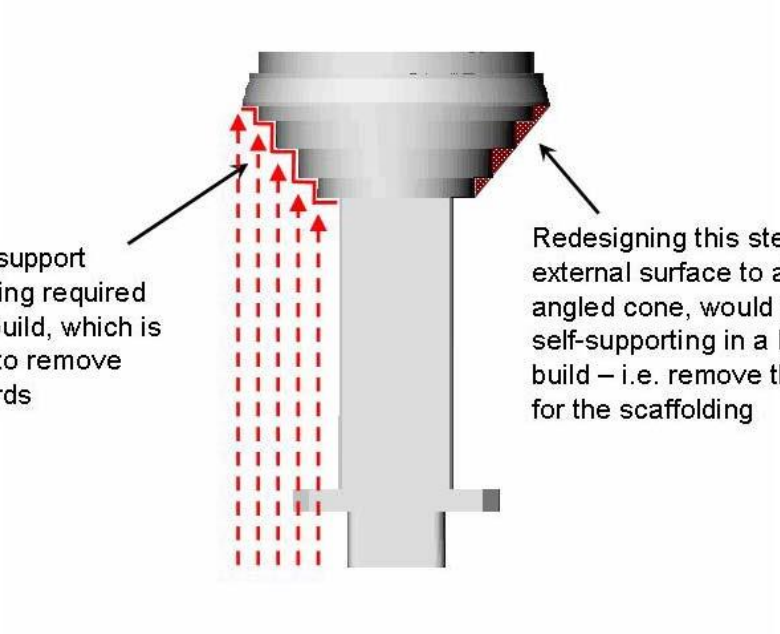

Figure 2.22, illustration showing the modification of a part to reduce support required, (Jacobson and Bennett, 2006.p.736), creator: Jacobson (2006)

There are many different support strategies used in laser AM but these differ between systems, software updates, part function and some are commercially confidential so it is not possible to review them all. The support strategy shown in Figure 2.23 is common enough to be representative of the technology. The shape of the support shown is similar to that used in SLA, the support is cylindrical in shape and ends in a cone when in contact with the work piece to aid in removal.

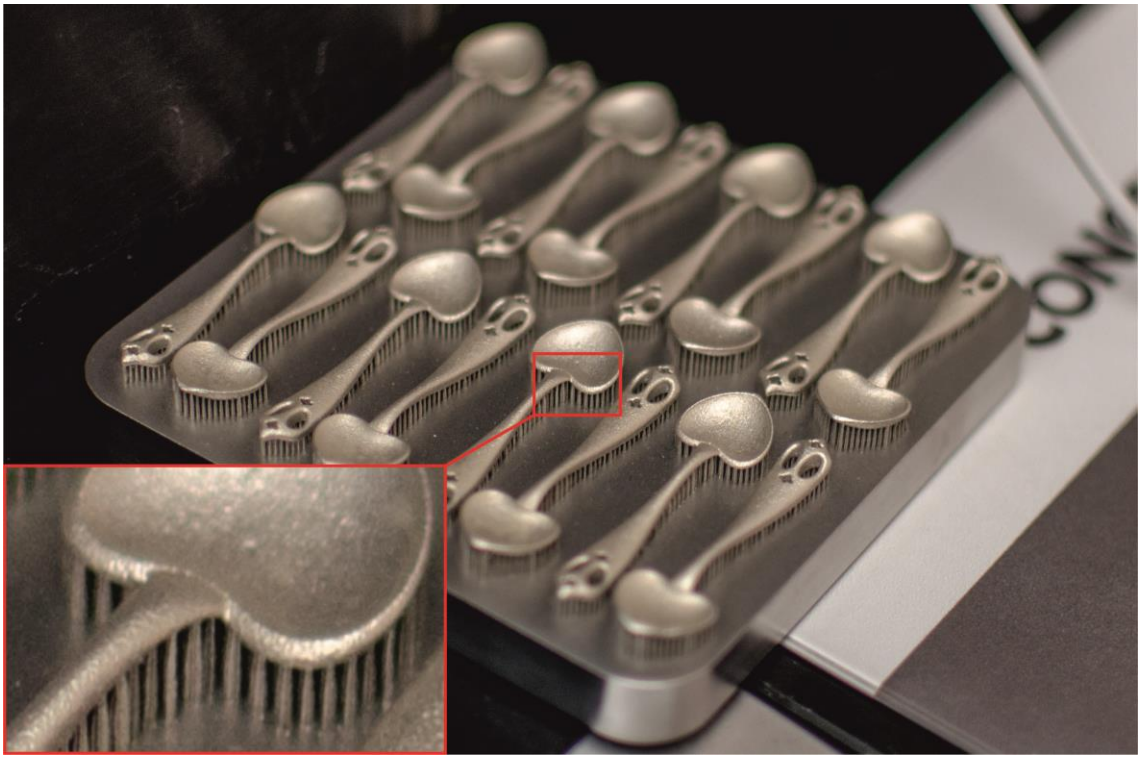

Figure 2.23, LaserCusing, details of build plate and support struts. figure by author.

The removal of support from parts is performed in two stages. Initially the whole part including supports is cut from the build platform using wire EDM; the support struts are then removed either mechanically by breaking them away by hand or using a range of tools to cut them away.

Surface finish

The surface of parts made with these processes does not feature the striation seen in other AM technologies as detailed in Figure 2.23. This is due to the particle size in the bulk powder and the layer height. As the layer height approaches the particle size of the powder used, the striation becomes indistinguishable from the grain texture left by the powder. In the examples shown in Figure 2.23 and Figure 2.24, the layer height was 0.015mm (Cater, 2013), however the system is capable is layer heights down to 0.05mm (Bechmann, 2010).

Figure 2.24, work piece just after the build is complete and loose powder brushed off (top left). Work pieces cleaned and shot peened (top right). Support removed (bottom left). And final piece polished (bottom right). Bottom piece designed and finished by Charlotte Parkhill 2013, images courtesy of estechnology (Cater, 2013)

After building is complete, any loose powder is brushed away, sieved and used for other builds. A more thorough cleaning is done using compressed air in a cabinet to recover as much powder as possible. Then the surface of the piece is cleaned with

plastic shot peening, and the support is removed and the piece polished using traditional methods. A breakdown of the process is shown in Figure 2.24.

Part density

The density of a part is dependent on a large range of parameters related to the process and material characteristics. Machine parameters include layer thickness, scan velocity (feed-rate), infill spacing and infill strategy. Laser parameters include; laser power, spot diameter, wavelength and laser power. Characteristics of the bulk powder used; particle size, distribution, shape also affect the density as well as material composition (Campanelli et al., 2010, p.238).

The parameters above can be used to control the porosity of a given part as demonstrated by Campanelli (2010, p239). He set out to determine parameters required to deliver the maximum mechanical strength. During the experiment only two parameters where changed; the scan speed and laser power while the rest of the parameters were set to produce a solid part. Energy density, a function of the scan speed, laser power and spot diameter is given by Equation 2.2 (Campanelli et al., 2010, p.238):

$$E_d = \frac{P}{v.d}\left[\frac{J}{mm^2}\right]$$

Equation 2.2, Energy density (E_d) equation, (P) laser power, (v) scan speed, (d) spot diameter

These experiments demonstrated that by changing the energy density the porosity of the test sample was affected, the more energy used the lower the porosity of the sample. The tests achieved a minimum porosity of 0.01%. (Campanelli et al., 2010, p.239)

The control over porosity presents a powerful tool where part density can be adjusted in different areas of a part, potentially reducing weight or allowing gasses to pass through the part. A practical application of part porosity was mentioned by Jacobson (2006, p.737) where the porosity of the material was used to help dissipate gasses trapped in a blow moulding tool made with DMLS. Controlling the density of the part can also speed up the build process where a core is made to a lower density and only the surface regions are made fully dense (Jacobson and Bennett, 2006.p.731).

Hybrid build

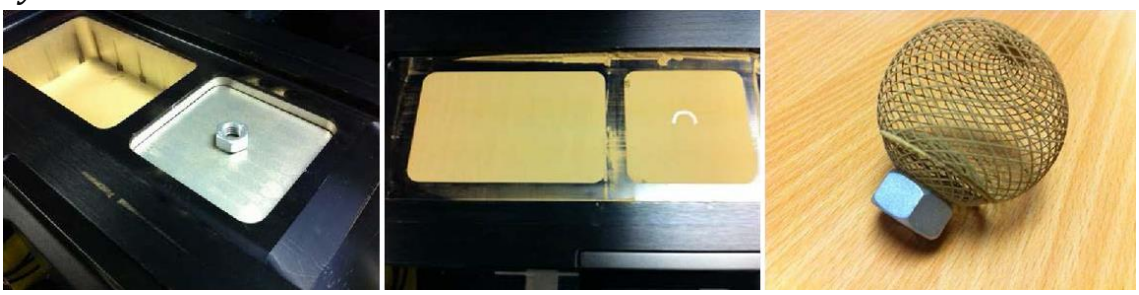

Figure 2.25, LaserCusing, hybrid build, steel nut and lattice sphere, Images: esTechnology (Cater, 2013)

Some applications of SLM might require the part to be built onto a pre-machined part rather than on the build plate to cut down on build times or because the part requires two different materials, this process was demonstrated by Concept laser using their LaserCusing technology (Cater, 2013). In the case study a lattice sphere was built bronze onto a stock steel nut (Figure 2.25), the nut was fixed in place onto the build plate using superglue, the offsets were measured and applied to the work piece in the slicing software and the Z offset was then filled with metal powder in the machine until just the top surface of the nut was exposed. The build then continued as normal building the bronze sphere onto the nut.

2.4.4 Inkjet 3d Printing (3dp)

3DP technology originated from MIT, the process was then licensed to Z-corporation for the production of the system; the term three-dimensional printing was also trademarked by Z-corporation.

Z-corp was acquisitioned by 3D systems in 2012, the line of Zprinters is discontinued and now sold by 3D systems as Projet, this can be rather confusing as their polyjet line is also called ProJet, for the sake of simplicity, in this section the powder based inkjet printers will be referred to as Z-corp system, or Zprinter.

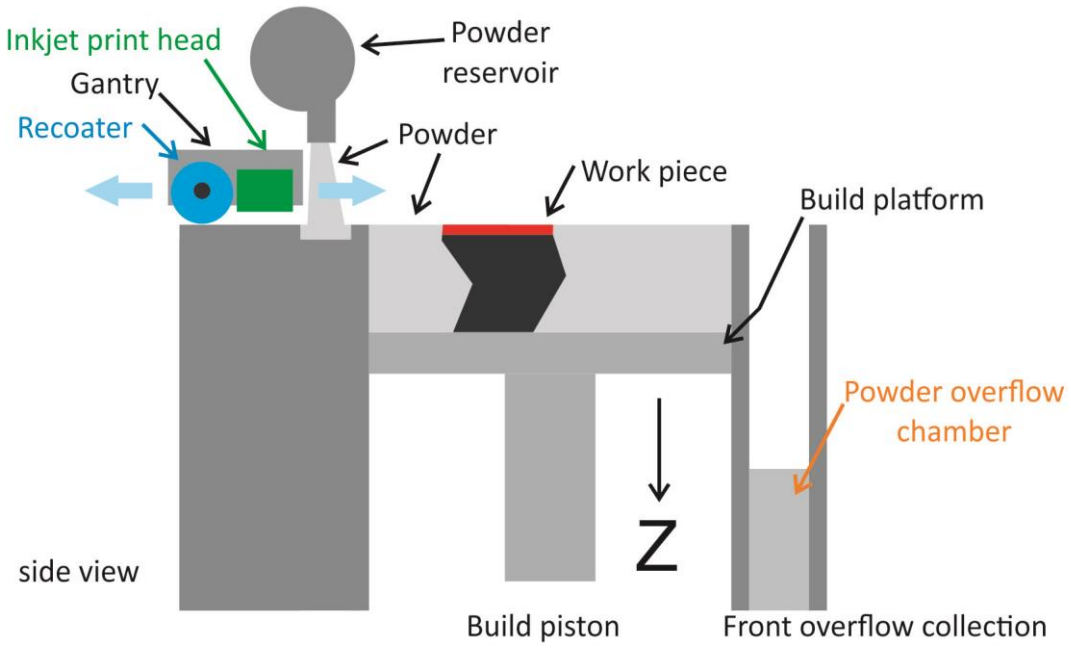

Figure 2.26, Z-Crop machine layout, figure by author

The arrangement of the Z-corp system (Figure 2.26) is similar to that used in SLS except there is no laser heating the build material. Instead an inkjet head is used to jet a binder onto the bulk powder -the binder acts as an adhesive that holds the particles together. The recoater and the print head are located on a gantry that moves over the build chamber, this saves some time as the recoating operation is done at the same time as the print head is repositioned for the start of the next layer; the layer resolution for this system is 0.1mm.

The Zprinter uses standard HP inkjet cartridges, "HP11" (Bibus, 2007, p.39) for each colour (CMYK) and the clear binder, the binder is pumped in from separate containers into the print heads. When a print head is installed system flushes the head with binder to clean the cartridge.

The system has a built in vacuum to recover unused powder which is automatically filtered and fed to the powder reservoir. The vacuum is also connected to the build plate and as a result the build chamber can be cleaned automatically.

Build strategy

The system builds each layer the same way an inkjet printer does, sequentially from the front to the back with the carriage moving left to right jetting the binder and ink. The binder is jetted in strategic areas to ensure good part strength but at the same time to use the least amount of binder as possible. The outside shell of the part (perimeters) receives a high saturation of binder while the interior receives less. Small areas in the interior are also treated with a high saturation of binder to form an infrastructure -this is similar to the infill of a part made with FDM. The areas of high saturation can be seen in Figure 2.27 where they show up as light grey. The colour for the work piece is only applied to the outside shell to conserve ink. The heads are cleaned regularly during the build by a clean station located to the side of the build chamber, a cleaning solution is sprayed onto the heads and a rubber blade cleans off the excess and any particle residue (iMakr, 2014).

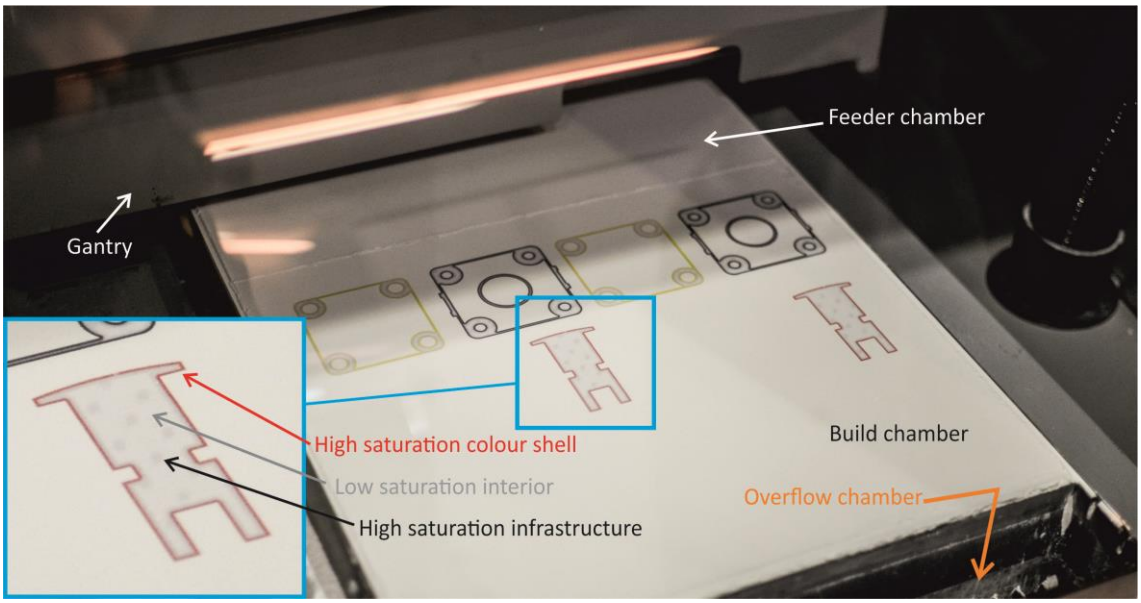

Figure 2.27, Z-Corp system building, left: detail of print strategy, figure by Author

There is no need for support as the powder surrounding the work piece supports the solidified areas, nevertheless the process of removing the work piece from the unused powder can break horizontal or fragile areas, so fixtures can be added that help reinforce the work piece while it is being handled (Bibus, 2007, p.13). The build

chamber is heated once the print is finished to dry the binder before the *'depowdering operation'* to ensure parts do not break during the process. Depowdering is done in two stages, first the large bulk of the powder is removed with the vacuum cleaner; the piece is then taken to another chamber where compressed air is used to blow away any loose powder still on the work piece.

The binder that is used to create the part is only strong enough to support the part during printing and some light handling, this is known as *'green state'*. The part will need further processing to give the part its final strength and this is done by infiltrating the work piece with Cyanoacrylate (super glue) when the work piece then takes on the strength of the infiltrating chemical uniformly (Bibus, 2007, p.12). In parts made with AM techniques the part is weakest in the areas where the layers meet, along the Z axis, this is also true for the green parts produced with the Z-corp, however by infiltrating the print, the strength becomes more uniform (isotropic).

The Z-corp system originally offered a large range of materials including materials for sand casting and flexible infiltration resins for rubber-like properties (Zsolutions, n.d.), however since the acquisition from 3D systems this is no longer the case and the materials are limited solely for the production of visual models. There are some options for the infiltration chemical but they only change the part strength (3DSystems, 2014 A, p.3).

Whilst the materials appear to be common, with names like ZP 130, or VisioJet PXL core, it is difficult to see what they are actually made of, however the material safety data sheet reveals that the main build material, VisioJet PXL Core, is 90% plaster (3DSystems, 2013 A, p.1) and the binder, VisiJet PXL, is an aqueous solution of 2-pyrrolidone (at 1%) (3DSystems, 2013 B p.1). As mentioned before the infiltration chemical, ColorBond, is Cyanoacrylate (3DSystems, 2014 B p.1).

Figure 2.28, 3D scan printed with Z-Crop, figure by author.

The real strength of the system lies in the ability to print full colour models. The vertical resolution of 0.1mm (3DSystems, 2014 A p.4) is not ideal for high resolution models but the use of colour helps bring out more detail, Figure 2.28 shows a full colour print from a 3D scan printed with the Z-Corp system.

Voxeljet

The Voxeljet system works the same way as the Zcorp, by Applying binder onto a bed of powder to build the model. However the focus of the system is different, it is intended for use in metal casting applications with materials suitable for investment casting and sand casting.

The investment casting materials come in two variations, both are PMMA (modified acrylic glass) but have different particle size, the first at 55 microns and the second at 85 microns. They also use different binders; the Polypor B binder is used for high accuracy and sharp edges and it also yields a stronger green part at 4.3 MPa (Voxeljet, 2013, p.3) which burns out at 700°C. The second binder Polypor C while still compatible with investment casting; can also be used for architectural models and can be dyed. It is weaker at 3.7 MPa and burns out at 600°C. Both materials can be printed at a layer height of 0.08 to 0.2mm.

Parts made with this process require hardening in an oven. The parts can be infiltrated with resin for architectural model applications or wax for investment casting pattern purposes; this also produces a smooth surface (Voxeljet, 2013, p.3).

Figure 2.29, Dragon made with Voxeljet system, material: PMMA with Polypor B binder for investment casting. figure by author

Figure 2.29 and Figure 2.30 show sample plastic models made with the Voxeljet system, the model in Figure 2.29 shows very little striation from the AM processing, this being due to the small size difference between the particle diameter and the layer height (55 and 80 microns respectively).

The model in Figure 2.30 shows the same characteristics as the model in Figure 2.29 but treated with resin and dye. This model demonstrates the capability of the system to cope with overhangs. The lattice beams are 1.6mm thick and the square gaps are 7x7mm and it also features a loose solid sphere encased inside the lattice.

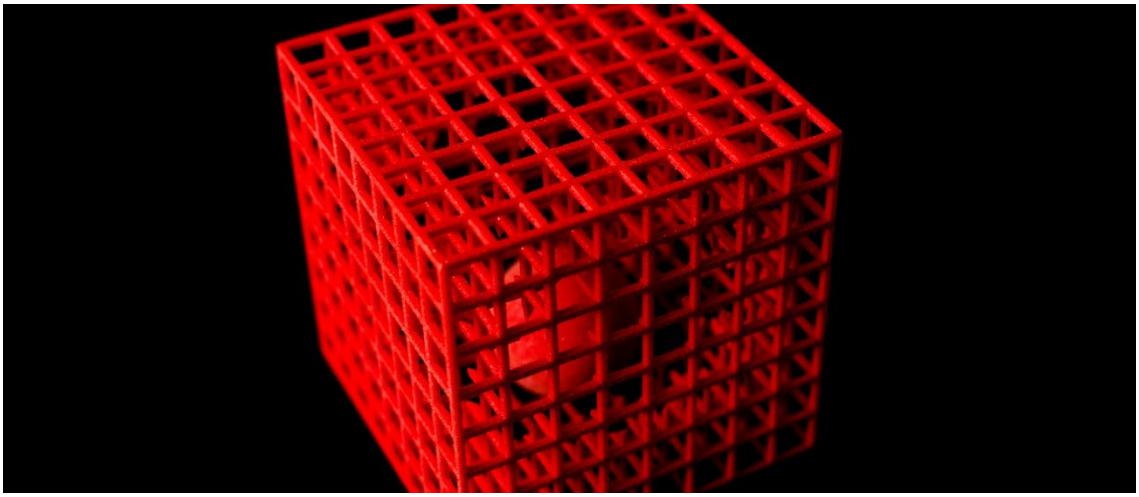

Figure 2.30 box lattice made with Voxeljet system, treated with resin and dye, 69.6mm x69.6mm x 69.6m,. figure by author.

The material used for sand casting applications is silica sand and it can be printed at a layer height of 0.2-0.3mm, with Furan resin as binder. The moulds made with this process have relatively low emissions during casting. This material is used for direct manufacture of sand casting moulds including cores for hollow parts and is manufactured in different grades to match individual applications (Voxeljet, 2010, p.7).

The systems offered by Voxeljet vary in size depending on the application but the biggest envelope available is 4mx2mx1m (Voxeljet 2013, p.10).Perhaps the most innovative system in their range is the VXC800 with an envelope size of 850mmx500mm and a continuous Z axis. (Voxeljet 2013, p.8)

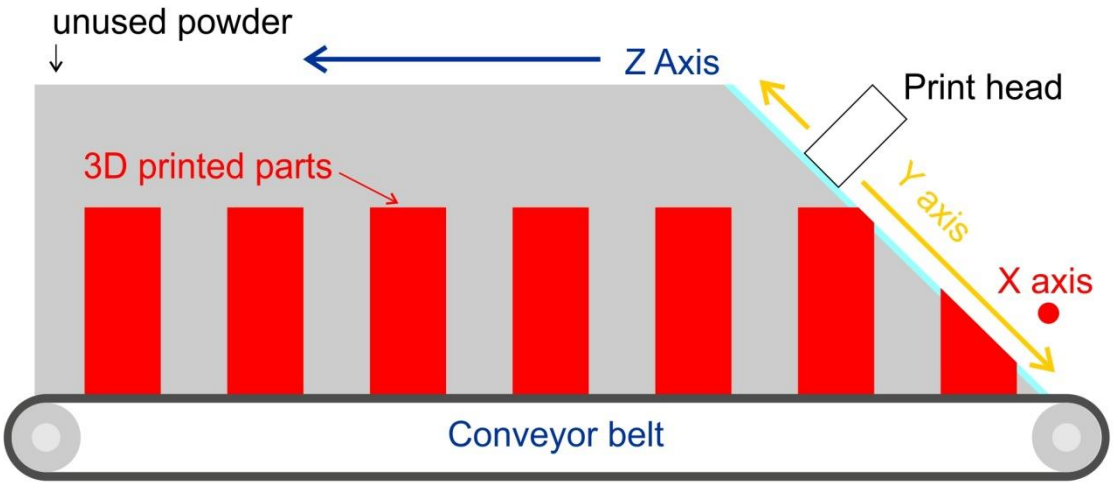

Figure 2.31, VXC800 continuous 3D printer layout, side view. Diagram by author based on process explanation video (Voxeljet 2013,B)

The layout of the axis on this system is unique, the Z axis is a horizontal conveyor belt that moves the whole print towards the back of the system where it can be cleared of the unused material (Figure 2.31), the X and Y axis are mounted at a slanted angle, this layout according to Voxeljet allows the system to continually print a large batch of parts or build long parts that exceed the dimensions of the system.

2.4.5 Inkjet 3DP in metals

This technology has strong parallels with the systems just discussed, the main difference being that instead of plaster or sand the binder is deposited onto a bed of metal powder. The technology is referred to as Digital Part Materialisation by EX One, or Digital Metal by Höganäs. The combination of the binder and the metal is still light enough to not require support; this as opposed to the laser sintering/melting systems discussed previously, which means that parts can be stacked on top of each other to fill

the whole build envelope. The parts also require heat treating in a kiln to sinter the material and the metal parts can also be infiltrated with bronze to make a composite metal part.

The Ex One system offers "420 and 316 Stainless Steel/Bronze, Tool Steel, Bronze"(Exone, 2012) at a minimum layer height of 0.1mm, and the Höganäs system only offers stainless steel but is working towards offering titanium, copper and silver (Honagas, 2013 p.3), the system is capable of resolutions of 0.045mm (Ipmd, 2013).

2.4.6 Polyjet, Multi Jet Modelling (MJM) And Multi Jet Printing (MJP)

MJM and MJP are the same process, the terms are used interchangeably by 3D systems; it is also virtually identical to PolyJet technology developed by Stratasys. An inkjet head is used to deposit droplets of UV curing materials on demand to create an object, a UV lamp mounted on the print head is used to cure the material. (Realizeinc, n.d.) Depending on the materials that are being used, this technology is capable of producing 0.016mm layers for the Polyjet (Stratasys, 2014, A) and 0.029mm for the MJM (3Dsystems, 2014, C, p.4).

Figure 2.32, Object printed on Objet system with rigid and flexible materials. figure by author

The technology has a wide variety of materials from rigid to rubber-like. An individual system is capable of using several of these materials in one print (Figure 2.32), the advantage of this being that parts can be made fully assembled featuring different and

functionally graded materials; this versatility is not normally seen in AM processes and is unique to this technology. The number of materials that can be loaded depends on the model of the system. The print head is also capable of mixing the materials to create composites, extending the range of mechanical features that are possible in one part (SlashGear, 2013).

For several years systems using this technology only produced prints in grey scale by combining white and black materials, that is still the case with the MJM systems, but the Polyjet systems are now capable of mixing up to three different colours, both transparent and opaque, in one print, extending the colour palette available (Stratasys, 2014, B).

Support is an area where MJM and Polyjet are different; with MJM the print head deposits a wax material to support overhangs (Vaezi, Chianrabutra & Mellor et al., 2013, p.25). This needs to be melted away in an oven and the part also needs to be cleaned in an ultrasonic cleaner to remove the fine wax residue. With Polyjet a viscous gel-like support is used (Singh, 2011) and this is removed using a water jet. This process is faster than the MJM method but it can be difficult in areas that are hard to reach or parts with a complex internal structure.

Wax jet

A system that is similar to the technologies just discussed is the Solidscape, it uses an inkjet head to deposit droplets of wax to create a part, this system however is aimed namely at the production of investment casting masters. It uses wax that has been heated to melting point, not UV curing resin. The system deposits two types of wax, the build wax and the support wax which is soluble in a chemical bath (Vaezi, Chianrabutra & Mellor et al., 2013, p.25) and it produces layers down to 0.025mm (Solid-scape, 2014).

The build method is similar to Polyjet with the difference that each layer requires cooling, as a cutter is used to level the build after each layer thus ensuring high dimensional accuracy.

2.4.7 Laminated Object Manufacturing

Laminated Object Manufacturing (LOM) was originally developed and commercialised by Helisys (Warnier, Verbruggen & Ehmann et al., 2014, p.13) it is a hybrid additive/subtractive Process; additive in that layers of sheet material are used to build the object, but also subtractive as the sheets of material are cut (Weisensel, et al, 2004, p.258).

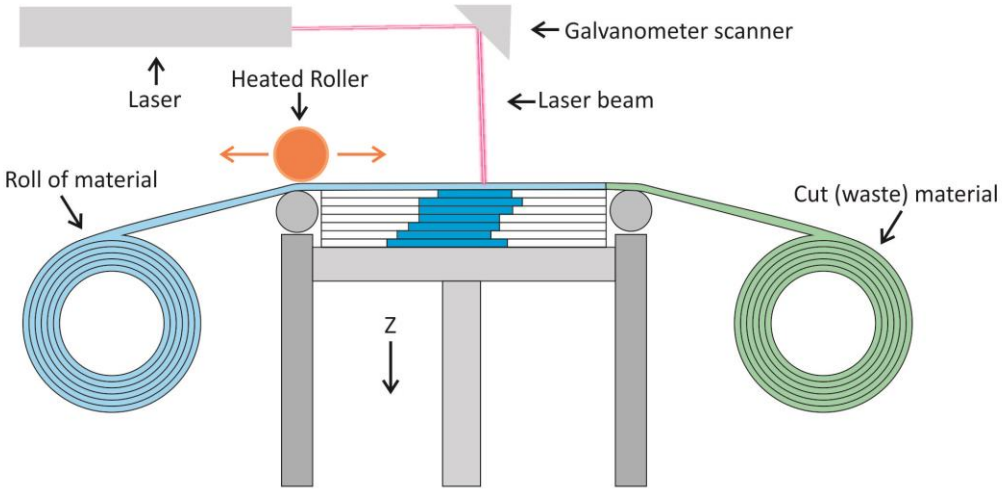

Figure 2.33, diagram of LOM process. figure by author.

It starts by loading a sheet of self adhesive material from a roll over the build plate then a laser is used to cut the material to form each layer of the object. A grid pattern is also cut in the unused areas to aid in removal after but the unused material also serves as support. The laser also cuts around the perimeter of the build plate leaving some excess around the edges so the sheet can be pulled into a waste roll. A heated roller is then moved over the build chamber to compress the cut sheets and activate the adhesive (Figure 2.33). This process can create parts from plastic sheets, paper, metals and ceramics (Custompartnet, 2009).

This process has been overtaken by other AM technologies and has seen very little commercial success with several systems developed over the years by companies that are no longer trading (Warnier, Verbruggen & Ehmann et al., 2014, p.13). There are still some companies that use this process but provide it as a service, such as Stratoconception, where they cut thick sheets of material using a CNC router to produce models and bespoke form fitting packaging for products, layer stacking is

done manually, guided by external registration fixtures that are later cut away (Stratoconception, n.d.).

This process is also more common in areas of research where equipment is developed for specific applications. The most common material used is ceramic where complex parts can be made without the need to manufacture moulds

Commercial LOM systems

Mcor is one is probably the only commercial system currently in the market and although it calls the process Selective Deposition Lamination (SDL), it is effectively the same strategy as LOM. Using standard A4 paper sheets instead of a roll of material, the system has a hopper loaded with the paper sheets, which are fed into the machine by a roller and moved into position by a manipulator mounted on the gantry (Figure 2.34).

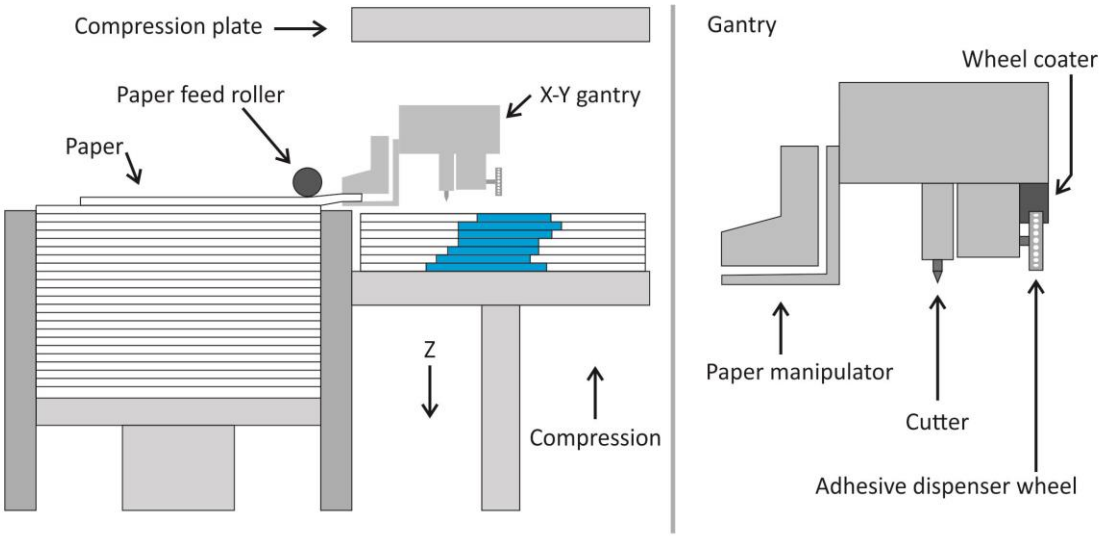

Figure 2.34, Mcor machine layout (left), Mcor gantry, including cutter, adhesive dispenser and paper manipulator. figure by author.

The machine uses a sharp blade to cut the paper and it cuts around the perimeter of the part and in a grid pattern over the waste areas facilitate removal. The sheets of paper act as both the build material and the support. Once a layer is cut, the gantry retracts the cutter and by means of a dimpled wheel the adhesive is selectively applied as dots over the sheet of paper. The gantry then locates a new sheet of paper over the build, the build plate moves up and compresses the whole stack against the compression plate, then the process repeats until the model is complete. Models can be made in full colour by printing the paper prior to loading into the machine; the

software produces the colour layers along with registration marks to guide the machine.

Figure 2.35, collection of Mcor samples in full colour. figure by author.

The main limitation of this process is that hollow objects cannot be made at it would be impossible to remove the support material from inside the build; considerations would have to be taken such as designing the object in two parts.

2.5 Ceramic Additive Manufacturing

Intro

This section introduces some AM projects that have been developed for the manufacture of ceramic parts and components and are available as commercial systems or services.

2.5.1 Robocasting

Robocasting is an AM method for processing ceramic and composite materials, which works by depositing filaments of ceramic slurry with a high solid content. The slurry is comprised of 50-65 vol.% ceramic powder, <1 vol.% organic binder and 35-50 vol.% volatile solvent (usually water) (Cesarano, King and Denham, 1998, p.697).

The solid loading of the slurry is carefully controlled to ensure good performance. The viscosity of the slurry must be low enough to allow deposition at reasonable rates but also maintain the filament shape. The solid content mentioned before is in a range where the rheology of the slurry is pseudo-plastic as at a solid content beyond 63 vol.% the interaction between the particles of ceramic in the slurry increase leading

restricted mobility and the slurry locks up into a dilatant mass (Cesarano III, King and Denham, 1998, p.698).

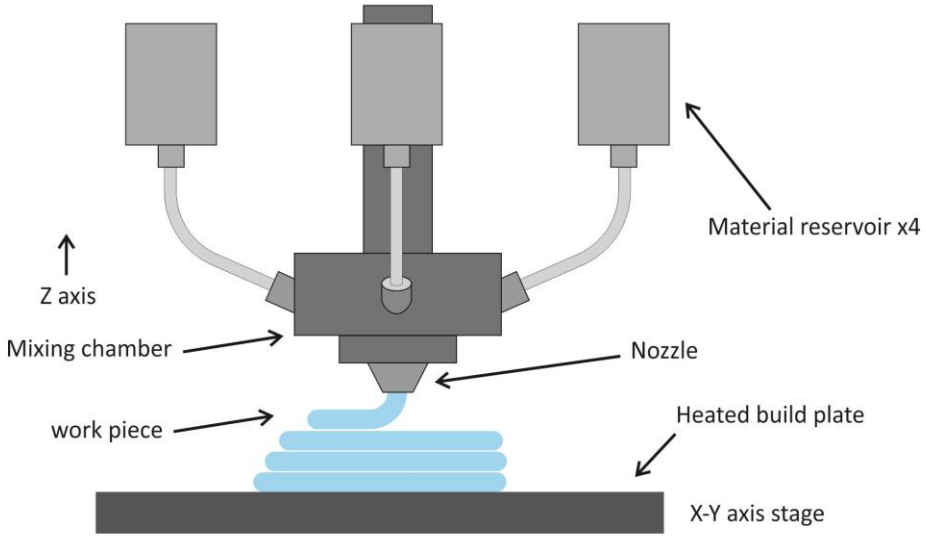

Figure 2.36, robocasting print head, four materials and mixing chamber (Cesarano III, King and Denham, 1998, p701) . figure by author.

The rheology of the slurry needs to be controlled so that it is close to the point before it becomes dilatant, which ensures good filament shape stability and quick drying performance. To ensure that the slurry dries at a fast rate, the build plate is heated to between 30 and 60°C, otherwise the filaments would deform under the weight of consecutive layers. For larger and thicker parts heaters are also used above the build.

The deposition head is fed from four material reservoirs (Figure 2.36) and the head also has a built in mixer, which means that the head can deposit up to four different materials in one build and also dynamically mix the materials at different ratios for functionally graded materials.

Figure 2.37 shows a typical structure made with Robocasting in ceramic. These parts can be used as high temperature filters or as an interface surface for mechanically joined composites, this has been demonstrated where molten steel was infused into the structure creating a strong mechanical bond (Robocasting, n.d. A).

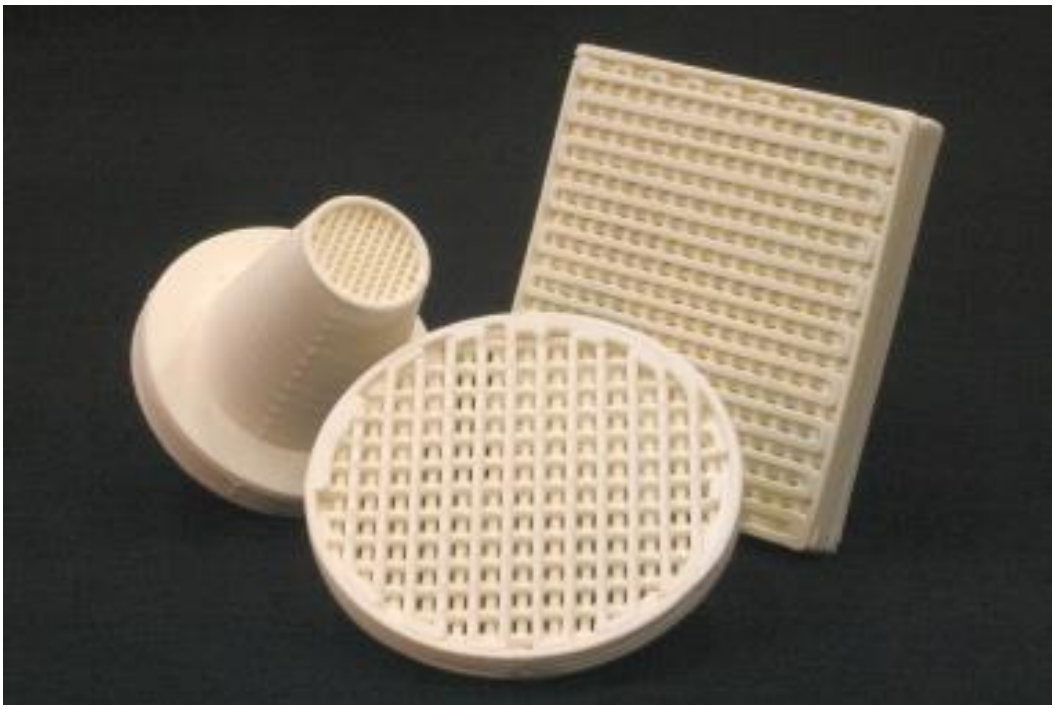

Figure 2.37, Robocast ceramic filters, photo courtesy of www.robocasting.net.

Robocasting is capable of creating parts in a large range of ceramics, metals, metal/ceramic composites and polymers (Robocasting, n.d. B). The company focuses on the manufacture of lab ware, lab equipment and bespoke parts for specific applications and they also provide this as a service.

2.5.2 Unfold

The ceramic deposition machine by unfold is built around an open source FDM machine, it uses a pressurised slurry reservoir that feeds into an auger valve to control deposition rate, the auger valve is driven by a stepper motor, the same way as an extruder in an FDM system.

Figure 2.38 Unfold ceramic printer, porcelain cup. photo by Kristof Vrancken (unfoldfab, 2012).

The projects run by Unfold using the ceramic printer are aimed at exploring the aesthetic qualities of the technique, they use large filaments, the nozzle in the picture is 0.6mm; this exaggerates the striation left by the process revealing how the artefact was made. This project displays AM not as a tool to emulate industrial processes but rather as a manufacturing method in its own right, with its own identity.

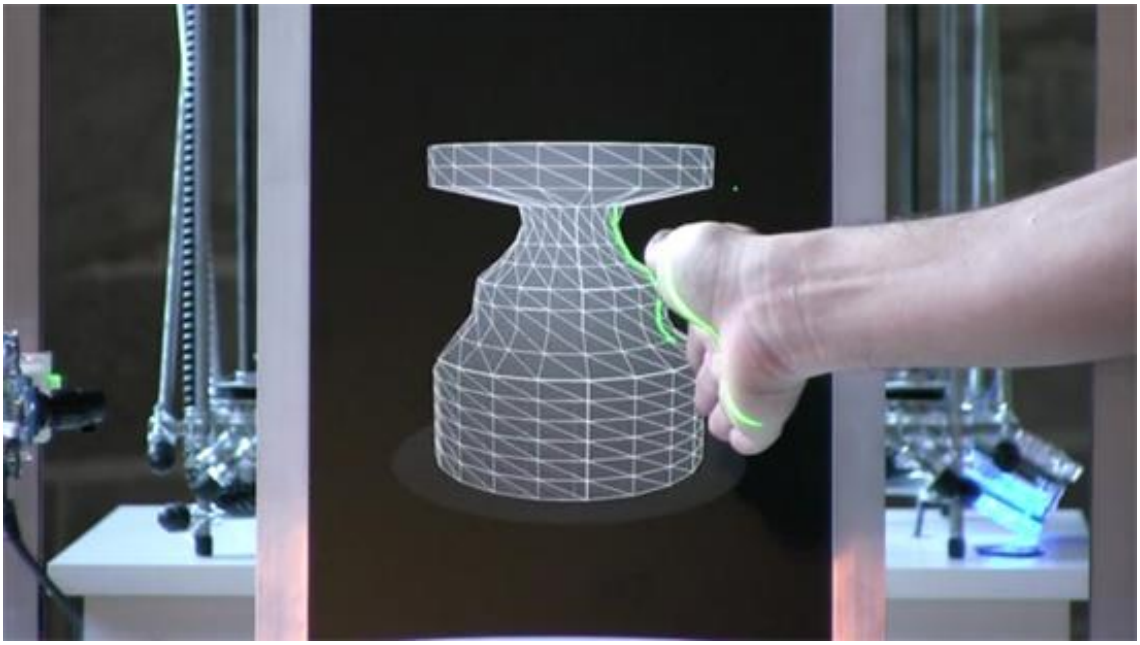

Figure 2.39, L'Artisan Electronique, virtual potters wheel. figure from (Designplaygrounds, n.d)

Unfold have also explored the possibility of creating a more inclusive design process. No matter how advanced AM technologies get, at some point the user will have to use

3D modelling software to create. This excludes a large portion of people who are less technical or too young. The Unfold L'Artisan Electronique project is aimed at creating a more inclusive modelling system (Shillito, 2013, p.93), the underling concept in this project is that it is operated the same way as a pottery wheel but using cameras to track the user's hands, the object is created in a virtual environment using intuitive tools everyone is used to, hands (Figure 2.39).

2.5.3 WASP - Large Delta

The information given in this section was obtained directly from the manufacturer during the 2013 3D print-show in London, specific references to information given are difficult to obtain as there is little information available online or otherwise. Therefore this section is focused on the aims of the WASP project, some general information on their systems and their approach to AM in large scales.

As mentioned in the FDM section; there are several configurations for linear slides in 3 axis machines. The system developed by WASP uses a Delta configuration to minimise footprint while maintaining a large build envelope. The Delta configuration is widely used in industry, particularly for high speed pick and place jobs in assembly operations. The biggest Delta system by WASP is 2m cubed (Microfabricator, 2014), however they intend to make these systems much larger to build housing in 3rd world poverty stricken areas, they plan to use local materials to minimise environmental impact.

So far the systems developed have not reached the scale to achieve this goal. The systems work rather as demonstrators of the technology. WASP plan to fund their research from selling machines, thus far they have designed Delta FFF (Figure 2.6) and clay systems (Figure 2.40).

The clay is mixed with alcohol which evaporates at a fast pace ensuring that the build does not collapse during deposition - this is imperative due to the scale of the builds produced. The clay is extruded using a pressurised reservoir; the flow rate is controlled using an auger valve linked directly to a stepper motor via a flexible coupling.

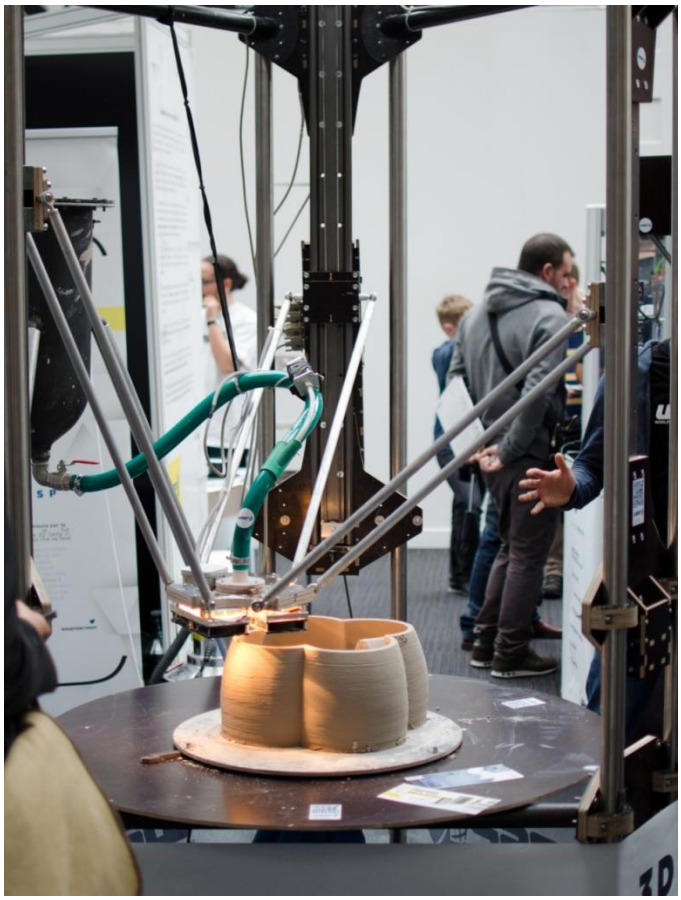

Figure 2.40, WASP clay Delta machine, building a model of the house intended for 3rd world poverty stricken areas.. figure by author.

Nozzle sizes for this system are generally large due to the size of the build and the viscosity of the materials and are in the range of 5-10mm. These are subject to change depending on the application of the system, it is expected that a system for building architectural scale parts would use much larger nozzles to reduce build time.

This process has a different approach to AM than that seen in most commercial systems as it is unconcerned by the Z-resolution of the build and more interested in the final form and how long it takes to get there. As mentioned in the 'Build times in AM' section, as the size of the build is doubled the time taken to build that part is increased by a factor of eight, using a larger nozzle overcomes this limit as the filament size is increased along with the scale of the build. It is much quicker to sand and fill a large build in clay than it is to make the same build at a high resolution. This is of particular importance to the WASP project as they aim at making building scale prints, such as housing, sourcing materials from the local area.

2.6 Architectural scale additive manufacturing

2.6.1 Additive Manufacturing Of Bespoke Bricks

Using an open-source FFF system Brian Peters (Warnier, Verbruggen & Ehmann et al., 2014, pp. 170-171) developed a novel approach for architectural scale AM in his project titled *'Building Bytes'*.

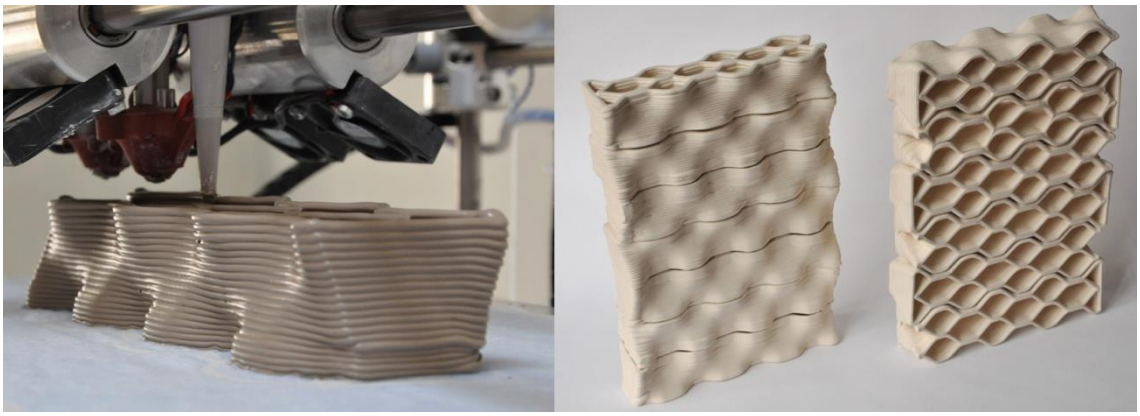

Figure 2.41, Bytes (bricks) designed by Brian Peters, in pictures is the Honeycomb Byte. figure by Brian Peters (Peters, n.d.).

He focused his research on the creation of bespoke bricks or, as he calls them *'Bytes'*, for creating larger objects (Figure 2.41). This approach allows for complex design to be made that utilise the advantages of AM; each *'Byte'* can be unique and the collective of all the pieces brings the artist intent forward. This method came from the size limitation of the desktop sized system he was using and his intent on creating architecture scale objects (Peters, n.d.).

The *'Bytes'* are made from a liquid slip cast recipe of earthen ware ceramics, the material is held in a plastic reservoir and extruded by pressurising said container with air.

2.6.2 Concrete Deposition

This AM technique is being developed for the manufacture of architectural components in concrete instead of full size buildings; the research is based in Loughborough University. The technique allows for gaps and pockets to be designed inside the structure and these can be used to reduce weight, add insulation or for the installation building services. The manufacturing method leaves a large striation texture, one which has been deliberately incorporated as designers and architects

expressed interest in the evidence of the process (Lim et al., 2011, p.666), the layer height range is 6mm-25mm (Lim et al., 2012, p.264).

The process uses a bespoke concrete formulation that is up to three times stronger than commercial cast concrete, in order to account for the inherit structural weakness left by the AM process, as the deposition leaves gaps that result in up to 20% reduction in strength (Lim et al., 2011, p.666).

The project has also developed optimisation algorithms for machine tool paths to reduce the amount of times the deposition has to be stopped to reposition the head. Stopping and starting deposition leads to under printing and over printing respectively due to the flow rate of material not coinciding with the movement of the head. So creating a tool path that allows for continuous deposition is desirable as it improves surface quality and accuracy (Lim et al., 2012, p.265).

2.6.3 Contour Crafting

Contour crafting focuses on large scale builds (Figure 2.42); similar to Loughborough's concrete printer but the main difference here is that a trowel mounted on the side of the deposition head is used to smooth the outside surface. Contour crafting produces hollow parts with a smooth outside finish; typical layer height used is 13mm (Lim et al., 2012, p.264).

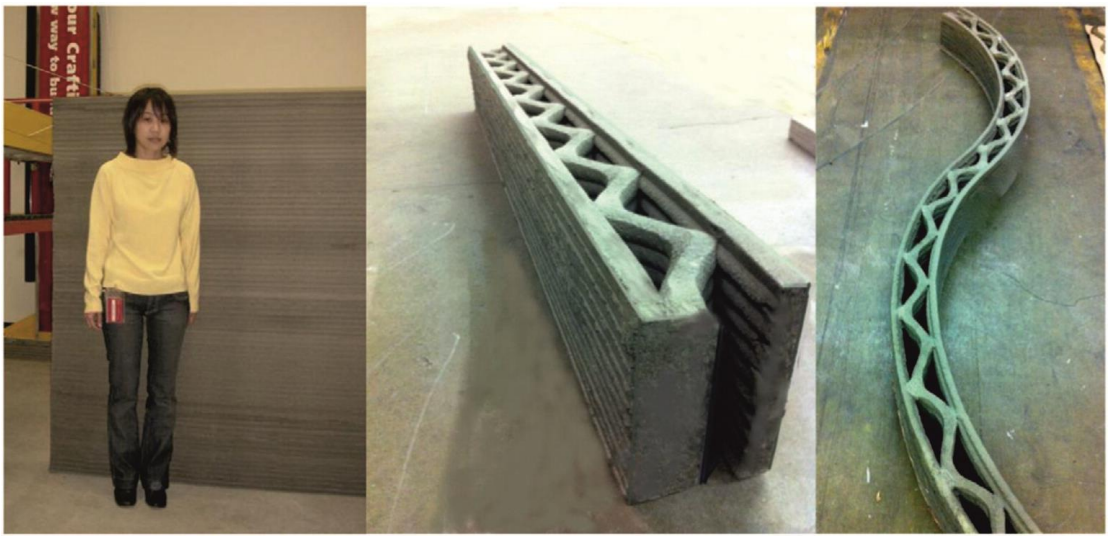

Figure 2.42, Wall sections built by Contour Crafting Machine. figure by Zhang (2013, p.52)

This process stands out from all other AM processes in that the deposition head can rotate 360° allowing the trowel to work the surface. The deposition head has a square

profile with sides that enclose the filament, which has the effect for moulding the deposited filament into a flat square profile of improved filament stability as subsequent layers are deposited onto a flat surface (Khoshnevis, 2004, p.2).

The main aim of contour crafting is to fabricate complete buildings, with electrical and plumbing fixtures and painting of surfaces. To achieve this, the system would need to use several different deposition heads to produce the structures required and manipulators to install fixtures (Khoshnevis, 2004, p.5) - however at the time of writing this has not been realised.

Another paper was published with the focus on building large structures such as walls and how to optimise this process for the construction industry. One of the focus areas was in cost; it is derived from the use of material and print time. The cost of material is constant once the structure is designed for Contour Crafting, however the build time required further work and it was divided into three sections (Zhang & Khoshnevis, 2013, pp.55-56):

- Time spent depositing.
- Travelling time, time in which the deposition head is idle and travelling between deposition operations, this was referred to as 'Air-time'.
- Time spent rotating the head, this is the time spent rotating the head to position as the extrusion nozzle has a square profile.

The time spent depositing could not be optimised, because it was dependent on the tool-paths of the actual geometry being built. The time spent travelling and rotating the head needed optimisation as this 'air time' was considered wasted time and therefore it unnecessarily increased build time and cost. To optimise the air-time the TSP (travelling salesman problem) model was implemented.

-The travelling salesman problem is a path optimisation model built around the idea of optimising the path taken to visit a number of cities only once and returning to the point of origin using the shortest possible path.-

The TSP model however, required some modification to include extruder rotation as walls that had the same orientation or required the least amount of rotation needed to be considered. The deposition paths needed to be ignored as these paths form the actual build. The tool-path was reduced to an array of vertices representing the start and end points of each deposition in order to implement the TSP model.

Once the TSP was produced for a given build, a TSP solver was used to produce the final solution. In Zhang's (2013, p.56) research Helsgaun's algorithm was used, which was an improved version of Lin-Kernighan's algorithm.

2.6.4 D-shape, Building Scale Printer

The D-shape system developed by Monolite UK is very similar to the powder systems mentioned where a binder is ejected over a bed of powder, in this case sand. More powder is added and subsequent layers are built up. D-shape does it at a larger scale, their current system having a build envelope of $6m^3$ and is intended for architectural applications (Figure 2.43), the layer height range is 4-6mm (Lim et al., 2012, p.264).

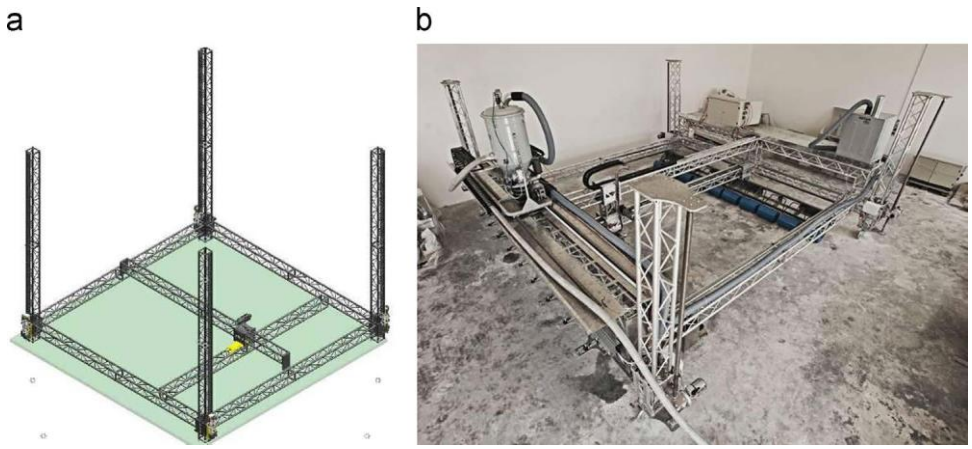

Figure 2.43, a: Schematic of the D-shape Material Depositing Unit and b: the complete D-shape printer. figure by Cesaretti (2014, p.440)

The 'print-head' is comprised of 300 nozzles that deliver droplets of binder and extends across the width build envelope. The nozzles are spaced 20mm apart and jet droplets of binder on demand. When the first pass is done an indexed actuator ram shifts the position of the nozzles in the Y direction to cover the areas that were left out, this is done four times as the average drop size is about 5mm in diameter (Cesaretti et al., 2014, p.441).

The granulated build material is distributed by the same gantry where the binder jets are mounted and a hollow pipe is used for this purpose. The granulated material is distributed inside this pipe by a series of rollers to ensure the whole build envelope is coated with precisely the same amount of build material. During this process a blade, also mounted on the gantry, removes excess powder and compresses the layers to ensure a precise layer height (Cesaretti et al., 2014, p.442).

Figure 2.44, large print "radiolaria" made on D-shape system during the 'evaluation process' (D-shape, n.d.)

The sand solidifies to sandstone (Figure 2.44) by a chemical reaction between Magnesium Oxide which is mixed into the sand (15-30 Wh%) and Magnesium Chloride Hexahydrate (65%) in the binder. This chemistry is known as "sorel cement" (Cesaretti et al., 2014, p.444) and the resulting parts can cope with tensile stresses and require no rebar to reinforce the structure.

2.6.5 'Endless' project, large scale FFF

The *'Endless'* project by Dirk Vander Kooij is focused on the production of furniture using a similar build method to FFF; in this case however the XYZ gantry is replaced with a large six axis industrial robot (Warnier et al., 2014, p.120). Instead of spools of

filament this technique uses a hopper filled with granulated plastic and the head uses an ogre screw to feed and extrude the plastic, similar to that used in an injection moulding machine.

Naturally using the FFF build method for parts this size would take a long time to build but this is overcome by using a large extruder opening which is a common technique seen in other large AM methods. The exaggerated striation of the products combined with bright colours gives a skewed sense of scale to the surroundings as the parts look like small scale parts made on an ordinary FFF system. The layer height range is not stated in any of the literature; however it has been estimated to be 4mm by dividing the width of the chair by the number of layers (100) which were counted from a photograph. Finer or coarser layer heights may be used for products in other collections.

Figure 2.45, Endless chair being built. figure by Endless. (Kennedy, 2011)

As the products made in the endless project feature very light geometry (Figure 2.45), with most products having a single or double perimeter, the parts are designed to be self supporting thus requiring no support material that would ruin the surface quality. None of the examples shown feature any infill and are purely made with just perimeters, with tool paths that allow for continuous deposition -meaning that objects are made with a single un-interrupted filament, hence the name endless (even though the filament has a definite start and stop).

2.7 Open Source

Additive manufacturing has the ability to democratise manufacturing of products on demand, allowing everyone to become a designer and manufacturer, perhaps not in the mass production scale but manufacturing nonetheless, it is essential that the evolution of these tools also be democratised. This is the idea behind open source, to allow the user to tailor the technology for individual applications, the manufacturer or software provider cannot anticipate every possible use for any given piece of technology, if left open to the user then new uses and innovation can occur, naturally for the manufacturer of the original hardware it is a risky business strategy as open source is provided with no IP protection allowing anybody to clone the system and gain from it. This trend can be seen in the 'Makerbot' system, originally open source now closed source, this was a decision brought forward by the number of manufacturers cloning the system and selling it at a lower cost, this naturally meant that 'Makerbot' lost revenue that would have been used to improve its current system.

"For the Replicator 2, we will not share the way the physical machine is designed or our GUI because we don't think carbon-copy cloning is acceptable and carbon-copy clones undermine our ability to pay people to do development." Bre Pettis CEO of Makerbot Industries (Brown, 2012).

2.7.1 Reprap-Family Tree

The RepRap family tree (Reprap, 2012) shows the evolution and dissemination of FFF technology since 2006 covering over 100 projects. It is impressive to see how one open source project could generate so many iterations and commercial ventures with some like Makerbot becoming market leader in hobby grade machines. The current version at the time of writing cuts off at 2012, but there are on ongoing efforts to expand this to include more recent developments.

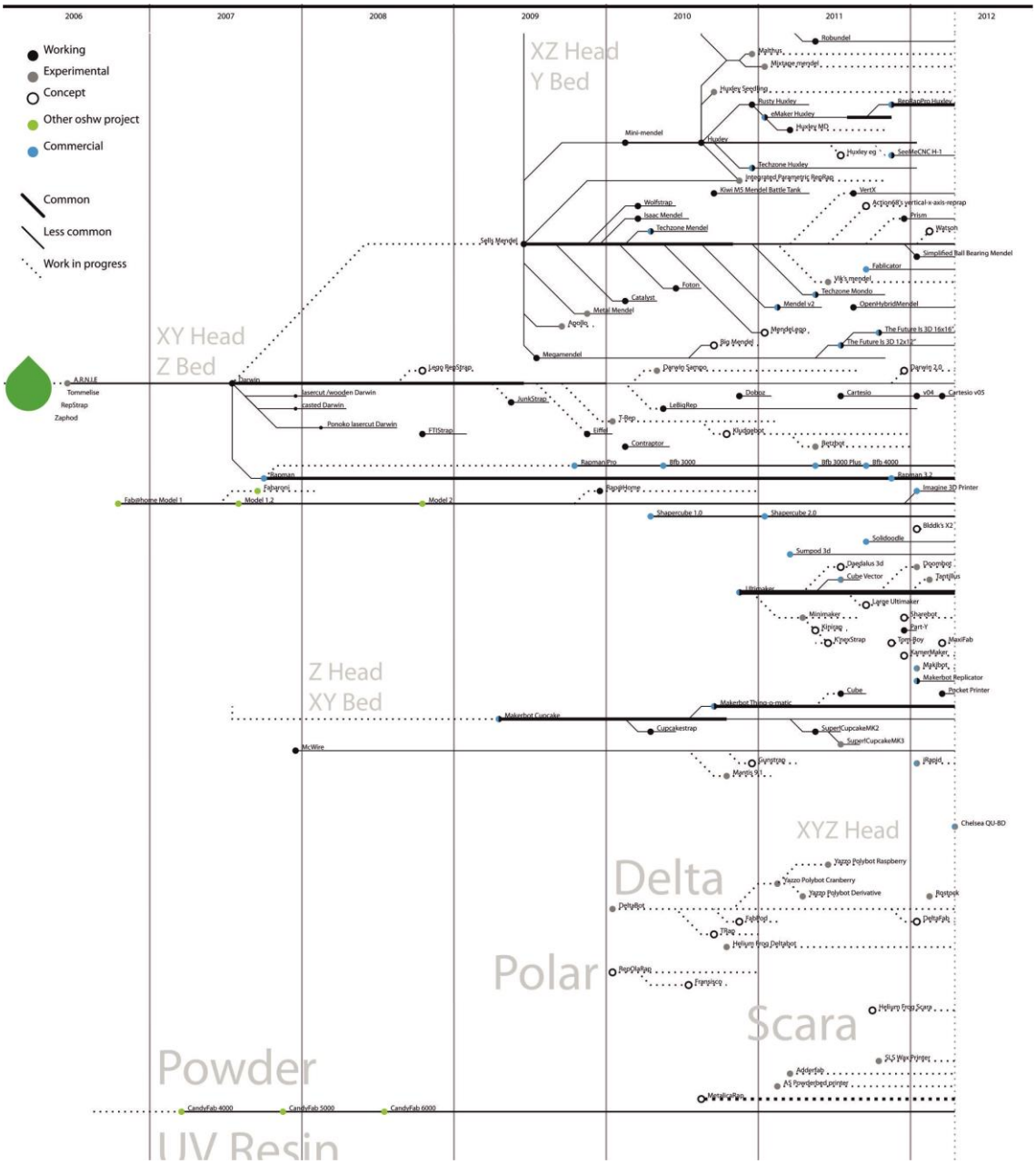

Figure 2.46, RepRap family tree, 2006 to 2012, cropped for illustration purposes. original illustration can be found at (Reprap, 2012)

2.7.2 Entry Level Systems

Makerbot is an FDM system developed as an open source project, it is very popular and generally hailed as the leader in the low cost systems; however the latest model is no longer open source to curb competition from clone systems that used the open source technology developed by Makerbot.

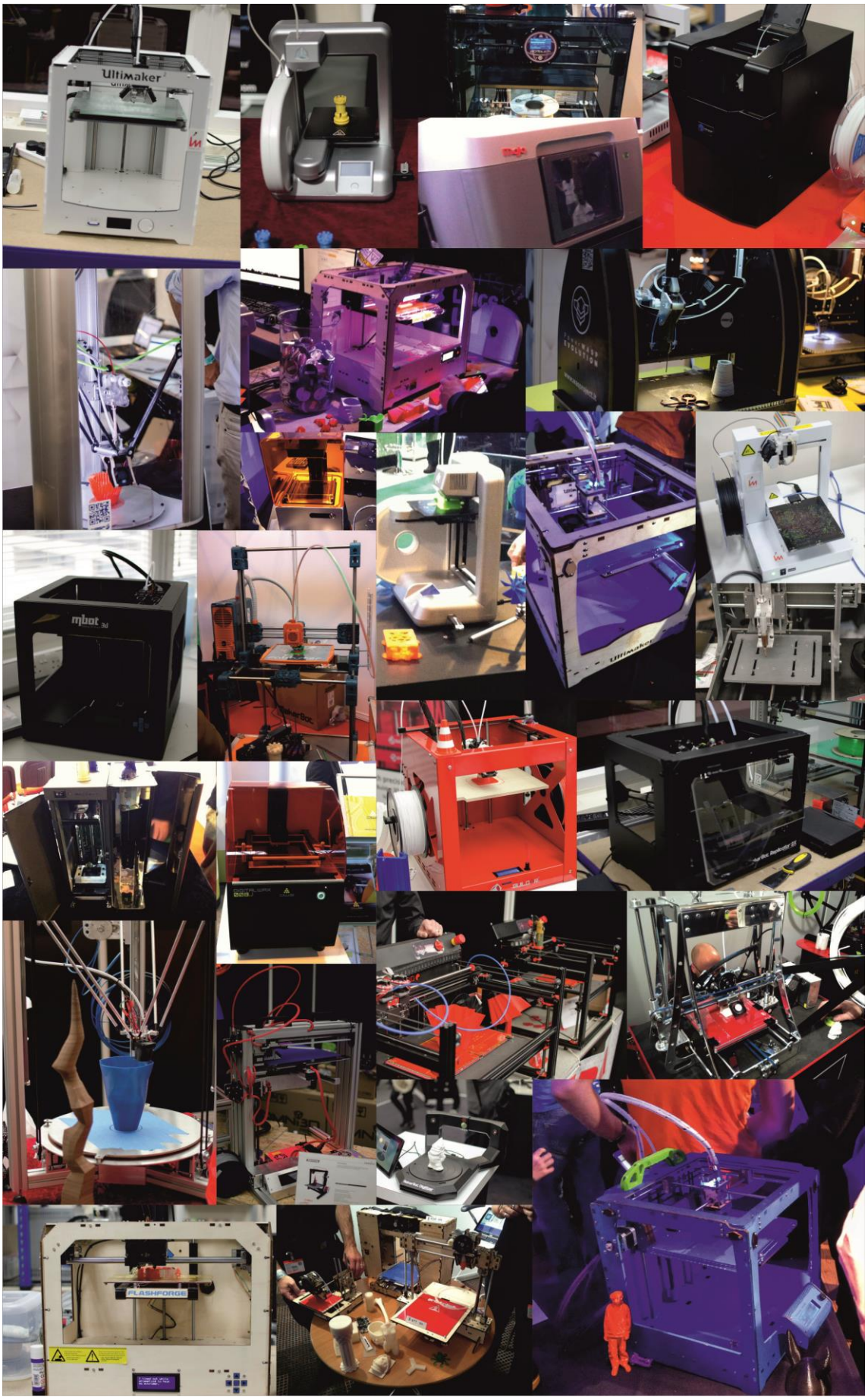

Figure 2.47, small cross section of AM systems. figure by author

2.7.3 Fab@Home

The personal fabricator developed by Fab@Home uses a similar build method to that of FDM, with the difference that the plastic extruder is replaced with two stepper motor driven syringes capable of a maximum pressure of 67psi (Malone & Lipson, 2007, p.248). The system is intended for experimentation allowing the user to modify the hardware and software to suit the intended application.

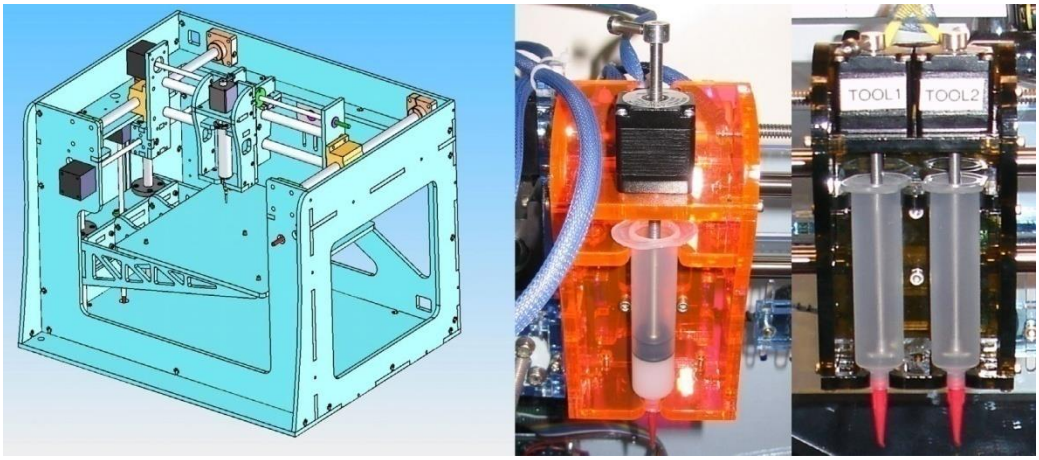

Figure 2.48, Left: Cad of model 1 Fab@home system. Right: Single syringe tool, driven by a linear stepper motor and two-syringe version. figure by Malone (2007, pp.247, 248)

Since syringes are used as the means of deposition, almost any material can be deposited with this system and is only limited by syringe loading and extrusion pressure required. This leaves the user free to prepare the build material for the desired application, nonetheless material properties must be considered as the material must be in paste form and self supporting. Materials such as chocolate which require heating involve hardware modification to add heating elements (Malone & Lipson, 2007, p.252).

What the system is capable of depends on the application the user develops; one example that is perhaps worth mentioning is AM of food. There are many demonstrations where this has been done, such as the edible rocket ship made at Cornel University (Doctorow, 2011), this demonstration however does not fully exploit the capabilities of AM systems; it is simply a food sculpture.

The application developed by Dave Arnold (2011) with the Fab@home system shows greater potential, developing structures and texture in forms that could only be done using AM. *'Masa'* -a corn based dough usually used to make corn tortillas, was used for

this demonstration, the dough can be fried but for it to be crispy all the way through it must be thin.

Figure 2.49, Stocharic 3D printed 'Masa Flower'. figure by (Arnold, 2011)

In order to build a structure that would fry to a crispy consistency Arnold used a process he called *'Stochastic printing'*. It involved depositing the *'Masa'* using parameters that would cause the extruded filament to coil randomly thus forming a loose weave (Figure 2.49). By adjusting the parameters it was possible to create a tight or loose structure allowing Arnold to dial in the proper parameters to make a structure that could be fried.

2.8 Food Additive Manufacturing

2.8.1 ChocALM

The ChocALM system was developed for the additive manufacture of chocolate forms in 3D, it uses a similar principle to FDM; where by a filament of chocolate is extruded to form the layers of the treat. It was originally developed by Dr. Liang Hao (2010) in a cooperative project that ran for two years with students from Exeter university, the technology has since then been commercialised and is sold under the brand ChocEdge.

There has been several iterations of the machine over the years and it is now very different from the system originally presented in the paper published in 2010 (Hao, Mellor & Seaman et al., 2010). The extrusion head was simplified from the original design which used a tempering chamber and an Archimedes screw to extrude the

chocolate (Hao, Mellor & Seaman et al., 2010, p.58). It is now a syringe controlled with a linear actuator (Figure 2.50) and is filled with molten tempered chocolate by hand.

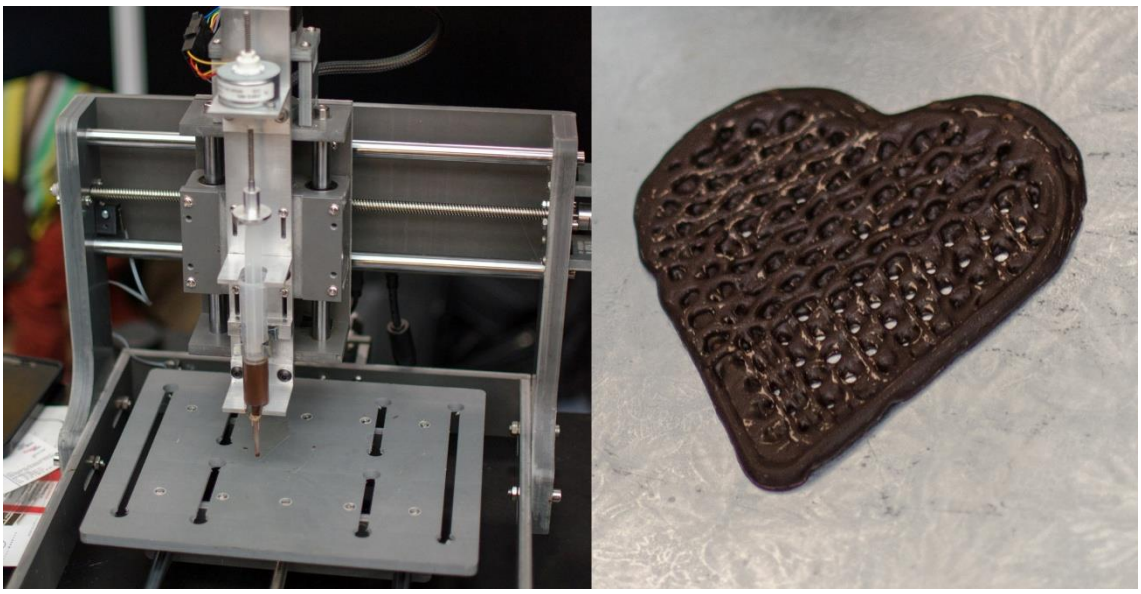

Figure 2.50, Choc creator v1 (left), chocolate heart sample (right), figure by author.

The chocolate is deposited onto a marble substrate, most samples feature 2D geometry, presumably more complex 3D forms are more difficult due to the rheology of the chocolate and the time it takes to cool down.

2.8.2 ChefJet

Chefjet currently under development by 3D systems and Hershe's confections and is a binder jetting system similar to the Z-corp but uses flavourings mixed with binder to 3D print sweets and is also capable of working with chocolate. The additive manufactured confections have the characteristic feature of parts made using powder (Figure 2.51).

Figure 2.51, Eddible 3D print made with ChefJet system. figure by (The sugar lab, 2014)

As the Chefjet is still under development at the time of writing there is very little information on the capabilities, however from press releases it has been observed that it is capable of printing in full colour and in a range of flavours (The sugar lab, 2014).

2.9 Research Projects in the Academic Field

2.9.1 Layerless Additive Manufacturing

The layer based build method common to most AM processes can make some applications challenging where the anisotropy of the part is detrimental to the desired mechanical properties. The method also inhibits the ease by which inserts can be added inside a part as it is built. This is especially true for SLA as any added fixture would potentially block the movement of a recoater.

Yong Chen (2011) of the University of Southern California has attempted to overcome some of these issues by developing a process called computer numerically controlled accumulation, based on similar principles as SLA, a UV light source is used to cure a liquid photopolymer, the main difference here is that the light source is immersed in the vat of resin and in direct contact with the material.

A UV LED is used as the light source, this is coupled to a fibre optic cable, the end of which is immersed in the resin vat; the light is focused with a sapphire ball lens. The light is directed by a 5 axis stage. (Chen, Zhou and Lao, 2011, p.220)

The system produces freestanding filaments of cured material and can be created in any direction. As the resin is cured in contact with the tool tip it is imperative to have a close control over the distance between the tool tip and the build surface, and also over the exposure time to ensure that the attachment force between the cured resin and the tool tip is less than the attachment force between the newly cured resin and the rest of the build to ensure that the structure can be successfully built. To reduce the attachment force between the tool tip and the cured resin, the tool tip is covered with a film of Teflon.

Tool path design for this process takes into consideration the direction of movement of the tool tip, as some downward moves are not possible. This is illustrated with the image below (Figure 2.52) where an arch was made following a 3D path.

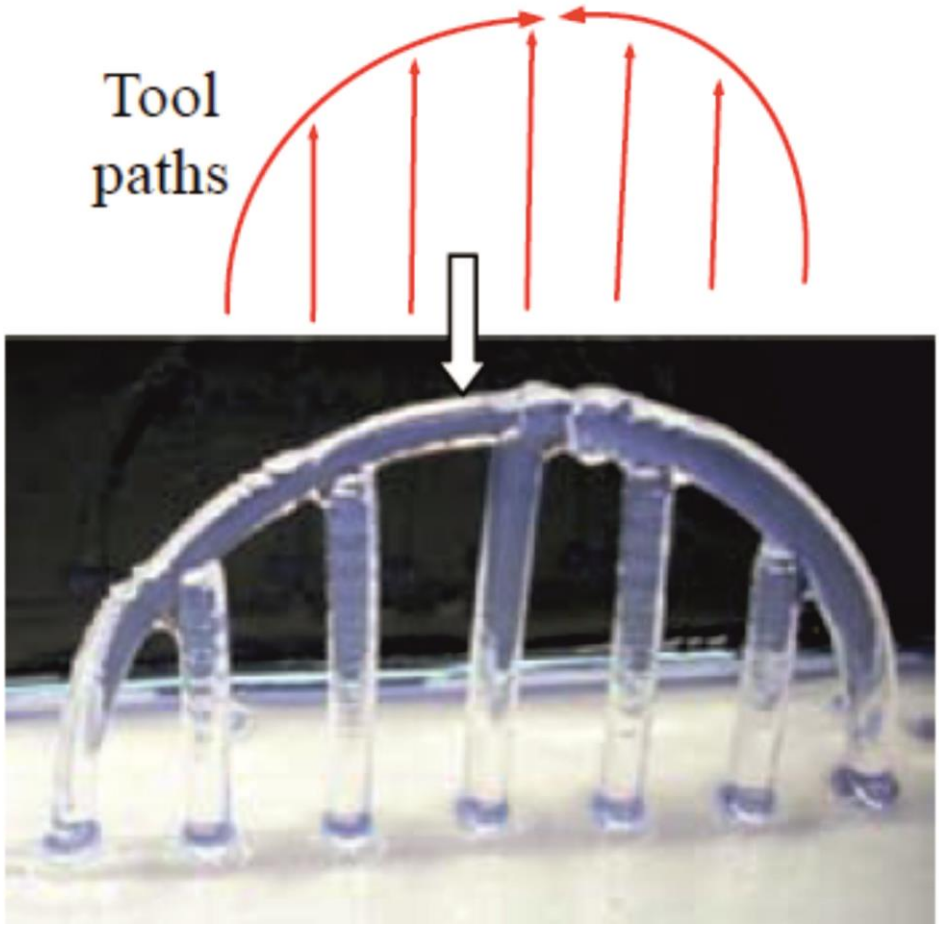

Figure 2.52, free standing arch, note the tool path direction illustrated by the red arrows. figure by Chen (2011, p.225)

Other applications demonstrated by Chen's research take the form of case studies include building letters onto the inside of a plastic bowl. This required the tool path to be contoured to the convex geometry of the bowl. The research demonstrated the capability of the system to build free standing structures as well as building around inserts.

2.9.2 3D Deposition of Chemical Reactors

A method for manufacturing bespoke chemical reactors has been demonstrated by Mark D. Symes (2012), The process uses a Fab@Home machine, setup for the deposition of silicone sealant "Loctite 5366 bathroom sealant" (Symes, Kitson & Yan et al., 2012, p.350).

The reactor, designed in Rhino3D, featured two solution holding chambers, a mixing chamber and a reaction chamber and non-printable parts were added at pre-programmed pauses. These included a glass microscope slide to view the reaction and a glass frit. Additionally, the reagents for the chemical reaction were also dispensed by

the machine into the appropriate chambers. The whole reactor was self contained, meaning that once printed it could be placed upside down without any leaking of the chemicals occurring (Figure 2.53).

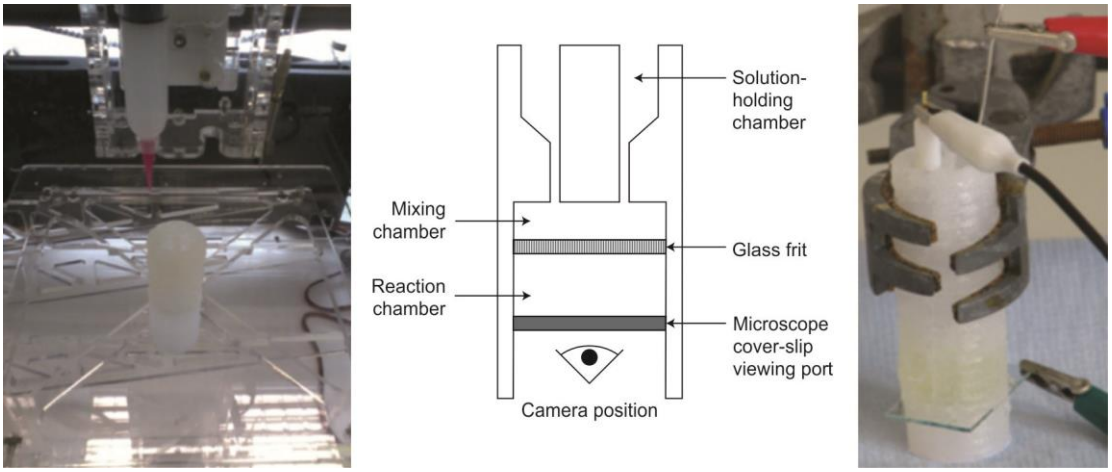

Figure 2.53, Left: The fabricator printing one of the devices used in this work. Middle: Schematic of the as-printed multipurpose reactionware used in the synthesis of compounds 1–3, which shows the key features of the design. Right: The reactionware as a cell for electrochemistry in a three-electrode configuration. figure by Symes (2012, pp. 350,351)

The holding chambers were designed to be self sealing so that the reagents would not flow prematurely into the mixing chamber and only when induced to do so. The reagents were drawn into the mixing chamber by inserting a needle attached to a vacuum into the reaction chamber, upon removal of the needle the silicone resealed itself.

Once the chemical reaction was complete the reactor was sliced open with a scalpel to remove the product of the chemical reaction, it was possible to reuse the reactor by applying fresh silicone into the cut edges and pressing it closed by hand.

The research also demonstrated a modified version of the reactor which included holes to insert electrodes and a fibre optic cable to monitor the reaction, further work also included building electrochemical cells with deposited electrodes, the electrodes were created by mixing the silicone with toluene to make a thinned gel and then mixing this with conductive carbon (Symes, Kitson & Yan et al., 2012, p.352).

The research demonstrated the versatility of the process for creating low cost bespoke reactors, and also provided new avenues of investigation into reactor design as it was demonstrated that the outcome of a reaction could be controlled by changing the architecture of the reactor (Symes, Kitson & Yan et al., 2012, p.353).

2.9.3 Printed Origami Structures

The technique established by Bok Yeop Ahn (2010) is capable of creating complex 3D geometry in titanium by combining AM methods with wet folding origami. The deposition method is similar to FDM, as the layers are made up of filaments of deposited material. The deposition head is directed via an XYZ stage, extrusion of the material is done by way of pressurising a syringe containing the material with pressures up to 600psi. The syringe featuring a standard luer-lok was equipped with a 0.25mm smooth-flow tapered nozzle; typical feed-rates were between 0.5-2mm/s (Ahn, Shoji & Hansen et al., 2010, p.2254).

The material is a specially formulated metal ink for deposition, it contains titanium hydride particles, an acrylate-based triblock copolymer and a graded volatility solvent system composed of 2-butoxyethanol and dibutyl phthalate (DBP).

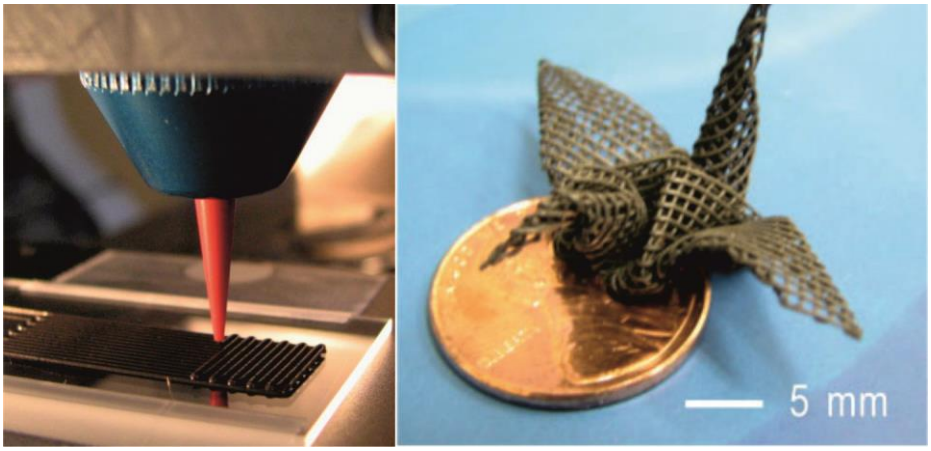

Figure 2.54, left, deposition of titanium ink. Right, folded titanium crane. figure by Ahn (2010, p.2251, 2253).

The system does not actually deposit 3D structures but rather it is utilised to produce the sheets of material that are then used to create the 3D structures (Figure 2.54, Left). Once the material sheet is deposited it is allowed to dry, but only partially so that it retains some flexibility. Folding of simple shapes such as a cube was done using a fixture to guide the folding and also hold the shape while the material fully dried. Subsequently the part was placed in a kiln for annealing. The shrinkage of the final artefact depends on the atmosphere inside the kiln, titanium hydride can either become titanium leading to 52% shrinkage, or it can oxidise to titanium dioxide and expand by 7.5%.

The composition of the titanium ink can be adjusted to specific applications, in areas where large gaps need to be spanned; the solid content can be varied between 70 wt% and 85wt%, the higher solid loading leading to more rigid filaments. The drying time can also be adjusted by changing the ratio of 2-butoxyethanol to DBP, this can lead to a larger working window for more complex geometry.

To demonstrate the capability of the technique for creating complex forms an origami crane was made (Figure 2.54, right) which was folded by hand and required 15 folding steps.

2.9.4 3D Deposition with Microcapillary Nozzles

The work presented by Gratson (2004) demonstrates a technique for the deposition of filament based periodic structures using microcapillary nozzles measuring 0.5-5 microns in diameter (Figure 2.55). Extrusion of filaments at this scale can be challenging as discussed by Lewis (2004), the deposition of colloidal gel based inks can suffer from clogging issues when the nozzle-particle diameter ratio falls below ~100 as given by Equation 2.3:

$$D/a2$$

Equation 2.3, relationship between nozzle and particle diameter, were 'D' is the nozzle internal diameter and 'a' is the maximum particle size (Lewis & Gratson, 2004, p.34).

Due to this limiting issue the project required development of polyelectrolyte inks that could readily pass through the microcapillary.

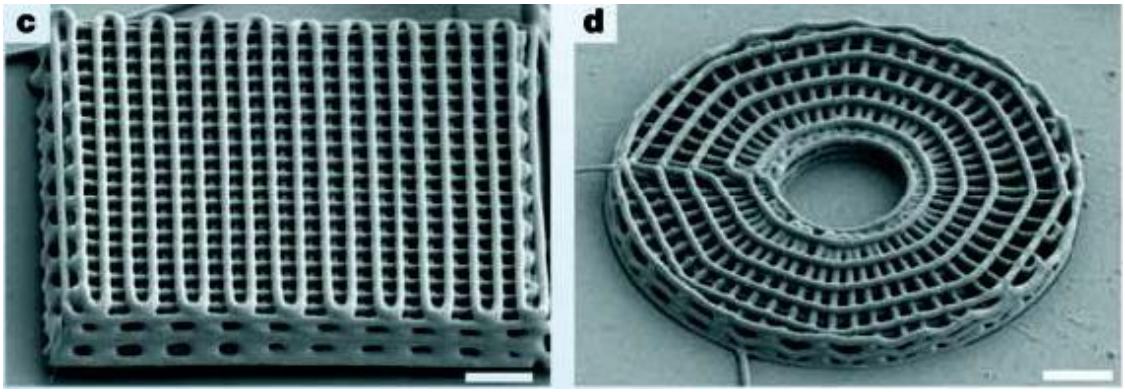

Figure 2.55, Microperiodic structures. 1 micron filament, scale bar 10 micron. Figure by Gratson (2004).

Further to this the deposited filaments also had to set rapidly to avoid filament deflection when spanning gaps, for this purpose Gratson developed fluid inks that could rapidly solidify in a coagulation reservoir into self supporting filaments. The

coagulation mechanism is driven by the electrostatic effect in the alcohol rich coagulation reservoir (83%-88% isopropyl alcohol) and the composition of the deposited polyelectrolyte ink, the elasticity of which rises from 1Pa to 10^5Pa when deposited into the coagulation reservoir(Gratson, Xu & Lewis, 2004).

The literature published by Gratson (2004) makes no reference as to the type of equipment used for this research, however from other related published works (Smay, Cesarano & Lewis, 2002 & Lewis & Gratson, 2004), it has been surmised that the apparatus used was a three axis stage for the positioning of the deposition head and a linear actuator mounted on the Z axis to exert pressure on a syringe containing the ink.

2.9.5 Additive Manufacturing of Hard Tissue Scaffolds

The research published by Yang et al. (2008) describes a method for producing hard tissue scaffolds with biphase calcium phosphate, implementing a filament based extrusion build method using a 3 axis stage and a syringe loaded with the material.

The structures presented feature a graded void hierarchy where the cell size between the filaments and layers is tightly controlled between 0.05mm to 0.5mm to produce dense strong load bearing areas that also promote osteoblast development and open areas intended for vascularisation (Yang, Yang & Chi et al., 2008, p.1802).

The materials used for the scaffolds were hydroxyapatite and β-tricalcium phosphate as they are widely used as biomaterials for bone substitute. The binder was made from a combination of polyvinyl butyral and polyetheline glycol, dissolved in propan-2-ol which was used as the volatile solvent. This was finally mixed with the ceramic blend to form the mixture (Yang, Yang & Chi et al., 2008, p.1803).

The extrusion of the ceramic was done by initially loading a syringe with the mixture; the extrusion force was applied using a high precision linear actuator. Whilst initial tests were done using standard hypodermic needles, the length of these combined with the orthogonal lead in limited the minimum nozzle size to 0.2mm. To reduce this, sapphire water-cut jet nozzles were used, which permitted a minimum opening of 0.08mm to be used. High speed linear motors were used for the X and Y coordinates, the whole system was integrated and controlled using labview and this made it possible to monitor and record extruder pressure. This was of particular importance as

the extrusion pressure needed to be adjusted while depositing to match the acceleration and deceleration of the XY stage to produce a filament with a constant cross section, this was controlled with Equation 2.2 given below, if $V_r < V_{XY}$ then the filament will be stretched, if $V_r > V_{XY}$ then the filament will curl.

$$V_r = \left(\frac{R}{r}\right)^2 V_R$$

Equation 2.4, Vr filament speed, R diameter of plunger, r diameter of nozzle, V_R plunger speed (Yang, Yang & Chi et al., 2008, p.1803).

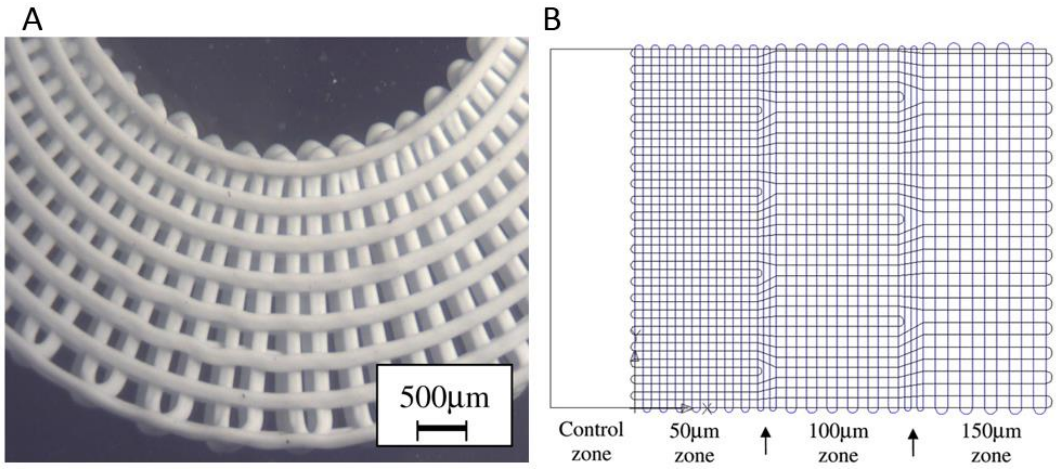

Figure 2.56, A, cylindrical scaffold 0.15mm filament diameter, spiral tool path. B, four zone scaffold tool path. Figure by Yang (2008, p.1805-1806).

The graded void size was based on an arithmetic series to gradually increase the void size in the cylindrical sample (Figure 2.56, A). This sample has two main structures, a set of spokes oriented toward the centre and a spiral tool path that forms the rest of the periodic structure, the distance between the filaments is increased in this spiral to form the graded void size. The second sample produced was rectangular featuring four distinct zones with different void sizes separated by solid zones, control, 0.05mm, 0.1mm, 0.15mm. This sample did not feature any size gradient in between zones, to increase the strength of the sample, the tool path was designed as one continuous movement as can be seen in Figure 2.56, B. This sample was used to test the ideal void size for tissue growth, the control zone was built as a large void to act as control to compare with the deposited structures (Yang, Yang & Chi et al., 2008, p.1806).

Beyond controlling void size of the macro structure, the pore size of the ceramic was controlled by adjusting the sintering parameters of the kiln when firing the samples. Yang (2008, p.1803) also mentions that the porosity of the fired sample could also be

adjusted by changing the ratio of binder to ceramic and by the addition of pore-formers.

2.9.6 Aqueous-Based Extrusion Fabrication

Introduction

Here Mason (2009) demonstrated the development of an aqueous-based extrusion fabrication (ABEF) system including a feedback control system to regulate the extrusion force during deposition. Extrusion was achieved by way of a linear actuator driven by a stepper motor linked to a plunger that applied pressure on a 60 ml reservoir. A load-cell was mounted between the actuator and the plunger. Nozzles measuring from 190 to 580 microns were used (Figure 2.57).

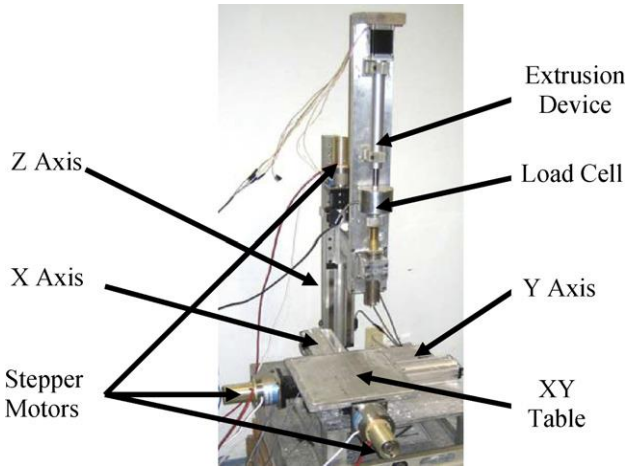

Figure 2.57,ABEF equipment. figure by Mason (2009, p.2947)

ABEF according to Mason is more environmentally safe than other ceramic suspensions used in solid freeform fabrication as it contains less binders (1 to 4 vol%) that would produce toxic fumes during burn-out in a kiln. The burn-out process is also more efficient as there is less material to burn. The slurries are suspended in water at 35 to 40 vol%.

Modelling of ABFE slurries has been done in the past however these only took into consideration a system where the extrusion ram was operated at a constant ram velocity. This, Mason claims is inadequate in order to produce good quality filaments, the extrusion force must be considered and the velocity of the ram adjusted.

In the study both models (ram velocity and extrusion force control) where considered and compared.

Deposition stage

The system built used three orthogonal liner axis (Parker Hannifin Daedal 404 XR) each having 254mm travel, maximum travel speeds of 250mm/s and acceleration of 250mm/s^2.

Extrusion dynamics

The material used in the study was Alumina (Al_2O_3) in concentrations greater than 50 vol%, this was mixed with water, polyetheline-glycol as the extrusion lubricant and Aquazol 50 as the binder. The particle size for the ceramic was in the range of 0.1 to 0.7 micron. The materials were ball milled for 24h to form a uniform paste, however it was not possible to eliminate all agglomerates (particles stuck together) from the mixture.

As the agglomerates reach the nozzle opening pressure is increased as they resist the extrusion force, the slurry continues to compress due to the presence of air bubbles. When the extrusion force reaches a threshold the agglomerates break into smaller agglomerates and allow for the material flow to continue, this is known as agglomerate breakdown.

Air is introduced into the ceramic slurry during the manual loading process, these small air bubbles coalesce near the nozzle forming larger bubbles which then pop when exiting the nozzle. The void left by the exiting air bubble then allows the slurry to expand to fill the void causing a drop in extrusion pressure. This and the formation and consequent break down of agglomerates cannot be predicted.

Model comparison

Mason found that when using a constant ram velocity the extrusion force changed constantly over time, this was demonstrated in a test where lines were deposited onto a surface (Figure 2.58, A), this change in extrusion force resulted in inconsistent track width. In sharp contrast when the same test was run using the extrusion force controller which was set to a constant 0.613kN, the track width was far more consistent (Figure 2.58, B). The method of measuring the extrusion force allows for quick adjustments to be made when agglomerates or air bubbles are encountered thus producing a better quality filament.

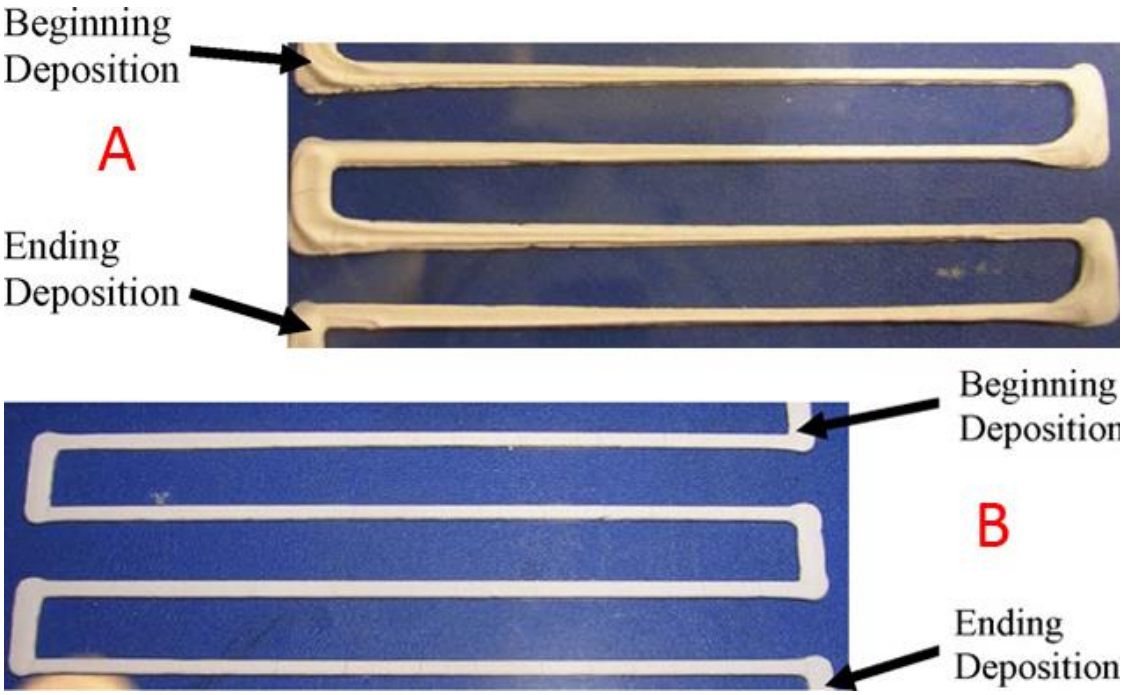

Figure 2.58, Track deposition test. A: constant ram velocity. B:Extrusion force controller. figure by Mason (2009, p.2954)

Another test was run this time with several layers stacked, the results were consistent with the track tests and the sample produced with the extrusion force controller prevailed (Figure 2.59).

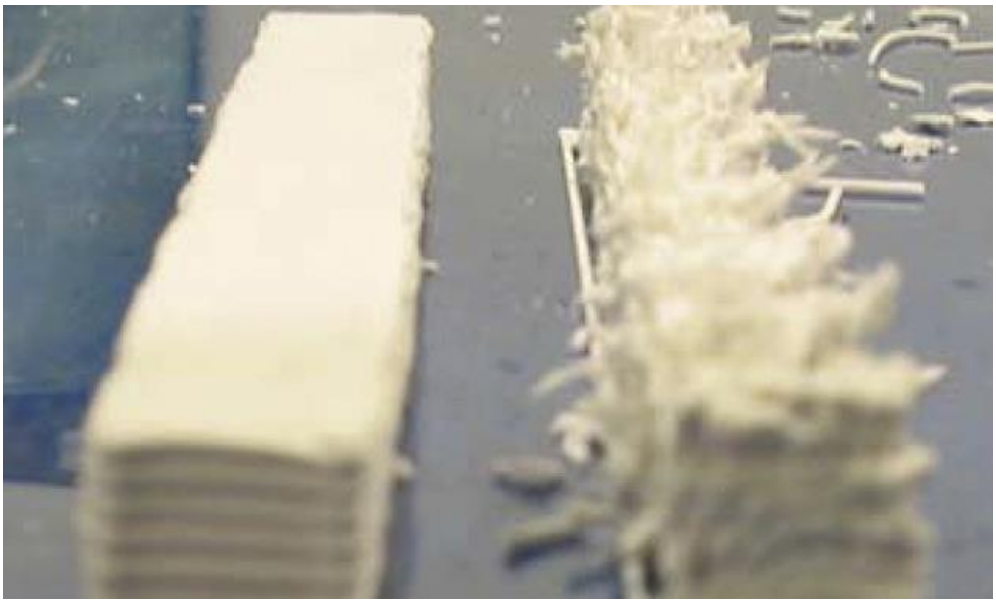

Figure 2.59, Side view of Al_2O_3 bars fabricated using extrusion force controller (left) and constant ram velocity (right, v =2_m/s). Table speed is 19 mm/s, standoff distance is 0.5mm, horizontal line shifts are 0.5mm, and nozzle diameter is 580micron.

The nozzle often clogs if a constant ram velocity is used for an extended period of time, this is due to material drying up along the length of the nozzle reducing the diameter and eventually causing clogging. With the force controller the ram velocity

changes constantly, Mason believes this variation loosens the dry material and prevents clogging.

2.9.7 Process Variables in Solid Freeform Fabrication with Ceramics

Whilst this paper written by Xueson Lu (Lu, Lee & Yang et al., 2009) highlights potential applications for Solid Freeform Fabrication (SFF), in areas such as hard tissue scaffolds and photonic crystals. The main focus of the paper is in deposition parameters and identifying the cause of deposition errors.

Extrusion equipment

The deposition setup used in the research presented in this article is similar to that used by Mason (2009), with an XYZ table and a ram driven syringe for extrusion, a load cell located between the syringe and the ram was used to measure the extrusion pressure.

Material

The materials used were ceramic particulate pastes, several ceramic pastes were used, Alumina (Al_2o_3), $La(Mg_{0.5}, Ti_{0.5})O_3$, TiO_4 and Silica, the binder used was a mixture of poly butyral (PVT) and poly ethylene glycol (PEG) with Porpan-2-ol as the high volatility solvent. The binders where mixed together with the solvent before adding the ceramic powder and dispersing the mix with an ultrasonic prove, after preparation, a paste was made by evaporation of the solvent until the concentration was at 12%.

Build bed level

Typically the layer height maintained for deposition of the ceramic pastes was 2-3 times the filament diameter, the vertical accuracy of the deposition head and the level of the X-Y table strongly influence the quality of the build. If the bed is not level then the deposition head may make contact with the build or the bed, this also limits the size of the build as the bed level angle would produce more drastic changes in height over a long distance. The bed level tolerance for a 38mm x 38mm build with a 0.1mm filament was stated to be 0.15°; however this value would be lower for a larger build or for a finer filament diameter.

Feed-rate and extrudate velocity defects

The feed-rate of the X-Y table must be equal to the extrudate velocity for deposition to be successful, if the extrudate velocity is higher then the filament will not be straight but rather it will form a snaking path due to the surplus material (overfilling), if lower then the filament may be stretched and broken in some areas (underfilling). This issue also means that extruate velocity must be adjusted when the axes decelerate to change direction as this may also cause similar defects.

Equation 2.5 shows the realtionship between the extrudate speed (Vpaste), the extrusion ram velocity (Vram), the syringe barrel diameter (Dbarrel) and the filament diameter (Dext). What the equation shows is that the size of the syringe barrel and nozzle can have a great impact on the build feed-rate that is possible, the ratio between the barrel size and the nozzle, limit the maximum pressure the ram can produce before it stalls, this in turn limits the extrudate velocity and so the feed-rate. For a 100µm nozzle with a barrel of 4mm the X-Y feed-rate must be 8100 time faster than that of the syringe ram.

$$\frac{Vpaste}{Vram} = \left(\frac{Dbarrel}{Dext}\right)^2$$

Equation 2.5, Relationship between extrudate velocity and extrusion ram velocity. Vram is extrusion ram velocity, Vpaste is extrudate velocity, Dbarrel issyringe barrel diameter and Dext is the extrudate diameter. (Lu, Lee & Yang et al., 2009, p.4656)

The equation shown deals with only theoretical values, in practice the extrudate velocity may be affected by agglomerates in the paste or leaking between the walls of the syringe and the piston, these issues may lead to under filling as the X-Y feed-rate would not match the practical extrudate velocity. When this issue occurred in the research it was greatly reduced by using a Teflon piston with tighter tolerances that limited the leaking between the piston and the syringe walls.

Vertical inaccuracy

The research produced square and circular log-pile structures with the ceramic paste, it was stated that the height of the sample did not match the theoretical height as it was lower. This was due to 'slumping' caused by the deformation of the filaments in the areas where they intersect the previous layer; the paste was not rigid enough to prevent deformation.

Die swell

Another issue that may lead to inaccuracies is the die swell that occurs when extruding and disrupts the relationship between ram velocity and extrusion rate.

Die swell causes the filament diameter to increase when exiting the nozzle this occurs because of the elastic strain produced when the paste enters the nozzle, this is released upon exiting causing the filament to swell. This issue may be compensated with a nozzle profile design or limiting the ram velocity.

2.10 Material Extrusion Methods

2.10.1 Introduction

In this chapter several extrusion methods have been mentioned, however the focus has been on additive manufacturing. As demonstrated in the research paper just reviewed, most researchers opt for building the extrusion equipment to suit the specific application. However there are plenty of manufactured solutions that are designed for industrial applications, particularly in the electronics and adhesive dispensing industries. This section will give a brief overview of these.

2.10.2 Valves

Spool valve

Spool valves are used for many industrial applications, more commonly they are used to control pneumatic and hydraulic equipment. However they are also used to extrude materials, the valve has an internal piston called spool; this is moved along the length of the valve and blocks or opens inlets and outlets.

In the Spool valve designed sold by Adhesive dispensing (Adhesivedispensing, 2005, A) there are two inlets, one for air to move the spool and another coming from a pressurised reservoir of material (Adhesivedispensing, 2005, M).

In its natural closed position the spool blocks the inlet of material, and only when air pressure is applied and the spool moved back is the material able to flow out through the outlet port (Figure 2.60).

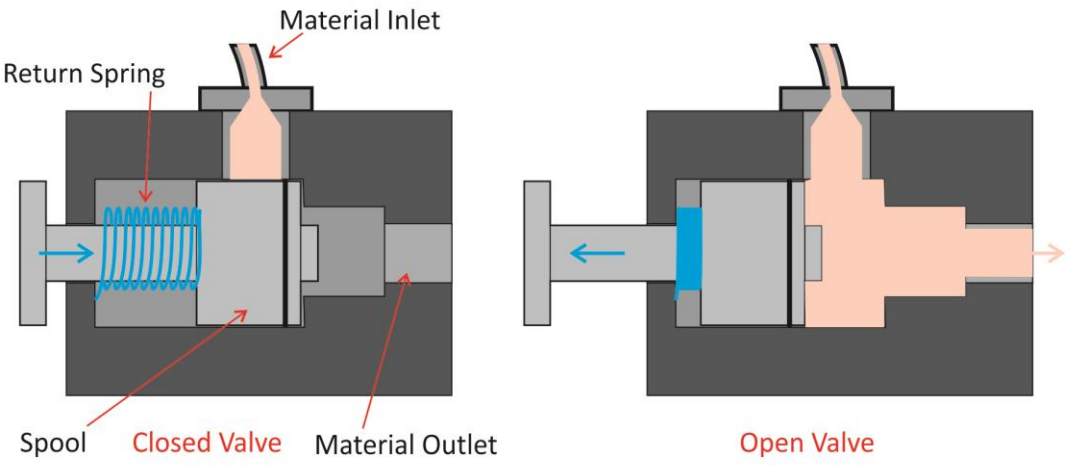

Figure 2.60, Diagram of spool valve. figure by author

Diaphragm valve

The diaphragm valve works in a similar way to the spool valve, but instead of a spool, a diaphragm is pulled back by a piston to allow the material to flow. The flow-rate can be controlled by changing the air pressure that drives the piston (Adhesivedispensing, 2005, B).

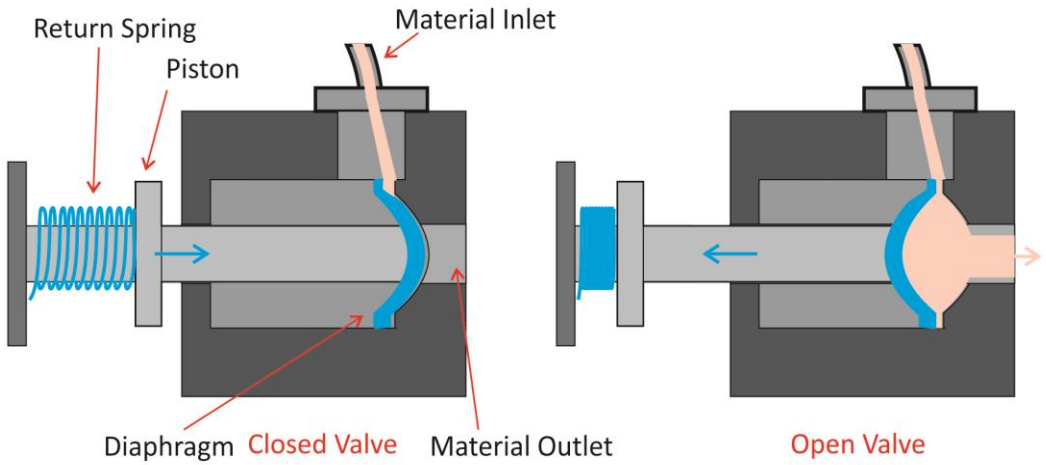

Figure 2.61, Diagram of diaphragm valve. figure by author

Needle valve

The needle valve also works in a similar way to the spool valve, but in this case the spool is replaced with a long tapered needle (Adhesivedispensing, 2005, C). The needle can be exchanged for different sizes to change the material flow rate.

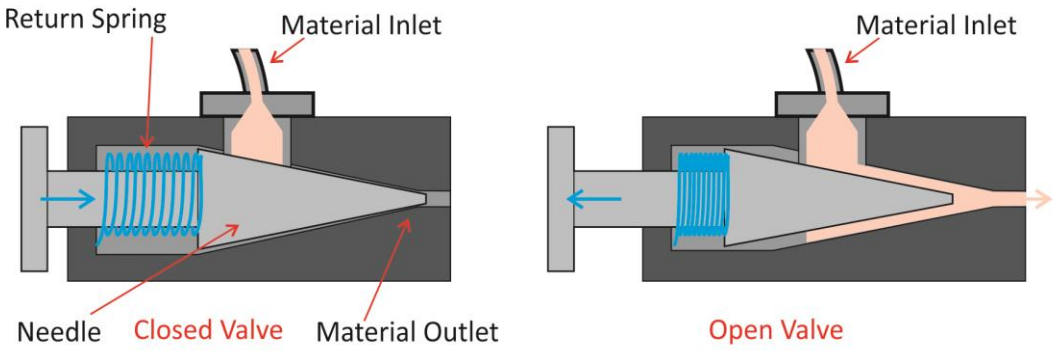

Figure 2.62, Needle valve diagram. figure by author

Auger valve

The auger valve is the same type of extrusion system used by Kristof (unfoldfab, 2012). The valve is fed from a pressurised material reservoir; an auger is used to control the material flow-rate (Adhesivedispensing, 2005, D).

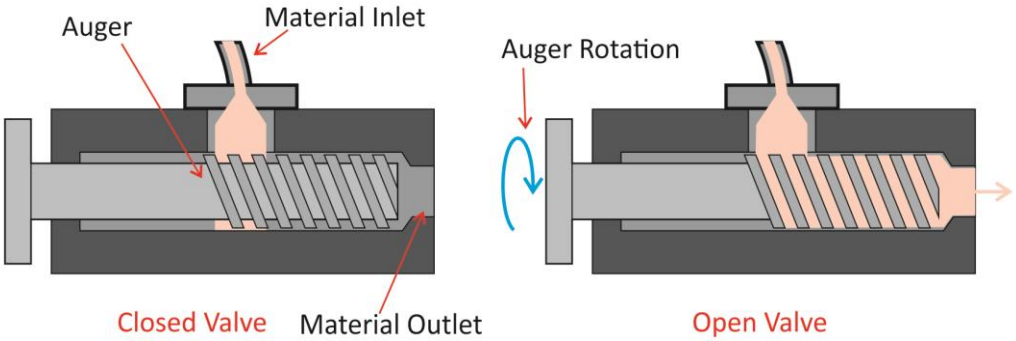

Figure 2.63, Auger valve diagram. figure by author

Pressurised syringe

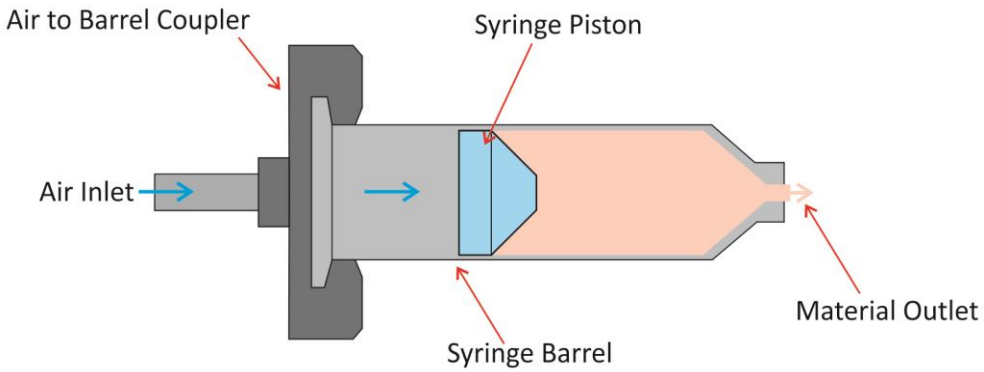

Figure 2.64, Pressurised syringe extruder diagram. figure by author

This type of extrusion is used in the electronics industry to deposit droplets or filaments of glue or solder (Groover, 2011, p.752). Deposition is controlled by

pressurising a syringe barrel with air, this is similar to the method used by Symes (2012), but in this case a stepper motor ram is not used.

2.11 New Design Freedoms

With current commercial AM systems the goal is to achieve near finished products so as to require little to no finishing by hand. The trend in AM system development is towards higher resolutions to eliminate evidence of the process by reducing the layer height (stepping). In doing so however, the opportunity to exploit the stepped quality of the process aesthetically; is lost, without intentional programming. The exploitation of the striation texture can be seen in the digital clock by Brian Podschies (Figure 2.65), where he intentionally exaggerated the stepping texture of the SLA process across the top of the piece to use it as an aesthetic feature; he then used this print as a form to cast in polyurethane which he then electroformed in silver.

Figure 2.65, Electroformed silver clock by Brian Podschies

The approach of leaving the evidence of the process leads to a more honest outcome, this is similar to the digital deconstruction method created by Drummond Masterton (2007), however instead of using additive manufacturing Masterton used subtractive methods; cutting into blocks of material using a CNC mill (Figure 2.66). CNC machining leaves cutting marks and patterns on the surface of the material, in the industry, these are usually polished away. However Masterton focuses on using these as the primary aesthetic feature of his work, he interferes and manipulates the machine code to create patterns and cutting marks that are distinctive to his visual vocabulary.

In doing so Masterton takes greater ownership of the final artefact. By modifying the machine code, decisions made by the machine on how to make the intended part are overridden and manipulated to achieve the desired outcome.

Figure 2.66, 'KOM' by Drummond Masterton (2012).

The question of ownership goes beyond the visual identity of the process, AM technologies such as SLS are able to manufacture objects with great complexity, this brings about new design freedoms that designer-makers did not have in the past. This has sprouted a new form of design using computer algorithms to create objects with complex forms, texture and tessellated macro/micro scale features that conform to parameters set by the designer, allowing the design to evolve and change through parametric changes. Lionel T. Dean (2013) applied such method to the design of a chair named "Holy Ghost" (Figure 2.67).

Figure 2.67, Back rest Holy Ghost chair, by Lionel T. Dean. figure by author

The design process starts with a standard build button (supposed to be reminiscent of button in leather furniture), the number of 'buttons' the chair will have is set up in the parametric program. Then a surface for the 'buttons' is designed; this is where the buttons are placed at random by the parametric software. The buttons then expand in a uniform axisymmetric manner until they cover the designed surface and almost touch. In a manual operation the buttons are connected together by a matrix of curved links that act as live springs allowing the whole structure to flex. This manual process, Dean claims could be automated with further programming.

Another example of this method can be found in the work by Mary Huang and Jenna Fizel from Continuum Fashion (Continuumfashion, 2011). Here the parametric design method was applied to the design of a bikini bra named 'N12', the design featured a complex tessellation of interconnected dots that change in size depending on the position on the contoured geometry; this array was generated using an algorithm. The resulting design was manufactured in an SLA system in nylon 12, the thin interconnections between the dots allowed the whole structure to remain flexible.

Figure 2.68, N12 Bikini by Mary Huang and Jenna Fizel. figure by author

Designer Carrie Dickens (2012) has taken a different approach for a similar result. Dickens created large wearable neckpiece made from small interlocking parts that change in size so the whole piece conforms to the wearer. However here an algorithm was not used, Dickens manually sized and positioned each of the parts to create the design; she created several variations of the "Tactile Neckpiece" with some made with SLS in nylon, silver plated plastic and others made with SLM in titanium as shown in Figure 2.69.

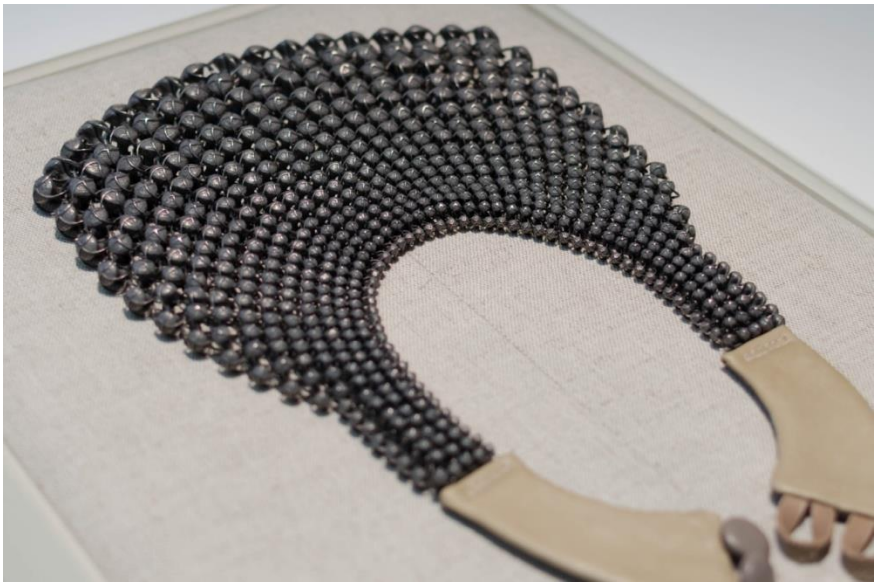

Figure 2.69, Tactile Neckpiece by Carrie Dickens made in titanium with leather clasp. figure by author

This manual process is more in tune with a craft approach, were the designer takes greater responsibility for the outcome of the work undertaken.

The use of algorithm tools where geometry is self generated brings forth a debate of ownership, with software making decisions for the designer not only in the manufacturing stage but also now in the design stage with the creation of self-generated designs. Where is the ownership for the piece? It can be argued that the ownership is in the parameters, the rules from which the design was formed; the ownership perhaps is also in the programming of the piece, a form of digital craft where code is one of the tools.

2.12 Chapter summary

2.12.1 Layer height

The current trend in commercial AM systems is to increase layer height resolution to the point where the striated surface texture is no longer visible and all evidence of the process is eliminated, this is ideal for high resolution meshes and is therefore suited for applications where a high level of geometry fidelity is required. However from a digital craft point of view such high layer resolutions may not be necessary and increase build time. It also limits the spectrum of materials and the creative freedom by working to tight operational windows where the practitioner is confined to a few variables; it shifts making from a process of uncertainty to an almost clinical process of certainty.

Precision, accuracy and resolution are terms often used to describe the capabilities of an AM system and are often considered to be mutually inclusive; you can't have high precision and accuracy without high resolution.

In reality that is not the case; precision is the capability of a particular machine to produce repeatable paths to a practical tolerance, this is in no way connected to accuracy as the machine might turn out consistent results but still produce a part that is over or under the desired dimension in any of the three axes. Resolution is often used to communicate the finest layer height the machine is capable of; the same system may produce layers at 1mm or 10 microns. The effect of this is similar to the bit-rate of an Mp3 compressed music file, there is still high precision and accuracy depending on the equipment used but the fidelity may be lowered (Figure 2.70). Fidelity is perhaps a more relevant measure of the capability of a manufacturing system. It can be used to determine how close the manufactured part is to the original

data, it takes into consideration precision, accuracy and resolution; this is a quantitative assessment. However this is not as clean cut as that, fidelity may also be a comparison between the final outcome and the maker's intent, not necessarily the data used to produce it, this then becomes a qualitative assessment.

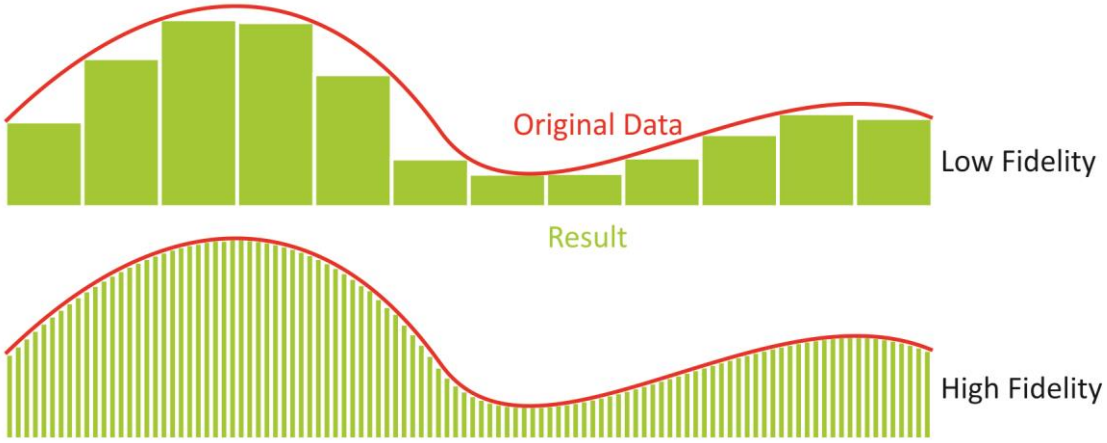

Figure 2.70, Mp3/build fidelity comparison, thick bars indicate thicker layers. figure by author

Given this interpretation of fidelity many practitioners such as Dirk Vander Kooij (Warnier et al., 2014, p.120) and Unfold (unfoldfab, 2012) have designed and made their own systems tailored towards their applications and intent. Others such as Masterton (2007) interfere with the automated code generation process to achieve what an automated *'one-size-fits-all'* solution cannot. The common theme with these practitioners is that they choose to exploit the idiosyncrasies of the manufacturing process and use them as a primary design feature in their work. Whether it is exaggerating the striation texture in an AM part or highlighting the rough cuts in CNC machining.

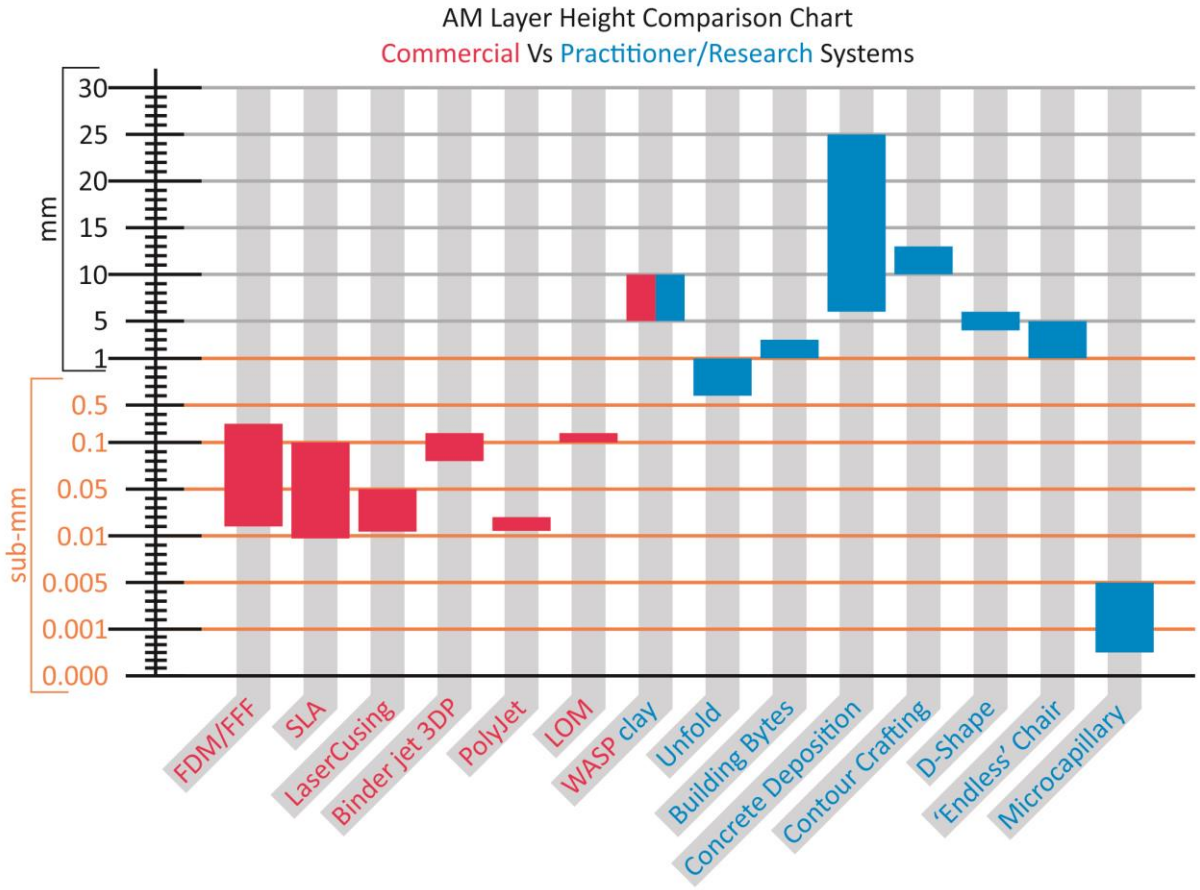

Figure 2.71, Layer height comparison, commercial Vs practitioner/research work, red: commercial, blue: practitioner/research. figure by author

As illustrated in Figure 2.71 , commercial system manufacturers tend to aim for higher resolutions than those used in practitioner and research work. There are a few exceptions such as the WASP Delta which deposits clay in thick layers, however at the time of writing this system was not yet commercialised and was used for research to develop an architectural scale machine so it falls into both commercial and research categories (Figure 2.71, shown in red and blue). Gratson's (2004) Microcapillary deposition system was developed for research into small scale AM; it is by a large margin the system with the thinnest layer height in the chart (0.0005 to 0.005mm).

Layer height is an important selling point for commercial AM systems, the higher the resolution the more intricate the parts it can make and therefore the more interest it attracts, but this is at the expense of build time which is dramatically increased the thinner the layers are made. This becomes a larger obstacle at larger scales, as stated by Carl Bass (2013) just doubling the size of an object, increases the volume by a factor of eight as well as the build time. This penance can be overcome by using a larger layer thickness, the use of thick layers make the build time of large architecture scale parts

practical. To illustrate this point a graph (Figure 2.72) was made showing how the build time was affected by the layer height.

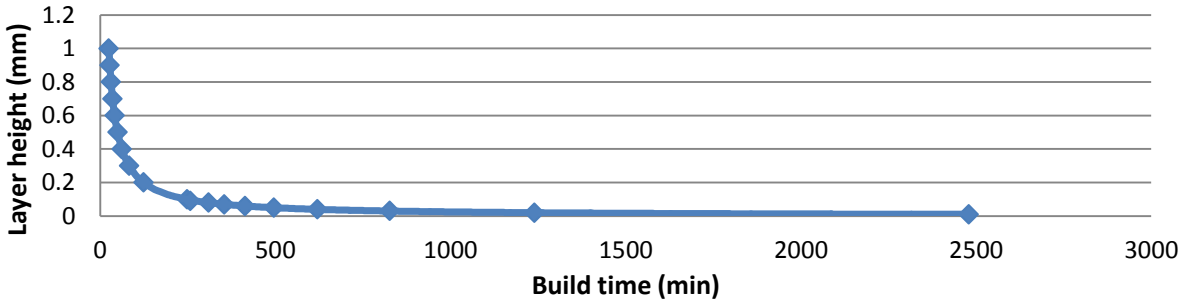

Figure 2.72, Layer height over build time graph, figure by author

The graph was produced from estimated build times using the FDM slicer simplify3D, a 100mm cube was sliced with no infill and one perimeter so the estimated build time was only affected by the layer height. The layer height range was from 0.01mm to 1mm, the feed-rate was kept the same throughout the test.

What these examples show is that build fidelity requirements change depending on the intention of the maker, it also shows that the design parameters of a commercial system are designed as a one size fits all solution and may not necessarily align with the parameters needed by a practitioner or researcher. Under those circumstances the options are to either build a new system from the ground up once the requirements are known, such as that seen in D-shape (Cesaretti et al., 2014), Contour Crafting (Khoshnevis, 2004), etc. Or modify an existing system as done for the Unfold project (unfoldfab, 2012) where an open source FFF system was modified to deposit ceramic.

2.12.2 G-code generation

Most if not all AM systems reviewed in this chapter make use of an automated slicer to generate the G-code required for the machine to produce the desired part. In some cases researchers or practitioners develop their own software or method to fit the requirements of the process, other practitioners such as Masterton choose to subvert this step in the process and manually interfere with the generated code. Achieving a higher degree of control over the tool-paths and thus claiming greater ownership of the outcome and the process. This method may be more time consuming but it is perhaps more akin to traditional craft methods where the responsibility of the outcome lies with the maker and not the automated solution. This practice also allows

for experimentation with parameters that would otherwise not be possible under the operational window designed by the manufacturer.

"Taking advantage of the unique circumstances that the tools can provide, and moving beyond using the tools to simply aid in the speed or ease of production."
(Campbell 2007, p.61)

2.12.3 AM machine architecture

The architecture of an AM machine is defined by the nature of the process and the targeted performance. Manufactures and practitioners go through an iterative process while developing the process to ensure the outcome meets the expectations and performance targets, with each revision the operational window is narrowed down and focused. The design of the machine varies greatly between the different AM processes however there is a common theme; they all work by adding layers of material in three axes to produce the part. There are a few exceptions such as Chen's (2011) five axis system that can produce parts in a layerless SLA like process, or Dirk's (Warnier et al., 2014, p.120) system that makes use of an industrial robot arm to deposit layers of softened plastic.

The arrangement of the axes also varies, even within the same AM process, the axes may be linked in different ways; the Z axis may be independent or linked to either the X or Y axis, or all three may be linked as seen on the Delta configuration used by WASP (Microfabricator, 2014). The axes may be driven by belts, lead screws or linear motors, these variations affect the overall speed, precision and footprint of the machine, the choice to use either depends on the budget of the project or the retail price of the machine and the target tolerances and material. How the axes are arranged depends on the size of the deposition head, the weight of the head, machining loads (if any), target machining tolerances, maintenance accessibility and the overall footprint and look of the final machine. These decisions can only be made once there is an understanding of the process and the performance requirements.

2.12.4 Materials

Current commercial systems use materials that have been specifically manufactured for the operational window of the intended system; these materials are often similar

to 'real' materials used in the manufacture of products but often fall short. The rubber like materials used in the Objet system replicate the flexibility of vulcanised rubber but lack durability, and do not replicate the chemical properties and so are primarily used for prototyping.

Current systems for AM in base metals are prohibitively expensive and are therefore not accessible to most practitioners unless through a service bureau, that level of access does not allow the practitioner to build important tacit knowledge on the process. AM in precious metals was not available at the time the research project started. Bok Yeop Ahn (2010) dealt with deposition of pastes containing titanium powder; the process was specifically designed for the purpose of creating thin 2D meshes that could be formed into various 3D shapes and not directly creating 3D parts. Bok's research was not focused on digital craft but rather on material science.

2.13 Research gap

Review of current literature suggests a gap exists in the materials used for AM, materials in some AM systems get very close to replicating a material used in the manufacture of products, but due to the nature of the process and the operational window the material properties are not fully replicated. It would be advantageous to start with the desired material and adjust the building parameters and machine to make it possible to AM with the chosen material without material re-formulation, this would be of interest as parts could be made with the intended material as opposed to a simulated one.

In order to push AM technology beyond where it is at the moment the limits must be found, to step out of the safety net designed by the manufacturer of a system. There is an element of risk associated with pushing the limits, a build might fail and waste money and time, but this is the nature of developing the tacit knowledge a maker needs to design objects that would otherwise be impossible to make. To develop this deep understanding of a process the maker needs to have direct access to the system to gain practical experience.

AM in metals is not very accessible to practitioners due to the costs involved, a possible solution for this is to reduce the cost of the system, or develop an AM process

in metals where it is less costly. A lower buy in price would be of great importance to practitioners as it would lower the risk of experimentation and push the technology further.

Software used to generate the tool-paths and G-code for AM can be quite limiting, it supplies only a few parameters to the user and leaves other parameters behind closed doors. The direction and shape of a tool-path can have a great impact on the final outcome, as well as how much material is used and where. The user is relegated to using automated tools that make decisions on how to make an object, these are pertinent to optimise build times and machine reliability, but can often subvert features that the maker feels are important - the machine has no understanding of the maker's intent. It is therefore imperative that the user be privy to all the decisions taken on how a part is made.

Surface quality is regularly considered one of the most important aspects of a build; support strategies and part orientation are often used to ensure the surface quality is as high as possible. The infill structure inside the build however is often ignored; in slicers there are different patterns the user can select, however these prioritise material consumption, structural integrity and build time; and so are rarely used in the visual vernacular of the designer. There, exists an opportunity to explore AM where the infill patterns go beyond the existing role and are implemented as elements that can elevate the design aesthetics and functionality of a build.

2.13.1 Research Questions

The research gap section identified a few gaps in the field where novel research in AM can take place; building with materials used in manufacture, exploring the deposition of base and precious metals with the aim of reducing the entry price of metal AM, developing a process where user originated infills and patterns are possible and encouraged.

What these gaps boil down to is a process where the maker intent is at the forefront of making with AM technology, a process where the practitioner can adjust the process to suit the desired outcome, not only in the preparation stage but also whilst the

process is taking place. This information was distilled down to a question aligned with the intent of the project:

Can the AM process be deconstructed so that the practitioner is free to choose how an object is made and experiment with a large range of materials and parameters?

And a few sub-questions:

Can craft methods be applied to AM where the practitioner has Influence and control over all aspects of the manufacturing process?

Is it possible to develop an AM system that can affordably process base and precious metals?

Can 'real' materials be used in AM to produce durable builds that take advantage of the properties of the material? And if so, what applications can arise from it?

Chapter 3 Methodology

"Craft relies on tacit knowledge. Tacit knowledge is acquired through experience and it is the knowledge that enables you to do things as distinct from talking or writing about them."
(Dormer 1997, p.147).

Introduction

For a designer to successfully make full use of a manufacturing process there must be an understanding of the process being used, CNC machines are easy to understand because they are just effectively automated versions of a milling machine, or a lathe. These are tools that most makers and designers have experience in using by hand and therefore some tacit knowledge has already been formed. This makes it easier to understand and therefore design for CNC systems, but when it comes to additive manufacturing there really is no analogous system in the workshop. Therefore it is difficult to form tacit knowledge with that process unless the designer has direct access to the system. This disconnect with the technology is a limiting factor in the exploitation of the process, as the expectations from the designer do not always match the outcome.

The closest manual analogous process to additive manufacturing dates back to Mesopotamia, in Coil pots, they were made by coiling long strands of ceramic to form the pot (Cooper, 1981), the technique was suitable for small vases as well as large ones. This coiling method leaves a striation texture similar to AM parts, as it is indeed a filament deposition process, albeit manual. The artist using this technique has the option of removing the striation created by the coils of clay, or using this texture to create patterns and decorations, using the process characteristics as the main aesthetic feature.

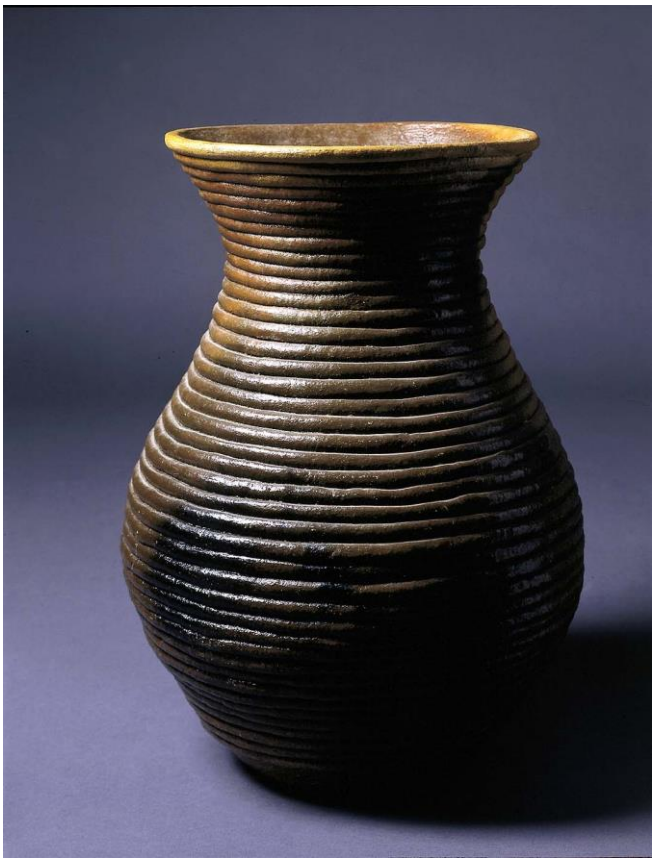

Figure 3.1, Coiled Pot by Louise Goodman ca.1986 (Americanart, n.d.)

The craft process can sometimes mean the devolution of technology. To take back the technology a few steps to explore the process not as a commodity that emulates other manufacturing processes but as a unique process with its own identity. This forms one of the main tenets of this thesis.

The literature exposed some areas where novel research can take place, particularly in the areas of materiality and tool-path generation. Working with a large spectrum of candidate materials and user originated parameters can be difficult, this becomes particularly challenging in complex AM technologies such as SLS or PolyJet and would steer the research towards a material science investigation and thus further from one of the themes of the project.

There is a lack of material diversity In AM as they are developed specifically for the process and as a consequence are limited. However there are examples where practitioners have attempted to overcome this by modifying or developing their own process, such as the work presented by Kristof (unfoldfab, 2012), Dirk Vander Kooij (Warnier et al., 2014, p.120) and several researchers (Cesarano III, King and Denham, 1998; Symes, Kitson & Yan et al., 2012; Cesaretti et al., 2014).

Based on these examples of work, it has been found that the process of filament deposition is perhaps the most commonly used AM method when developing AM for different materials or applications. This is perhaps due to the complex chemistry required in SLA, or the expensive laser systems required for SLS that makes filament deposition a more viable and attractive method for experimentation. As such this project was also developed around the filament deposition process. This allows the project to focus on the craft of making rather than developing and optimising a complex technology - more time can be spent on the process for new materials whilst also developing ideas of form and function for these materials.

3.1 Methodology design

The research design was based on Poggenpohl & Sato's (2003 p.127) Empirical/Experimental model for research in design, it was slightly modified to include case studies in phase 3 (Figure 3.2). The model uses three phases; the first phase uses the literature review to help define the research question, validating it against existing literature. Phase 2 uses trial experiments (or pilot studies) to help refine both the research question and the method in a feed-back loop, it is also used to evaluate the equipment and pose appropriate modifications. Phase 3 uses the experience and information gained from phase 2 to produce a series of case studies implemented as a qualitative validation device.

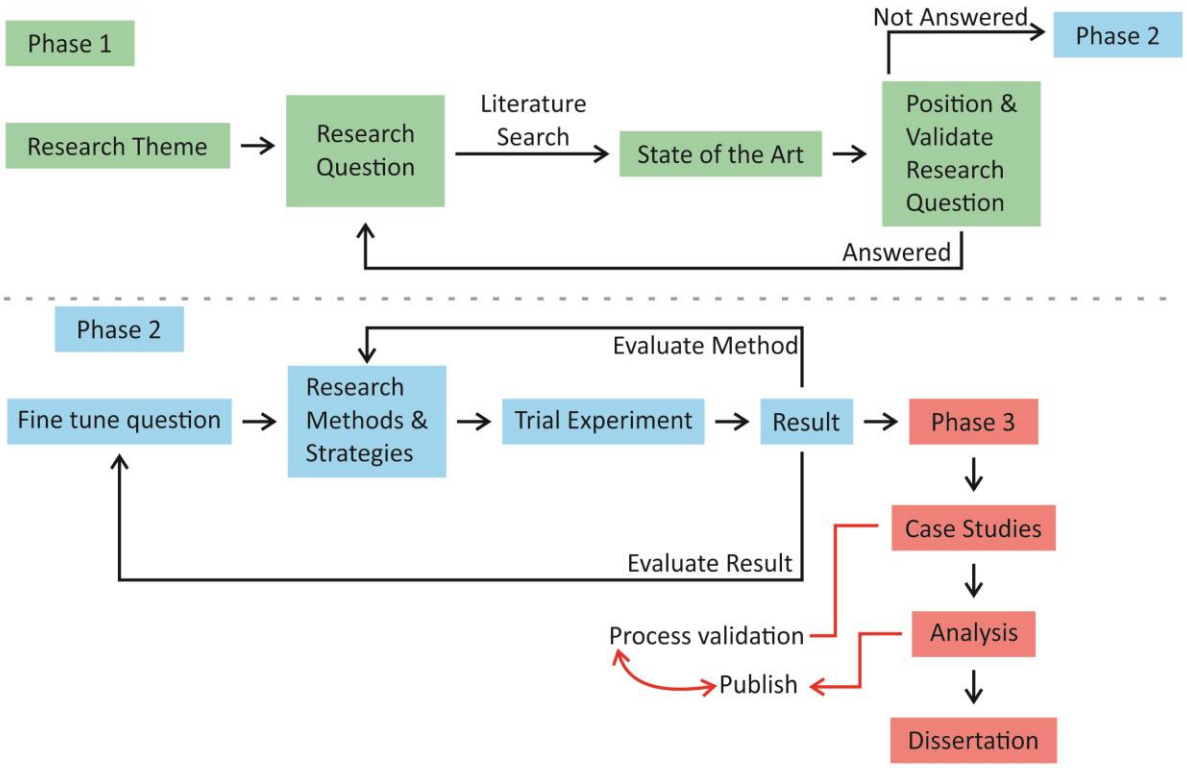

Figure 3.2, Empirical/Experimental model used for the research project, figure by author, based on Poggenpohl & Sato (2003 p.127).

The Empirical/Experimental model works on a feed-back loop, each test with the equipment informs the parameters for the next test. This can lead to changes in the hardware, building parameters, tool-paths or object geometry. This iterative workflow helps create tacit knowledge; which in turn helps focus the operational window for a given material and ultimately lead to more ambitious and complex tests that push the build method further.

Traditional scientific methodologies for process development are based on mathematical modelling and practical quantitative analysis and validation. In some circumstances this model requires statistical analysis of the results, this would have required a large volume of objects to provide a suitable sample size; given the nature of the AM process this would have been impractical. The research aims to answer a very broad question with many variables; the traditional quantitative methodology would not have been suitable to answer this question, as the craft enquiry theme of the research would have been subverted. There is a human element in craft that cannot be quantified.

3.2 Research Equipment

The question of what positioning equipment to use for deposition was difficult to answer. One thing was clear, whatever equipment was chosen had to be open for experimentation; there could not be any firmware issues that could prevent something from being made where the hardware was capable of performing the task. Firmware causes issues because the machine is designed to expect certain conditions, such as the size of the print head, when these change it can lead to unpredictable behaviour. The firmware also expects code generated with the tools provided by the manufacturer, which are designed to work in a tight set of parameters.

Commercial systems had become too focused on the intended applications with automatic tool changers, auto home etc. Features intended to make the system more user-friendly. Modification of such a system would be time consuming and the trade-offs not clear so early in the project, what was needed was to go back a few steps in the development tree of the technology and start from a less focused point (Figure 3.3).

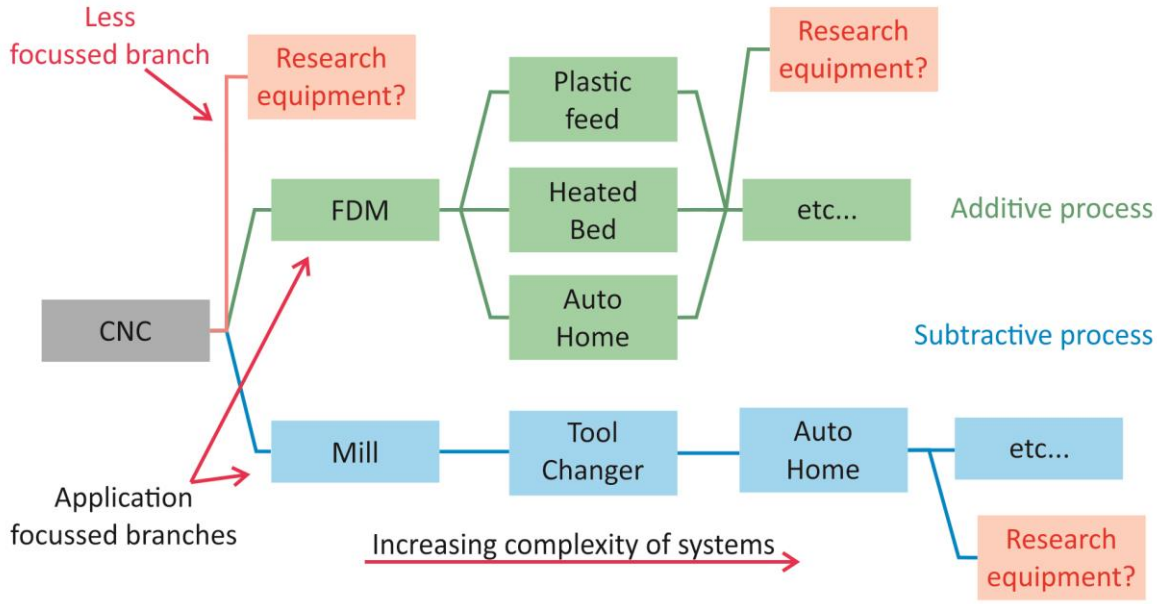

Figure 3.3, Small cross section of AM development tree, started from the positioning technology for CNC. figure by author

There are existing methods for machine design; however these generally require knowledge of machining performance and parameters to then make appropriate assertions on what the architecture of the machine should be and what translation methods to use. One of the main factors to consider when designing a machine is the

cutting forces, as these will stress the frame and lead to inaccuracies or in some cases structural failure. For AM cutting force is not a major consideration as the process is contactless by nature and therefore there is little to no machining force exerted on the frame, the main consideration then is accelerating the tool when moving as it can stress the frame depending on the weight. The other concern is the machine feed-rate and axis acceleration required for successful deposition, knowing these, a decision could be made whether to use lead screws or belt drives so the mechanics can match the performance of the process. However given that one of the aims of the project is to experiment with different materials; the requirements for the process are not known and so an accurate assertion as to what specific machine to use was not possible at the start of the project.

The literature review demonstrated that the process of filament deposition is possible with a large range of positioning equipment, from industrial robots (Warnier et al., 2014, p.120), high precision linear stages (Lewis & Gratson, 2004) to low cost open source FDM printers (Symes, Kitson & Yan et al., 2012).

To narrow down the search for appropriate research equipment a feasibility study was needed, then based on the evaluation of results from this study either the equipment would be modified or new equipment would be selected, this study required a three axis positioning stage

3.2.1 Extrusion method

The feasibility study required extrusion equipment to be selected. The literature revealed several methods for filament deposition used in the industry. The method used in FDM is widely used and extruders are available at a low cost, however this method of extrusion was deemed inappropriate for this research as it would require spools of filament to be manufactured for the intended material before even knowing if the material would work. The spectrum of materials would also be limited to only those that could be softened with heat. These constraints would limit the scope of research.

The method used by Cesarano (1998) for the extrusion of ceramics in RoboCasting while effective in the deposition of high viscosity pastes would require constant

maintenance due to the contact between the material and mechanical elements inside the extrusion head. The simplified form of this extrusion method, such as that developed by Kristof (unfoldfab, 2012) would have similar drawbacks, albeit part replacement and repair would be cheaper than that with Cesarano's equipment.

The methods applied by Hao (2010) and Symes (2012), offered a more viable route and the extrusion equipment in these projects is not in contact with the material and the use of cheap syringe barrels means that if clogging issues arise then replacing the syringe would be simple and cheap. However because the project aims at depositing with a range of materials, the viscosity of the material will not always be known or be under controlled conditions. Therefore the extrusion method of using a linear stepper motor/slide would be at risk of bending or stripping threads if the viscosity of the material is too high, such risk would potentially limit what materials are experimented with.

Methods used in the adhesive dispensing industry, while not designed for 3D deposition could be suitable. As mentioned in the literature review there are several methods currently used in the adhesive industry, most common of which are the high precision valves. However these would have the same issues as using the methods applied by Cesarano and Kristof. There are also simpler systems that use an air solenoid to pressurise a syringe barrel filled with material (Groover, 2011, p.752). The advantage such a system has over all others discussed is that the risk of equipment breakdown is very low. If the viscosity of the material is too high; it will simply not deposit. This type of equipment also makes material change effortless as the syringe barrel can be quickly changed without having to deal with lead screws or any other mechanical parts.

As discussed by Mason (2009) the extrusion of aqueous suspensions is more reliable when a constant force is maintained instead of constant ram velocity, a pressurised extrusion head would provide the closest resemblance to Mason's extrusion method shy of replicating the complex setup. However the main disadvantage is that the pressure is controlled manually and not in software meaning that pressure adjustments cannot be automated. On the other hand the use of a manual system leaves the operator at the helm, taking responsibility of the outcome, one in which

judgement, dexterity and care play a bigger role in the process thus leaving the outcome open to 'happy accidents'.

According to David Pye handwork can be understood as two aspects of workmanship: workmanship of certainty and workmanship of risk. Craft, he argues typically falls into workmanship of risk owing to the uncertainty of the outcome caused by lack of complete control over materials and processes *(Pye, 1995).*

"If I must ascribe a meaning to the word craftsmanship, I shall say as a first approximation that it means simply workmanship using any kind of technique or apparatus, in which the quality of the result is not predetermined, but depends on the judgment, dexterity and care which the maker exercises as he works."
(Pye, 1995, p.20)

The control of the air solenoid is also simpler than the other methods that require hardware controllers and software setup as the air solenoid only requires an on/off. Thus signal making it simple to integrate with the positioning equipment.

The use of the air solenoid is therefore ideal for this research project with the combination of low risk of mechanical break-down and the palette of materials that could be deposited with a syringe based extrusion head making for an unconstrained environment open to experimentation.

3.3 Practical research methods

Due to the iterative development of the machine and the methods, it is not practical to include every method and process used in a small concise section, as the methods changed from the early stages of the project, methods were also developed for specific materials, therefore these methods will be discussed in depth at the relevant sections where they were used. This leads to a rather long hybrid methodology chapter but makes it easier to follow. This concession also helps demonstrate how the experience of the operator allowed the methods to evolve through tacit knowledge, something that would have been complex and difficult to read with a more traditional methodology chapter where the methods are stated and not necessarily how they developed throughout the research.

3.3.1 Build strategy and equipment

The build strategy chosen for the project is filament deposition with pneumatic syringes controlled with an air solenoid. This strategy allows for a large range of materials to be tested as the only prerequisite is that they can pass through a syringe nozzle, properties such as air drying/curing and self supporting make for better candidate materials but are not necessarily imperative.

The material will be deposited using a three axis positioning stage, with the layers parallel to the X and Y axes and the layer height linked to the Z axis.

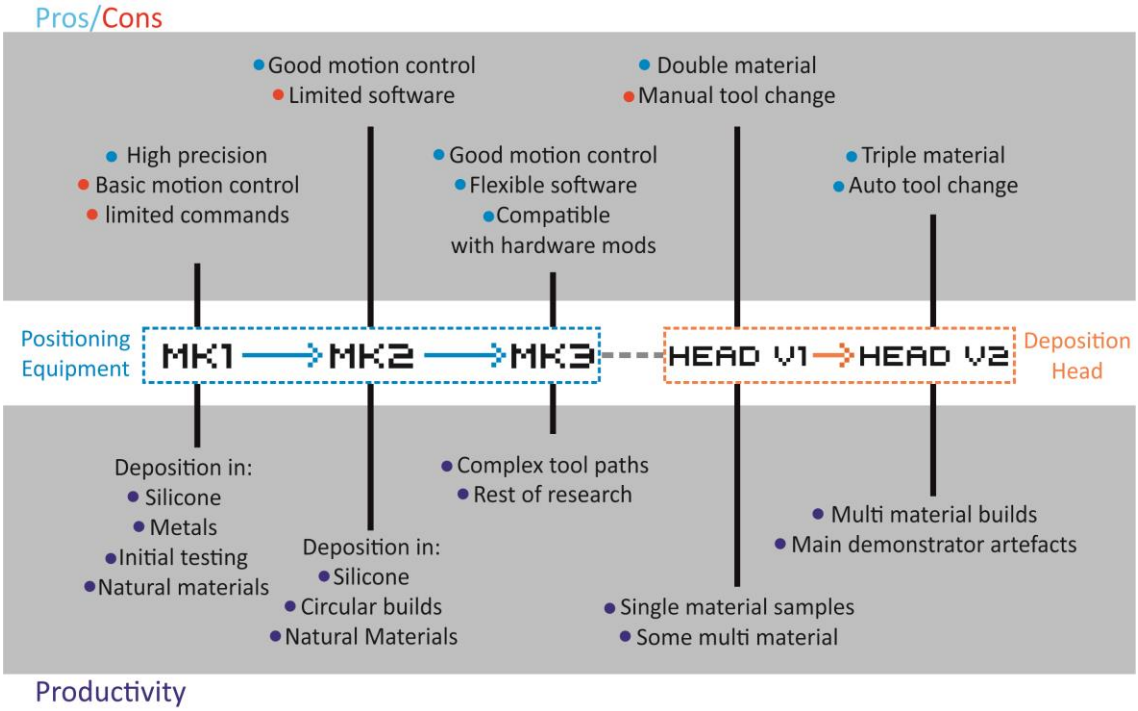

Figure 3.4, Practical research equipment development timeline. figure by author

Figure 3.4 charts the iterative development of the positioning equipment used in the practical research. As progress was made, the requirements for the equipment became more evident. At each key stage where it was deemed that continued research on a particular machine would not yield further results the research was moved to another machine or modifications made that could allow for further development of the process.

3.3.2 Design and programming methods

This section acts as a primer for the main methods used in the design and programming for the artefacts and tests performed, more in-depth information can be

found later in the chapter. These methods were used primarily on the Mk3 iteration of the research equipment (Figure 3.5).

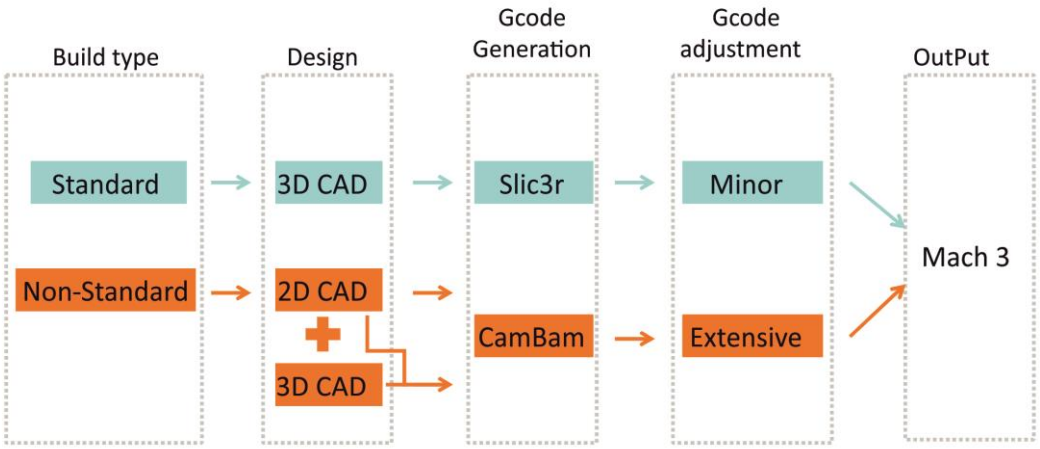

Figure 3.5, Programming methodology flow chart. figure by author

There are two main methods and a third hybrid method:

2D: Here the tool-paths for each layer is drawn in Corel Draw (vector design software), then exported and processed using CNC engraving software; this converts each vector into G-code. The code is then manually modified to include extrusion commands, feed-rates and layer heights for the Mk3.

3D: This method is similar to that used for commercial FDM systems, an open-source slicer (slic3r) is used to generate the G-code from a 3D STL file; the code requires some modification to make it compatible with the Mk3.

2D+3D: This method is an evolution of the 2D method; the main difference is that the 2D vector layers are modified in a 3D environment to produce more complex builds, after the 3D step the layers are processed the same way.

The methods used in the project grew in complexity as the research progressed, however the first few tests were simple and aimed at gaining an understanding of the process dynamics. The next section (3.4 preliminary tests) introduces the extrusion equipment and then shows some tests done to determine if it was an appropriate method, later in the section, the extrusion tests are moved to a three axis positioning stage (Mk1) to test simple 2D deposition.

3.4 Preliminary Tests And Deposition Equipment Development

3.4.1 Rationale

The next sections details a series of tests with different pieces of positioning equipment to establish what equipment is needed for research and a framework for how to work with the equipment. Since the point of the project is to reduce constraints designed into the process, it is reasonable to start at the point of designing and building a new machine with fewer constraints. The literature review has documented the wide variety of equipment used in filament deposition ranging from high precision linear stages (Yang, Yang & Chi et al., 2008) to low cost open source FDM machines (Symes, Kitson & Yan et al., 2012). The methodology of how the equipment is used changes depending on the equipment; therefore it is imperative to gain tacit knowledge with different types of machines to evaluate the appropriate components to use for the exploration proposed. Information gained during these tests informed the development of the design of the machine and of the functional parameters used in later stages of research.

3.4.2 Extrusion Feasibility Trials

Extrusion equipment

As discussed the extrusion method is by way of a pneumatic syringe actuated by an air solenoid, the equipment is comprised of several components; air solenoid, syringe barrel air hose, syringe barrel and piston heads (Figure 3.6).

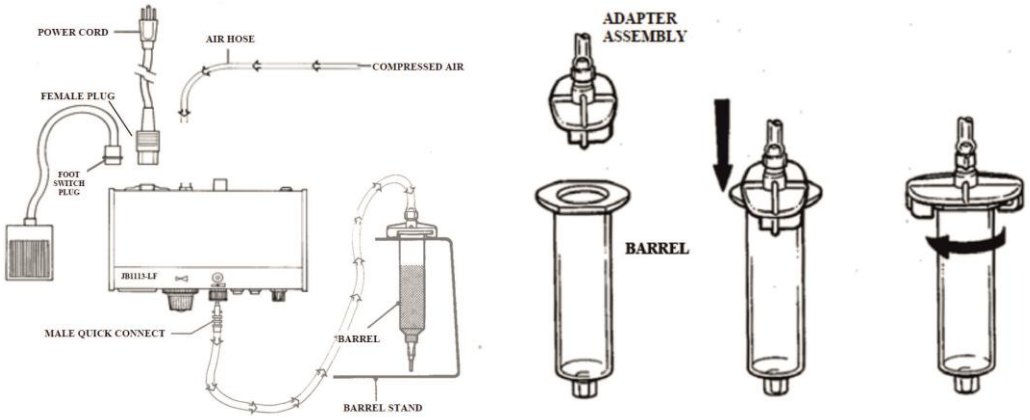

Figure 3.6, Air solenoid assembly diagram and barrel adaptor fitting. figure scanned from user manual. (Fisnar, 2009)

Air solenoid

The specific model used was the JBE1113-LF manufactured by Fisnar (2009). As supplied the air solenoid is controlled with a foot pedal but this is removable to allow for other triggering methods and the maximum air input/output possible is 7 bar with output pressure being adjustable via an inbuilt air regulator.

Syringe barrel air hose

The syringe barrels are connected to the air solenoid via an adaptor hose, which latches onto the air solenoid with a quick release fitting whilst the other end locks onto the syringe barrel with a bayonet style fitting (Figure 3.6). This fitting is manufactured in different sizes to accommodate the volume of the syringe barrel (Adhesivedispensing, 2005, F).

Syringe barrel

Syringe barrels for the air solenoid are sold in several different volume capacities, the internal diameter (ID) of the barrels changes depending on the capacity. The barrel used for these trials was 30cc, with an ID of 22.63mm, sold in packs of 20 and up to 1000 (Adhesivedispensing, 2005, G).

Syringe piston

Pistons are made from different materials and are designed for specific material viscosities, the pistons used in this study were:

Straight walled for high viscosity (Adhesivedispensing, 2005, H).

Wiper piston for low to medium viscosity (Adhesivedispensing, 2005, I).

Pistons are manufactured to different sizes; the size used in this study was selected to match the 30cc syringe barrel.

Syringe nozzle

The Air solenoid was supplied with a range of deposition nozzles, for these tests a blunt 0.6mm nozzle was used (Adhesivedispensing, 2005, J).

Selecting the material

The material used for this trial was a Silicone dioxide ceramic powder combined with a thick nozzle dispensing medium (NDM) called JM0001 manufactured by Johnson Matthey, this is a gel composed of 95% water and 5% solid material (see Appendix A). The thick gel was designed for use in ink suspensions and its use in this study was suggested by Dr. Richard Bateman as a starting point for ceramic suspensions.

Mixing method

The two materials were mixed at a proportion of 20 grams of silicon dioxide to 11 grams of NDM in a three roll mill; this proportion was arrived at empirically by combining the materials in different proportions until the desired consistency was reached, this proportion was designated B007. The resulting paste having a composition of a large solid content, water and a small amount of binder and lubrication agents is similar to that used by Mason (2008).

The three roll mill mixes materials with shear force as they are fed into the two counter rotating rolls. When the mix is ready the apron roll is moved closer to the centre roll and the gathering knife is positioned. This then transfers the viscous mix from the centre roll to the apron roll which is in turn gathered by the knife.

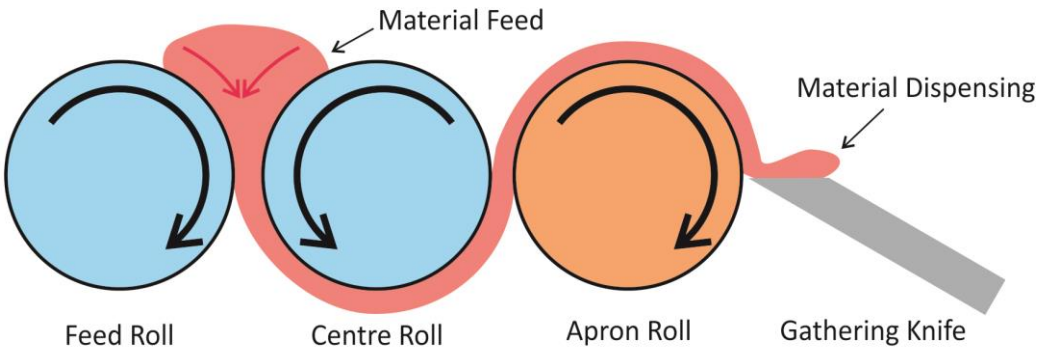

Figure 3.7, Diagram of three roll mill. figure by author

This material was chosen for these trials as it was identified in the literature review that ceramic colloids are among the most challenging materials to deposit. It was therefore advantageous at the initial stages of the project to understand the dynamics of depositing such materials.

The plasticity of the colloid affects the material flow rate at a given pressure. If the material is pseudo-plastic the increase in flow rate will be proportional to the increase in extrusion pressure. This relationship was demonstrated in colloid deposition by Cesarano (1998, p.698), however if the material is non-Newtonian, increasing the pressure will not increase the material flow rate proportionally.

Syringe loading method

Initially the ceramic paste was loaded directly into the syringe barrel with a narrow palette knife. This method introduced a substantial amount of air into the paste, so much so that tests could not be run. This method was modified to loading the paste into a loading syringe barrel which was then coupled to the deposition syringe with a female to female luer-lok adaptor (Adhesivedispensing, 2005, K), the deposition syringe barrel was then loaded from the front, this ensure that the large air bubbles were dissipated into the paste. This method was based on an established method used in the adhesive dispensing industry, where syringe barrels are loaded from the front using large material reservoirs (Adhesivedispensing, 2005, L).

Extrusions trials

To determine the flow rate of the material the deposition was timed at two minutes at various pressures intervals increased by 5psi each time. The material deposited in that time was then weighed, each measurement was repeated three times. [The results of this trial are shown in Table 3.1]. A gauge 20 (0.6mm) blunt end needle was used for this trial.

Pressure (psi)	*Weight deposited (gm)*	*Average (gm)*	*Flow rate (gm/min)*
30	*0.26, 0.25, 0.27*	*0.260*	*0.130*
35	*0.31, 0.24, 0.31*	*0.315*	*0.156*
40	*0.38, 0.4, 0.38*	*0.380*	*0.190*
45	*0.39,0.34,0.38*	*0.385*	*0.193*
50	*0.39, 0.38 0.35*	*0.385*	*0.193*
55	*0.36, 0.62, 0.58*	*0.600*	*0.30*
60	*0.61, 0.61, 0.6*	*0.600*	*0.30*
65	*0.69, 0.69, 0.63*	*0.670*	*0.335*
70	*0.78, 0.85, 0.86*	*0.830*	*0.415*

Table 3.1, deposition rate trial 1 of B007 ceramic mix. table by author.

The data obtained from this experiment was very inconsistent. The numbers highlighted in red were measurements that were too low when compared to the other

measurements under the same conditions. These experimental errors could be due to agglomerate break down, also the nozzle clogged on several occasions. It is likely that this was caused by dry material gathering at the end of the nozzle between tests, this resulted in the deposition rate falling and eventually stopping. As such these measurements had to be omitted from the average.

Based on the difficulties encountered during this trial another trial had to be run. The ceramic B007 was mixed more thoroughly to reduce the number of agglomerates in the paste and the pressure intervals were also reduced to 2psi providing more data points. Also the duration of the deposition was increased to 10 minutes to allow lower pressures to produce a measurable result.

To decrease the chances of material drying at the tip of the nozzle the deposition was left running between sampling runs at a low pressure to keep fresh material on the nozzle tip. The results of this trial are on Table 3.2.

Pressure (psi)	*Average weight (gm)*	*Time (min)*	*Flow rate (gm/min)*
10	*0.04*	*10*	*0.004*
12	*0.086*	*10*	*0.0086*
14	*0.0133*	*10*	*0.0133*
16	*0.25*	*10*	*0.025*
18	*0.337*	*10*	*0.0337*
20	*0.407*	*10*	*0.0407*
22	*0.550*	*10*	*0.055*
24	*0.26*	*5*	*0.052*
26	*0.350*	*5*	*0.069*
28	*0.356*	*5*	*0.071*
30	*0.617*	*5*	*0.123*
32	*0.687*	*5*	*0.137*
34	*0.38*	*2.5*	*0.152*
36	*0.43*	*2.5*	*0.172*
38	*0.463*	*2.5*	*0.185*

Table 3.2, deposition rate trial 2 of B007 ceramic mix. table by author.

The consistency of the results was improved, but not by much as some results still show a large difference within the same conditions. This could be due to inconsistencies brought forward due to the need to refill the barrel with more paste. Also due to agglomerates in the paste or even dry fragments of B007 ending up in the barrel. Nonetheless the trend of the results is very similar to that of the first trial but only for the first few data points.

This trial was run a third time but with one further improvement to the mixing method, the paste was first mixed with a homogenizer (RW-20) and then milled with the three roll mill. The temperature of the lab was also monitored and recorded at the time of each measurement.

These improvements to the mixing method yielded far more regular results, the trend was consistent with the previous tests, suggesting that the viscosity and plasticity of the material were similar and the measurements across each repetition were far more consistent, giving a better average to work from. The results were tabulated (Table 3.3) and a graph produced comparing all three trials (Figure 3.8).

Pressure (psi)	*Average weight (gm)*	*Time (min)*	*Flow rate (gm/min)*	*Ambient temperature °C*
10	*0.01*	*10*	*0.001*	*12.7*
12	*0.053*	*10*	*0.0053*	*12.6*
14	*0.127*	*10*	*0.0127*	*13.7*
16	*0.227*	*10*	*0.0227*	*16.4*
18	*0.313*	*10*	*0.0313*	*16.7*
20	*0.260*	*7*	*0.0371*	*16.5*
22	*0.233*	*5*	*0.0466*	*16.7*
24	*0.306*	*5*	*0.0612*	*16.7*
26	*0.403*	*5*	*0.0806*	*17.1*
28	*0.237*	*2.5*	*0.0948*	*16.9*
30	*0.273*	*2.5*	*0.1092*	*16.7*
32	*0.227*	*2*	*0.1135*	*16.9*
34	*0.307*	*2*	*0.1535*	*16.9*
36	*0.353*	*2*	*0.1765*	*16.7*
38	*0.360*	*2*	*0.180*	*16.9*
40	*0.390*	*2*	*0.195*	*17.1*
42	*0.227*	*1*	*0.227*	*17.0*
44	*0.257*	*1*	*0.257*	*17.0*
46	*0.273*	*1*	*0.273*	*17.3*

Table 3.3, deposition rate trial 3 of B007 ceramic mix. table by author.

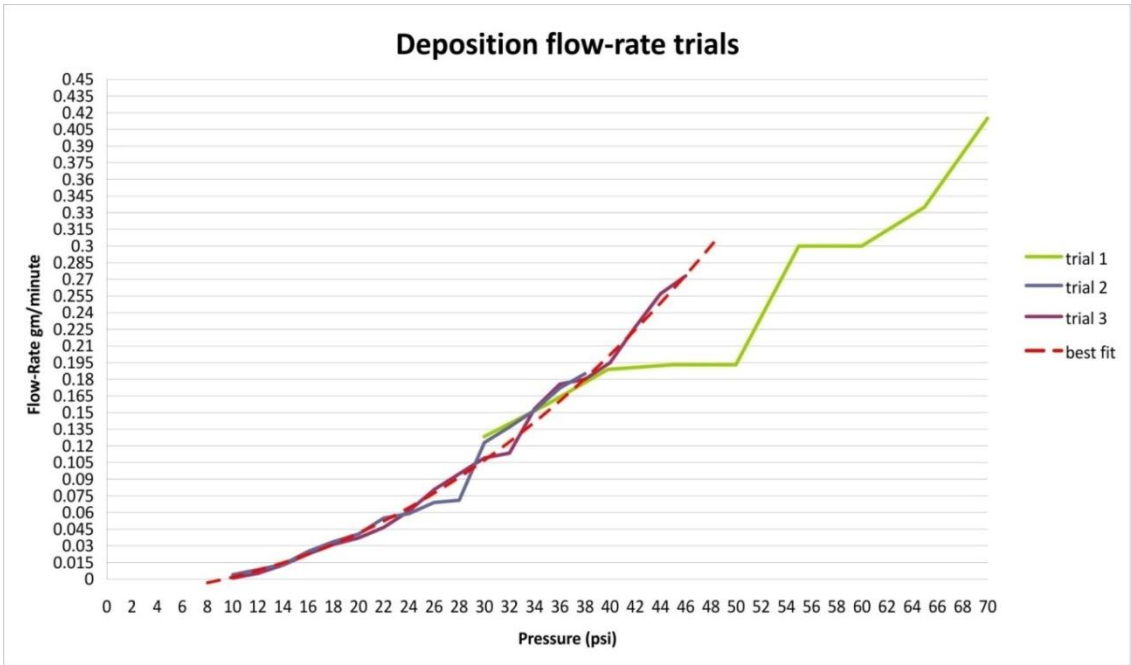

Figure 3.8, graph deposition rate (gm/m) against pressure (psi). graph by author.

The results from these trials show that deposition of a material with a high solid content is possible with this equipment, but the tests also highlighted the issue of material drying on the nozzle causing clogs.

3.4.3 2D Deposition Trials

Introduction

This new experiment was aimed at testing the deposition of the B007 ceramic material onto a substrate to form straight lines of material. In order to accomplish this; the barrel and nozzle were mounted onto a clamp-stand and placed over a high precision X-Y stage. The stage comprised two PI M-410.dg linear slides, the slides being capable of feed rates up to 1.5mm/s and a repeatability of 0.1 microns (Physikinstrumente, 2008).

Equipment

Motion control is a complex topic and hardware is usually customised for a specific combination of hardware and software. For these trials it was decided that the controllers bundled with the slides would be used; then if the slides prove effective a more comprehensive solution would be developed.

The model of the controllers used was C-860.10, manufactured by PI. Each controller is only capable of driving one stage so each slide required its own controller. The controllers are then daisy chained together and connected to a computer terminal via a serial port interface. Configuration of parameters such as feed-rate, acceleration, soft-limits and origin were setup via a purpose built terminal program designed by PI which communicates with the controllers (Figure 3.9).

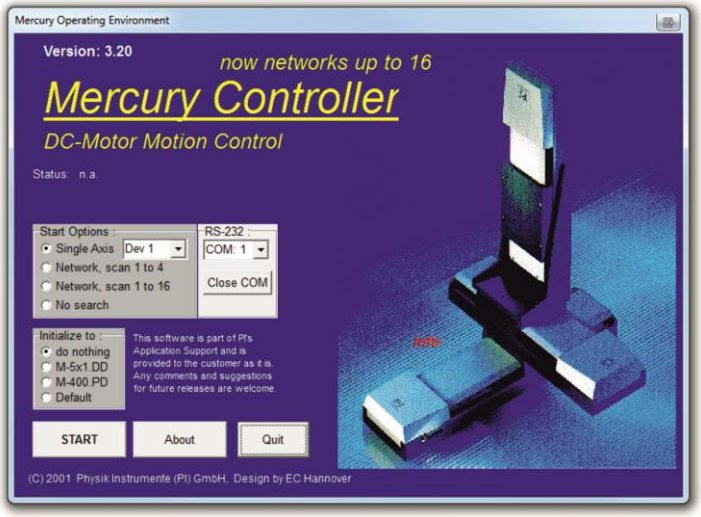

Figure 3.9, Screenshot PI slides controller software. figure by author

The positioning of the stage was also controlled via the terminal program. It is important to note that the serial interface only allowed one command to be sent to a single slide, so each slide needed to be addressed in turn. The coordinate commands sent to the slides were in the form of positive or negative steps and not in standard units of measurement and the resolution of the slides was 118,400 steps/mm. Commands such as MA5000 would move the selected axis 5000 steps in absolute coordinates (relative to the origin) or the command MR5000 would move the axis 5000 steps in relative coordinates (relative to the current position).

The limited interface with the motion controllers meant that deposition with this equipment was rather labour intensive with individual coordinates needing to be sent to each axis. This simplistic manner of working also meant that deposition could be studied in a closely controlled environment without any quirks or unknowns that would be brought on by using more complex motion control software/hardware.

Deposition pressure trials

The purpose of this test was to determine the effect of deposition pressure over deposited line quality. The same B007 mixture and nozzle size (0.6mm) as the previous test were used in order to estimate the material flow rate by using the results from the last test. The feed-rate was kept constant throughout the test at 1mm/s.

For the line deposition test it was imperative to find a suitable substrate so that the quality of the line was only affected by the extrusion pressure. Several materials were tested for this purpose; high density polyurethane foam, latex, grease paper, steel and Teflon. The ceramic adhered with varying degrees of success to all materials except Teflon; however the high density polyurethane foam performed the best, probably due to the porous surface (Figure 3.10).

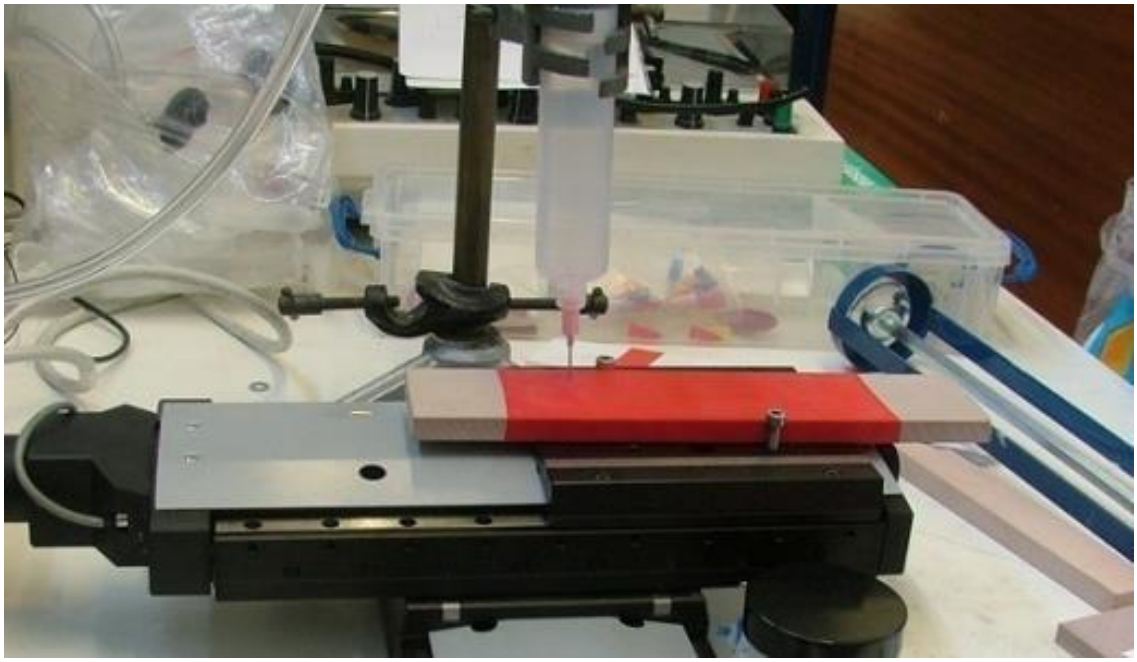

Figure 3.10, equipment used for the line deposition trial, 2 x Pi-M-410.dg slides in X-Y configuration, latex substrate (red) in picture. figure by author

The first trial was performed at pressures of 21, 25, 30, 35 PSI; Figure 3.11 shows the results from the trial. As can be observed the filament at 21 PSI appears to be the best as it is closest to the original size of the nozzle. The quality of the filament shows that the material is neither being pulled by the stage nor accumulating at the nozzle, thus the material flow rate matched the feed-rate, a concern of great importance as discussed by Yang (2008). At higher pressures the filament became engorged and the deposited material started to overtake the nozzle.

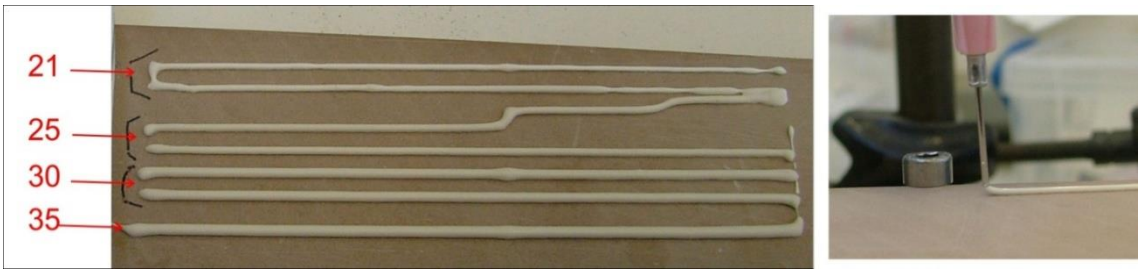

Figure 3.11, filament line deposition trial 1, pressures from 20 to 35 psi (left), profile view of the filament being deposited as 21 psi (right). figure by author.

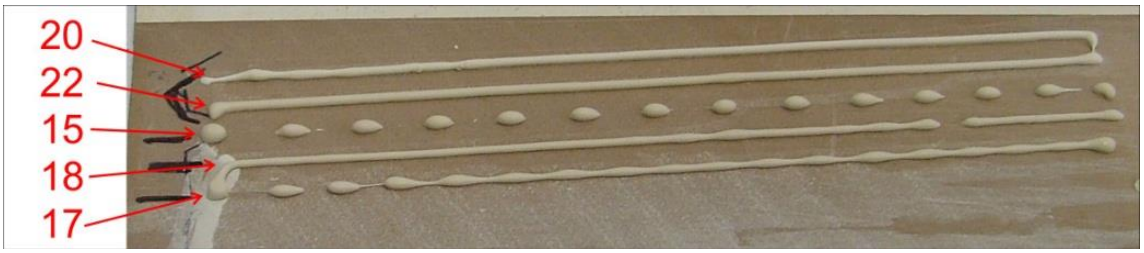

Figure 3.12, filament line deposition trial 2, pressures from 15 to 22 psi. figure by author

The lowest pressure tested in the first line deposition trial was found to be in the operational window for successful deposition. As a result the trial was run again with pressures below the operational window to observe how the line quality was affected at lower pressures.

For this second trial the pressure was first tested at 20psi and then at 22psi to compare with the first trial and observe how the quality was affected by small changes in the extrusion pressure. It was found that these small changes had only a small effect on the line, with the line at 22 psi showing a marginal improvement in quality. This test determined that the operational window for this material was 21 +/- 1 psi at a feed-rate of 1mm/s which coincides with 0.04 grams per minute. The original plan for this trial was to then decrease the pressure from 20psi down to 10psi in 5psi steps. However the line at 15psi (Figure 3.12) produced a series of dots suggesting that the extrusion pressure was well below the operational window and lowering the pressure would only exacerbate the effect and not yield any new information, so the line test was performed at 17 and 18psi. These lines showed signs of dotting similar to that seen at 15psi where the filament was stretched over the substrate leaving small accumulations of material.

Summary of 2D deposition trials

During the substrate tests the drying behaviour of the ceramic mix was also observed and it was found that B007 shrank a small amount owing to the water content

evaporating. For most substrates tested this caused the deposited filament to crack as the filament adhesion to the substrate was too strong to allow the filament to release as it dried. However it was possible to release the filament fragments from the substrate once ceramic was dry. The grease paper substrate was flexible enough to allow the filament to shrink without breaking but the dry material did not release. This would probably not be an issue as in the event that the ceramic is eventually fired the paper would burnout anyway.

Further work could have been done on the formulation of the ceramic colloid to improve the green strength in order to alleviate this cracking issue. The viscosity would also need to be increased to allow for consecutive layers to be built up. However owing to the complexity in the chemistry of ceramic pastes it was decided at this point that developing the project down this ceramic materials route would probably distract from the creative exploration of the deposition process.

During the flow-rate trials an important point was raised; these tests were very wasteful. The trial was useful in helping to understand the relationships between deposition pressure and material flow-rate for the given material, for example, if the material is shear thickening or shear thinning or if it could be extruded. Nonetheless it was not particularly helpful in determining the operational window for deposition and this test was deemed too wasteful for the information gained and subsequently removed from the methodology of later tests.

The filament deposition trial was however useful and helped determine operational windows quickly and with minimal amount of waste and this method was streamlined in later tests. Instead of producing long lines and slowly incrementing the pressure after each line it was deemed that this process could be made faster by starting deposition at a low pressure and increasing the pressure gradually as the filament was being deposited until the operational window was found, then a further line deposited to confirm the finding. As mentioned earlier in the line deposition trial the operational window is large enough so as to not require high precision when setting the extrusion pressure.

3.4.4 3D Deposition of Silicone Periodic Structures

Introduction, Mk1 equipment

The following test was designed to determine operational window for the deposition of 3D objects, the periodic structures designed featuring a periodic configuration were intended to test the deposition of consecutive layers while keeping the complexity of the geometry relatively simple. The same equipment as the previous tests was used save for with a few additions:

- A third slide of the same model was added for the Z axis.
- The syringe clamp was mounted onto a small manual slide with a digital readout to allow fine tuning of the Z height; this in turn was fixed onto the Z axis with a laser cut acrylic plate.
- An acrylic frame and plate were mounted onto the X-Y stage and a build plate, made of steel, was placed inside the frame so that the substrates could held in place on the build plate with neodymium magnets. The acrylic frame was designed to locate the build plate to exactly the same place every time, thus allowing several build plates to be prepared and exchanged when needed and also for builds to be set aside to dry or cure without risking damage to the build or delaying the next trial. Because of the low force or non-contact nature of this process the plates do not need to be bolted or clamped down.
- The XYZ stage was mounted on a 25mm thick aluminium plate and bolted to a steel T-slot table and the whole machine placed inside a cabinet to keep dust out.

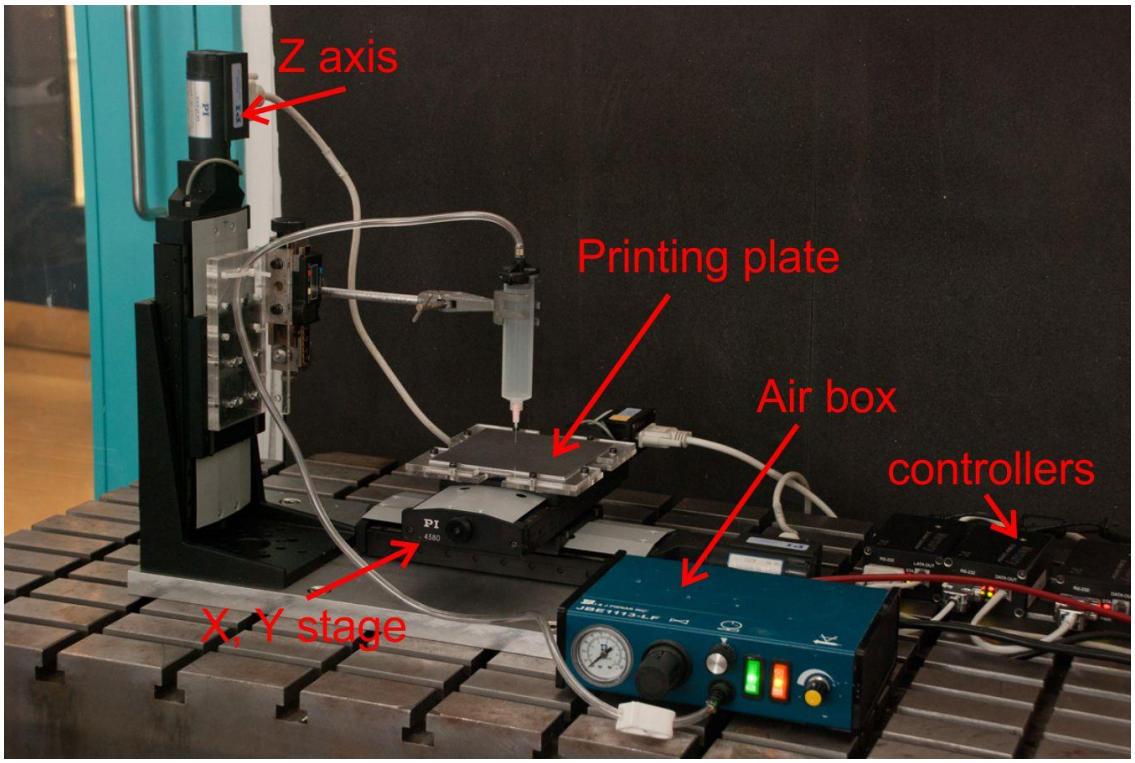

Figure 3.13, second iteration of the deposition equipment. figure by author

With these modifications the equipment was now suitable for 3D deposition and was designated as Mk1, the setup can be seen in Figure 3.13.

Deposition of the test structures

To successfully print complex shapes and geometries a baseline must be established; i.e. a set of parameters and methods that can be used to develop a tool path for the desired build.

A basic tool path was developed, consisting of a periodic structure of layers of material of evenly spaced filaments, each layer being rotated 90° to the layer to produce a 'cross grain' (i.e. log-pile, periodic) structure.

For preliminary testing this structure has several merits. Due to its simplicity, changes between parameters or any problems that arise during deposition are evident as the structure is composed of straight lines. Problems and uncertainties that might arise from complex tool paths such as curves and angles are eliminated and the deposition in its basic form can be observed and improved upon.

The spacing between the filaments reduces deposition time and at the same time allows the bonds between the layers of material to be observed.

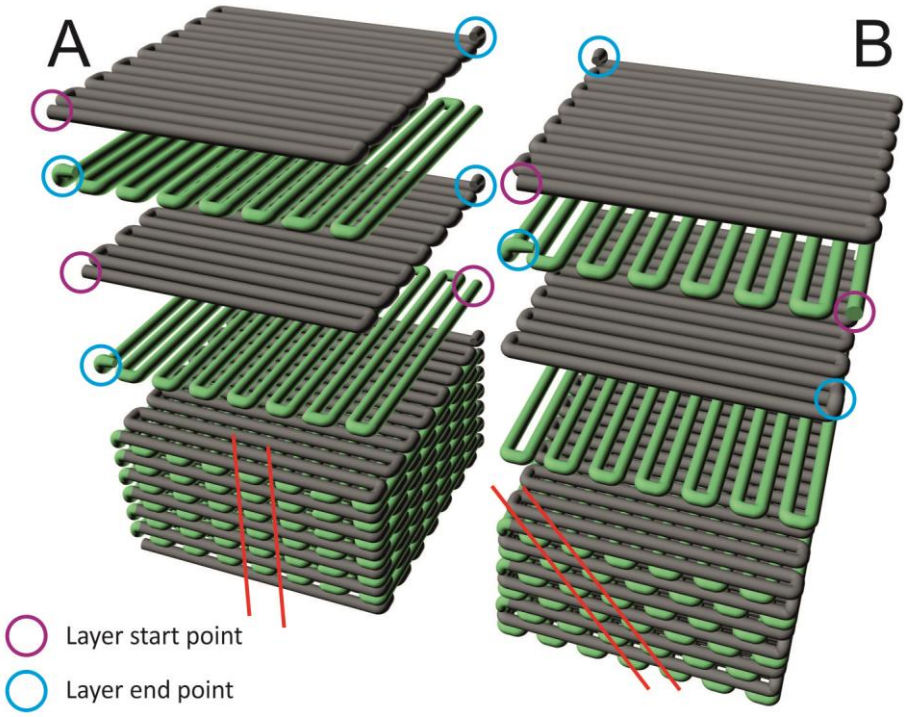

Figure 3.14, periodic tool path, left linear pattern, right diagonal pattern. Direction noted by the red lines. layer start point indicated in purple, layer end points indicated in blue. figure by author

The periodic structure is repetitive and as such, patterns are expected to occur. It was observed while designing the structure that depending on the number of filaments the structure developed either a linear pattern (Figure 3.14 A) or a diagonal pattern (Figure 3.14 B) along the perimeter. This is due to there being either an even number of filaments per layer which would produce a diagonal pattern or an odd number of filaments which would produce a linear pattern. It is important to note that these patterns only form when the end X and Y coordinates of the previous layer are the same as the start of the next layer, this strategy also decreases build time as there is no build air-time when positioning the nozzle for the next layer.

The patterns also repeat at different layer numbers, the linear pattern with odd number of filaments per layer repeats every two layers where as the diagonal pattern with the even number of filaments repeats every four layers, where the end point of the previous layer is the same as the start point of the new layer.

While CAD models of the structure were produced, these were only used to help plan the experiment. How the equipment is used has not changed and each axis is instructed in turn as described earlier in the ceramic line trials section. The size of the builds produced in the following trials and other parameters such as layer height will on occasion have small decimal non- whole numbers. This is because the slides are

controlled in steps and not in a standard unit of measurement and during the trials numbers that were easy to repeat were used: 100,000 or 80,000 or 50,000 steps (0.42mm). This is one example of how the idiosyncrasies in software forces the user to adapt to the environment and has an unexpected influence on the outcome.

Material choice

Unlike previous tests with the equipment, during these experiments the ceramic mix B007 was not used.

Instead the material chosen for these tests was Acetoxy silicone (caulk), a clear material of the type used for sealing sanitary ware (Dow Corning 785). This material was chosen as it was designed for extrusion through nozzles and meant that issues that arise during deposition would not be due to improper material formulation, mixing or variations between batches but rather directly linked to the operational parameters, such as nozzle size, feed-rate, extrusion pressure and deposition height.

The first periodic structures

The plan for this build was to build a 23.6 x 23.6mm x 13 layers periodic structure with a 1.7mm pitch between filaments using the same 0.6mm blunt end needle used in the previous tests.

To build the layers the axes are controlled individually and addressed in turn, this means that once a single line is completed the deposition is stopped; the next axis is addressed and sent the new coordinates and the deposition is resumed again until the axis completes the instruction. The deposition is only triggered when the axis are moving, because addressing the axis takes time and if the deposition was not stopped every corner would have a large accumulation of material.

The diagram (Figure 3.15, A) is a visual representation of the points (red) where the deposition is stopped the next axis is addressed and deposition resumed.

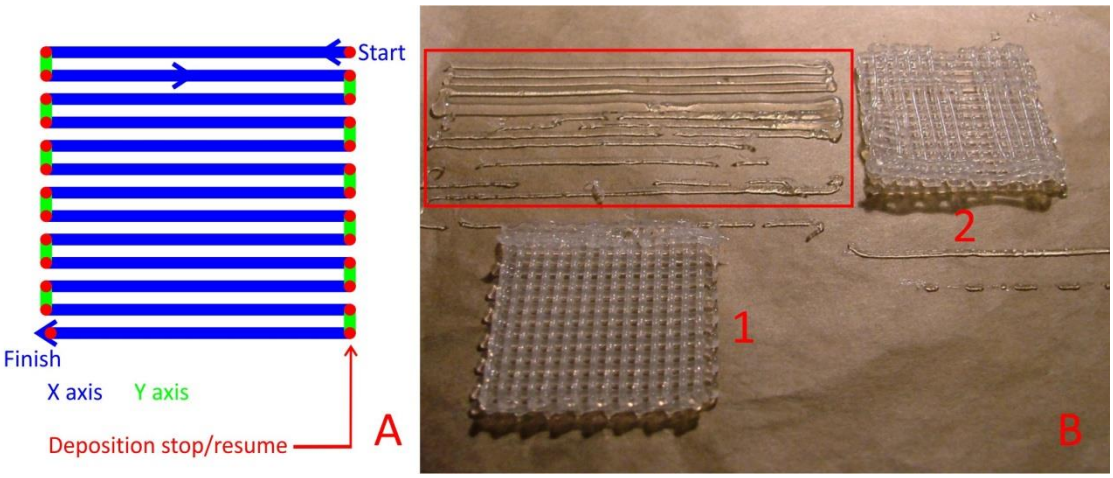

Figure 3.15, A: periodic structure tool path for one layer. B: first attempts at building in 3D, red rectangle calibration filaments, B1: tree layer periodic structure, failure from clogged nozzle. B2: failed build due to clogged nozzle. 23.6mm^2 deposited at 2bar with 0.6mm blunt needle. figure by author

The feed-rate was set at 1mm/s. The height of the nozzle was set at 1mm and the same 0.6mm blunt end nozzle as the earlier ceramic tests was used. Several lines were deposited onto the grease paper substrate and the pressure was adjusted to find the ideal extrusion pressure, which was found to be 2bar.

Some more test lines were deposited to ensure that 2bar was indeed the correct pressure, and during this the nozzle clogged with cured silicone (Figure 3.15, B red rectangle). After the nozzle was replaced, the deposition of the periodic structure was re-started. The build failed after three successful layers were deposited; again from a clogged nozzle (Figure 3.15 B1).

The build was reattempted after replacing the nozzle; this build failed again with issues at the first, second and third layer. Figure 3.15 B2 shows the results of the second build attempt.

Upon inspecting the clogged nozzle it was discovered that the silicone compound was curing inside the luer-lok hub producing a mass of silicone that blocked the nozzle, as opposed to small dry fragments of material blocking the cannula as originally thought. This would suggest a faster drying time than that specified by the manufacturer and under conditions where the silicone was not exposed to air. It is believed that the silicone was suddenly agglomerating under pressure with the shallow lead in from the hub to the cannula of the blunt end needle probably being a contributing factor in this issue. This is a similar issue to that faced by Yang (2008) where the length and lead-in angle of the hypodermic needles he was using for depositing ceramic were the major

contributing factors that limited the diameter of needle that could be used. This problem was solved by using nozzles specifically designed for high viscosity fluids.

Figure 3.16, Tapered Nozzle, 0.6mm. figure by author

To solve this clogging issue, tapered nozzles were sourced (Figure 3.16). This type has a longer transition taper making it more suitable for high viscosity applications; it is also made from a single material so there are no seams or joints leading to a smooth flow of material.

The build was attempted again with the same parameters as the two previews builds, except for the pressure which was found to be ideal at 1 bar with the new 0.6mm tapered nozzle. This build was completed successfully at 13 layers; the only issue encountered was an air bubble that momentarily interrupted deposition but this did not compromise the build (Figure 3.17).

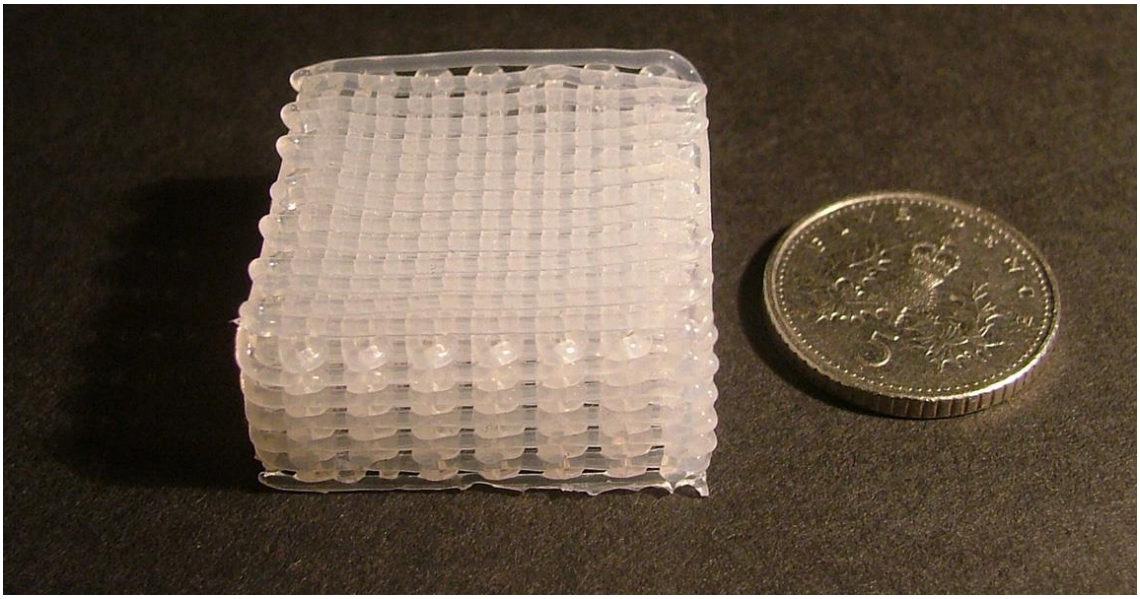

Figure 3.17, silicone periodic structure, deposited at 1bar with 0.6mm tapered nozzle, 23.6mm^2 x 13 layers, 5p coin for scale. figure by author

This build provided some very valuable information namely that the silicone was found to be viscous enough to be self-supporting. As a result it does not need time between layers to let the material cure and harden, at least at this scale.

The grease paper was not suitable as a substrate; the silicone could not be separated without assistance. The build had to be soaked in water for one hour to release it from the grease paper substrate.

The structure shows some interesting mechanical properties, when a force was applied at 45° (corner to corner) the structure hinged on the inter layer filament bonds and the whole structure was able to collapse (Figure 3.18) however when a force was applied at 90° the tendency of the structure was to buckle under the load. When a compressive force was applied along the Z axis the structure compressed with no apparent buckling.

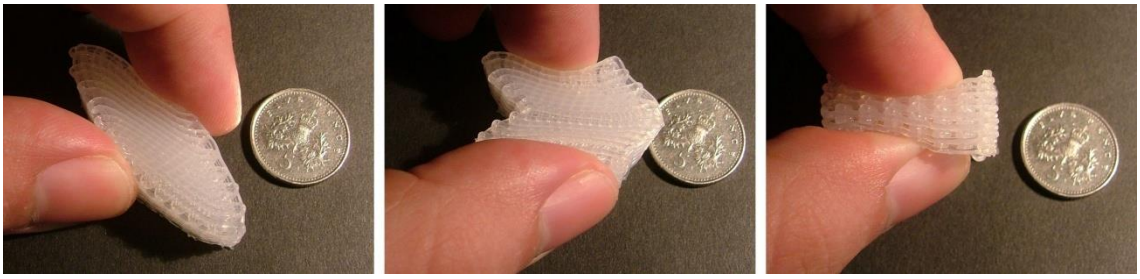

Figure 3.18, 23.6mm^2 x 13 layer build, behaviour when compressed at 45°(left) , 90° (middle) and along the Z axis. figure by author

This was noted as a very promising structure with interesting properties, and deemed worthy of further study at some later date.

Deposition of with small diameter nozzles

The previous build highlighted the need for an alternative substrate so two candidate materials were tested, a silicone sheet and a Teflon sheet. The silicone sheet was not suitable as the acetoxy silicone simply welded itself to the sheet. However the Teflon sheet bonded well to the wet silicone but once cured the silicone peeled off, thus making the Teflon sheet an ideal substrate for this material.

The previous build also indicated that some form of recording and viewing equipment was required to help with the building process. A digital microscope was installed on the Z axis. This made it possible to photograph and record the deposition as well as view the deposition from a better vantage point.

The test demonstrated that it is possible to build a three dimensional object with the silicone material, so new trials were planned building on what was learned but using a finer nozzle of 0.2mm ID.

While trying to set the correct extrusion pressure for the 1mm/s feed-rate it was noticed that the deposition height also played a major role in the successful deposition of the filament, deposit too high and the filament will coil onto the nozzle and not adhere to the substrate.

The height was set at 0.338mm, this provided a good quality line but it also broke up or failed to adhere to the substrate at unpredictable moments, almost as if there was grease on the substrate, however the parameters seemed to work well in some areas of the substrate so a build was set up, which had an vertical and horizontal dimensions of 25.34mm with a filament pitch of 0.76mm and the pressure set to 1.5bar.

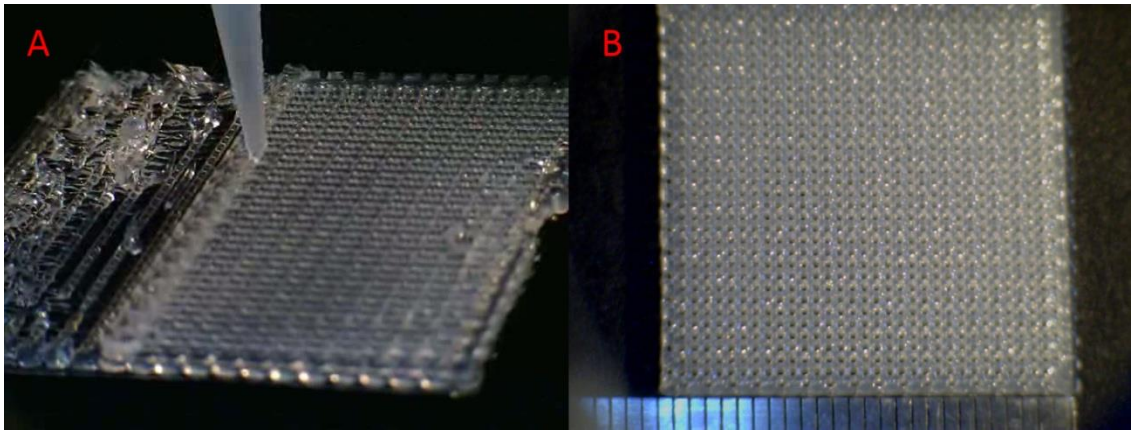

Figure 3.19, silicone periodic builds with 0.2mm nozzle . A:partial failure of build. B: completed build at ten layers. figure by author

This build partially failed but only in 1/3 of the build footprint, where the filaments failed to adhere properly to the substrate, this area was too damaged to deposit consecutive layers on top so the build was continued for ten layers on the area that did deposit properly (Figure 3.19, A).

During deposition the filaments did break up at several points on the top layer so to alleviate the problem the layer height was decreased during deposition to 0.25mm and this seemed to solve the problem.

It was determined from this build that the nozzle height had to be close to the filament diameter in order to deposit properly-this figure of 0.25mm is very close to the actual diameter of the filament which is 0.203mm.

This build was repeated with the same parameters and the new nozzle height and this attempt was successful. The layers were almost flawless, however there was one instance of the nozzle clogging up, this was replaced and the build resumed. It was virtually impossible to reset the nozzle to the exact same point where the build stopped so the structure was slightly offset to one side (Figure 3.19, B).

This particular structure stands at a height of 2.5mm and is almost like a textile due to the size of the filament. It was expected that the build would be very fragile because of the small bonds and the thin filaments, however it was completely the opposite with the structure being very resilient to handling.

Another build was planned with the same parameters as the textile build but with the intention of building a structure with a higher aspect ratio. However at 20 minutes per layer making a tall structure would have taken a long time so the size was reduced to 10 x 10mm with a pitch of 0.71mm this reduced the layer build time to eight minutes.

The first attempts at this build failed on three different occasions due to filaments breaking and being dragged across the layer, this usually occurring in the second layer and leading to large accumulations of silicone (Figure 3.20). These defects were considered large enough to compromise the build and therefore no more successive layers were deposited and the build was repeated in a different area of the substrate.

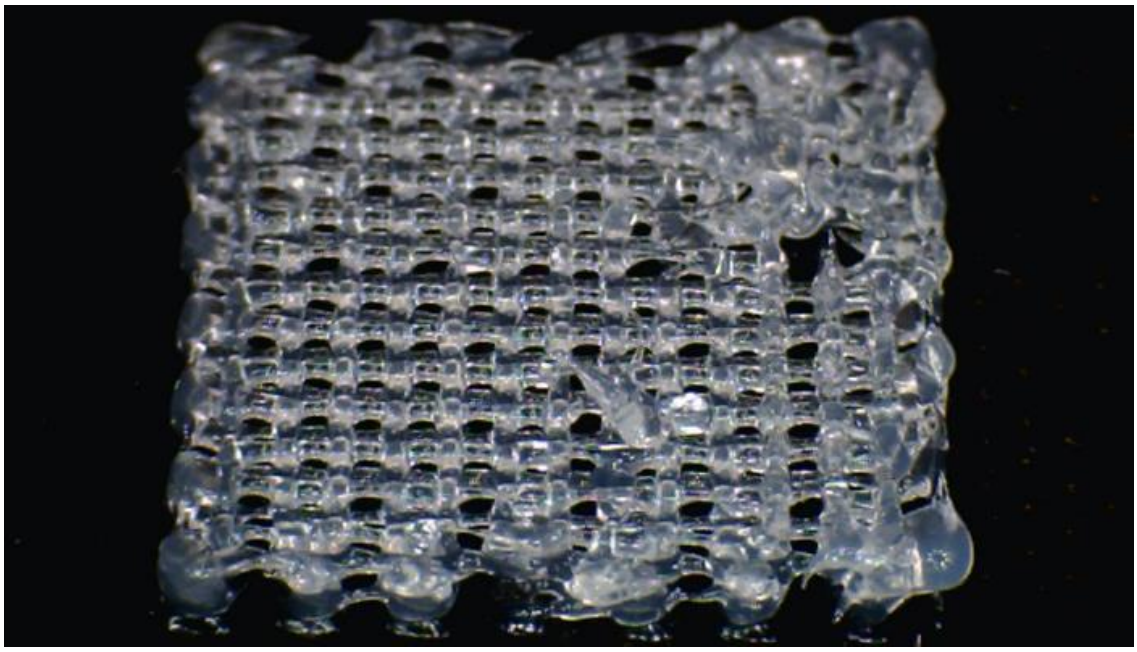

Figure 3.20, failed 10mm^2 periodic build, 0.2mm nozzle. failed at the second layer. figure by author

Although the trial was eventually successful and was completed at 8.2mm in height, the build was not free of defects. Filament break-up developed but was localised to the perimeter of the build, particularly in the areas where the deposition was stopped and restarted at the ends of the filaments. These areas are shown in red Figure 3.15, A. The perimeter filament break-up was cumulative and once this happened the damage was irreversible and consecutive layers amplified the damage spreading it deeper towards the centre of the build.

This issue could be partially due to human error, the timing of deposition was critical when starting or finishing a filament line. At this stage the timing still manual, this occasionally led to the accumulation of material or its lack at the perimeter of the build. These flaws most likely led to the perimeter filament break-up issue discussed.

The images (Figure 3.21) show the end result; the filament break-up did not occur at the first few layers but rather later in the build as the small defects accumulated.

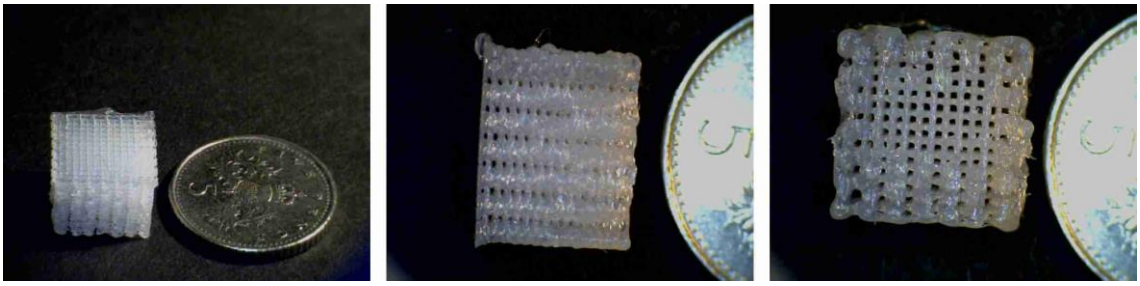

Figure 3.21, the 10 x 10mm x 8.2mm structure, the filament damage at the edges is evident in the figure to the right.5p coin for scale. figure by author

Deposition With 0.4mm Nozzle

At this stage it was not clear why the initial layers were failing so often so to shed some light on this question another build was planned. This time with a 0.4mm nozzle; it was believed that the larger nozzle would make inspection of the defects easier to see and would help to diagnose both the second layer issues as well as the perimeter break-up.

With this trial, the method for determining layer height was modified. With the nozzle at a height just over the diameter of the filament, several lines were deposited. The pressure was then tuned until a good quality filament was deposited, then with the pressure tuned the height was lowered to zero and the height was increased in small increments until the filament stopped adhering to the substrate. The height was lowered again in small increments while still depositing until the filament started to adhere to the substrate.

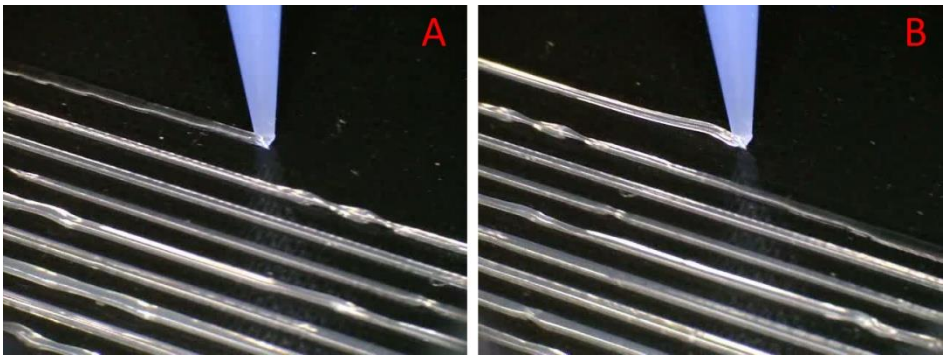

Figure 3.22, 0.4mm nozzle, layer height calibration tests. Right: deposition is too low. Left: deposition is too high. figure by author

This method provided a range of heights where the filament could be deposited onto the substrate. The figure shows the deposition of the filament at a low height (Figure 3.22 A) and the filament coiling onto the nozzle when it was too high (Figure 3.22, B).

The height range was found to be between 0.4mm to 0.59mm, beyond this the filament coiled and it was impossible to deposit a line of filament.

Based on this, the height chosen for this trial was 0.55mm; the dimensions were 12.7 x 12.7mm and 0.84mm filament pitch. This build failed at the second layer but this time it was possible to observe the how the defect was formed; the filament appeared to coil as if the nozzle was too high. The height was lowered to 0.42mm and the build was repeated, this time the failure occurred at the third layer (Figure 3.23).

The defects in this build were clearer and easier to observe. It showed that the failure was due to two reasons; the first was weak bonding between the layers, suggesting that the layer height was still too high and the second was due to the timing of the deposition. When the deposition was started for a cross beam filament it was on occasion stretched at the start. This, combined with the weak inter-layer bonding, pulled the filament off in the nozzle travel direction (as indicated by the red arrows in Figure 3.23). During this build the layer height was lowered from 0.42mm to 0.34mm in the area shown in blue in Figure 3.23. This adjustment improved the layer adhesion enough to correct the issue.

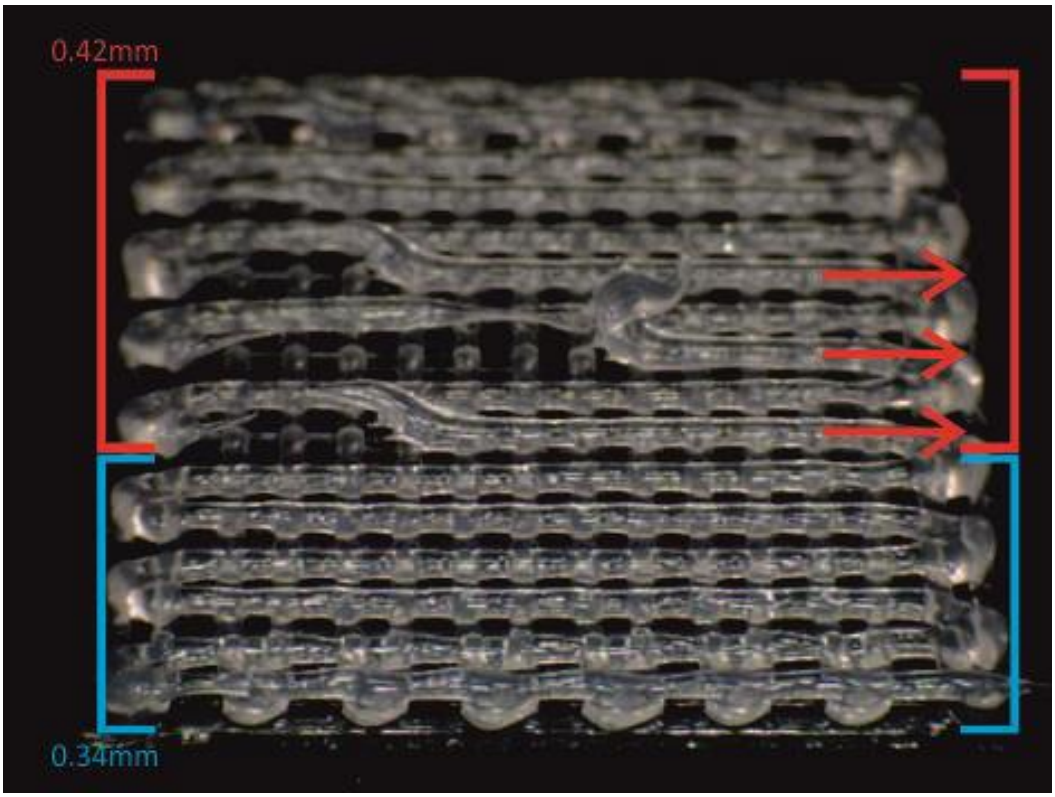

Figure 3.23, second attempt at silicone periodic structure with 0.4mm nozzle, 12.7x12.7mm. Layer defects at layer three, red arrows indicate nozzle travel direction. Brackets indicate layer height used in the top layer. figure by author

Considering that the first two layers of this build completed with no issues suggests the notion that a deposition height that is suitable for the first layer will not necessarily be suitable for subsequent layers. It is important to note that the layer height of 0.34mm is actually lower than the filament diameter by 0.06mm, so perhaps the ideal layer height needs to press the filament into the previous layer a small amount to promote layer adhesion.

To test the layer height of 0.34mm steps for a larger number of layers a fresh build was prepared with the same parameters as the previous build.

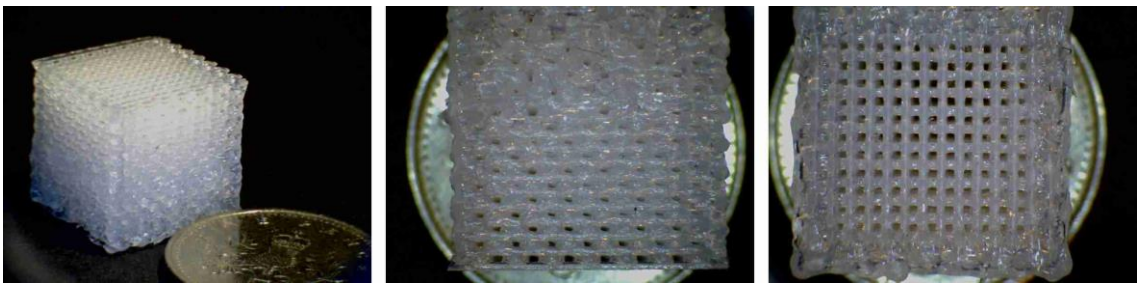

Figure 3.24, 12.7mm3 cube made with a 0.4mm nozzle, 5p coin for scale. figure by author

This build was completed successfully at 12.7mm in height and at four minutes per layer (Figure 3.24). The perimeter filament break-up occurred again for this build but was contained closer to the perimeter when compared to the 0.2mm build. (Figure 3.21)

Summary of findings

The issues with the first layer failing and not adhering to the substrate seen in the first 0.2mm build (Figure 3.19) is related to the delimitation problem caused by depositing too high as seen in the 0.4mm three layer trial (Figure 3.23). The pattern observed at the 0.2mm deposition was not due to the wrong height being used as a large portion of the build deposited successfully. This issue was most likely caused by the surface height deviation of the substrate sheet. As it was fixed to the build plate with magnets at the corners there was little control over the actual surface flatness of the substrate.

Considering the small height adjustment needed to build the 0.4mm (0.9mm) this sort of variation would not be noticeable to the eye yet could still cause the build to fail. To fix this problem the method of fixing the substrate to the build plate was modified from using magnets to spraying the surface of the build plate with adhesive spray. This allowed the surface to be secured and evened out with a lint free cloth thus ensuring a more flat build surface.

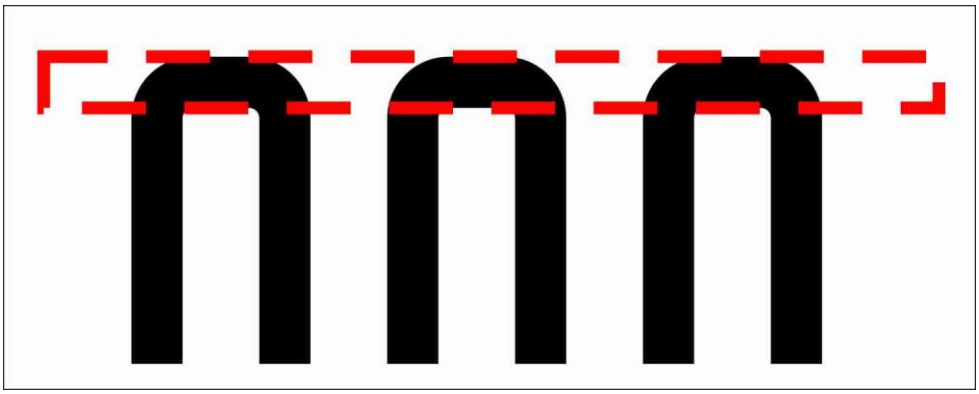

Figure 3.25, area where perimeter filament break-up occurs, the black lines represent the bottom layer filaments, the red rectangle represents the top layer filament. figure by author

The cause of the perimeter filament break-up is not fully clear, however it was attributed to a combination of human error and the material's natural tendency to be pulled at the start of the deposition, thus leaving a larger gap between filaments. Figure 3.25 illustrates the area where the perimeter break-up took place; the red rectangle represents the layer deposited on top of the previous layer (in black). This problem might be solved by automating the movement of the stage instead of the manual addressing of each axis in series as had been done up to this point.

3.4.5 Periodic Structures In Metal Clays

Introduction

The previous tests with the use of 'off the shelf' silicone material helped develop a methodology for determining the operational window for a given material. To refine these methods and test them further, a more complex material was selected for deposition of 3D periodic structures, namely 'metal clay'. The basic geometry of the structure remained the same, and the equipment did not require any further modifications.

During these trials two types of metal clay were used: the first was PMC3 (Mmc, n.d.), a paste containing silver particles. The second was BronzClay (Riogrande, n.d.), a clay containing bronze particles. These materials are sold in different forms; PMC3 is sold in paste form in a preloaded syringe and BronzClay is sold as a malleable lump of clay. The methods by which these two materials are prepared for the deposition process differ greatly, therefore it is advantageous to test both materials to determine which form, paste or clay, is more suitable for deposition.

Despite some of them containing precious metal, metal clays are comparatively low cost and it is therefore of great interest to develop parameters for these materials as current metal AM systems are expensive and the use of metal clays would reduce the cost of metal AM significantly.

Introduction to metal clays

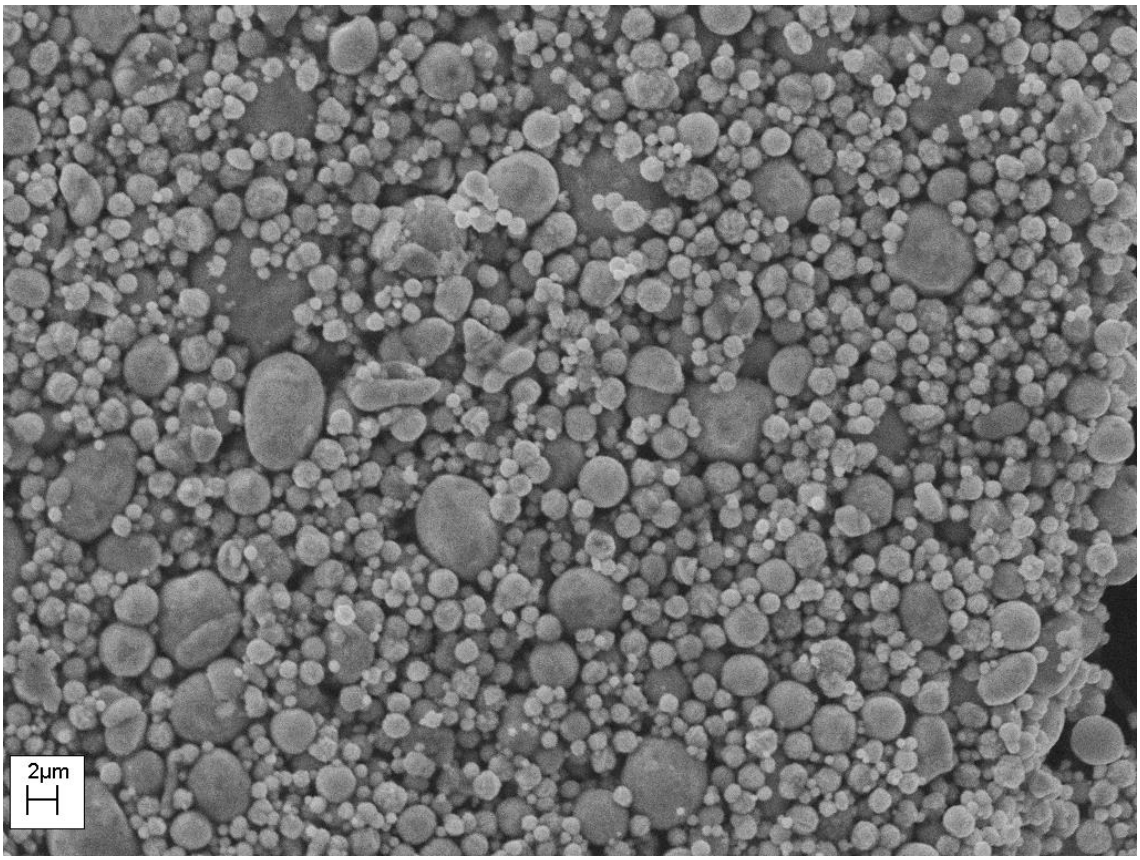

Figure 3.26, Scanning Electron Microscopy of dry PMC3 metal clay, 5000x magnification at 20Kv. figure by author

Metal clay is a colloid containing metal particles suspended in an organic binder (Figure 3.26); it is manufactured in several different consistencies ranging from sheets to block clay, paste and powder. Once fired the organic binder burns out and the metal particles sinter together to form a solid metal part (Rahaman, 2003, p.335). Widely used in the 'hobby' jewellery market for which this material was developed, it is normally worked using hand tools and it is similar to working with plasticine or clay.

Material loading

As PMC3 is sold in paste form, the material does not require any modification, nonetheless the syringe it is supplied in is not compatible with the extrusion equipment and as such the syringe was coupled to a compatible 5ml barrel with a female to female luer-lok coupling and the PMC loaded into the barrel. This reverse

loading method ensured that no air was introduced into the paste, the 5ml barrel being setup with a piston head inside before loading with material.

Silver PMC3 substrate suitability test

A quick test was run to indentify a suitable substrate for deposition and a very small amount of material was used on each test to minimise waste. All dry material from this test was collected and stored as it could be reconditioned with distilled water; this is standard practice with precious metals in the jewellery industry.

The results from the test are shown in Table 3.4:

Material	***Wet adhesion***	***Separation once dry***
Silicone sheet	*No*	*N/A*
Grease paper	*Yes*	*No*
Teflon sheet	*No*	*N/A*

Table 3.4, PMC3 substrate test. table by author

Grease paper was the only substrate of those tested that allowed deposition to take place, however it was not possible to separate once the PMC was dry. Further tests with PMC3 used this substrate as it was thought the paper would burn in the kiln without damaging the samples.

Deposition test

The focus of this test was to determine the parameters required to deposit periodic structures with the PMC3 material, then, if tests were successful, determine if the structures could be fired in a kiln.

To test this material several samples close in size were required. The plan was to fire the samples in small batches and correct the firing program if required. This way, if the firing failed and the samples were destroyed there would still be enough samples to adjust the firing program.

For this test a safe 0.6mm taper nozzle was used as deposition with this nozzle has had the least issues in previous tests. A total of 10 grams of PMC3 were used during these tests.

Figure 3.27, PMC3 line deposition test on grease paper. figure by author

Setting up the layer height for the PMC3 was easier than the tests with the silicone; the material was quite dense so the tolerances for layer height were large and not as critical. The material bonded very well to itself. The height was estimated to be between 0.6mm and 0.67mm steps as the diameter of the filament was 0.6mm. Line deposition tests were run with both heights (Figure 3.27) and 0.67mm steps was found to be suitable. A pressure of 2bar was used to deposit the material and the feed-rate was set at 1.5mm/s.

Several structures were built varying from two to three layers in height (Figure 3.28), although no clogging or curling was encountered during the build the air pressure needed frequent adjustment between 1.5 and 2.5 bar. Also there was one instance where deposition was interrupted due to an air bubble (Figure 3.28.B).

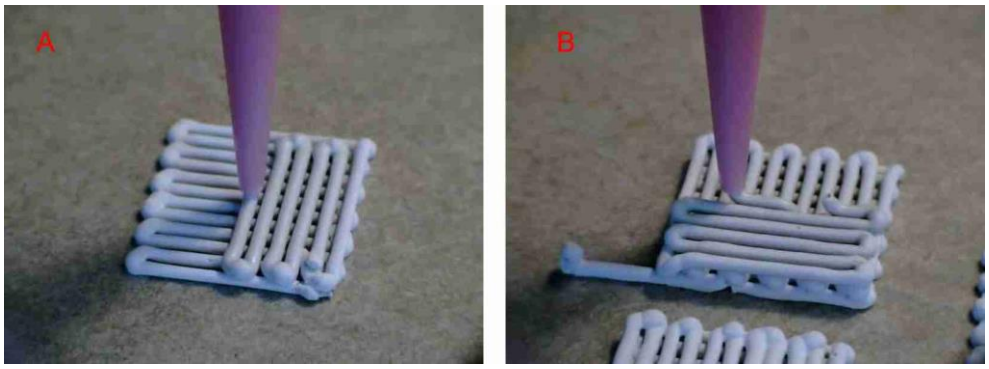

Figure 3.28, Deposition of MPC3 periodic structures. A: 2 layer sample, B: 3 layer sample with air bubble. figure by author

The final sample (#6) produced with the remnants of the 10g of PMC3 was partially completed. In order to use the material remaining inside the nozzle, silicone was used

to flush the PMC3 while the deposition of the periodic structure continued; this led to silicone being deposited in the final three filaments of the structure (Figure 3.29).

Figure 3.29, Final PMC3 periodic structure sample #6, silicone was used to flush the remaining material inside the nozzle as can be seen in the last three filaments. figure by author

Summary of deposition tests

The method of using the silicone to extract the last remnants of PMC3 from the nozzle worked well, almost three layers were deposited from the remainder inside the nozzle. The photo (Figure 3.29) shows the last moments of deposition where the PMC3 finished and silicone was deposited; as expected the pressure was far too high for the deposition of silicone so the filament lacked definition; the silicone was excepted to burn in the kiln during firing.

The 10 grams of PMC3 paste (standard amount in pack) yielded 6 samples including the line test. Whilst the method of spraying adhesive onto the printing plate kept the grease paper flat and even it also made it very difficult to remove from the printing plate without breaking the samples. Acetone was used to aid in the safe removal of the substrate from the printing plate; the samples did not suffer any damage from this.

The variation in the pressure required to deposit of PMC3 from 1.5 to 2.5 bar suggests that either the material is not very well dispersed or it contains agglomerates of material. This is not very likely considering the manufacturing precision of the product. The more likely reason is the fact that there was some uncertainty as to how much material to use for the tests and the barrel was reloaded with PMC3 several times during experiment. This exposure to air could have introduced some dry material; also

the material used during this test may not have been fresh; leading to a variation in viscosity.

Sample firing

Figure 3.30, PMC Kiln, Even Heat 360. figure by author

A specialised kiln for firing PMC was used to fire the samples (Even Heat 360). The kiln controller has a set of predefined programs specifically designed for each type of PMC, the program used for the PMC3 was program 3 F -this program does a full ramp to 700°C and holds that temperature for 10 minutes, the kiln then takes about 40 minutes to cool down. The full program takes less than an hour to complete the firing process.

Two samples were selected for the first firing test, one sample was three layers high the other sample only had one layer; the one layer sample was used to determine if there was any warping. The results are tabulated below (Table 3.5).

Before firing				***After firing***		
Sample #	*Number of layers*	*Weight (grams)*	*Size (mm)*	*Weight (grams)*	*Size (mm)*	*Shrinkage %*
1	*1*	*0.16*	*9.5*	*0.15*	*N/A*	*N/A*
2	*3*	*0.54*	*9.5*	*0.52*	*8.5*	*10.52*

Table 3.5, First firing test of PMC3 periodic structures. figure by author

Sample #1 warped, this was expected as warping of PMC3 pieces is normal. It was impossible to determine the shrinkage due to the warping. (Figure 3.31, B)

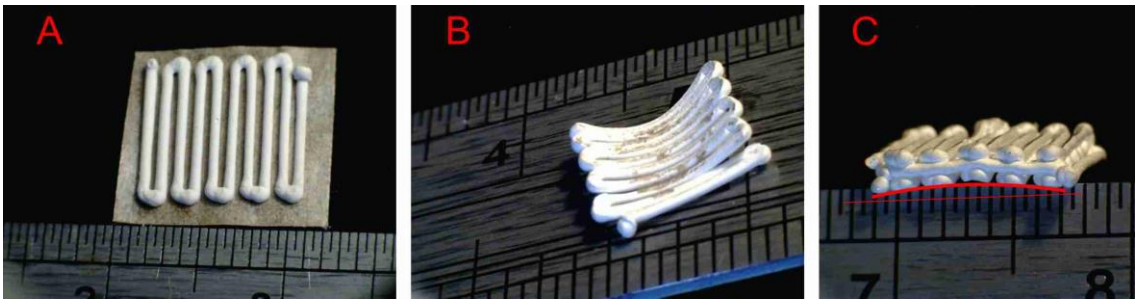

Figure 3.31, First batch of fired samples, A: one layer sample before firing. B: one layer sample fired and showing warping. C: Three layer sample fired, showing some warping. figure by author

Sample #1 warped, this was expected as warping of PMC3 pieces is normal. It was impossible to determine the shrinkage due to the warping (Figure 3.31, B).

Sample #2 showed less warping (Figure 3.31, C) of about 0.5mm. A thicker sample with four layers would probably show less warping. What is perhaps important to note is that there was no layer delamination -it was feared that the layers would delaminate due to warping.

The rest of the samples were fired under the same program, the results from this are in Table 3.6.

Before firing				***After firing***		
Sample #	*Number of layers*	*Weight (grams)*	*Size (mm)*	*Weight (grams)*	*Size (mm)*	*Shrinkage %*
3	*2*	*0.37*	*9.7*	*0.34*	*8.6*	*11.30*
4	*3*	*0.50*	*9.5*	*0.47*	*8.6*	*9.50*
5	*2*	*0.45*	*9.6*	*0.43*	*8.5*	*11.45*
6	*3*	*0.49*	*10*	*0.46*	*8.9*	*11.00*

Table 3.6, Second firing test of PMC3 periodic structures. figure by author

These samples also show a similar warping to that of the previous firing test, the surface appearance is matt silver; this is because the surface is very rough due to the small sintered particles on the surface scattering light. The samples were cleaned with a fine brass brush.

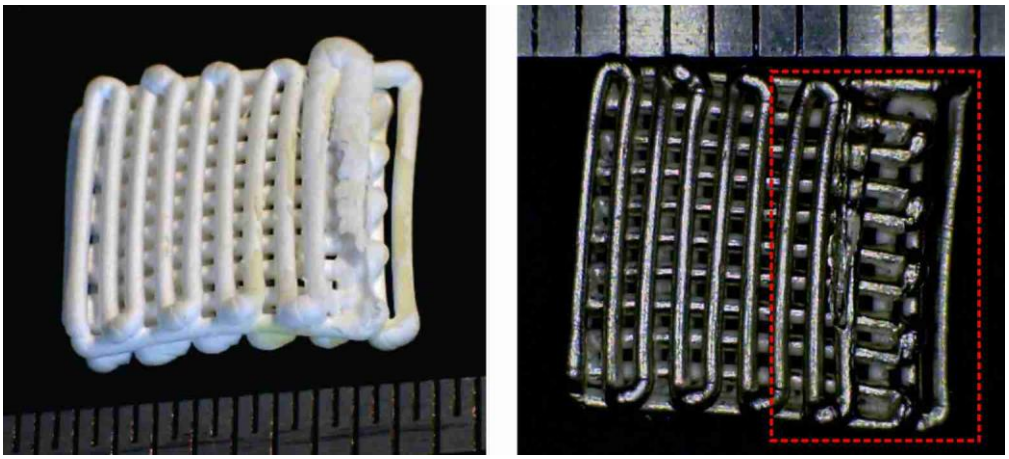

Figure 3.32, PMC3 periodic structure, sample #6. Left: sample before cleaning with wire brush. Right: sample cleaned with wire brush, silicone area in red square. figure by author

Sample #6 was very interesting; The silicone formed a cavity inside the deposited PMC3 filament before the PMC3 depleted; this formed a tube like geometry filled with silicone ashes (Figure 3.32, Left) most of this shell was removed during cleaning but the tube was still present in the structure as indicated by the red square in the figure.

Summary of PMC3 firing tests

These deposition tests have demonstrated that deposition with PMC3 is possible; the technique needs to be improved to produce more consistent complex shapes. A more suitable substrate need to be identified as the grease paper is thought to add to the warping of the pieces, as these showed some warping even before firing.

The shrinkage of the PMC3 was consistent with the 10% shrinkage the manufacturer claims (Thepmcstudio, n.d.), however sample #4 shrank less than the others, this could have been due to the placement of the sample in the kiln.

The samples were also brittle; it is known that PMC3 is usually weak in thin areas. To improve this, the samples could be annealed to improve the ductility.

Bronze clay deposition

The following tests use the same methodology and equipment as that used in the PMC3 tests. The purpose of this test with BronzClay was to determine how using a different form of metal clay (block of clay instead of paste) affected the operational window and to establish working parameters for BronzClay.

Material preparation

The BronzClay is supplied in a dense clay form, so to make a paste it was thinned with distilled water, 10wt% water to 90wt% bronze clay. A glass sheet was used as the mixing substrate and two spatulas were used to mix the BronzClay. The clay was spread thinly on the glass and the water was applied in small amounts to ensure a consistent mixture was produced. This method was chosen over the three roll mill used in the ceramic experiments because the consistency of the material would jam the mill.

Bronzclay deposition substrate test

The Issues with the grease paper substrate in the PMC3 tests warranted a new substrate suitability test. In this test the original grease paper was used to determine the performance with the bronze clay and to compare with the PMC3 results. Then the test was run on a 1mm thick alumina sheet. The test method was identical to the test run for the PMC3, with several lines of filament being deposited. Two factors determine a good substrate: Good adhesion to the wet material and easy release from the substrate once the clay is dry.

The grease paper test was run with a 0.4mm tapered nozzle, this served the purpose of determining if the clay would extrude through the smaller aperture and also test the substrate.

While the BronzClay successfully extruded with the 0.4mm nozzle, the higher water content of the BronzClay paste bloated the paper and made consistent deposition impossible. The extrusion pressure used was 2.2bar (Figure 3.33, Left).

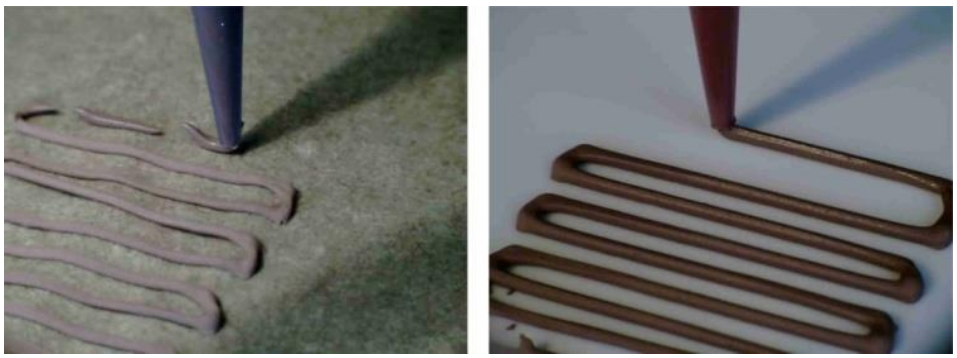

Figure 3.33, Left:, BronzClay clay deposition on grease paper. Right: BronzClay deposition on alumina sheet substrate 0.6mm nozzle. figure by author

The second test with the alumina substrate produced better results. The wet BronzClay adhered well to the alumina; the dry paste was also easily removed from the alumina substrate thus making it a suitable substrate, Figure 3.33 (right) shows the successful deposition test onto the alumina substrate.

Deposition of periodic structures in BronzClay

The parameters used for these tests were: pressure: 2.1 bar, feed-rate: 1.5mm/s. The layer height was initially set at 0.6mm for the first layer; this was lowered to 0.5mm for consecutive layers. The samples were made to the same size as the PMC3 tests but with four layers, a total of three samples were made.

During these tests there were no issues with air bubbles, clogged nozzles or sudden drops in material flow-rate, such as those encountered with the PMC3.

However the filaments deposited were not perfectly straight on the consecutive layers, the filaments had the tendency of being pulled at the start of every filament giving the filaments a slight angle. It was thought this could have been caused by the consistency of the clay, with the fresh filament pulling on the previous one, it could have also been caused by incorrect deposition parameters, Figure 3.34 shows the deposition of the four layers of clay of the first sample.

Figure 3.34, The process of depositing a four layer sample. BronzClay, 0.6mm nozzle, 2.1 bar pressure. figure by author

The first two samples were easily removed from the alumina substrate. However the third and final sample was damaged due to impatience, it was removed too soon and the bottom layer was damaged, some of the material was still wet. The 'green' bronze builds and the line test show an unexpected level of flexibility, the samples could be handled quite roughly and flexed without breaking.

Firing the BronzClay samples

Firing of BronzClay is more complex than the PMC3 because an oxygen free atmosphere is required to stop the bronze from oxidising. The firing program is also not preset in the kiln and the manufacturer doesn't provide any information on firing samples thinner than 3mm.

For the first firing test both the line test and one of the three samples were fired. The purpose of firing the line test was to determine if the firing was successful by bending the sample, under firing would cause the sample to be weak and brittle.

To provide the oxygen free atmosphere the bronze samples were placed in a steel pan filled with 50mm of activated carbon according to manufacturer recommendations (Riogrande, 2008, p.8). The samples then had to be spaced 20mm or so apart and towards the back of the pan to avoid cooling from the kiln door. The samples were then covered with 50mm more of activated carbon and the pan lid was placed on the steel pan -this stops the carbon from igniting and turning to ash in the kiln.

The firing program

Table 3.7 below contains the firing program recommended by the manufacturer for 3mm thick pieces (Riogrande, 2008, p.9).

Ramp up	*Hold time*
260°C degrees per hour to 843°C	*2 hours*

Table 3.7, BronzClay firing program. table by author

This firing program would take 6 hours and 20 minutes to complete including 1 hour for cool down, it was decided that the program would be modified to shorten this time, Table 3.8 shows the firing program used for the first set of samples.

Ramp up	*Hold time*
400°C degrees per hour to 843°C	*1 hour 20 minutes*

Table 3.8, Streamlined BronzClay firing program. table by author

This program took around 4 hours to complete including cool down.

The samples fired successfully, the four layer sample had a copper hue on its surface, and the line test sample showed signs of oxidation; indicated by the blue and green colour on the surface.

The four layer sample was cleaned with a brass brush to reveal the bronze colour underneath. The line test sample was fired to observe the flexibility and strength of the fired bronze, this was ascertained when the sample was bent back and forth several times beyond 90° until the metal broke. This level of ductility demonstrates that the bronze clay fired successfully; if it had not fired properly the material would have been weak and brittle.

Based on these observations the firing program for the next samples was reduced further, Table 3.9 shows the revised firing program.

Ramp up	*Hold time*
550°C degrees per hour to 843°C	*1 hour*

Table 3.9, BronzClay, revised quick firing program. table by author

This program reduced the firing time to 3 hours including cool down. The rest of the samples were fired using this program.

This second batch of samples was of identical quality as the previous firing run.

All the samples were weighed and measured before and after firing, Table 3.10 below shows the results for the samples.

Before firing			*After firing*			
Firing program	*Weight (grams)*	*Size (mm)*	*Weight (grams)*	*Size (mm)*	*Shrinkage %*	*Identifying characteristic*
1	*0.42*	*9.7*	*0.40*	*8.10*	*16.5*	*Flaw in corner*
2	*0.41*	*9.5*	*0.40*	*8.02*	*15.6*	*N/A*
2	*0.39*	*9.5*	*0.37*	*7.93*	*16.5*	*Bottom layer damaged*

Table 3.10, Results of second firing test of BronzClay. table by author

Summary of BronzClay results

The quality and definition of the bronze samples showed a definitive improvement in the building technique. The paste exhibited very positive characteristics such as layer adhesion and filament strength which bodes well for self-support. Drying times were also very short and the green material showed great handling durability.

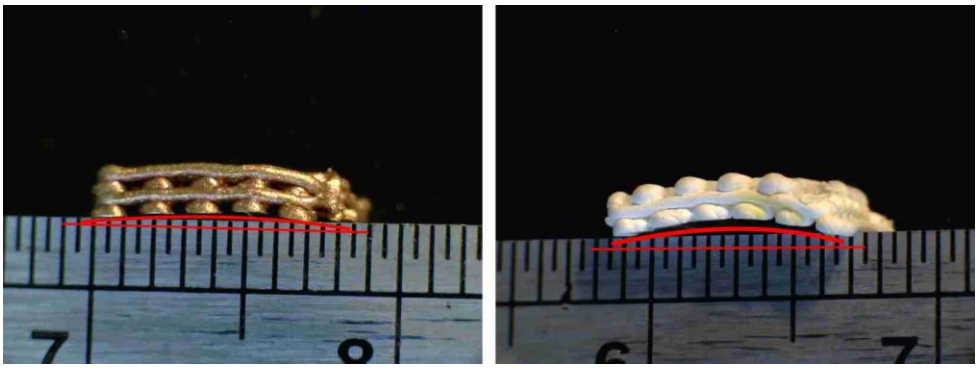

Figure 3.35, Comparison of warping between Bronzclay (left) and PMC3 (right). figure by author

The samples did have the tendency to warp during drying but not by much, these samples showed the least amount of warping at 0.3mm when compared with the silver samples at 0.5mm. (Figure 3.35) but they were also thicker at four layers. The shrinkage of the bronze was lower at 16.5% than the 20% claimed by the manufacturer (Riogrande, 2008, p.5).

3.4.6 Summary of Mk1 Equipment

Ceramics

Whilst the deposition of ceramic will not be pursued further, the tests helped to determine if the extrusion equipment was suitable to warrant further tests with the same equipment. The tests also helped to develop the material loading and filament extrusion methods which were applied and streamlined in the silicone and metal clay tests.

Silicone

These tests helped to further refine the deposition technique with samples featuring a large number of layers. The deposition with fine nozzle sizes demonstrated the capability of the extrusion equipment in handling low pressures for the small material volume being deposited. The silicone material also showed great potential for filament deposition which warranted further tests.

Metal clays

Additive manufacturing in metals is generally expensive, the systems are developed and priced for industrial applications and therefore are rarely accessible to the public. It is only until recent years that this has changed and the process is now offered by service bureaus (Shapeways, n.d.). The deposition of metal clays has the potential of

democratising metal AM using low cost materials and equipment. The results of the tests with both PMC3 (silver) and BronzClay were promising and warranted further experimentations, it was demonstrated that the deposition methods developed thus far are suitable and that the extrusion equipment can handle the materials.

Mk1 equipment

Whilst the deposition equipment had been demonstrated to be effective at depositing the simple geometries for the preliminary tests, the project reached a point where better motion control was required to create more complex parts and to automate the deposition process. Up to this point deposition timing and axis control had been done manually, this was very labour intensive and led on some occasions to undesired deposition defects. Initially this was pursued by sourcing a more comprehensive controller from PI, -the manufacturer of the slides used. It was soon discovered that such controllers would require motion control software to be developed. This would have distracted from the aims of the project as developing the software would have taken a considerable amount of time. So at this stage it was decided to retire the Mk1 equipment and source a better solution.

However from the Mk1 system the extrusion method was carried on for the next iteration of the equipment as the tests with the different materials demonstrated that the extrusion equipment was capable of handling the pressures required and did not limit the exploration with the materials.

If a spool valve would be considered for deposition of metal clays, the main limiting factor would be the volume of material required to prime the valve. When considering precious metals such as silver, the material used to prime the valve would not be recoverable as the valve would need to be flushed after each use to avoid build up of dry material inside the valve (Adhesivedispensing, 2005, M p.5).

3.5 Development of PDM Mk2 Equipment

The past experiments performed with the Mk1 equipment have highlighted the need for automation. To test automated deposition a CNC machine was used, Modela MDX-20 manufacture by Roland, this would serve as a test platform for automated deposition.

The Modela is a compact desktop CNC milling machine; it is capable of feed-rates up to 15mm/s. The software driver is compatible with most CAD packages which meant the tool paths sent to the machine could be fine tuned and more complex shapes could be made.

Figure 3.36, Modela MDX-20 manufactured by Roland, figure from (Creativetools, n.d.)

To fit the extrusion system onto the Modela the original spindle was removed, as the machine needed to be changed from a subtractive process to additive. This was done by removing two bolts on the Z axis carriage. The machine was designed to allow quick removal of the spindle which simplified installation of the extrusion head. A bracket was made from aluminium to hold the syringe barrel in place (Figure 3.37). The bed of the CNC machine was coated with spray adhesive and a Teflon sheet was laminated over this to form the build surface for silicone deposition. After these modifications and combination of equipment, now capable of additive manufacturing, was designated as PDM Mk2.

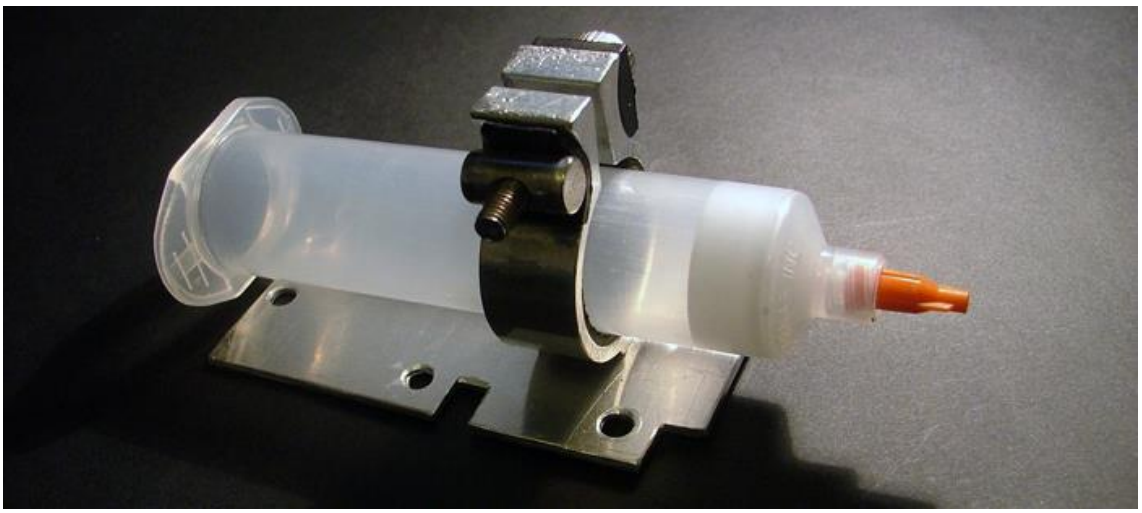

Figure 3.37, Syringe barrel mounting plate for Modela CNC machine. figure by author

The air solenoid was manually operated during these trials just as the case with the Mk1 equipment, the intention was to integrate the air solenoid to the rest of the equipment for automation if deposition with the Mk2 equipment proved successful and an appropriate way forward.

A camera was also attached to the deposition head to record the builds, as this was a valuable tool in the Mk1 equipment, and it was thought it could help identify issues and faults when testing the Mk2.

3.5.1 Setting up the Mk2 Equipment

The machine driver is compatible with both 3D and 2D CAD programs such as Corel Draw. In this 2D vector drawing program the Modela works as a 2D engraver, this was the function and software used to create and send the tool-paths for deposition.

Software parameters

The Modela CNC machine appears as a 'printer' in Corel Draw, so setting parameters here is as simple as setting up duplex for a laser paper printer.

The software recognises RGB colours in the vector drawings from Corel Draw. These colours can be used to assign 'cut' depth data to a particular vector line; up to eight different colours can be assigned per tool. Several tools can then be used to create objects with more than eight layers, with each tool having a set of eight 'cut' depths associated with it (Figure 3.38).

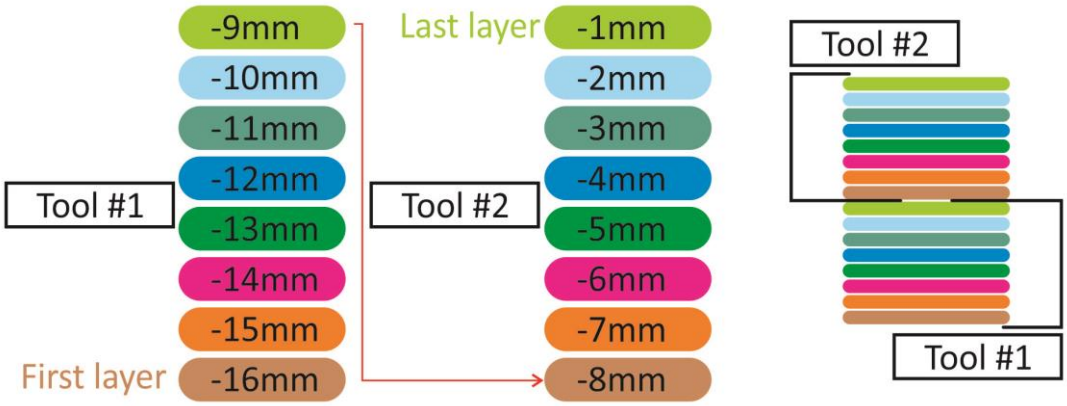

Figure 3.38, Modela colour and tool, layer height set-up example. figure by author

Tool set-up

The CNC machine was designed for a subtractive process and not additive and as such the tool setup does not allow the user to set positive height values, the parameters are designed to cut into material, so a negative value is expected with the surface of the object being cut set as Z origin. Therefore the Z origin had to be set at a level higher than that of the build plate and then use negative Z values to set the height of the nozzle, Figure 3.38 illustrates the issue.

e.g. If the Z origin is set at 17mm above the build plate and the desired nozzle height is 1mm above the build plate, the depth of cut in the parameters would be set to -16mm. this would move the nozzle down by 16mm to the height of 1mm above the build plate.

Tool-path order and 'cut' depth is set in the Modela 'print' dialog; these settings are linked to the colour of the vector drawn that makes the tool-path. A total of eight different colours can be set-up. If two objects have the same colour then the first one cut will be the one that was created first.

In the 'printer' dialog it is important to turn off the 'sorting' option, as this lets the software decide the start and end points for each tool path and overrides the preferences set by the user. The sorting option works like "point to point machining", where the path the tool takes to reach the start coordinate of a tool path has a lower priority than the target coordinate (Stenerson & Curran, 2007, p7). This type of sorting algorithm is used to optimise the time taken to complete a set of machining operations by picking the ideal start an end point for each operation. This method however was developed for a system designed to cut into material where the direction the machining operation takes is not necessarily relevant; however in additive 3D deposition of materials the direction has a higher priority as this must be carefully considered to ensure a successful build. The direction of the designed tool path is set in the design software, in this case CorelDraw, were each vector line has a start and an end point.

3.5.2 Mk2 Deposition Trials

Build method

For these tests a 26.1mm thick piece of aluminium was used to set the height, based on this, the height for the layers was set in the 'printer' dialog for the Modela as described in 'Software Parameters'.

The nozzle chosen for this series of tests with Mk2 was a 1.6mm blunt end nozzle, it was chosen for several reasons:

The layer height tolerance in such a large nozzle is very large so problems seen in previous tests with the Mk1 are reduced.

The large scale makes mistakes and changes to parameters very easy to identify so as to adjust the system parameters accordingly.

First deposition trial

The first test used the same periodic tool-path that had been used in the previews builds; it was made larger to accommodate the 1.6mm nozzle (Figure 3.39). Using the same tool-path as the Mk1 experiments allowed for direct comparison of both systems. The parameters used were: feed-rate: 15mm/s, layer height: 1.6mm, pressure 3 bar and the dimensions of the build were 40mmx40mm.

This build attempt failed, this was due to an unexpected behaviour from the CNC machine; once a layer was complete the Z axis moved up to return to origin before positioning the X and Y axis, this is done to avoid crashing the spindle against the work piece when the machine is milling, however in this additive process all the machine did was pull off the last filament from the layer. This build was allowed to continue for seven layers, Figure 3.39 shows the end result.

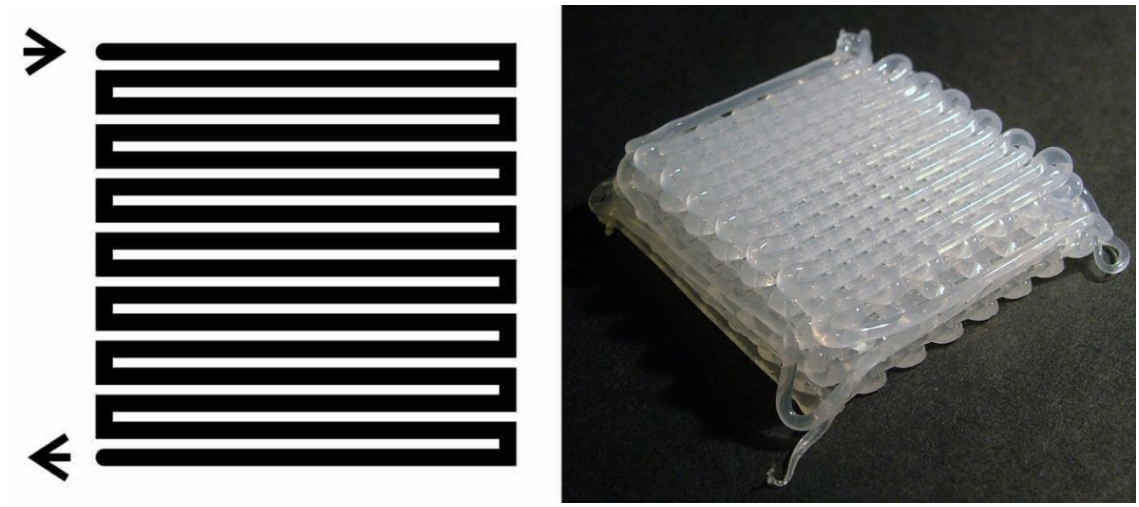

Figure 3.39, Left: machine tool-path. Right: First build on Mk2, failed due to unexpected machine behaviour when creating consecutive layers. figure by author

The issue with the Z axis moving up after every layer is a built in function that cannot be overridden by the user, therefore steps had to be taken to ensure that filaments were not pulled off during this operation. The issue was fixed by modifying the tool path; both the start and end point of each layer were set to overlap with the adjacent filaments, this modification meant that the last filament was reinforced and was not pulled off (Figure 3.40). This tool path was tested by depositing one layer to determine if any filaments were pulled off by the retraction of the Z axis once the layer was completed.

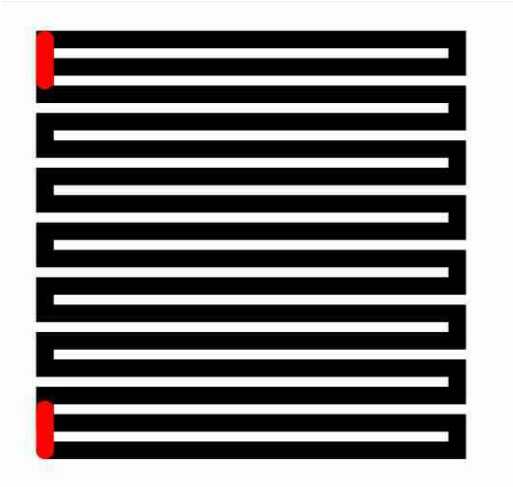

Figure 3.40, tool-path with the corrections for the Mk2 to reinforce the last filaments. Corrections shown in red. figure by author

A build was made to further test this new tool path, the layer height was reduced to 1.5mm as it was noticed that in the previous build the layer height was getting too large for the topmost layers.

This structure was completed at five layers; the tool path modification solved the retraction issue. During deposition It was noticed that at layer five of the build (last layer) the nozzle was too high. It seems the large filaments were losing some height to the previous layers, probably due to the deformation of the filaments as they adhere to each other between layers. The weight of the consecutive layers might be have played a contributing factor.

The final height of the build was measured, it was 6.5mm at five layers instead of the expected 7.5mm (5x1.5mm); this meant the average layer thickness was 1.3mm. The layer height was reduced to this value for the next build attempt.

A further improvement was done to the tool path; a perimeter box was added to provide better support to the structure (Figure 3.41). The tool-path was designed to be one continuous movement including the perimeter box to avoid any issues that might arise from the tool moving up to reposition for the perimeter tool-path, this also reduced tool air-time for quicker layer build times.

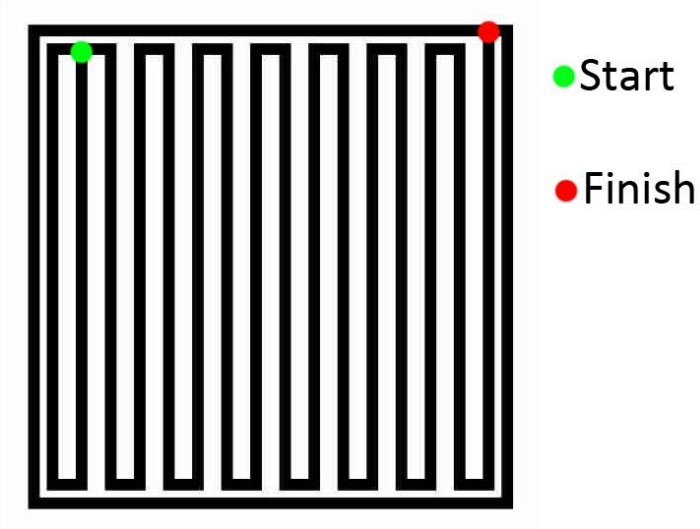

Figure 3.41, tool path revision, now with perimeter box. figure by author

A new build was setup to test the tool path with the bounding box, the height setup used can be found in Table 3.11.

layer	*Cut depth (mm)*	*Layer Height (mm)*
1	*-24.8*	*1.3*
2	*-23.5*	*1.3*
3	*-22.2*	*1.3*
4	*-20.9*	*1.3*
5	*-16.6*	*4.3*
6	*-18.3*	*1.3*
7	*-17*	*1.3*
8	*-15.7*	*1.3*

Table 3.11, Third build with Mk2 equipment, height set-up, highlighted in red is the error that caused this build to fail. table by author

This build failed, the tool path worked very well but there was a mistake in the layer height set-up, the cut depth at layer five was accidentally set to -16.6mm instead of -19.6mm effectively depositing 3mm too high. Figure 3.42 shows the result of this error.

This error was corrected and the build was repeated, the build was successful, all eight layers were completed at one minute per layer; this build was repeated once more to confirm the results, both builds were identical.

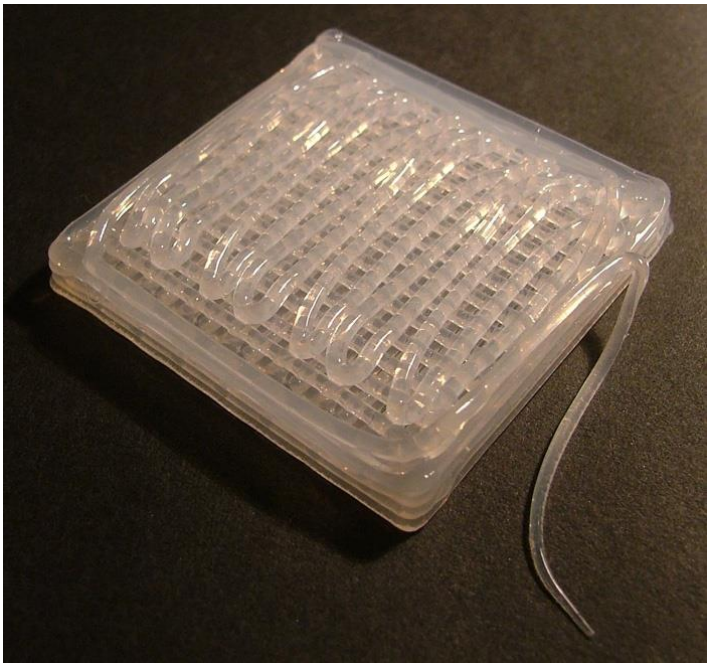

Figure 3.42, Third build on Mk2, Error in height set-up. figure by author

It was noticed that by layer eight the nozzle height was again becoming too large, it was thought at the time that is would not be possible to further reduce the layer height to correct for this issue as this could potentially damage the early layers

The solution developed was to reduce the nozzle height every few of layers to keep up with the vertical 'shrinkage' of the structure.

The deposition head on the Mk2 equipped with a camera allowed for the footage of both builds to be reviewed after deposition to pin point the exact moment where the layer height was no longer suitable. It was found that by layer five on both builds the layer height was beginning to become too large, not enough to compromise the build but enough to be noticeable. Based on this, layer five was chosen to be the adjustment layer, the adjustment was 0.3mm lower than the 1.3mm layer height for the rest of the layers.

To test this; a 16 layer build was planned; it was chosen to be this high because if the adjustment layer did not work, then this build would fail, giving a clear indication, the layer setup for this build is in Table 3.12.

Layers 1-8			*Layers 9-16*		
layer	*Cut depth*	*Layer height*	*layer*	*Cut depth*	*Layer height*
1	*-24.8*	*1.3*	*9*	*-14.8*	*1.3*
2	*-23.5*	*1.3*	*10*	*-13.7*	*1*
3	*-22.2*	*1.3*	*11*	*-12.4*	*1.3*
4	*-20.9*	*1.3*	*12*	*-11.1*	*1.3*
5	*-16.6*	*1*	*13*	*-9.8*	*1.3*
6	*-18.3*	*1.3*	*14*	*-8.5*	*1.3*
7	*-17*	*1.3*	*15*	*-7.5*	*1*
8	*-15.7*	*1.3*	*16*	*-6.2*	*1.3*

Table 3.12, Layer height set-up for 16 layer build on Mk2, correction layers highlighted in blue. figure by author

The tool path was also modified for this test, it was noticed that the area of contact between the inner tool path and the perimeter box was too large. The inner tool path dimensions were increased by 0.5mm on all sides to increase the area of contact with the perimeter box.

In order to print the 16 layers with the eight colour limitation the tool selection in the 'printer' dialog was exploited as described in 'Software Parameters'. The parameters for the first eight layers were loaded onto tool#1, and the parameters for the next eight layers were loaded onto tool#2, there was a pause in deposition in between while the data for the next eight layers was sent to the machine.

Figure 3.43, 16 layer build with Mk2 equipment. figure by author

The build was completed successfully, the adjustment layer worked well, 65% of the capacity of the barrel was used. Figure 3.43 shows the complete structure, the build was completed in 15 minutes, the material took 10 hours to fully cure but it was cured enough to handle at three hours.

One of the limitations of the Mk1 equipment was not being able to produce circles, this is a limitation not shared with Mk2, a tool path similar to the one used for the square builds was modified to have a circular perimeter. This build used the exact same layer and deposition parameters already established; but limited to five layers, to reduce the time taken to build this test.

The perimeter tool-path design went through two iterations to find the correct size, in the first try the perimeter was too close to the inner tool path, the print was not ruined but the circle lost some of its shape; the second test yielded much better results with the perimeter wall appearing more rounded. Figure 3.44

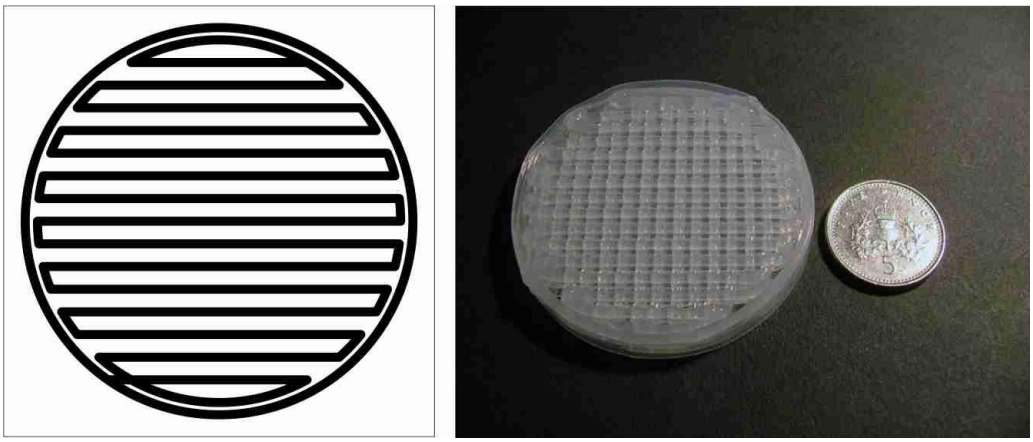

Figure 3.44, round tool path build, Mk2 equipment, five layers in height. figure by author

The tests performed up to this point have helped determine that the Mk2 is suitable for 3D deposition, with parameters that produce consistent results, however further work was required to integrate the air solenoid to the Mk2 to allow for automatic deposition.

Programming the Mk2

The CNC Machine (Modela MDX-20) uses a serial interface to communicate with the computer, the translation of vector graphics to instructions and coordinates is done by the printer driver provided by the manufacturer, data is sent by the printer driver straight to the machine. However it is possible to intercept this data for modification, an online tutorial for the implementation of a fourth axis onto the Modela provided the method for this procedure (Fourthaxis, 2009). The process starts by setting the printer driver to 'print to file' instead of communicating directly with the Modela, once this file is saved to the computer it can be modified using any text editor, then once the modifications are complete the file can be sent to the Modela using the command prompt in windows, addressing the serial port the machine is plugged into.

What follows is a table of commands and their function, the function of some of these commands was obtained from the tutorial mentioned, others were determined from context and experimentation with intercepted code, such as sending a file with just one straight line of a known length set to a known cut depth.

command	*result*
IN;	*Initialize*
PA	*Set coordinates to absolute*
PR	*Set coordinates to relative*
!MC0	*Turn off spindle motor*
!MC1	*Turn on spindle motor*
VA n	*Set feed-rate n= 0.1 to 15 mm/s*
!VZ n	*Set Z axis feed-rate n= 0.1 to 15 mm/s*
!PZ0, 6050	*Move Z axis to origin*
PU x, y	*Move to X Y coordinates, Z goes back to zero and comes back down*
PD x, y	*Move to X Y coordinate, Z axis does not move*
;	*End of instruction*
!PZ- a, b	*Set cutting height (a) and Z up position (b)*

Table 3.13, Modela MDX-20 programming instruction set. table by author

Air-solenoid integration

The plan was to remove the spindle from the modela and use the electrical signal to trigger a relay on and off, this would in turn trigger the air solenoid, the instructions !MC0 and !MC1 could be used for this, by modifying the intercepted code with these instructions the air-solenoid could be triggered in the appropriate time to allow for automatic deposition.

This plan was however never put into action, before modifications could be made the machine malfunctioned and required repairs, the time frame of this repair was far too long and therefore new equipment had to be sourced to continue with the research project, this marks the end of the development of the Mk2 equipment.

Whilst modifying the Modela would have produced the desired outcome such as the ability to produce complex tool paths and automatic deposition, the system was too limited by the firmware and the software designed by the manufacturer of the system. While 3D deposition was possible the eight layer limitation would have caused more problems further down the research project as the builds would increase in height and complexity, the new equipment needed to be less limited and more open to modification to allow for more room for expansion as the project developed.

3.6 Development of PDM Mk3 Equipment

3.6.1 Equipment Selection

Hardware selection

With the abrupt end of testing with the Mk2 system due to equipment malfunction it was necessary to source new equipment, however several things were learned from using the Mk2 that helped inform the requirements for the Mk3 system. First and foremost the system needed to be open to modifications, whilst the Mk2 worked well future expansions such as multi material would have been very difficult to implement given the nature of the hardware. Secondly the system needed to be simpler, the Mk2 featured functions that assisted the user in setting up the machine for milling or engraving. These were aimed at creating an inclusive system so users with less experience could operate the machine; these functions hampered the development for 3D deposition of materials.

At this stage it was decided that the Mk3 system needed to be based on a CNC mill running in real-time from a computer, it needed to do so without any firmware assisted functions such as origin finding and instruction interpretation, as these would interfere with any modifications done to the machining spindle and would need to be overridden.

What was required was a more primitive system that would move to where it was instructed, as opposed to a complex system built and refined towards a specific application.

Several systems were considered, one of those was the RepRap, as it was open source and therefore open to modification, however the system would have required new firmware to match the intended application, this coupled with unreliable hardware it was thought that perhaps this route would have been more trouble than it was worth.

Building a system from scratch was also considered, purchasing the slideways and a controller to build the machine, such as those seen in some of the publications in the literature review (Chen, Zhou and Lao, 2011; Ahn, Shoji & Hansen et al., 2010; Lewis & Gratson, 2004).

The other option would be to source a prebuilt CNC mill; this would have similar performance to the DIY system but without any unexpected issues that could arise from building the system.

It was decided that a prebuilt CNC mill would be used, the model obtained was a three axis Sherline 5410 (Sherline, n.d.), it is a compact and simple system. There is plenty of room around the Z-axis for modifications and mounting the deposition head. The envelope size is X: 230mm, Y: 150mm, Z: 150mm (Figure 3.45).

Figure 3.45, Foreground: Sherline 5410 CNC mill. Background: retired Modella MDX-20. figure by author

The Sherline runs in real-time from a computer using a parallel port interface, it does not have any form of feedback built in and relies solely on the instructions sent by the computer, the code interpretation and motion control is managed by software installed in the computer.

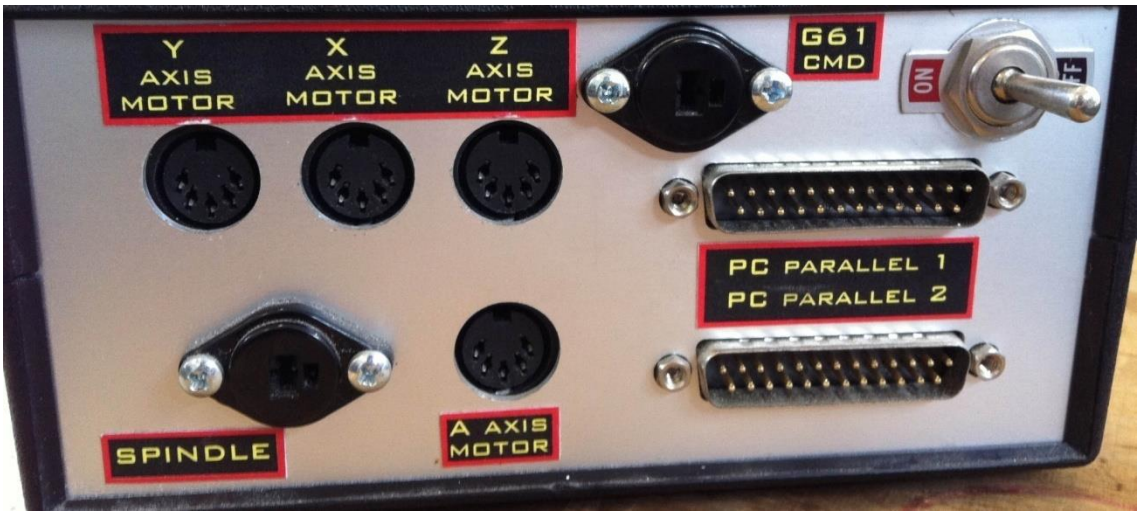

Figure 3.46, Sherline 5410 CNC mill controller. figure by author

The controller for the Sherline mill has four axes, a spindle output, a spare input and two parallel ports, only three axes are required so the spare outputs for the spindle and the fourth axis could be used to control external devices such as the air solenoid.

Software selection

There is a plethora of software designed for CNC motion control, however when considering the parallel port interface three pieces of commercial software rise to the top, EMC2, Mach3 and Labview.

While Labview (ni.com/labview/) is not specifically designed for this type of application, the programming language would allow for motion control to be implemented, it would also be possible to utilise sensor feedback to monitor machine parameters and accuracy. This software is commonly used in research environments and would be suitable; however it would also require a steep learning curve and software to be written for the specific application.

EMC2 is a Linux based CNC program (Linuxcnc.org), this software would be capable of running the CNC mill, this software runs on G-code, so designs would need to be converted to G-code prior to deposition, the software still has a learning curve but it is not as steep as that in Labview. The limitation lies in the fact that the software runs on Linux, this would mean that a dedicated workstation would be required and any design software would need to be used on a separate Windows based system.

Mach3 (machsupport.com) works the same way as EMC2 but it runs on Windows, it is limited to the 32bit version of Windows but that is not an issue for the project, it is also capable of running up to two parallel ports meaning that there are enough inputs and outputs between both of those ports for any future additions to the Mk3 system.

The plan was to first test the Sherline mill with a trial version of Mach3, if there were any compatibility issues with the hardware then EMC2 would be tested, failing that then Labview would be used.

Mach3 hardware compatibility test

Initially the hardware was unresponsive to signals sent from Mach3; there was no documentation on how the controller was wired to the parallel port. Most CNC

controllers use two pins from the parallel port to interpret instructions for each stepper motor, one for direction, the other for steps. With these signals the controller will move each motor in the indicated direction a set number of steps, each step can be converted to a specific amount of linear movement depending on the pitch of the lead screw coupled to that stepper motor. When configuring Mach3 the user needs to indicate what pins are used to control each axis motor before any movement can be seen on the CNC mill.

To set up Mach3 the manual was consulted to find out what needed to be configured and where it was. The first step was to configure the step and direction pins, as these were not known this had to be done by trial and error. All possible combinations of output pins 2-9, 1, 14, 16 and 17 were tested yet there was no response from the hardware. The parallel port on the workstation was tested using a Loop-back cable to rule out any hardware issues with the workstation; this test connects the outputs to the inputs of the port and is used to check if it is operational (Passmark, n.d.), the test concluded that it was operational. The solution was found in the port configuration of Mach3, the controller for the CNC mill was a Max NC-10 wave drive and it required a different configuration than that used in other CNC mills. Mach3 features a mode designed for this type of controllers, enabling this option allowed the software to communicate with the controller. The Sherline 1/2 pulse mode was also enabled; this setting uses large 40µs pulses to control the axis, which gives the motors time to mechanically catch up to the data being sent and produce a smoother travel, Figure 3.47 shows the configuration used.

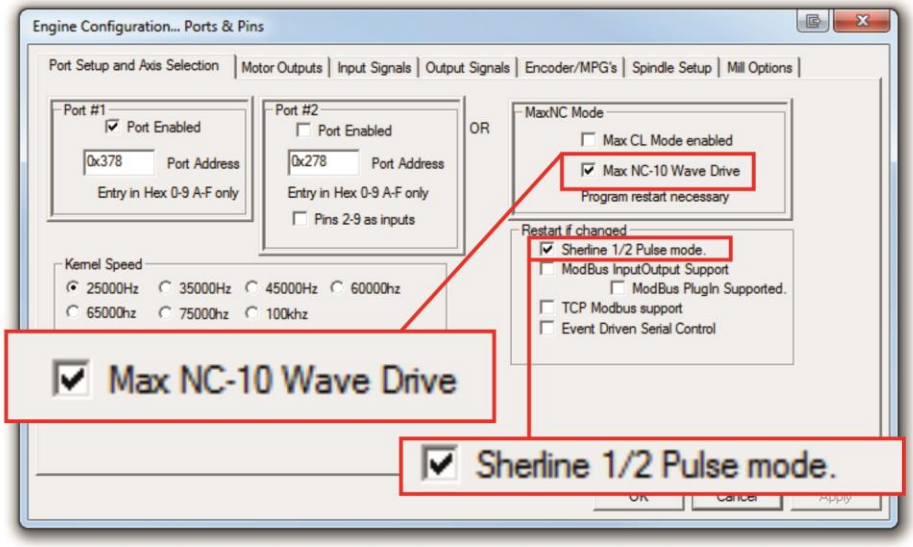

Figure 3.47, Screen shot of Mach3 Software, Sherline port and pin configuration. figure by author

Max NC-10 Wave drive controllers differ from other CNC controllers in that step and direction pins are not used, instead all four cables from each stepper motor are wired to the parallel port, when the Max NC-10 mode is enabled in the Mach3 configuration these pins are configured as part of that mode, further reading revealed that this type of controller is referred to as a Phase Controller, this in turn also led to a table by MaxNC showing all the pin assignments for the controller (MaxNc, n.d.).

Axis calibration

The Sherline CNC mill has three axes X, Y and Z, in order to function properly three settings must be calibrated for each one; steps per millimetre, Feed-rate and acceleration.

Steps/mm

This is calculated from the lead screw pitch and the resolution of the stepper motor (Machsupport, 2008, p.76), for the Sherline all the axes use the same model of stepper motor and lead screws with the same pitch. The lead screws have a metric thread with a pitch of 1mm, the stepper motors have a resolution of 1.8° so 360°/1.8° = 200 steps per revolution which means that the setting should be 200 steps/mm. However as there is no documentation on the controller being used this figure could be larger. Some controllers do not move the motor a full 1.8° step and instead run in half or micro-steps (typically 10 steps per step) and thus increase the number of steps per revolution, according to the Mach3 manual; micro stepping reduces the vibration in

the system giving a faster and smoother operation (Machsupport, 2008, p.76) but at the cost of torque. The stepping configuration is usually fixed and cannot be changed as it is built into the controller.

Feed-rate

Calibrating this setting was done on trial and error, testing from a low velocity of 100mm/minute and slowly increasing it until the axis stalled and could not move. It was found that a maximum of 600mm/minute was possible for the X and Y axis, however this was at the edge of stability and some stalls did occur at this setting. It was lowered to 500mm/min where the system was more stable; the Z axis reached a stable point at 400mm/min

Acceleration

Similar to how the feed-rate setting was found the acceleration was found by trial and error, in this case the setting was tested by performing linear moves on each axis and quickly changing direction, it was found that the system was stable at 100mm s^{-2}.

Testing mach3 settings

Up to this point the axes were being controlled using the computer keyboard to jog them, using this method there was no indication whether the axes were moving accurately. To test if the axes were moving as intended G-code was written to move the axes in a 10mm square, graph paper was used fixed to the X and Y axes and the spindle was positioned to just above the paper. Executing the G-code revealed that there was something wrong with the calibration of the machine; the axes produced a 5mm square. This was solved by increasing the number of steps per millimetre to 400, it appears the controller was running in half steps meaning that the number of steps per revolution was doubled. The 10mm square test was run again and it confirmed that the axes were now functioning as intended.

3.6.2 Sherline Setup for 3D Deposition

Initial modifications

Before deposition could be started several modifications were necessary. The stock cables for the CNC mill were far too short, extensions were made using Din5 connectors which matched those already used on the controller and the stepper

motors. Also there was no emergency stop button, for this the input labelled as "G61" on the controller (Figure 3.46) was used.

E-stop buttons are normally wired between a pin on the parallel port and ground with a normally closed button, if at any point the connection between the pin and ground is broken, either by pressing the button or pulling the cable out the machine will immediately stop.

For the Sherline controller the input used was located on pin 13 on parallel port 1, two E-stop buttons were wired in series, one near the machine and another near the workstation keyboard.

As the Mk3 does not require a machining spindle, the outputs labelled as "spindle" were used to control the air solenoid. These outputs were located on pins 6 and 7 on parallel port 2 and output 24v. The original spindle had a manual speed controller built into the assembly mounted on the Z-axis, so it was safe to assume that this voltage was constant as opposed to PWM.

By using two pins on the parallel port instead of just one pin and a ground connection the spin direction of the spindle could be controlled by changing which of the two pins was energised and which one was connected to ground. In G-code this is controlled by the M3 (forward) and M4 (reverse) commands.

As the reverse was not necessary a 24v relay was connected to the spindle output, the switching pins of the relay were connected to the air solenoid foot pedal connector.

In Mach3 the spindle output was setup as a relay and tied to output #1 in the configuration, then output #1 was configured to pin 6 on parallel port 2, the output for pin 7 was also setup so it wouldn't remain as a floating pin (Figure 3.48).

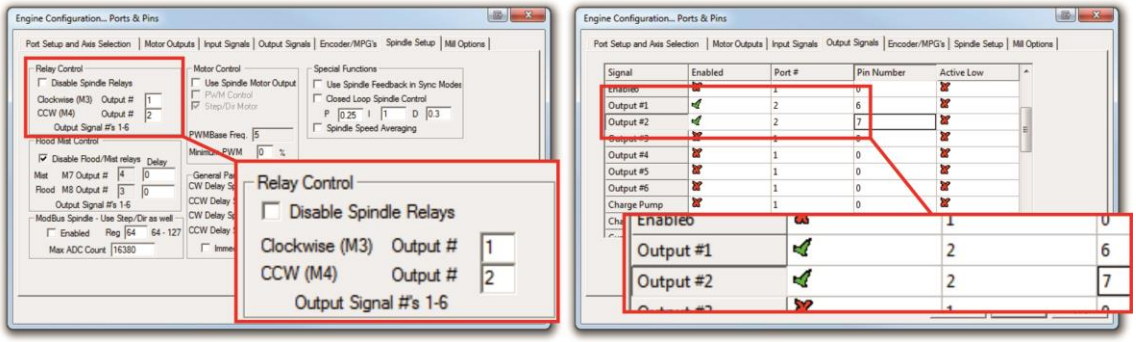

Figure 3.48 ,screenshot of Mach3 software, spindle/air solenoid configuration. figure by author

This modification allowed Mach3 to trigger the air solenoid whenever an M3 command was encountered in the G-code program, the M5 command cleared the output signal to turn off the air solenoid.

Deposition head v1 for Mk3

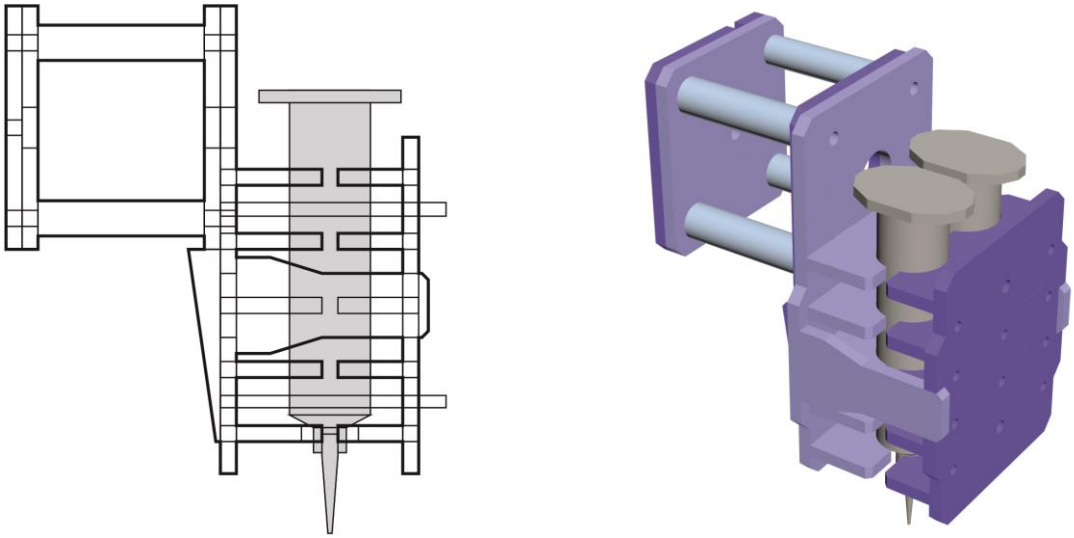

Figure 3.49, Deposition head v1. Left: side view of design, syringes in grey. Right: 3D rendering of assembled deposition head, syringes in grey. figure by author

The deposition head was designed in 2D in Corel Draw (Appendix B), it was laser cut from 5mm clear acrylic sheet and assembled (somewhat similar to a 3D puzzle Figure 3.49), 52mm long aluminium tube spacers were added to the mounting assembly to match the machining centre (100mm) of the original spindle. The deposition head featured space for two syringes to allow for future experimentation with dual materials. The syringe clamp was designed with narrow holes at the bottom so that the syringes would always be at the same height when installed. A digital microscope camera was also installed onto the deposition head (Figure 3.50).

The deposition head was laser cut for two reasons: laser cutting provides a short lead time so any modifications to the design can be quickly implemented and if any parts break there is a limitless supply of spares.

Deposition plate V1 for Mk3

For initial trials with the Mk3 equipment the same deposition plate as that used in the Mk1 was used. To install it onto the Mk3 four holes were drilled in the bottom plate to fix the plate onto the X axis t-slots. The plate was installed off centre from the Y axis to increase the travel range of the Y axis. If installed in the centre the plate would hit the Z axis post before the full travel of the Y axis.

Mk3 cabinet installation

The footprint on the Sherline mill was too narrow to be operated free standing so the mill was fixed onto a 20mm thick aluminium plate, this in turn was installed onto a steel t-slot table and enclosed in a cabinet, Figure 3.50 shows the installed Mk3.

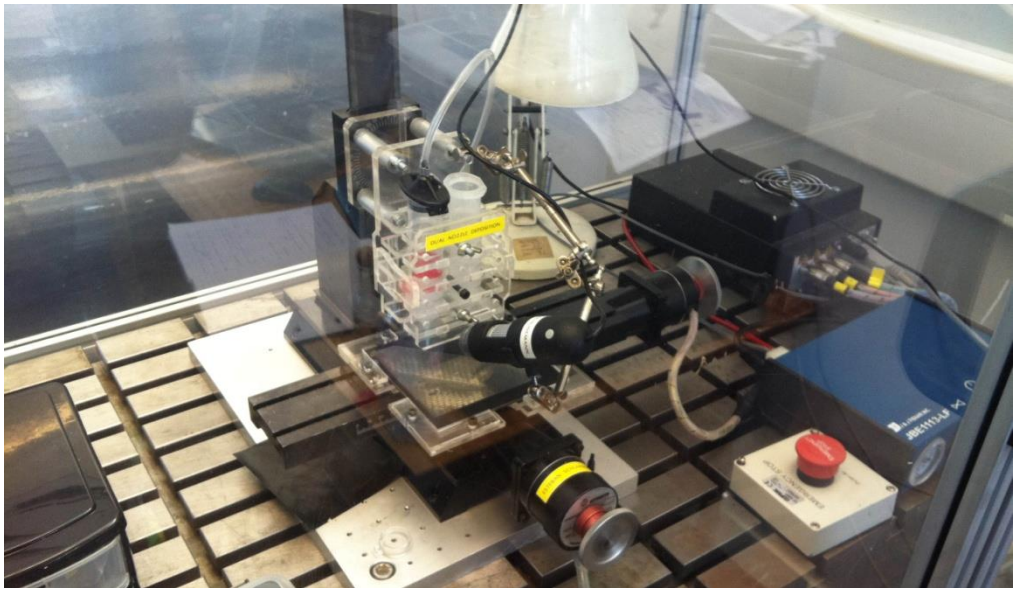

Figure 3.50, Mk3 machine with v1 deposition head + digital microscope camera and v1 deposition plate. figure by author

Control pendant

Most CNC machines, particularly large industrial models have a device called a pendant, this works as a control pad to position the axes, zero coordinates, calculate machining centres... most of the operations that can be done from the workstation can be done from the pendant, but with the convenience of close line of sight with the

machine. As the cabinet for the Mk3 is about two meters from the workstation it was thought that a pendant would be an appropriate addition.

There are USB CNC pendants available in the market, however there was a spare Xbox 360 controller available that could be used instead. Mach3 supports user created plugins, searching though the list a plugin for the Xbox controller written by Lee Davis (Davis, n.d.) was located and installed once configured the plugin allowed for easy control of the Mk3 with the two analogue sticks; one of the buttons was used to trigger the air solenoid.

3.7 Early Deposition Trials with PDM Mk3 Equipment

3.7.1 PDM Mk3 Workflow Development

The method for working with the Mk3 was very different from the other two systems, it required as much programming for the G-code as it did for tool path design. Reading through chapter 4 of Computer Numerical Control by Stenerson (2007) and the G and M code help tool in Mach3 helped get to grips with how to write and understand G-code, it was also useful to try out some of the code on the machine to appreciate the kinetic effects different instructions had. It was not very different from programming for the Mk1, there were just more commands and functions available.

First deposition trial

As with the development of the Mk1 and 2 there was only so much that could be read before practical experience was needed to move forward. For this test the code written to test the Mach3 configuration (10mm square) was modified to produce a square profile tube. This was done by copying and pasting the same code over and over and increasing the Z value with each repetition.

For this first build a similar layer height strategy as that used with the Mk2 was used, every five layers has an adjustment layer to account for vertical shrinkage of the soft silicone layers, Table 3.14 shows the setup for 30 layers, the parameters used were: Feed-rate: 400mm/min, Pressure: 1.5Bar, Nozzle: 0.6mm, Layer height: 0.6mm, Adjustment layer height: 0.3mm, Material: Acetoxy silicone.

Layer no.	Layer height (mm)	Layer no.	Layer height (mm)	Layer no.	Layer height (mm)	Layer no.	Layer height (mm)
1	0.6	9	5.1	17	9.3	25	13.5
2	1.2	10	5.4	18	9.9	26	14.1
3	1.8	11	6	19	10.5	27	14.7
4	2.4	12	6.6	20	10.8	28	15.3
5	2.7	13	7.2	21	11.4	29	15.9
6	3.3	14	7.8	22	12	30	16.2
7	3.9	15	8.1	23	12.6		
8	4.5	16	8.7	24	13.2		

Table 3.14, Layer height setup for first build on Mk3 equipment. in blue: adjustment layers, adjustment 0.3mm. table by author

The build completed successfully, but the surface finish was uneven and collapsed, this was because it was a single filament build and therefore unstable. The purpose of the test was to see how the whole system worked together, the air solenoid was triggered correctly with the M3 and M5 commands and the G-code ran with no issues, Figure 3.51 shows what the tool path looked like in Mach3.

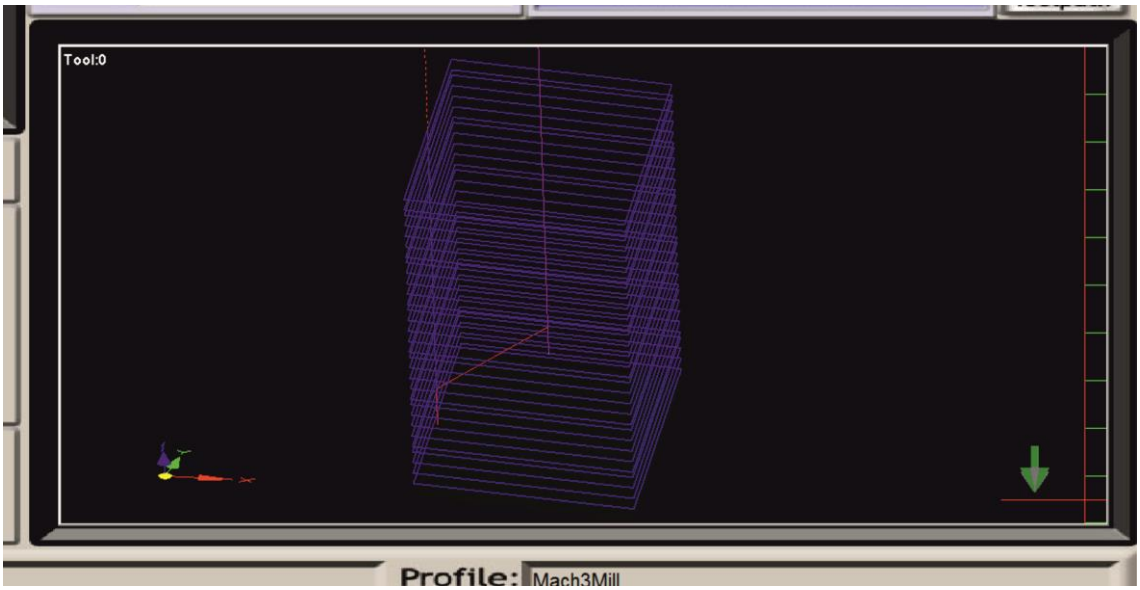

Figure 3.51, Screenshot of Mach3 software, first deposition test, 30 layers 10mm square tool-path view. figure by author

Vectors to G-code method

The previous test demonstrated that the Mk3 was functioning properly and that G-code instructions could be easily written. More complex tool paths such as the periodic structures in earlier tests or the circle in the Mk2 tests would be very complex and difficult to write, a method was needed to export vector lines drawn in Corel Draw to G-code that could then be modified and spliced together to form a 3D shape. Mach3 is usually sold with an accompanying program called CamBam, this program works almost like a slicer for additive manufacturing but instead it produces tool-paths for

subtractive manufacturing. One of the tools in this program is for setting up engraving operations, this was the tool used for converting vector files into G-code.

The process starts in Corel Draw where the vector lines that form the tool-path are drawn, the vectors are then exported to *DXF, an AutoCad file format compatible with CamBam. Once imported each vector object can be selected and the engrave tool applied to each, once all the engravings have been setup a button that generates machining paths in CamBam is pressed. This generates the actual tool-paths that will be converted to G-code but at a default height of -0.4mm; this, of course could be changed to the desired height in the engrave settings but it is much faster to do this in the G-code file instead of changing settings for each object. CamBam maintains the original position and direction set in the vector object when it was drawn meaning that no other settings need any attention.

Once the machine tool-paths are ready (this can take some time depending on the complexity of the path) then the G-code can be generated. On the default settings CamBam produces a *.Gcode file with no line breaks between individual instructions, however changing this to *.tap (G-code format compatible with Mach3) line breaks are inserted and the code is easier to understand and edit.

This method took some time to develop as there was plenty experimentation with different formats until the process could be streamlined and applied to 3D deposition.

3.7.2 45° Periodic Build on Mk3

45° build with coarse pitch

This trial was aimed at testing the process of converting vector files to G-code just described but in a practical application. A similar design to the already well established periodic tool-path was used but with the filaments aligned to 45°, this was a cosmetic choice.

The design of the tool-paths can be seen in Figure 3.52, the filament pitch of 1.6mm accounts for the filament thickness so the space between the filaments is reduced to 1mm as shown in orange, this is true only if this tool-path is built with a 0.6mm nozzle. Only two layers were designed and the G-code for each layer was repeated in sequence, the layer height values were written in manually.

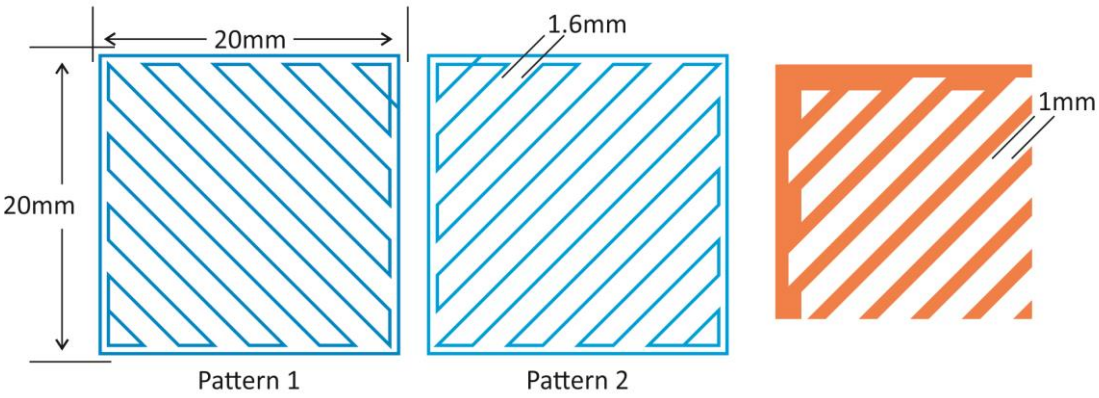

Figure 3.52, 45° coarse pitch tool-path design, both layers in blue. orange shows the design with the deposited filament thickness and actual pitch. figure by author

Initially this build used the same layer height strategy as that used in the previous build (Table 3.14) however the build failed on the second layer, the layer height of 1.2mm was too high. So the build was retried but with a different layer height strategy, the first layer would remain at 0.6mm but all consecutive layers were 0.4mm.

The parameters used were: Feed-rate: 400mm/min, Pressure: 1.5Bar, Nozzle: 0.6mm, Fist layer height: 0.6mm, Consecutive layer height: 0.4mm, Adjustment layer height: None, Material: Acetoxy silicone, Number of layers: 10.

This build completed successfully, it was also re-build several times to ensure that the Mk3 was functioning consistently, on the third build however the X axis stalled for a short period leading to an offset on the position of the axis and also the build, at this time it was not clear why this occurred, but lubricating the lead screws helped.

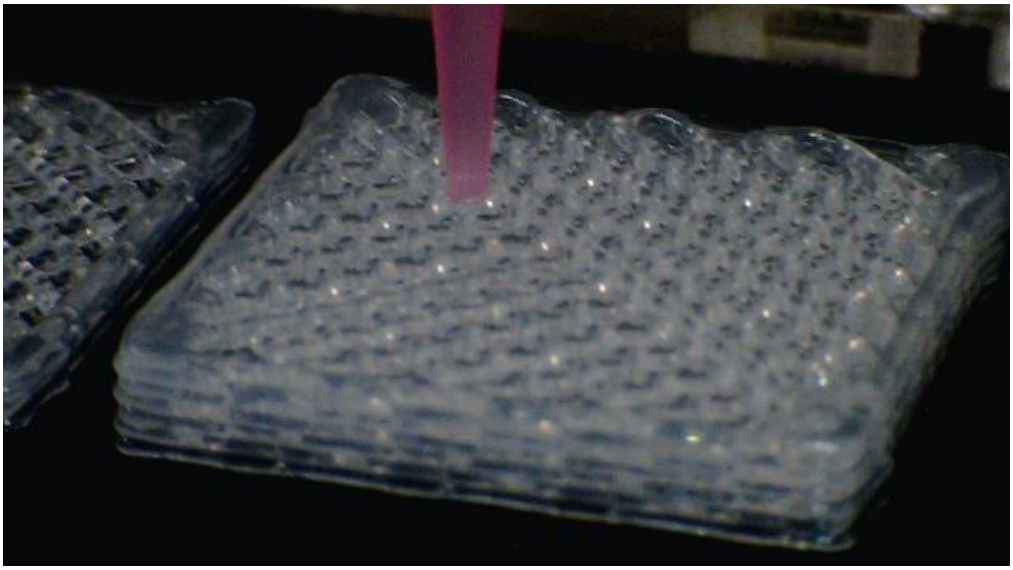

Figure 3.53, 45° build in silicone with 0.6mm on Mk3, on the far left: failed build due to X-axis stall. figure by author

When this batch of samples was made a new feature of mach3 was learned, the software uses two sets of coordinates, one called machine coordinates and the other called tool coordinates. When creating more than one sample the tool was zeroed to a new area and the build was made there, zeroing the tool did not affect the machine coordinates making it possible to return to origin. This process simplified the building of samples in batch as no changes needed to be done to the G-code, the machine origin was not lost and the build plate did not need clearing.

45° build with fine pitch

A build using the same parameters as before was planed, with the difference that this build would have a finer filament pitch of 0.8mm, this would leave a spacing of 0.2mm between filaments and test the repeatability of the Mk3 Figure 3.54 shows the tool-paths designed.

The same process of building the G-code was used, however there was an issue. The trial version of Mach3 was limited to 500 lines of code, the G-code for the 45° coarse build had 494 lines of code, the fine pitch build had 760 lines, so the two options left were either build the sample with less layers or figure out a way to use less lines of code.

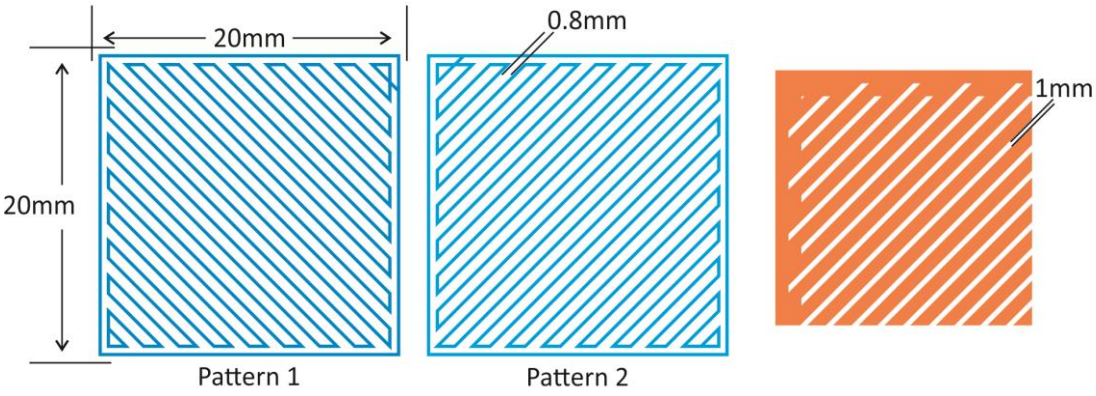

Figure 3.54, 45° fine pitch tool-path design, both layers in blue. orange shows the design with the deposited filament thickness and actual pitch. figure by author

2D programming method

looking at the G and M codes library in Mach3 two useful commands were found, M98 and M99, these codes are used to call a subroutine (M98) and indicate the end of a subroutine (M99) meaning that it was possible to reduce the lines of code required to build the fine pitch tool-path, the following shows the syntax of the command:

M98 P3 L2

This command calls a sub routine, the P defines which one and L defines the number of repetitions, in this example it is subroutine '3' and it is repeated twice.

o3 (subroutine name, command starts with the letter 'o', the integer is the name)
(subroutine content here)
M99 (end of subroutine)

The process of using subroutines also required changes to how the Z layer heights were written into the G-code file. They could either be set up as a list with calls to the subroutines containing the tool-path between them or variables could be used.

The command '#n' where 'n' is an integer can be used to define a variable, the variable can contain numbers, variables can also be used in movement instructions. The practical effect of this is that a variable can be used to store the Z layer height, then the Z axis can be positioned using the data stored in the variable:

#1 = 0.6 (define variable and inject value)

Z #1 (move Z axis to value stored in variable #1)

Arithmetic operations are also possible with variables:

#1 = 0.6 (define variable and inject value)
#2 = 0.4 (define variable and inject value)
#1 = [#1 + #2] (variable #1 injected with the value of #1 (0.6) plus #2 (0.4))

The arithmetic operations can also be used when moving an axis without changing the value of the variables:

Z [#1 + #2] (moves the Z axis to the sum of variables #1 and #2)

This subroutine method of programming was applied to the fine pitch code and it reduced the number of lines of code from 760 lines to 177, Figure 3.55 shows a flow chart on how the code works. Variable '#3' was used to retract the Z axis to a safe position before moving to the start of the next layer.

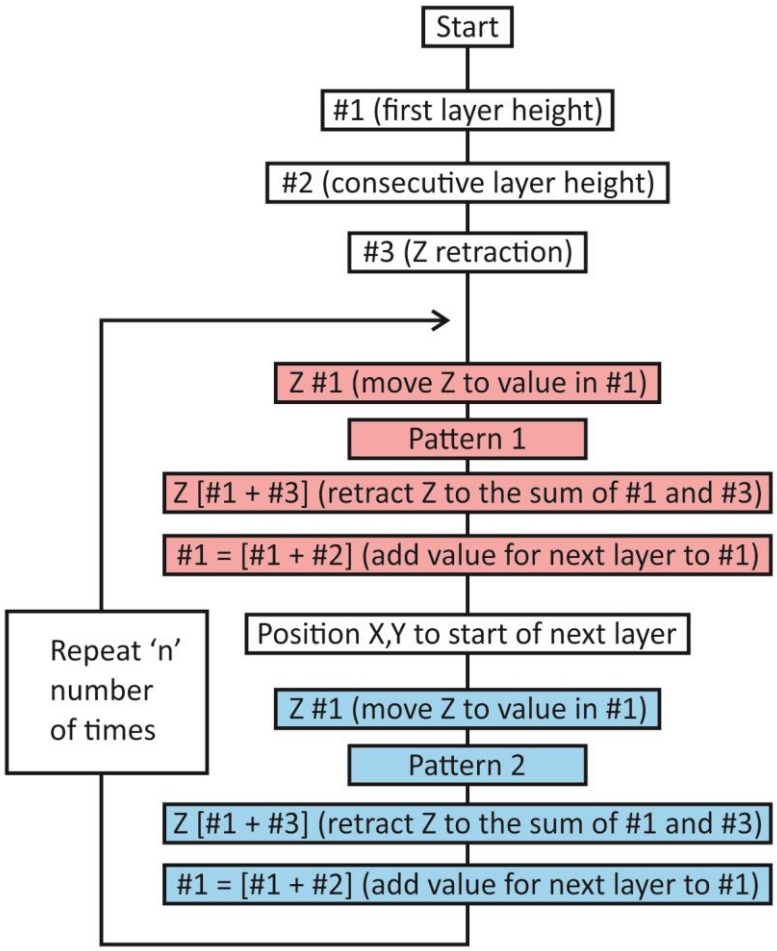

Figure 3.55, Programming flowchart for G-code subroutines and variables. figure by author

The first sample built with this new code completed successfully however there were some issues with the internal structure not mating properly with the perimeter wall where the filaments had a sharp change of direction.

Mach3 has two path control modes, constant velocity and exact stop, switching between these modes is done by using the commands G64 and G61 respectively. In constant velocity the program looks ahead for the next coordinates and maintains a constant velocity, this can lead to some inaccuracies in sharp corners due to the acceleration required. in Exact stop mode the program accelerates and decelerates between coordinate points stopping momentarily at each point thus producing sharper corners.

The code was modified with the G61 command and deposition was retried, the first sample failed, the Z axis was zeroed too high and the layer quality suffered, once this was corrected the build was tried again and this time it successfully completed and the

mating of the inner structure with the perimeter wall was much better. this build was done several times to confirm the results, Figure 3.56 shows the builds.

The parameters used were: Feed-rate: 400mm/min, Pressure: 1.5Bar, Nozzle: 0.6mm, First layer height: 0.6mm, Consecutive layer height: 0.4mm, Material: Acetoxy silicone, Number of layers: 10.

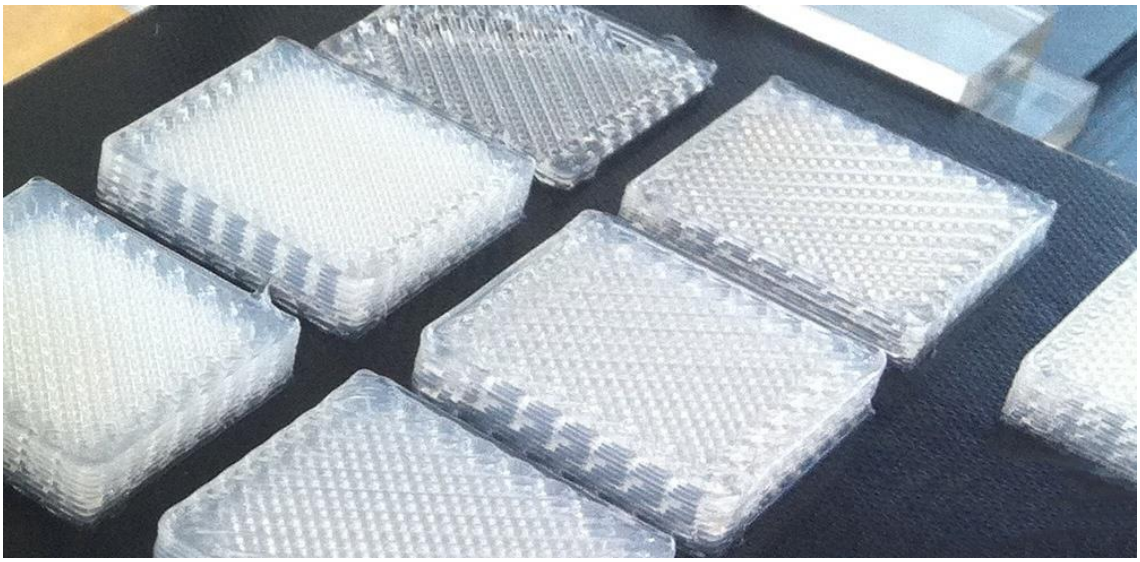

Figure 3.56, Batch of fine pitch 45° builds, failed print at the top. figure by author

The filament line spacing in the samples was kept consistent throughout all the builds demonstrating that the Mk3 was capable of delivering consistent results. The tests have helped develop a good methodology for creating complex tool-paths, the programming method allows for quick changes to the build parameters such as layer height, feed-rate and number of layers with very little effort meaning that the programs can be repurposed and changed to suit a desired application in a short lead-time. This is exactly what was done for a collaboration project with a masters student, the details and experiments from this collaboration can be found in the next section.

3.8 Deposition of Natural Materials (Collaboration)

Masters student Efthymios Drakos (2012) research was based on additive manufacturing with natural and renewable materials to lessen the environmental impact that AM might have, the MK 1 was initially used by Efthymios to test some of the materials and determine basic print parameters such as air pressure and nozzle height. This took place during the transition period between the MK2 to MK3. His research was then moved to the MK3 where square periodic structures were built to

test if the materials were self supporting and could hold a 3D shape without becoming an indistinguishable mass.

For these tests the 45° coarse pitch tool path developed in the previous section was used (it was rewritten with subroutines), however a small change was made. From the preliminary testing of the materials with the Mk1 it was found that the filament quality improved if each layer pattern was repeated twice, this decreased the appearance of filament deformation by depositing a layer of the same pattern over the previous layer, Figure 3.57 shows the result of this modification, note the wavy surface of the filaments under the top layer.

Figure 3.57, Deposition of two layers of the same pattern, improved filament quality. Material: Talc + PVA. figure by author

The same tool-path was used on all the materials to aid in comparison between them; all builds also used the 0.6mm nozzle.

3.8.1 Dextrin

The first material tested was Dextrin, it is a starch based adhesive with a translucent caramel colour.

This material proved to be very challenging to deposit because it is mixed by hand from powder and water leaving air bubbles in the mix; these bubbles were big enough to occasionally cause interruptions in the filament deposition leading to gaps. Nonetheless deposition was possible.

The parameters used were: Feed-rate: 200mm/min, Pressure: 4Bar, Nozzle: 0.6mm, First layer height: 0.6mm, Consecutive layer height: 0.4mm, Material: Dextrin, Number of layers: 10, Teflon substrate.

The Layers deposited with Dextrin lacked definition (Figure 3.59A & Figure 3.58), filament deformation was present due to the viscosity of the material which was similar to that of a thick molasses. Only a small number of samples were fully completed, the failure rate of this material was too high.

Figure 3.58, Left: deposition of Dextrin with Mk3, Right: explosive structural failure of Dextrin while drying. figure by author

The samples produced were solid enough to handle within an hour of deposition. They were left to dry further over a period of three days. However the samples never made it past the third day as the internal stresses from the shrinking exceeded the strength of the Dextrin which resulted in the structure exploding (Figure 3.58). This structural failure could have been due to the air bubbles present in the material, however the mixed Dextrin does not degas naturally due to the viscosity and applying centrifugal forces did not help reduce the amount of trapped air.

From this test Dextrin was found to be unsuitable as a primary material for AM due to its self destructive tendencies. Nonetheless Dextrin could be a candidate material for support structures, as it is soluble in water. The time frame for the explosive structural failure could be long enough for the build to finish, and if left to the side the support would be self removing.

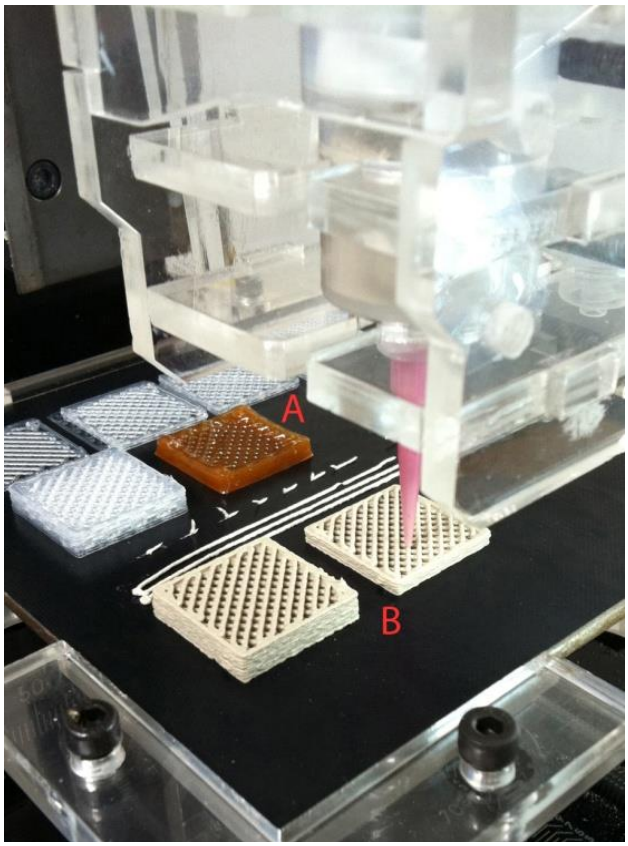

Figure 3.59, Deposition of natural materials with Mk3. A: Dextrin, B: Clay. figure by author

3.8.2 Clay

Nylon reinforced clay

The first clay tested was Nylon reinforced; it was reduced from its original block form to a paste with the same techniques used for the metal clay in the Mk1 tests. The deposition of this material was very troublesome; the first attempt the Nylon clay failed to extrude past the nozzle, it was remixed with more water. This mix successfully extruded, however a 0.8mm nozzle had to be used, the tool path was scaled up to account for this. During deposition of the sample the extrusion pressure varied greatly from 2Bar up to 6Bar in the production of one sample.

The parameters used were: Feed-rate: 400mm/min, Pressure: 2Bar-6Bar, Nozzle: 0.8mm, First layer height: 0.8mm, Consecutive layer height: 0.6mm, Material: Nylon clay, Number of layers: 10, Teflon substrate.

It is thought that the issues with the extrusion pressure were caused by the Nylon fibre content in the clay causing blockages. The clay also had to be mixed to a low viscosity to permit extrusion; this viscosity was too low for good detail. Aside from the extrusion

pressure issues, the clay also had air bubbles in the mix, which caused the failure seen in Figure 3.60.

All these issues meant that Nylon reinforced clay had to be dropped from further experimentation.

Figure 3.60, Deposition with Nylon reinforced clay, 0.8mm nozzle, moment the build failed. figure by author

Clay

The next material to be tested was regular clay; this was mixed from powder with water using the same technique as before.

The clay was an excellent material for deposition, the filaments exhibited little to no deformation, and the structure did not distort as the layers built up on the still wet material. The grain size of the clay however left a rough quality to the filaments but this did not affect the construction.

The parameters used were: Feed-rate: 400mm/min, Pressure: 1.1Bar, Nozzle: 0.6mm, First layer height: 0.6mm, Consecutive layer height: 0.4mm, Material: clay, Number of layers: 10, Teflon substrate.

Upon drying the samples showed very little warping; shrinkage was also very small, the structures shrunk from the original 20.6mm down to 19.6mm which equates to a total shrinkage of 5.102%. Figure 3.59B shows the clay structure as it was being deposited.

3.8.3 Talc

Talcum powder was chosen because it is a relatively inexpensive and naturally occurring mineral, making it suitable under Efthymios' criteria. Talc however is not soluble in water, so to mix it into a paste a small amount of PVA to act as a binder was added along with water. The resulting paste, displayed excellent deposition qualities (Figure 3.57).

The parameters used were: Feed-rate: 400mm/min, Pressure: 4.7Bar, Nozzle: 0.6mm, Fist layer height: 0.6mm, Consecutive layer height: 0.4mm, Material: Talc + PVA, Number of layers: 10, Teflon substrate.

Out of ten samples produced only two failed due to air bubbles in the paste, it worked better than expected. The surface finish of the filaments was better than the clay samples; this was probably due to the finer grain size of the talc. The shrinkage at 8.42% was acceptable given the DIY nature of the mixture, yet the samples warped once dry, the once straight filaments were curved in all three axes as shown in Figure 3.61.

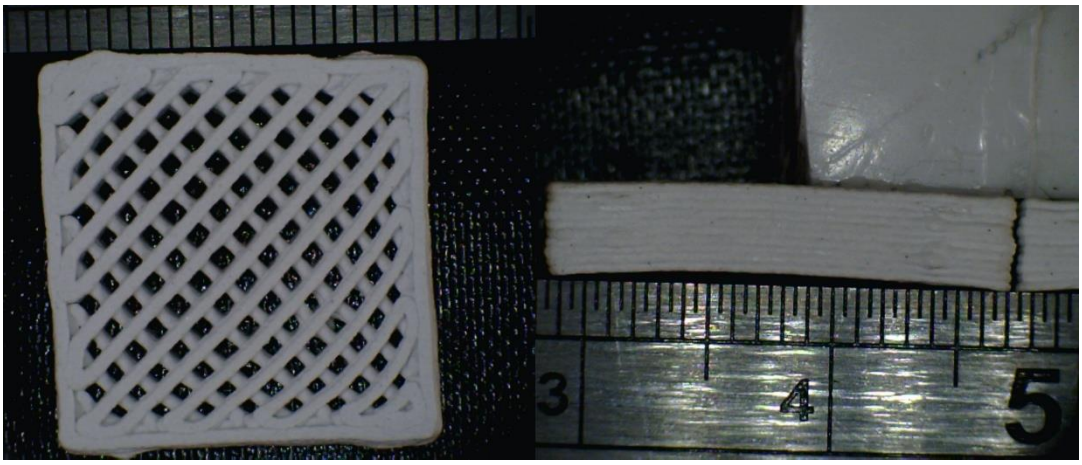

Figure 3.61, Talc and PVA dry samples, images showing warping. Left: top view, Right: side view. figure by author

3.8.4 Latex

Latex by all accounts would be an excellent material for AM, it is cheap, natural, and comes from a renewable source, it is also air drying and elastic which would be useful for some applications.

The original viscosity of Latex was too low for deposition; thickener was added to help raise the viscosity. With this it was possible to deposit and form layers, however it was

soon discovered that the material could not sustain the layers on top, causing the whole structure to droop and spread. This was alleviated by some degree by allowing the Latex to dry for one minute between layers, however this was not enough to solve the problem completely and the structure still drooped. A longer drying time might have helped but the latex was also drying at the tip of the nozzle which in some cases blocked the nozzle.

Due to the issues encountered this sample was built using a 90° periodic tool path as it was simpler to deposit (Figure 3.62).

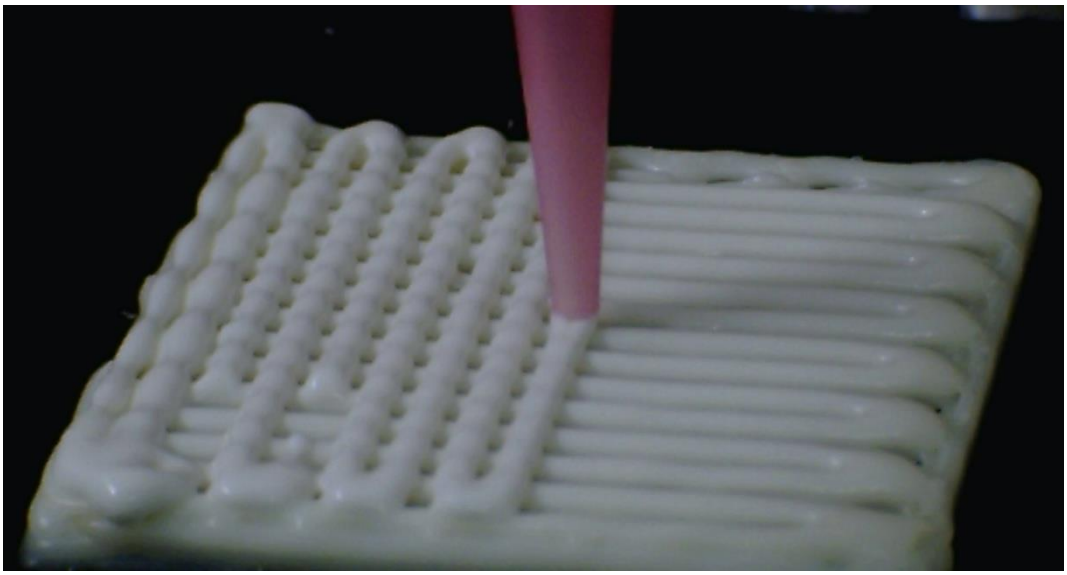

Figure 3.62, Deposition of Latex, 90° periodic structure. figure by author

The parameters used were: Feed-rate: 450mm/min, Pressure: 1Bar, Nozzle: 0.6mm, First layer height: 0.6mm, Consecutive layer height: 0.4mm, Material: Latex + thickener, Number of layers: 10, Teflon substrate, One minute pause between layers.

Due to the low pressure required to deposit the Latex, the feed-rate was raised from the usual 400mm/min to 450mm/min to compensate for the high material flow-rate.

3.8.5 Bees Wax

The tests with the Bees Wax were the last of this collaboration project; the wax was supplied in pellet form and required heating to permit extrusion. For this a syringe barrel, nozzle and piston were designed, both the barrel and the nozzle with an opening of 0.5mm were machined out of aluminium, the piston was machined from PTFE. The barrel was wrapped in a flexible silicone 12v heater pad and a thermocouple

was placed between the barrel and the heater (Figure 3.63). During deposition this assembly was wrapped in insulation to help maintain a stable temperature.

The deposition of the bees wax was difficult, aside from the regular deposition parameters such as layer height, air pressure, feed rate and nozzle size. The temperature of the wax and therefore the voltage used to heat up the barrel had to be adjusted and monitored.

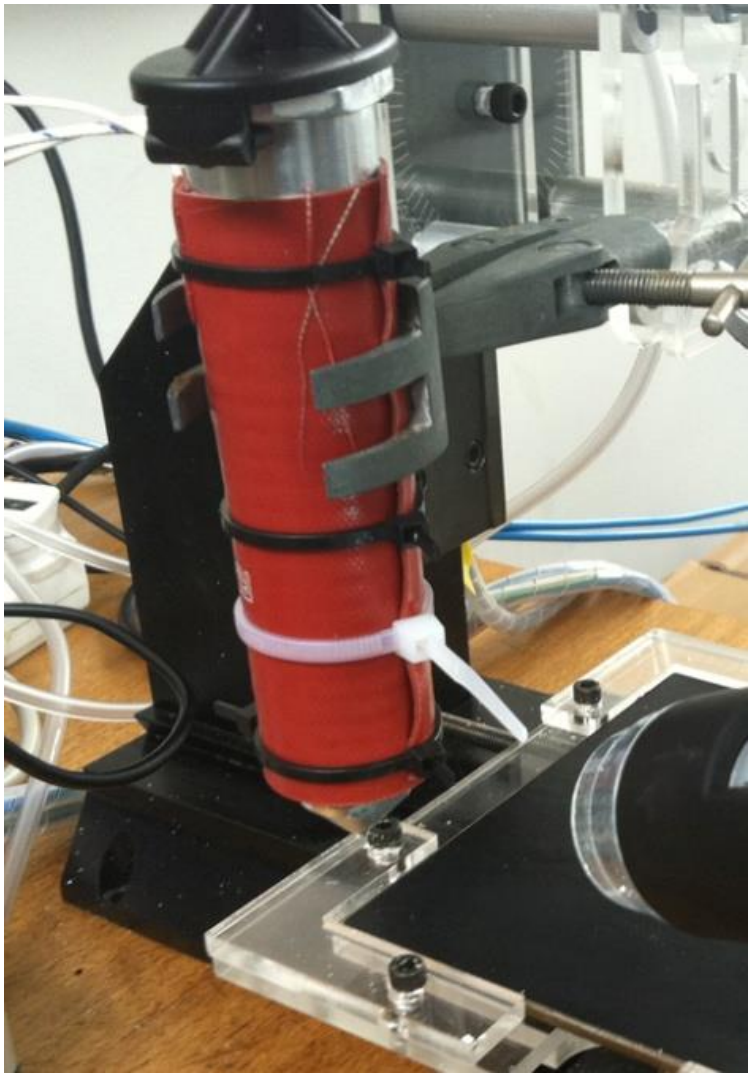

Figure 3.63, Bees Wax extruder set up. Aluminium barrel and nozzle, PTFE piston. figure by author

Extrusion test

The main issue to overcome was how to determine the ideal deposition temperature and heater voltage. Extrusion was successfully achieved at around 50°C however maintaining that temperature was next to impossible as the temperature kept increasing until eventually the wax was too liquid for 3D deposition. The initial temperature was correct, but the voltage to the heater was too high.

By setting the voltage to 7v and leaving the wax filled barrel to heat up for one hour prior to extrusion, it was found that the temperature was maintained stable during extrusion; and therefore the viscosity of the wax was kept constant, this experiment was repeated with a thermal imaging camera to record the temperature of the extruded wax.

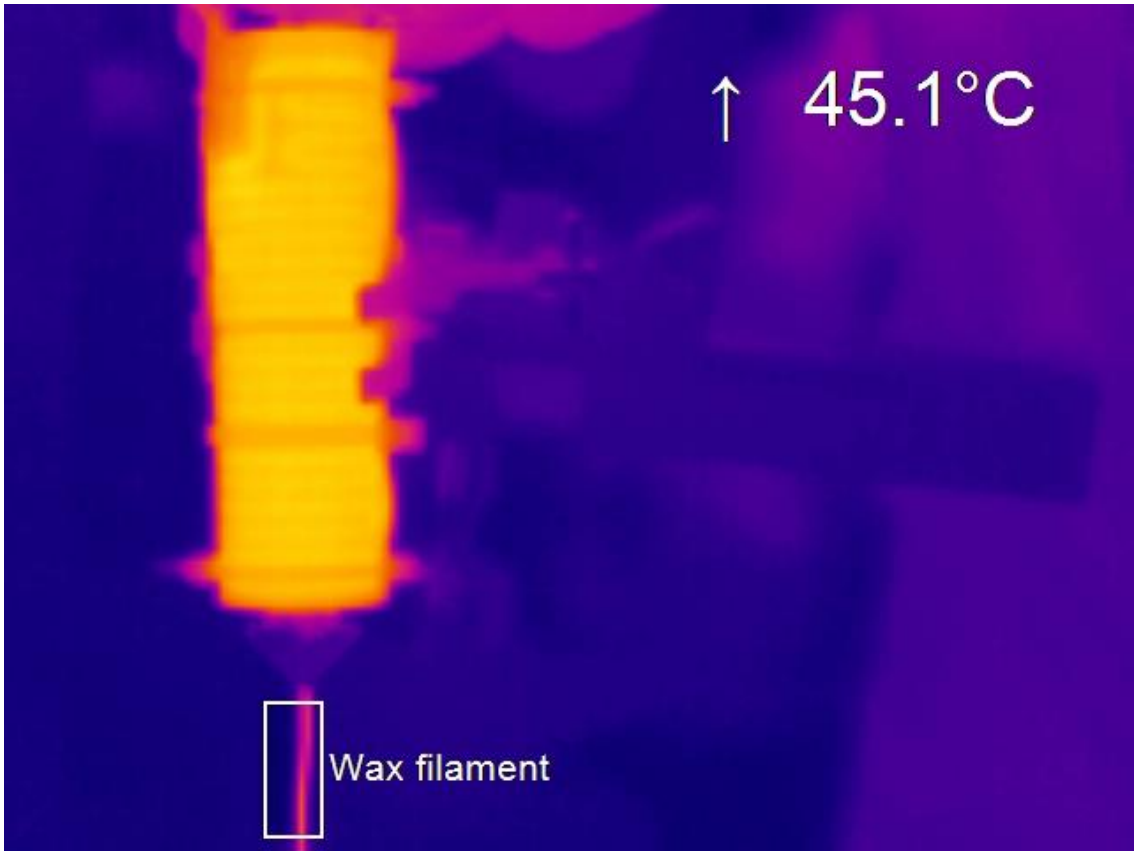

Figure 3.64, Thermal image of wax extrusion test, wax was left to warm up for one hour prior to test

The thermal imaging picture (Figure 3.64) taken without the insulation around the barrel, shows the temperature of the filament as it was extruded from the nozzle. The syringe was left to warm up to 50°C for one hour prior to this photo, the thermocouple showed a temperature of 50°C but the extruded wax was at 45.1°C according to the thermal image. This discrepancy could be attributed to the fact that the thermocouple was mounted outside the barrel and not inside measuring the actual temperature of the wax.

Deposition test

The air pressure and voltage needed some small adjustments during deposition of the samples due to there being less wax in the barrel but these changes were no bigger than 0.8V and 0.5 bar.

During the test several samples were produced with varying degrees of success, finding the ideal deposition parameters was difficult because it was not always clear why a particular sample failed.

One of the issues encountered was layer bonding, particularly at the start of layers, the freshly deposited filament would be dragged across the surface of the layer and the build would fail. This was solved by adding a small 0.5s delay between starting the extrusion and the axes moving, this gave the wax enough time to bond to the layer and the filament was not dragged. The feed-rate was decreased from 400mm/min to 300mm/min to reduce the strain on the wax filament and the first layer height was decreased to 0.5mm to match the nozzle size.

The extruder temperature was kept at 50°C (thermocouple) as established from the extrusion test; the voltage used was slightly lower than 7v as the syringe was covered in insulation. One test was run at 60°C but this failed as the wax was too liquid.

The parameters used were: Feed-rate: 300mm/min, Pressure: 2.7Bar, Nozzle: 0.5mm, Fist layer height: 0.5mm, Consecutive layer height: 0.4mm, Material: Bees Wax, Number of layers: 10, Teflon substrate, Temperature:~50°C, Heater voltage, 6.79v to 6v, Current: 467mA to 418mA, Layer delay: 0.5s.

With these parameters the deposition of bees wax was successful (Figure 3.65); producing several identical samples. On the other hand, the parameters that made it possible to deposit the wax also meant that the temperature of the wax was too low to ensure good layer adhesion; the samples were prone to delamination.

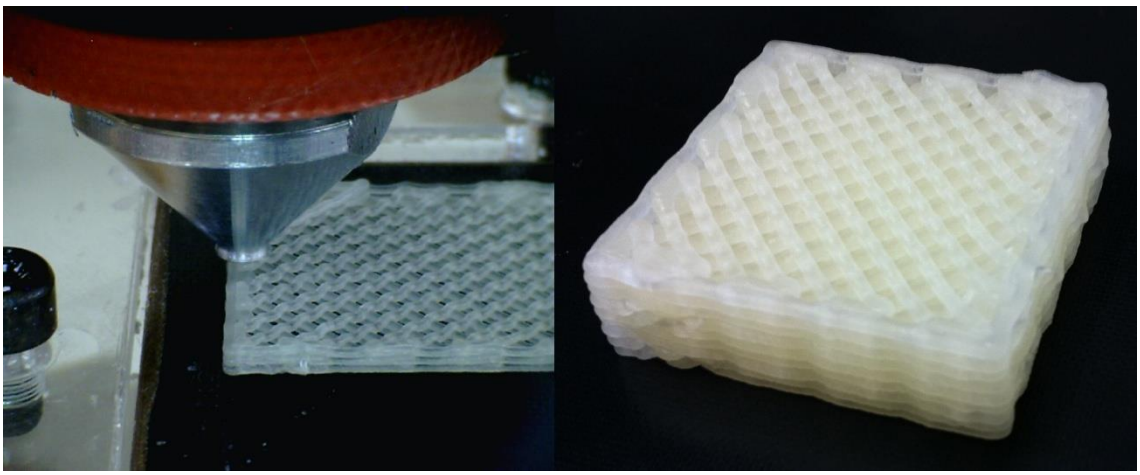

Figure 3.65, Left: deposition of Bees Wax sample with 45° coarse tool-path, Right: finished sample. figure by author

Delamination is not really an issue as the purpose of 3D deposition in wax would be to either form support structures or to be used in investment casting. So the strength of the part would not be a big issue. Other waxes particularly those designed for the purpose of investment casting might yield better results as they are more refined and homogeneous.

3.8.6 Deposition of Natural Materials Project, Closing Remarks

Whilst Efthimios, the masters student, was happy with the results obtained from the proposed materials, the results of the collaboration project were not particularly useful as experimentation would not continue with those materials. What was useful however was the experience and tacit knowledge gained through such diverse range of experiments. The working methodology with the Mk3 developed and became more efficient to deal with constantly changing parameters; this experience was something that was carried over to the rest of the research project. This collaboration project also demonstrated how versatile the chosen equipment was and confirmed it as a good platform for experimentation in AM. If the collaboration had run for a longer period then the focus of the experiments would have changed toward practical applications of the materials, and perhaps more complex and aesthetically pleasing samples.

3.9 Continued Deposition with Mk3

3.9.1 Development of parametric G-code

The 45° tool-path developed during the early tests with the Mk3 has up to this point worked well; the samples made in the Acetoxy silicone had an interesting feel to them. It is difficult to put into words how entertaining it was to play with the samples, yet the size left something to be desired, so work was set out to produce a bigger tool path.

Line limits

The first attempt at a larger version of the 45° tool path was met with disappointment, the path was designed to be 100 x 100 mm with the same 1.6mm pitch as the coarse tool-path. But the line limit of 500 lines of code on Mach3 was reached before the full code for one layer.

This build would require a different approach if the 100 x 100mm target was to be reached, an idea came up of using variables in G-code to build the tool-path, then any changes such as size and filament pitch could be adjusted with simple variables. The idea was to make a piece of code that could scale up or down to any size whilst remaining in the Mach3 line limit.

The code took some time to develop, the easier way would have been to do away with the 45° filaments and set them at 90°, the math would have been simpler. The advantage of using 45° filaments is that the machine can be run at a higher feed-rate, if both the X and Y axes are moving at 500mm/min, then using Pythagoras the resolved feed-rate should be 707mm/min, it was thought this increase in speed would be an advantage considering that the aim was to make a larger build.

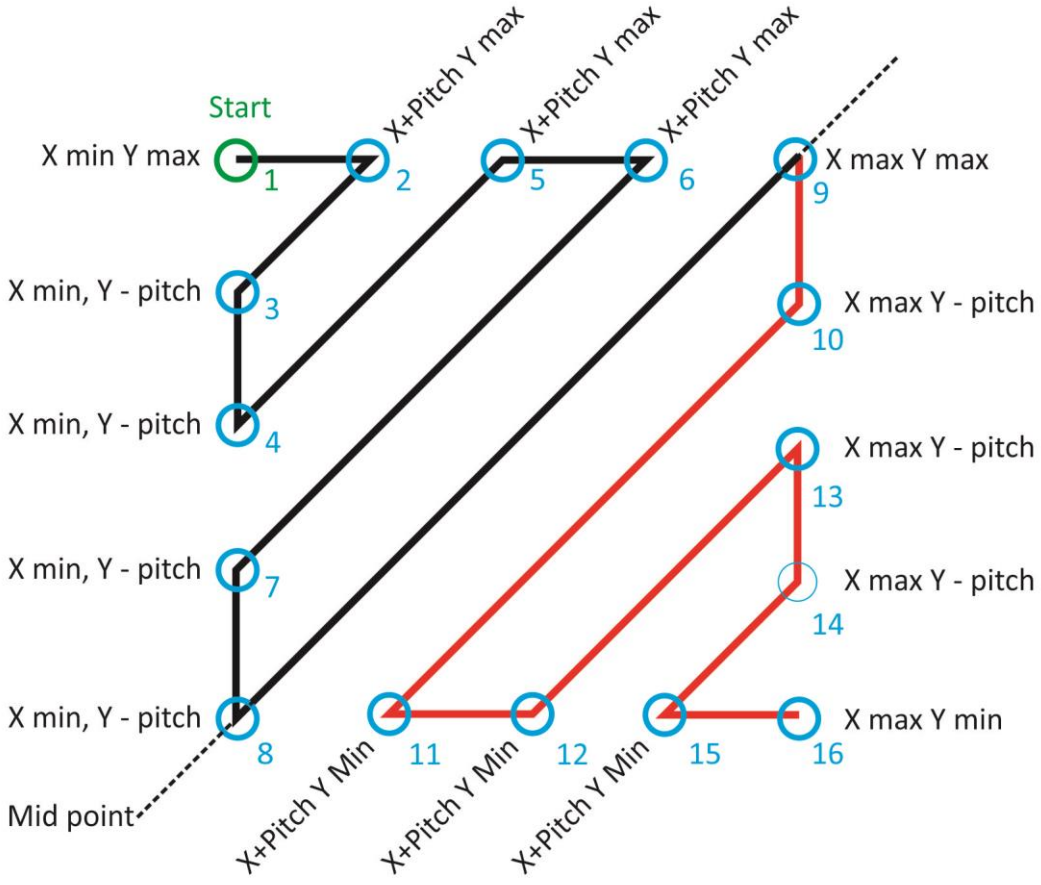

Figure 3.66, Parametric G-code, 45° tool-path, one layer. figure by author

There are two main parameters that are used to generate the tool-path, the dimension (both X and Y use the same) and the pitch, the code then sets the starting point as X zero (minimum) and Y as the largest dimension (max), essentially starting from the top left corner. The code then goes through a sequence of four commands which are

repeated (using a calculated number of repetitions) until the mid point is reached where both X and Y are at the largest dimension, this is the first pattern for layer one, shown in black in Figure 3.66. The second pattern (red in Figure 3.66) does another repetition of four commands and ends with X at the largest dimension and Y at zero (bottom right corner). The repetition of the four basic commands is calculated by dividing first the desired dimension by the pitch to determine the total number of filaments required then dividing that number by two to get the number of filaments each pattern must have to form a complete layer

When initially testing the code in Mach3 (no deposition yet), it worked well, the parameters set were 100mm for X and Y dimensions and 1mm pitch, however the code broke when the dimensions were not divisible by the pitch.

To fix this, the code needed to automatically adjust the desired dimensions to a value that was divisible by the desired pitch, to calculate this, the command 'FIX' was used. This command rounds down any given value or variable to the nearest integer, the number used to calculate the number of filaments ((dimension/pitch)/2) for each pattern was rounded down and then multiplied by the twice the pitch.

(FIX ((dimension/pitch)/2)) x (pitch x 2)

It is multiplied by twice the pitch because in an earlier calculation the dimension is halved to calculate the number of repetitions required to form half of one layer, conceivably this calculation could have been done without dividing the result of the dimension/pitch by two, then the rounded number wouldn't have needed to be multiplied by twice the pitch. But the way it was done reduced the number of lines and variables needed to make the corrections to the dimension and calculate the number of repetitions.

The result from this calculation gives a number that is divisible by the pitch and the tool-path can be generated properly, if the original dimension was divisible by the pitch, then the calculation would return the same number.

The second layer, which is rotated through 90° to the layer to form the cross-hatch pattern was programmed using the same method as the first layer, the only difference was that the starting point was at X zero and Y zero (see Appendix C).

Deposition with the parametric G-code

Deposition with this parametric tool-path was fairly straight forward as enough experience with the Mk3 had been gained by this point that only one quick test print was required to dial in the parameters. The tool-path was tested with different nozzle sizes from 0.2 up to 0.8; the most challenging one was the 0.2mm.

The first deposition test with the parametric code was done with a 0.2mm nozzle, the code was set to 100mm with a 1mm pitch, the first layer height was 0.2mm and the second layer was 0.1mm.

The build failed, there was a lot of filament curling present on the second layer, the nozzle also accumulated some silicone around the tip suggesting that it was touching the layer and picking up some parts of the deposited filaments. This suggested that perhaps the second layer height was too low; the test was repeated with a second layer height of 0.15mm. This did have some improvement but the nozzle was still accumulating some silicone around the tip which caused some damage to the rest of the layer.

The problem with silicone accumulating on the tip of the nozzle was solved by coating the exterior of the nozzle in machine oil (WD40), the layers produced with this modification had a big noticeable improvement, yet there was some curling present around the edges of the build, similar to the issue encountered during the Mk1 deposition trials. This curling was limited to an area of 10mm around the perimeter of the build, this was attributed to the acceleration of the axes and it was reduced from the original 100mm s^{-2} down to 50mm s^{-2} and the build was repeated. This did not completely remove the curling issue but it was reduce to an area of 5mm around the perimeter.

This build was completed at ten layers for a total thickness of 1.55mm, the parameters used were: Feed-rate: 700mm/min, Pressure: 5Bar, Nozzle: 0.2mm, First layer height:

0.2mm, Consecutive layer height: 0.15mm, Material: Acetoxy silicone, Number of layers: 10, Teflon substrate.

Initially the plan was to produce a scaled up version of the 45° tool-path used in the earlier tests, however it was soon found that this would not be practical, even with the increased feed-rate a single layer was taking 22 minutes when depositing with the 0.2mm nozzle, so reaching a thickness comparable to those builds would have taken a long time.

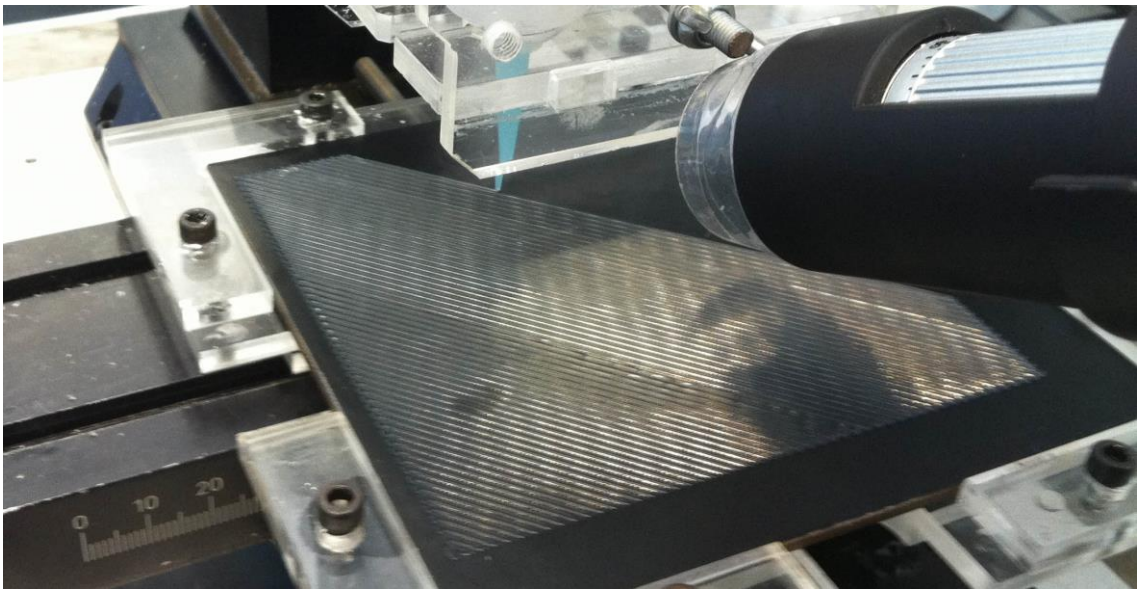

Figure 3.67, Deposition of Parametric tool-path, 0.2mm nozzle. figure by author

Several more samples were made with this tool-path using different nozzle sizes and coloured silicone, the results of these builds are in the Deposition of Silicone Fabric-Like Structures section in Chapter 4.

3.9.2 Shock Absorbing Jar Build

Radial tube build

The breakdown of the Mk2 equipment came at a time when experimentation with circular tool-paths had just started, it was decided at this stage that this should be revisited with the Mk3.

The tool-path designed for these trials was based on the work on 3D deposition with microcapillary nozzles by Gratson (2004), here the tool-path had two distinct layers, one with an array of radial oriented filaments (or spokes) and the other in a spiral-like pattern with the filaments intersecting the radial layer at 90° (Figure 2.55).

The spiral-like layer in Gratson's work was not exactly a spiral, it was a series of concentric circles increasing in size and joined at the top by a straight line.

The tool-paths were designed and programmed with the same '2D programming' method used for the 45° fine pitch build, these trials also used the same clear acetoxy silicone.

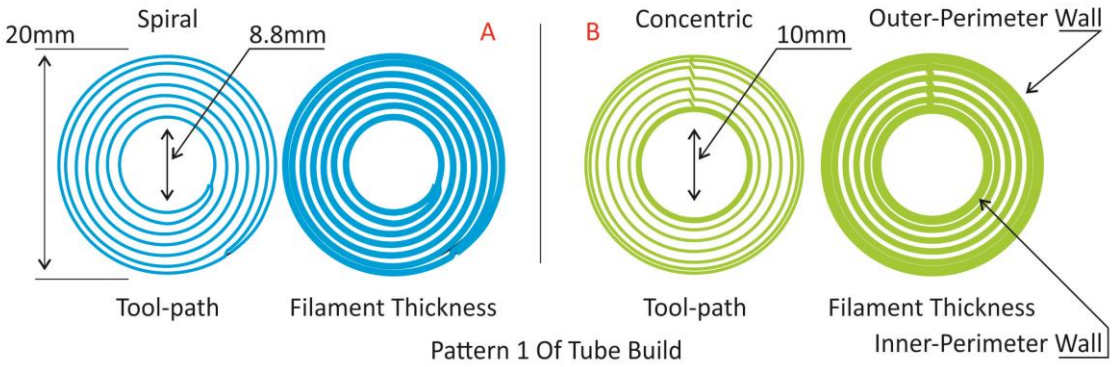

Figure 3.68, Spiral and concentric tool-paths for tube build. figure by author

The tool-path designed had 20mm outer diameter and an 8.8 inner diameter, instead of using the concentric circles to form the spiral-like layer pattern a spiral was used. The radial pattern designed had a spoke pitch of 5°; both the spiral and the radial pattern were combined to produce the full tool-path (Figure 3.68 A, Figure 3.69 A). However when depositing (with 0.6mm nozzle) this tool-path it was found that the spiral pattern did not perform well with some filaments binding due to close proximity in some areas and the radial pattern was too dense, producing almost solid layers.

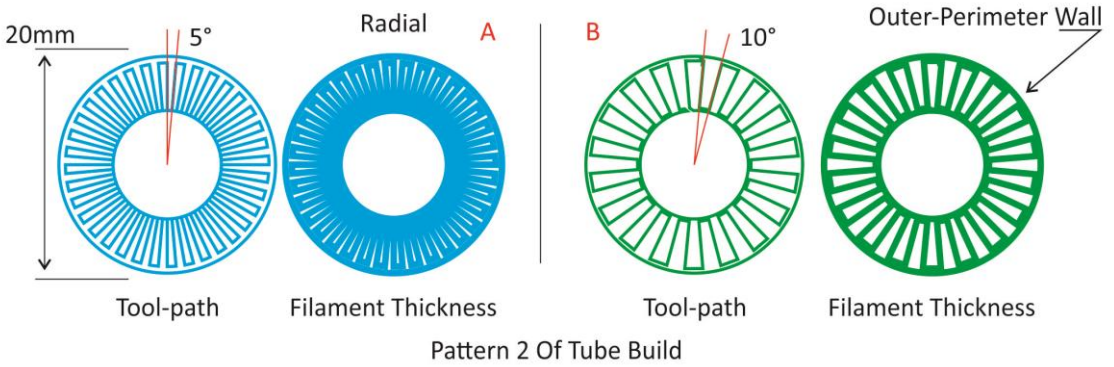

Figure 3.69, Radial tool-paths for tube build. figure by author

The tool-paths were modified to address these issues, the spiral pattern was changed to a series of concentric circles joined by straight lines (Figure 3.68 B) and the spoke pitch of the radial pattern was changed to 10° (Figure 3.69 B). The outer edges of the

radial pattern were moved closer to the outer-perimeter wall to improve the interaction between the infill and the perimeter. The inner diameter was also increased from 8.8mm to 10mm on both patterns.

The build with this improved tool-path was more successful with better filament definition and spacing, however the outer edges of the spokes in the radial pattern were struggling to meet the outer-perimeter wall properly, for these builds the G-code had been set to G64 (constant velocity mode), this issue was attributed to that mode as the tool head was not reaching the full extent of the spokes in the radial pattern due to the acceleration required. So the G-code was changed to G61 (exact stop mode) and the build was repeated, this caused another problem, the perimeter circles were made up of several arch moves, with the G61 mode it caused the machine to stop and accelerate several times at each arch move when producing the perimeter, this produced a very rough circle. The solution was to use the G61 mode only when the machine was producing the straight lines for the spokes, then switching to G64 for the circles.

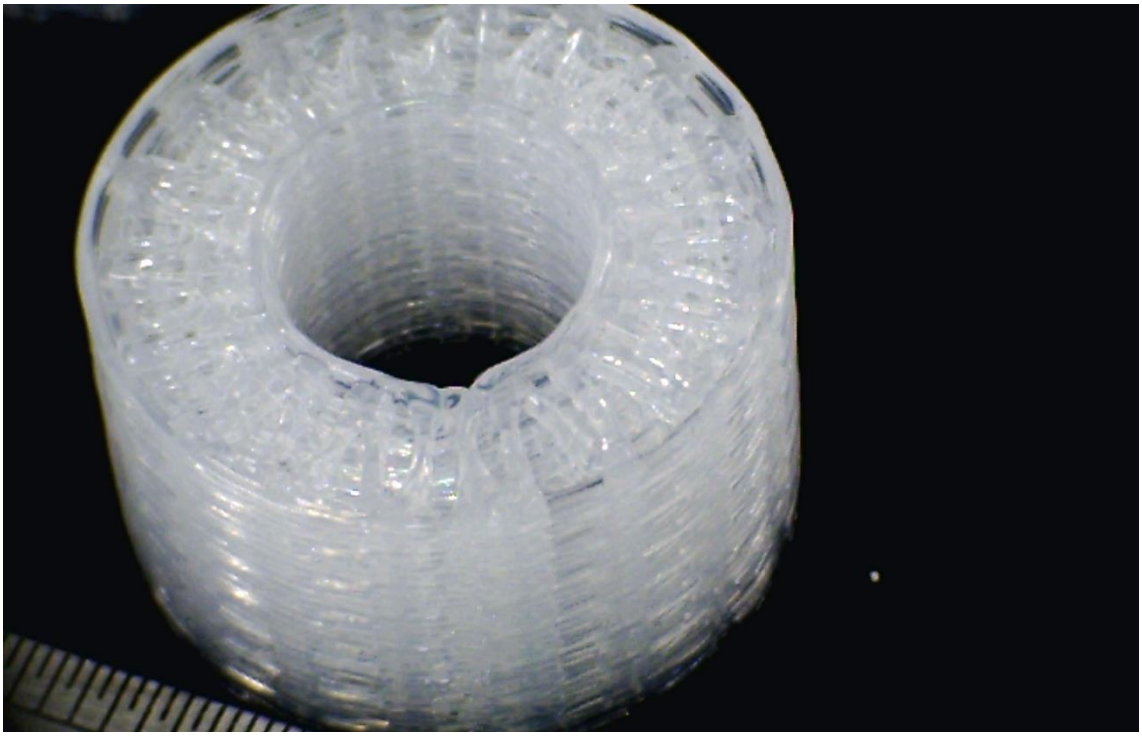

Figure 3.70, Tube build, completed at 20 layers with 0.6mm nozzle. figure by author

The build using both the G64 and G61 modes worked well (Figure 3.70) and completed at 20 layers, but the filaments from the concentric pattern sometimes struggled to span the gap between the spokes at the outer edges of the build. This was

to be expected, there is nothing much that can be done about this issue as the solution would be to increase the density of the radial pattern which would end up producing near solid layers, so the issue was left alone as it was not big enough to compromise the build.

The parameters used were: Feed-rate: 400mm/min, Pressure: 1.4Bar, Nozzle: 0.6mm, First layer height: 0.6mm, Consecutive layer height: 0.4mm, Material: Acetoxy silicone, Number of layers: 20, Teflon substrate.

Summary of the radial tube build

The tool-path for this build went through many iterations until it could be successfully deposited, the use of the G61 and G64 modes although already known from the 45° square build were crucial in this build.

The tube tool-path was developed further to create a practical application for the build; this could then be used to demonstrate a potential application for the process. The application was to use this as a jar or container for fragile objects, the structure of the tool-path and the thickness meant that it could be used to absorb impact shock, with the radial pattern acting as a 'crumble zone' dissipating the impact.

Sample jar tool-path development

The first step in transforming the tube build into a jar was to add a bottom that would close one end of the tube. The tool-path was based on the circular tool-path used during the Mk2 trials, but made to the same diameter as the tube.

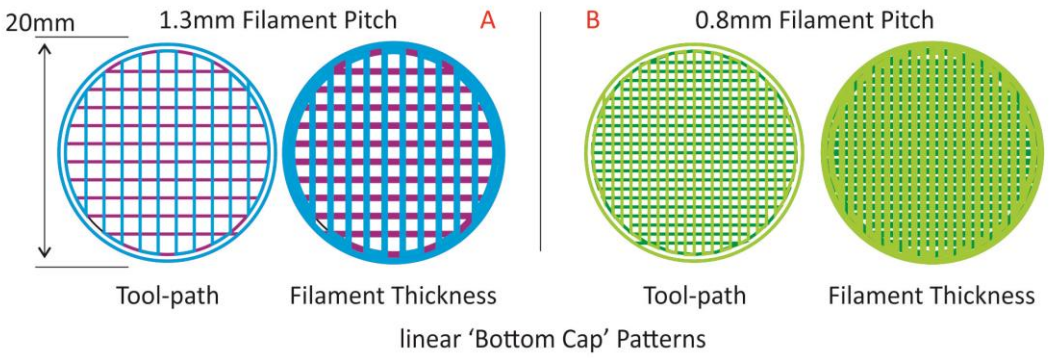

Figure 3.71, Tool-paths for the bottom of the jar build. figure by author

The first tool-path drawn had a pitch of 1.3mm between the filaments (Figure 3.71 A), after deposition it was noticed that the pitch was too large and the structure was not

very rigid, this was not a desirable property for a jar designed to protect fragile objects. So the tool-path was redesigned with a finer pitch at 0.8mm (Figure 3.71 B).

The build with this pitch was completed at 16 layers and it was much more rigid but there was an issue with silicone accumulating at the nozzle tip, this was surprising as the nozzle was coated in machine oil to avoid this exact problem. This could have been due to the layer height being too low and as a result the nozzle was touching the deposited silicone, to alleviate the problem the layer height was raised from 0.4mm to 0.5mm and the build was repeated. The modification did not completely remove the problem but it was greatly reduced and the quality of the build was perceptibly improved.

With the tool-path for the bottom of the jar now working it was added to the tube tool-path to produce the jar (Figure 3.72 A).

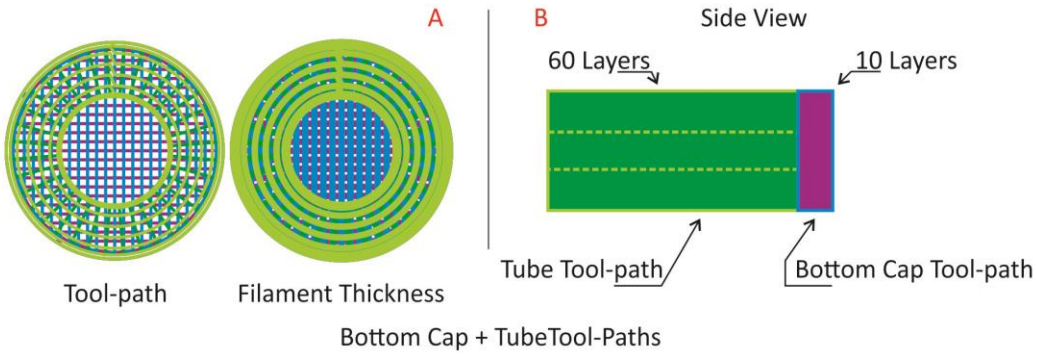

Figure 3.72, Layer plan for jar build, both the tube and the bottom cap tool-paths combined. figure by author

The Layer plan (Figure 3.72 B) for the jar was to deposit the bottom cap first to a height of 10 layers (5mm) and then deposit the tube tool-path to a height of 60 layers (30mm) giving a total height of 35mm. The deposition was successful but the accumulation of silicone on the nozzle tip lowered the quality of the deposition towards the top, this was particularly noticeable on the infill patterns and not so much on the perimeter surface.

The parameters used were: Feed-rate: 400mm/min, Pressure: 1.4Bar, Nozzle: 0.6mm, First layer height: 0.6mm, Consecutive layer height: 0.5mm, Material: Acetoxy silicone, Number of layers for bottom: 10, Number of layers for tube: 60, Teflon substrate.

With the main body complete, the jar now needed a cap, the same tool-path as the bottom cap was used for this purpose and a 8.5mm diameter 'post' was added so the cap could be held in place (Figure 3.73 A and B).

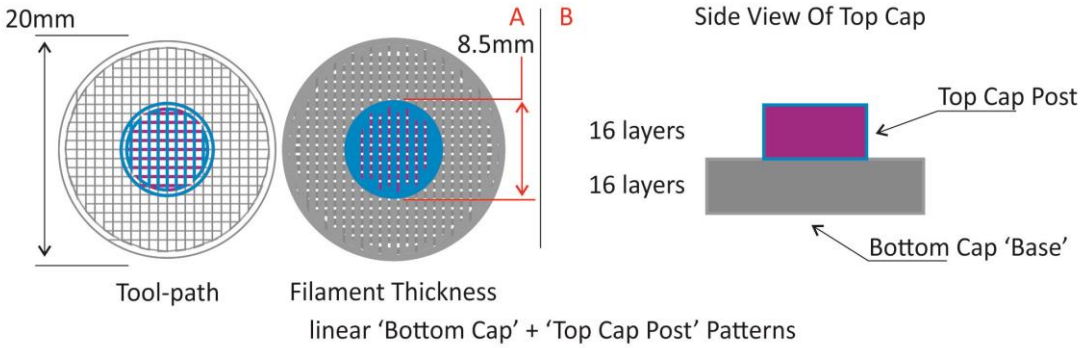

Figure 3.73, Tool-path and layer plan for jar cap build. figure by author

The deposition of this tool-path was tricky, not so much with the base as it was the same as the one used on the jar, the issue was with the cap post, it did not work well as it was too small for the density of the infill and it did not form well. To overcome this issue the build was repeated but this time with a smaller nozzle size, the layer heights were adjusted to 0.4mm for the first layer and 0.3mm for consecutive layers.

This build was much better and the cap post had good definition, but the interaction between the infill and the perimeter wall of the cap base was insufficient leading to weak bonding of the perimeter to the infill. The tool-path had to be redrawn to correct this, the infill paths were made longer so there would be better bonding, also to improve adhesion further the first few filaments of the infill were set to a smaller pitch at the beginning and end of the infill layer so they would be solid, a staggered pitch tool-path (Figure 3.74).

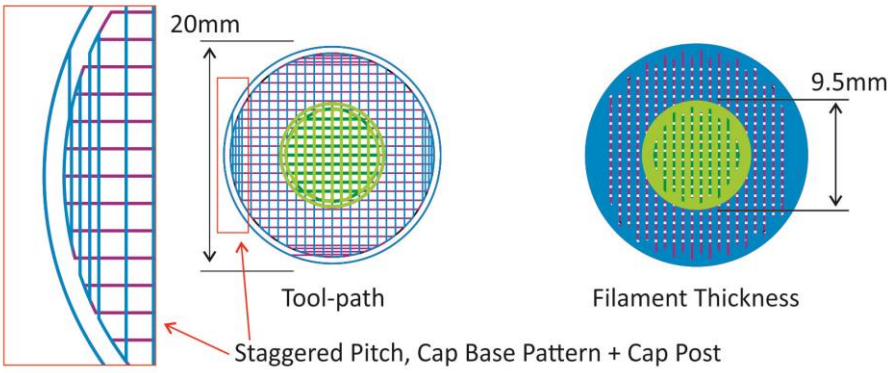

Figure 3.74, Revised tool-path for jar cap, staggered pitch strategy in red square. figure by author

Even though the cap base had issues, the cap post was good enough to test fit with the rest of the jar and it was found to be too small, this tool-path was redrawn as well to a larger diameter of 9.5mm.

The new tool-path deposited well with no issues, the parameters used were: Feed-rate: 400mm/min, Pressure: 1.6Bar, Nozzle: 0.4mm, First layer height: 0.4mm, Consecutive layer height: 0.3mm, Material: Acetoxy silicone, Number of layers for bottom: 16, Number of layers for post: 16, Teflon substrate.

Summary of sample jar

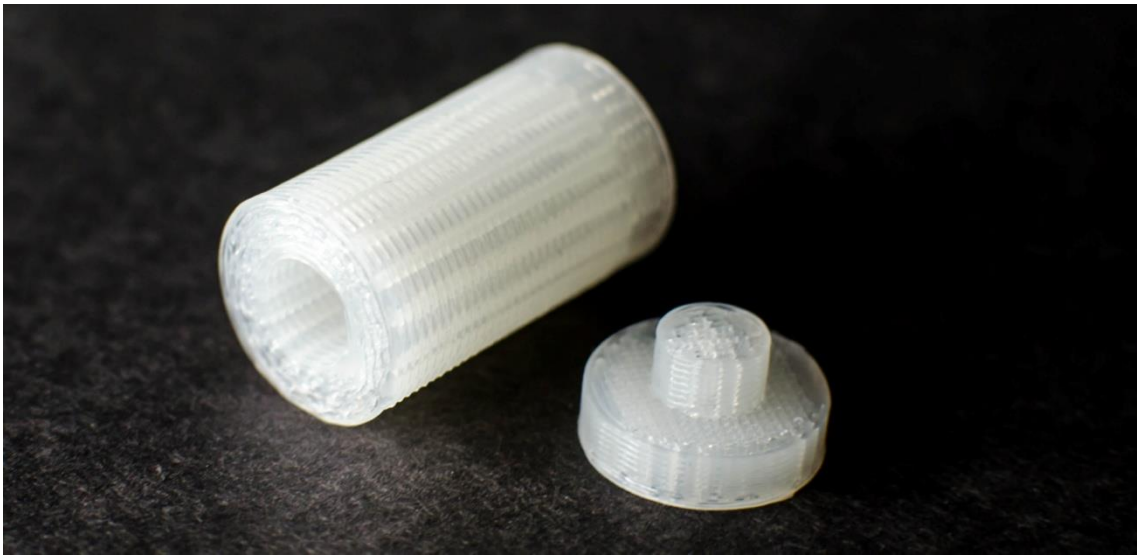

Figure 3.75, finished sample jar, left: jar main body, right: cap. figure by author

The code for the sample jar worked very well (Figure 3.75), up to this point this was the most complex tool-path made. The subroutine programming method used made it possible to manage all the different tool-paths and repetitions with ease.

Whilst the jar has not been tested with any standardised methods or equipment it was tested with a small glass vial and dropped 10m onto pavement, it was found to provide adequate protection against drops.

The radial tool-path used in the tube while effective for this application, the distance between the spokes towards the outer edges must be kept under control, if the wall thickness were to be increased then this distance may become too great for the concentric tool-path to span the gaps, the radial tool-path therefore has limited scalability.

3.9.3 Large cylindrical builds

The results from the sample jar test warranted further exploration into thick walled tubes. Up to this point the scale of artefacts and samples made were small, so the next series of tests were aimed at increasing the scale of builds whilst also exploring thick walled tubular structures.

When comparing the filament quality of the radial tube build with the 45° coarse square sample it was found that there were less flaws in the 45° sample, this was surprising as the tube build had the same pitch at the outer edges of the spokes as the 45° build (1.6mm). This however is a straight line measurement, the concentric tool-path that goes over the radial tool-path is round so this distance is actually slightly larger, however it can be surmised that perhaps the silicone can span gaps better when deposited in straight lines than it can when deposited in curves. This makes sense as the filament is under slight tension when spanning gaps in a straight line, when the tool-path is curved this tension is reduced and the filament is free to deform during deposition. This issue limits how thick the walls of a deposited tube can be made as the gaps become larger.

To address this issue a new tool-path had to be designed, one in which the infill patterns have straight lines so the wall thickness could be increased.

In commercial FDM machines, tubes are treated the same as any other type of geometry, this means that a tube or a square would receive the same infill, may it be rectilinear or honeycomb. The only other option available would be a concentric infill, but this would produce a tube either filled with thin concentric tubes or solid.

It was therefore necessary to design a whole new type of infill pattern specifically designed for thick walled tubular builds; this was called tessellated tube tool-path.

In the time between the sample jar build and these tests, the full license of Mach3 was purchased.

Tessellated tube tool-path

The tessellated tool-path is similar to the radial pattern used in the tube build (Figure 3.69) but the spokes are set at an angle and instead of a concentric pattern for the second layer the tool-path is mirrored forming the pattern shown in Figure 3.77B.

The main difference between the radial + concentric pattern (tube build) and the tessellated pattern, is that filaments are joined at 90° in the radial pattern whereas in the tessellated pattern the filaments are joined at a shallower angle, the filaments are also kept straight reducing the chance of filament breakup when spanning the gaps between filaments.

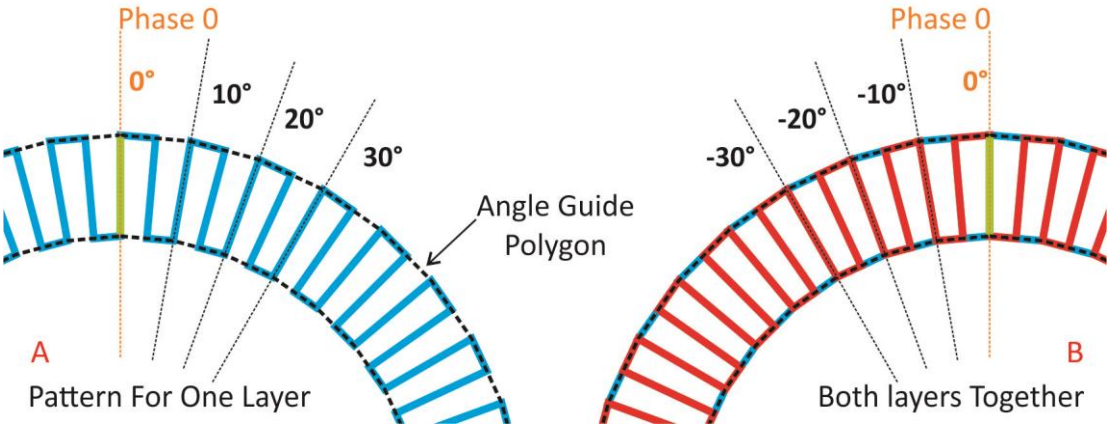

Figure 3.76, Tessellated tool-path at phase 0, A:pattern for one layer, B: patterns for two layers combined. figure by author

The pattern for a single layer is based on a 36 sided polygon, each spoke in the pattern stems from this polygon and is repeated every 10°. To draw this pattern the polygon tool in Corel Draw is used, this tool automatically repeats the pattern depending on the number of sides the polygon has; it is a simple process to arrive at the tessellated tool-path.

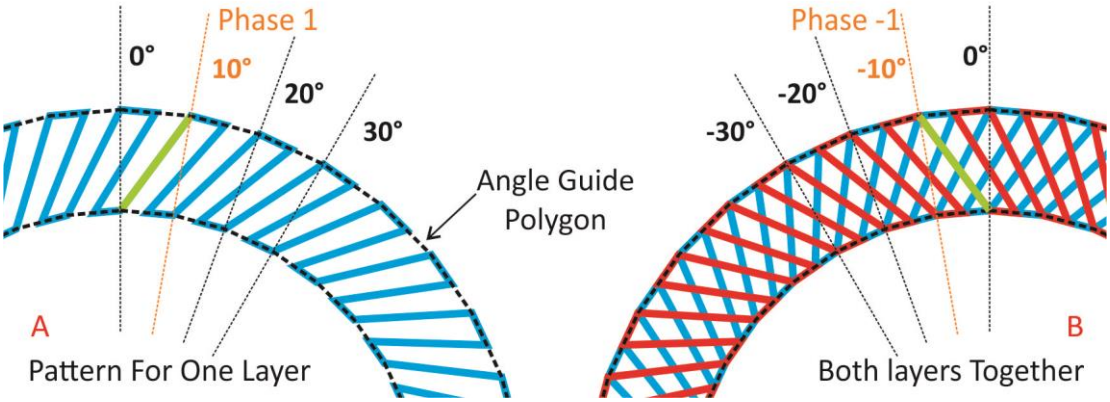

Figure 3.77, Tessellated tool-path at phase 1, A:pattern for one layer, B: patterns for two layers combined, Filaments cross over five times. figure by author

Figure 3.76A, shows the polygon with the spokes in a position that has been referred to as phase 0, this path is no different from the radial path. Using the angle guide polygon the edges of the path are shifted by 10° Clockwise into phase 1 (Figure 3.77 A), then to draw the second pattern and complete the tool-path a second polygon is created and shifted to phase -1 (-10°) (Figure 3.77 B). At phase 1 each filament in the tool-path crosses five filaments from the previous layer, shifting to phase 2 (Figure 3.78) increases the number of filament interactions to nine and makes the gaps between filaments smaller without increasing the number of spokes. So to increase the wall thickness of a build it may be necessary to shift to a higher phase if the gaps between filaments get too large to span across.

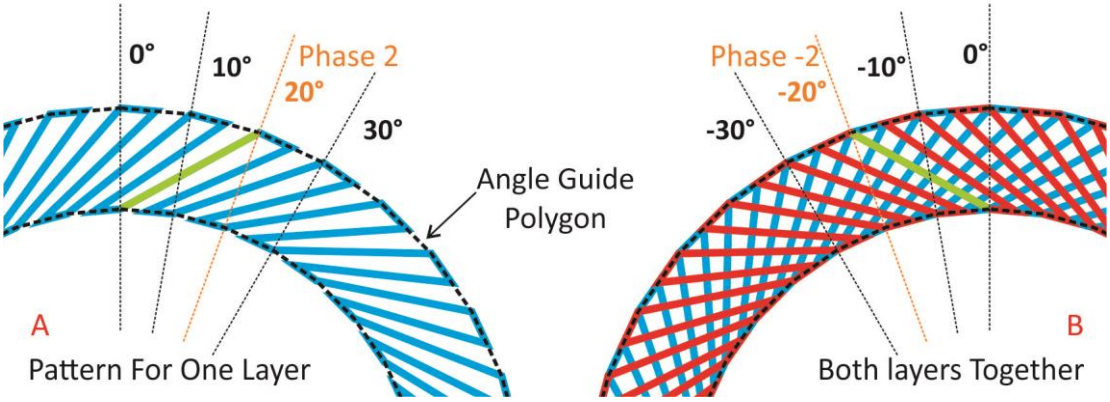

Figure 3.78, Tessellated tool-path at phase 2, A:pattern for one layer, B: patterns for two layers combined, filaments cross over 9 times. figure by author

It is important to differentiate the phase from the offset angle of the patterns, with a 36 sided polygon each phase is 10°, but with a 72 sided polygon each phase would be 5°, these polygons would produce a pattern with 36 or 72 spokes respectively.

Deposition with tessellated tool-path

Initial testing was done in a small scale with an outer diameter of 30.5mm and an inner diameter of 24.5mm, the tool-path was based on a 36 sided polygon. Because the walls were very thin the phase for the tool-paths was set to 0.5 (5°), this produced an open structure so observations could be made (Figure 3.79). Using the same subroutine programming method as before, the patterns for the tessellated tool-path were exported and the G-code program was built.

The first deposition was done using a 0.4mm nozzle, it was only built to four layers and the deposition quality was assessed. The outer edges of the spokes failed to adhere to the layers below, this was a similar issue to that encountered with the 45° build when using the G64 mode, so the build was repeated and the G61 mode was added to the infill, this somewhat helped but the problem was still present.

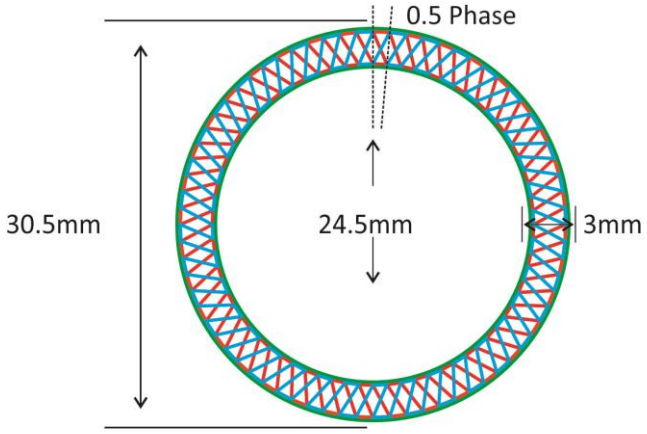

Figure 3.79, Tessellated tool-path for small scale test build of pattern. figure by author

Due to the scale of the build it was difficult to see what exactly was happening, so in Mach3 the scale was set to 200% to produce the same build but at a larger scale. It was made using a 1.2mm nozzle, the first layer height was 1.2mm and the consecutive layer height was 1mm. The build produced was 61mm in diameter and 11 layers (11.2mm) thick.

Figure 3.80, Build with 1.2mm nozzle showing the defects at the outer edges of the spokes. figure by author

This revealed what was going wrong, the area where the corner end of a spoke met the previous layer was too small, this caused the filament to be pulled off and drop in the gap between the filaments as show in Figure 3.80, the solution to this problem required a redesign of the tool-path.

The solution to this issue was to increase the size of the area where the outer edges of the spokes were interacting; this was done to only one of the two layers. As can be seen in Figure 3.81, the pattern of the second layer was designed to meet the previous layer not at the corner of the spoke but a third of the way on the perimeter filament of the spoke.

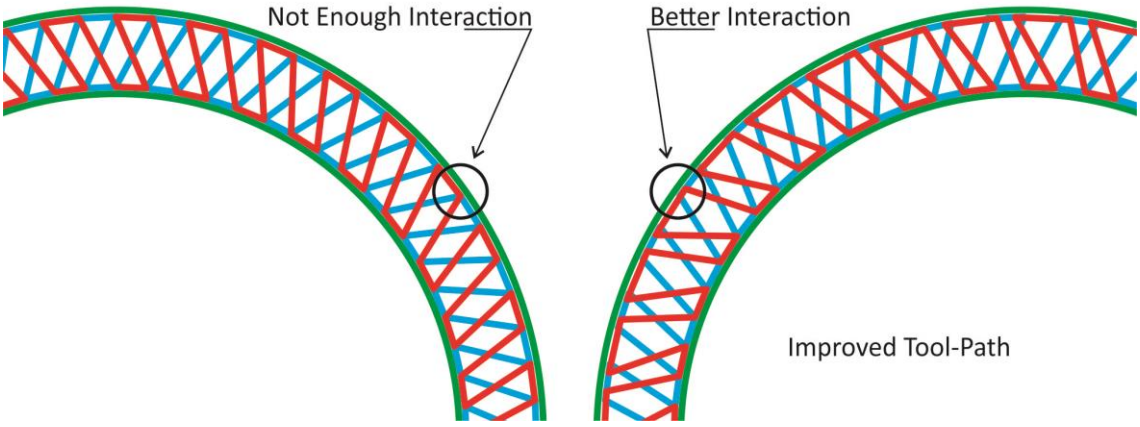

Figure 3.81, Improvement to tessellated tool-path to correct problems with the outer edges of the spokes. figure by author

To test the improvements of the tool-path it was decided that a small scale build would not be appropriate as the filaments would be too small, while redesigning the tool-path it was also scaled from the original 30.5mm to 61mm and adjustments were made to the perimeters (green in Figure 3.81) so that this tool-path could be deposited with a 0.8mm nozzle.

This build was successful and was completed at 20 layers (14.1mm), the layer heights were 0.8 and 0.7mm; there was some accumulation of silicone at the tip of the nozzle. Encouraged with this build, the number of layers was increased to 80 (56.1mm), this build failed due to a stepper motor stall. This time it was not due to lack of lubrication in the axes but rather to a windows update causing the computer to lag, after the update finished, automatic updates were promptly disabled to avoid this issue in the future.

The build was repeated using the same parameters as before, however by layer 25 the accumulation of silicone on the nozzle tip was starting to cause problems, so the build was paused and the silicone was cleared off the nozzle and the build was resumed, this was done every 20 layers or so until the build completed (Figure 3.82).

The process of pausing the build required timing as it had to be done when the nozzle was being lifted to reposition for the next layer, otherwise the silicone would have kept extruding as the 'spindle' in Mach3 is not turned off during a machining pause. The build consumed almost all of the silicone in the syringe (30cc).

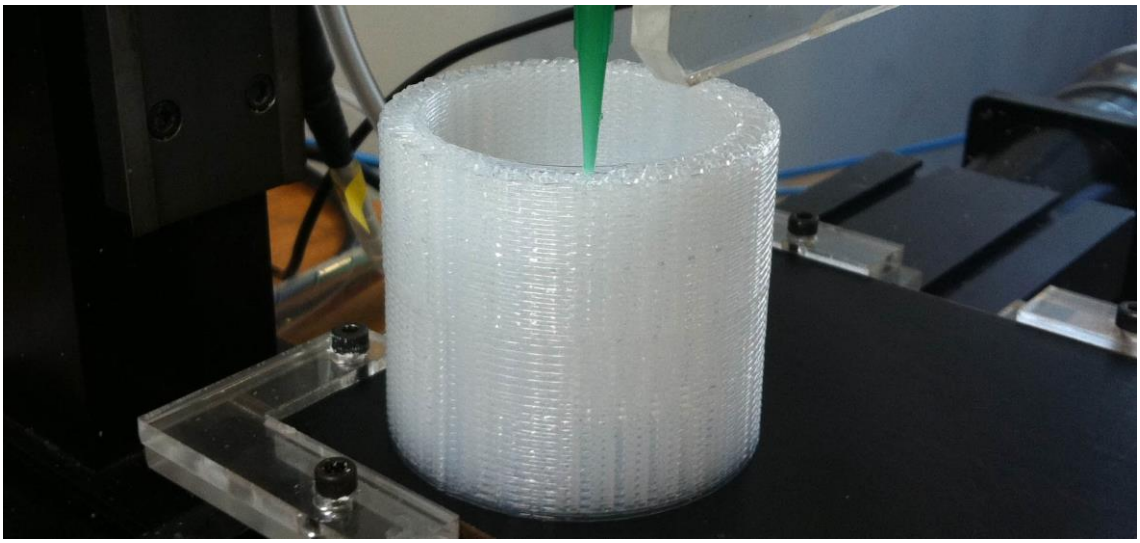

Figure 3.82, Large 61 x 56.1mm tube build with tessellated tool-path,0.8mm nozzle, clear silicone. figure by author

For the next build, the scale of the tool-path was scaled to 120% in Mach3 to see if a larger build could be made, also to allow for easy cleaning of the nozzle a pause and retraction routine was added to the code, this was done using the M1 (optional program stop) command to pause the build the nozzle was then retracted to 30mm above the build height, this was programmed for every 20 layers.

The modifications of the code were tested, however this build was cancelled at 10 layers because the perimeters were not adhering well to the infill pattern, so to quickly solve this without having to redraw the tool-path the layer height was changed from 0.7 to 0.65mm to create slightly wider filaments to improve perimeter bonding.

The parameters used were: Feed-rate: 400mm/min, Pressure: 1.1Bar, Nozzle: 0.8mm, First layer height: 0.8mm, Consecutive layer height: 0.65mm, Material: Acetoxy silicone, Number of layers for bottom: 80, Teflon substrate.

This solution worked well and the build completed successfully at 80 layers, which due to the lower layer height of 0.65mm was 52.15mm (the previous build was 56.1mm). The programmed pauses worked well and caused no issues with the quality of the build, the nozzle was recoated with lubricant at every pause to reduce the accumulation of silicone at the nozzle tip. This build felt softer than the build at 100% scale, this was most likely due to the infill having a lower density because of the scale up to 120%.

This tool-path was rescaled down to 50% to produce a 30.5mm diameter sample, it was made to a height of 32 layer (16.1mm) with a 0.6mm nozzle, this build completed with good surface and filament quality which demonstrated the scalability of the tessellated tool-path, Figure 3.83 shows the three samples produced with this tool-path.

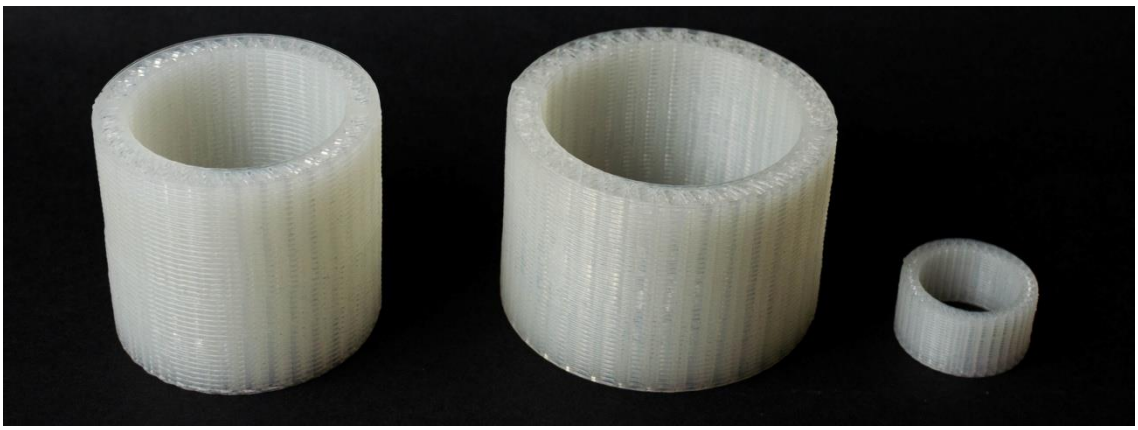

Figure 3.83, Collection of samples made during initial testing of tessellated tool-path, from left to right: 61 x 56.1mm, 77 x 52.15mm and 30.5 x 16.1mm (0.6mm nozzle). figure by author

3.9.4 Multi material builds in silicone

The deposition head v1 was designed with space for two syringes with the intention of exploring multi material deposition; this was the aim for the next series of tests.

The plan was to use the tessellated tool-path for these tests, for the multi material portion of the test another acetoxy silicone was sourced, Mapesil AC manufactured by Mapei in a large range of colours.

Considering that the builds produced during the previous test almost depleted the material in the 30cc syringe, larger 55cc syringes were sourced, also manufactured by Adhesive Dispensing.

In the time between the tessellated tool-path test and this test, the Mk3 was tuned further from the initial calibration and feed-rates of 550mm/s were now possible.

Material switching method

The first step in preparing a multi material build was to load two syringes (55cc) with silicone; both syringes were then installed onto the deposition head. The deposition head was designed to limit how far down the syringes could be installed, with the intention of keeping both syringes at the same height.

Both syringes were fitted with the coupler to connect them to the air solenoid, but only one syringe could be connected at a time, so during the switching routine the hose for the current material was disconnected from the air solenoid and the hose for the second material was installed, this routine included a pause (M1) to switch the hoses around.

The nozzle tips of both syringes were around 35mm apart, so for the deposited layer to line up, a fixture offset was used. In Mach3, up to six different fixture offsets can be set up, these are selected in the G-code using the commands G54 (fixture 1) up to G59 (fixture 6).

To set up the fixtures each nozzle had to be zeroed to the same point while either fixture 1 or fixture 2 was selected in Mach3. Due to manufacturing tolerances of the syringes and the nozzles, the fixtures had to be re-zeroed every time the nozzle or the syringe barrel was replaced. These slight differences in dimensions also meant that the fixtures also included offsets in the Z axis as no two nozzles were the exact same length.

In theory setting up the fixture offsets sounds simple, in practice that was not the case, zeroing each nozzle to the same spot was rather difficult, so each time the fixtures are calibrated a test had to be run. For this purpose the 10mm square test G-code written at the early stages of the Mk3 was used while alternating between the two materials every other layer. This test helped confirm if the calibration was correct.

The original plan for deposition with two materials was to leave both syringes fixed in the deposition head, however early in the tests it was noticed that this would not be possible; leaving both syringes in the same position meant that one nozzle would always be dragged over the freshly deposited layer. So during the material switching routine the syringe that wasn't being used was raised so it would clear the build. The limiter built into the deposition head v1 helped return the syringes to the original position.

Deposition with multi material

For this build a similar tool-path to the one used in the previous tests was drawn, but to a slightly larger scale, this path had a diameter of 85mm and a wall thickness of 9mm (Figure 3.84), it also had two perimeters per wall instead of one and the corners of the inner spokes were adjusted to improve adhesion with the previous layer (same as the outer spokes in the previous test).

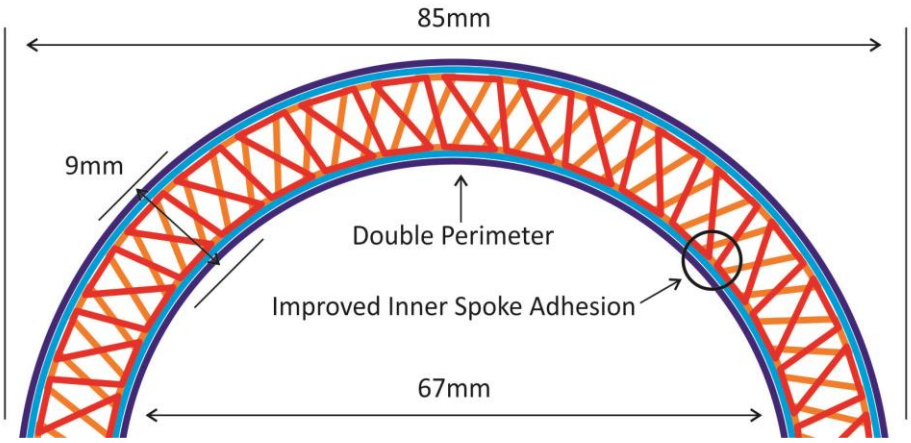

Figure 3.84, Tessellated tool-path for multi material test. figure by author

This build was made with clear silicone for the perimeters and orange silicone for the tessellated infill (Figure 3.85), both materials used a 0.8mm nozzle. Initially it was thought that the air pressure would need to be adjusted when switching materials; however both materials deposited well with the same pressure (1.3 Bar) at 550mm/s.

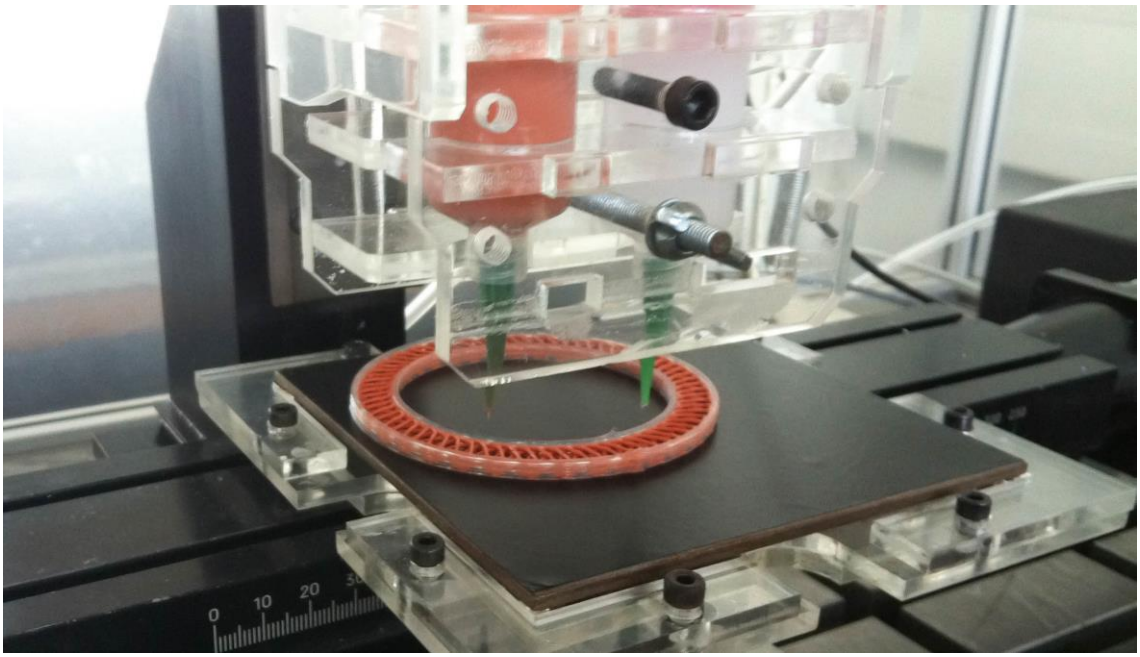

Figure 3.85, Deposition of tessellated tool-path with clear and orange silicone, nozzle: 0.8mm. figure by author

Deposition of two materials in practice was difficult and it took a few tries with this tool-path until enough experience was gained so that it could be done reliably, when switching materials there was enough time to also clean the nozzle tips from silicone residue which improved deposition quality. The purpose of these tests was to establish what was needed for multi material deposition so the samples made were only a few layers thick. The limiter built into the deposition head v1 worked well and the syringe was returned to the same position every time the material was changed.

To reduce deposition time layers with the same material were doubled up to make the least number of material changes per layer.

Summary of multi material deposition

The tests run helped develop the methods for multi material deposition but also highlighted the need for automatic material changing, as the manual method of moving the syringes was time consuming and bound to introduce operator error.

So at this stage it was decided that a multi material deposition head with an automatic tool changer was required, so it was designed and made. During this time deposition experiments were briefly suspended.

After the deposition head v2 was finished, experimentation with multi material and the tessellated tool-path was resumed, but with a different aim. This time

demonstrator artefacts were made that took advantage of the promising multi material capabilities of the Mk3 + deposition head v2 equipment. The process of making these artefacts is covered in the Embedded Electronic Components and Water-Tight Structures section in chapter 4.

3.10 Development of Deposition Head v2

3.10.1 Aim

From the multi material experiments it was learned that both nozzles could not be fixed at the same height as the inactive nozzle would drag over the surface of the freshly deposited layer. This was solved by manually moving the syringes so the nozzles would clear the current layer and not damage the build.

The deposition head v2 needed to move the syringes up or down depending on what material was required.

3.10.2 Actuation

To do this there were several options, the syringes could be mounted on small linear slideways and the position adjusted as any other axis, however this option would have been time consuming to design and build. The syringes could have also been mounted on a carrousel, which would rotate to the selected material, similar to that used in large CNC machines with tool-changers, however this option would have been even more complex to build, and the Sherline CNC was far too small for this option to be feasible.

3.10.3 Tool Positioning Strategy

The deposition head v2 needed to be simple, quick to make and easy to make spare parts for. So it would be better to use a linear actuator that would move the syringe between the highest and lowest position, an 'off the shelf' solution that would perform this action at a low cost. The solution was to use a central locking linear actuator, this actuator is usually used in cars to toggle the door lock, it is an inexpensive and reliable component.

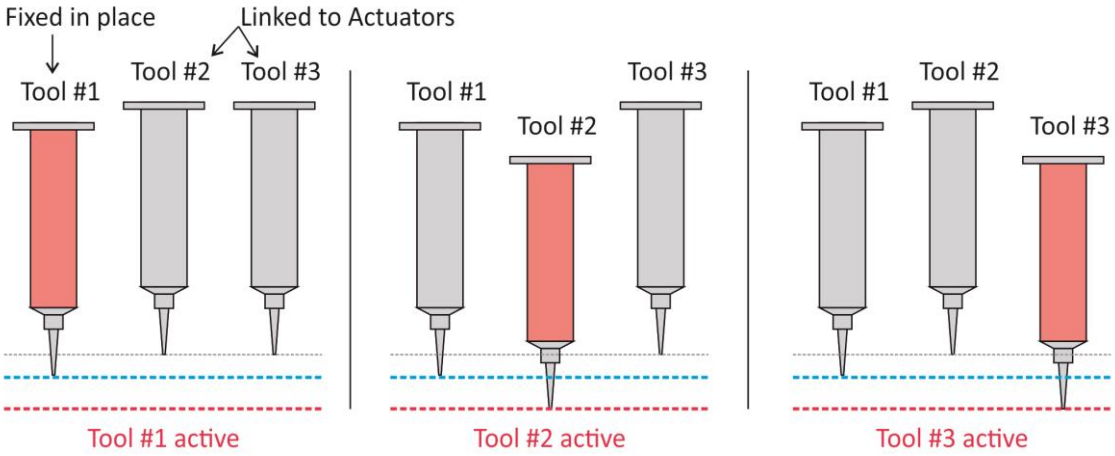

Figure 3.86, Diagram of triple material deposition head, one fixed syringe and two on actuators. figure by author

Early on in the design of the deposition head it was decided that each syringe would be moved independently from the other. This meant that if so desired, two builds could be done at the same time if they were not bigger than the space between the nozzles. In view of this, space for a third syringe was also designed; this was to remain fixed in position and would only be used if the other two syringes were set to the highest position (Figure 3.86).

3.10.4 Implementation of the Linear Actuator

As with the deposition head v1, v2 was also made using a laser cutter and assembled from flat parts, however this design was more complex and so the actuation mechanism was prototyped first to test the tolerances of the design.

The mechanism was designed by the author in Corel Draw and 3Ds Max, it was then laser cut and assembled by the author.

Linear actuator prototype

This prototype was used to test if the central locking actuators were strong enough to move the mechanism and also test the durability of the design.

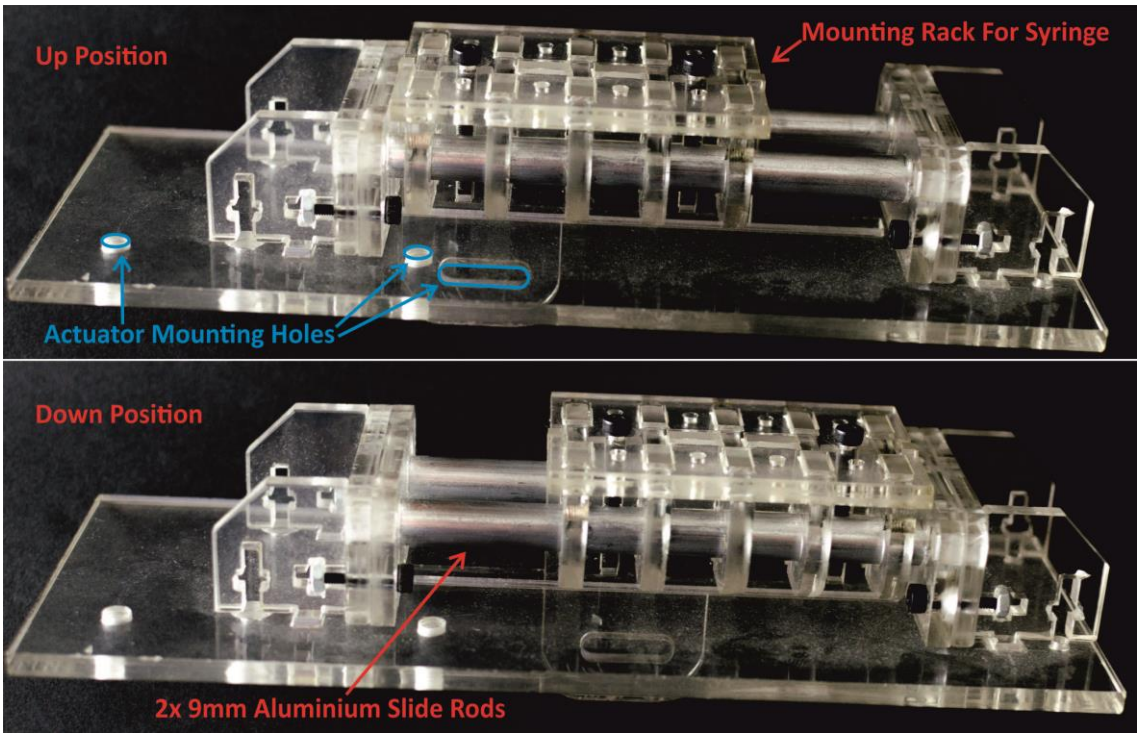

Figure 3.87, Prototype syringe sled for deposition head v2, central locking actuator not in picture. figure by author

The prototype worked well, some of the holes particularly those in contact with the slide rods (Figure 3.87) needed to be sanded so the sled would move more freely. The central locking actuator was more than strong enough to move the syringe sled, however once the actuator was powered down, there was not enough holding force to keep the sled in position. To solve this, a sliding plate that could be fixed in position with a screw was added to the back in contact with the sled, this plate added enough friction to stop the sled from sliding freely.

Deposition head V2

The prototype helped determine the final dimensions of the holes and fixtures so that the sled would move smoothly and reliably, all these adjustments were implemented into the final design of the deposition head (Figure 3.88) so that no sanding would be required when assembling. The design also included a cable management comb to help keep the air lines and actuator wires out of the way of the Z-axis. The full design had a total of 67 individual parts, many of these were duplicated, the puzzle pieces can be found in Appendix D.

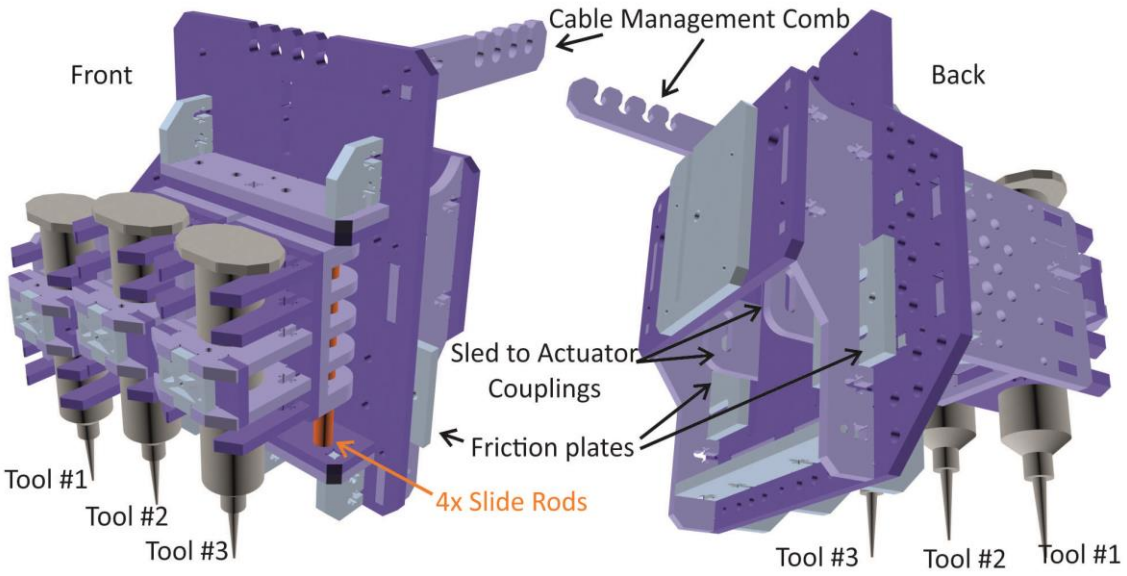

Figure 3.88, Render of the deposition head v2, 3/4 front and back views. figure by author.

The slide rods were made from stock 9mm aluminium tube to reduce weight and friction plates were added to both sleds to ensure that they did not slip, this was an area of particular concern as the vibration from the axes could exacerbate the slipping.

3.10.5 Electronics

PCB

The actuators each having two leads could have been driven by the sherline controller with four outputs from the parallel port, however this would have been wasteful as there were a limited number of outputs available and some of these were also required for the air solenoids, so it was decided that the actuators would be driven by a custom made PCB, this solution reduced the number of required inputs to just two, it was also safer as any malfunction or mistake would only damage the PCB and not the controller or the computer, the actuator controller was wired to a parallel port break-out board instead of using the existing outputs from the Sherline controller, as any mistake here would cause permanent damage.

The actuator controller was based on the 16F628 Programmable Integrated Circuit (PIC), this chip has a total of eight inputs available and eight outputs, so four of the inputs were used for communication with the parallel port, two of these would be used for the actuators and the others were left as auxiliary or future expansion. The other four inputs were set up as switch inputs, one of these was used as a diagnostic switch to move the actuators in case there were problems with the communication

with the parallel port. Four of the eight outputs on the chip were used for the actuators, these were linked first to an opto-isolator (TLP621-4) which then fed the signals from the chip to two motor driver chips (L293D), each motor driver has a total of four inputs and four outputs, it can power motors up to 12v at 2.6A per output. The actuators required 12v at 5A to run, so in order to power the actuator the four inputs of the driver were connected together to form two inputs, the same was done to the output pins (Figure 3.89).

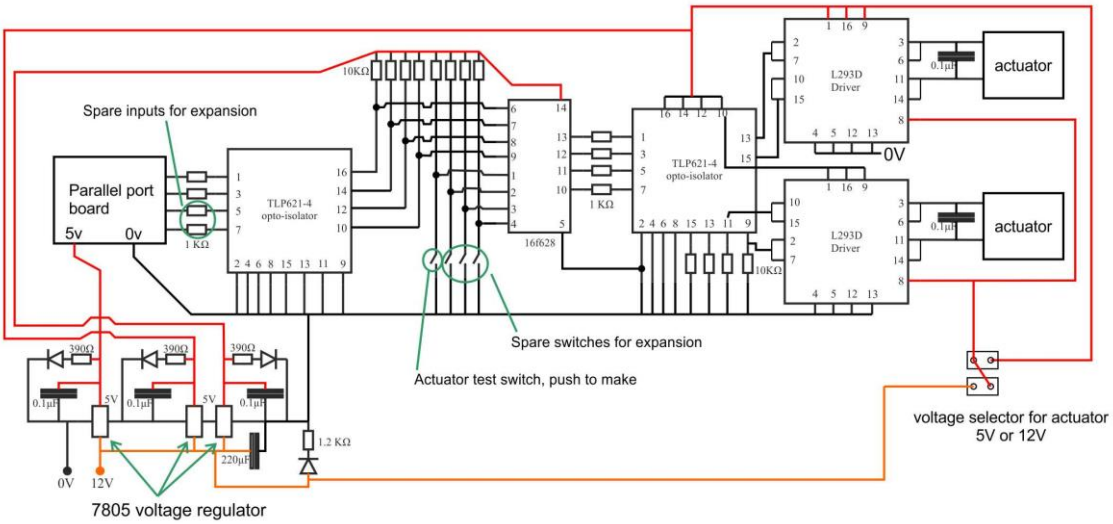

Figure 3.89, Schematic for actuator driver PCB. figure by author

The power was supplied to the PCB at 12v 6A, so only one actuator could be run at a time, also the PIC and the opto-isolators ran at 5v, so voltage regulators (7805) were added to step the 12v down to 5v, diagnostic LEDs were also added to each regulator and the 12v line for diagnostics. A double pole double throw toggle switch was connected between the 12v line and the motor drivers, the 5v line was also connected to this switch, this allowed the actuators to run at either 5v or 12v, this was done in case the actuators were too strong and needed to be run at a gentler voltage, the artwork for this PCB can be found in Appendix E.

This circuit board was designed, made and programmed by the author.

Firmware

The PIC is programmed in a language called assembly, the author has previous experience with this language and programming circuits similar to the actuator

controller, nonetheless PIC in Practice (Smith, 2006) was used for reference for the programming of the controller.

Actuator A	*Actuator B*	*Binary*
up	*up*	*01 01 0000*
down	*up*	*10 01 0000*
down	*down*	*10 10 0000*
up	*down*	*01 10 0000*

Table 3.15, Logic table for actuators A and B, blue signifies the bits responsible for the movement of actuator A, red for actuator B. table by author

Each actuator has two inputs, one positive and one negative, in the normal polarity the actuator is extended, reversing the polarity retracts it. With the PIC it was possible to switch polarities by selectively powering the pins connected to the motor drivers, a breakdown of the logic and binary used is in Table 3.15.

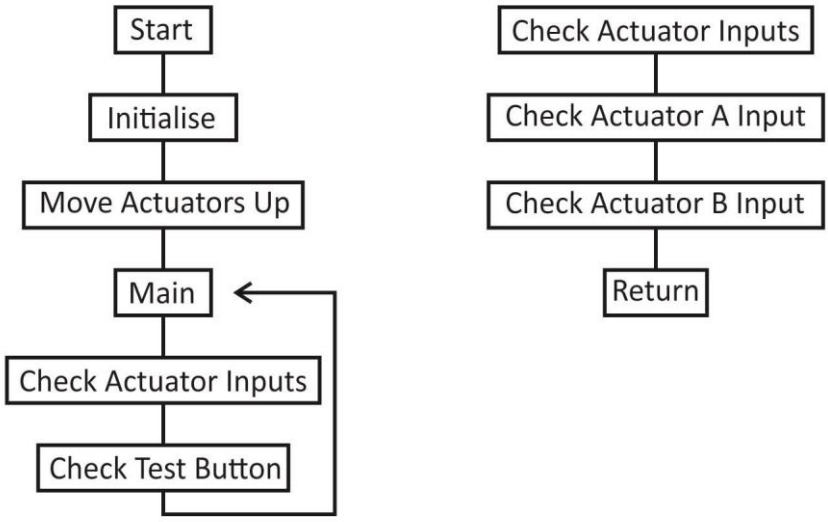

Figure 3.90, Flowchart of main routines in the actuator controller. figure by author

The firmware written for the actuator controller works by polling the inputs from the parallel port and the test button, if it the test button is pressed, the program first moves actuator A (tool #2) then waits until the button is pressed again to move actuator B (tool #3) down, another press then moves actuator A up and another finally moves actuator B up. In test mode the program overrides any signals from the parallel port, this is used to control the deposition head when the parallel port is not available or malfunctioning, it also helps troubleshoot any communication issues that might be occurring.

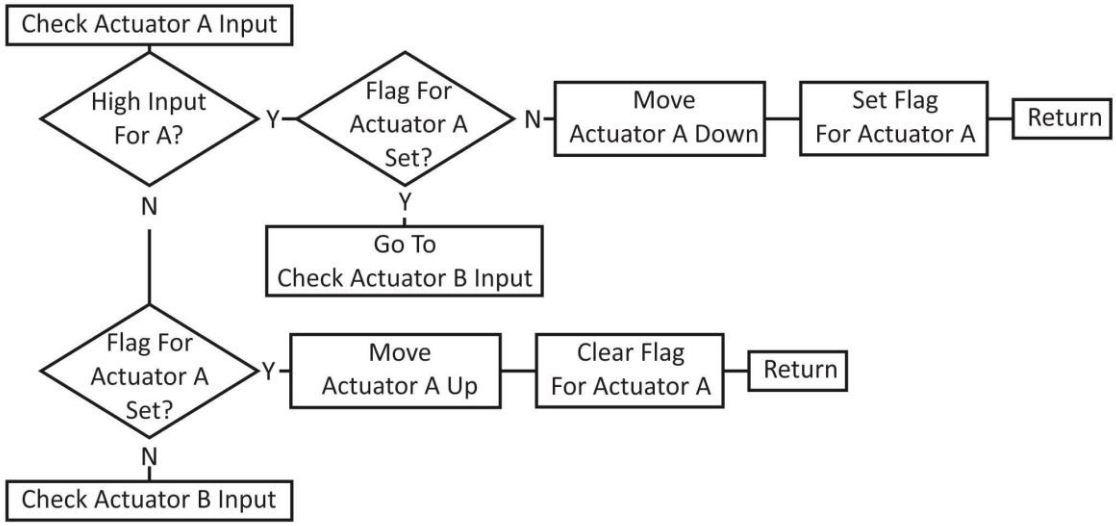

Figure 3.91, Flowchart for the polling of inputs for actuator A, it is the same for actuator B. figure by author

If a signal is received from the parallel port to move down a particular actuator, the program first checks if the actuator is already down, this is done by checking a flag that indicates if it is already in the down position, if not it moves the actuator and sets the flag for the next polling loop. The actuator does not move instantly, there is a small mechanical delay while it completes the stroke, to account for this the program has a small delay were the output is left on, the actuator cannot be powered constantly as it was designed for momentary movement only, so after the delay the program clears the bits and powers down the actuator.

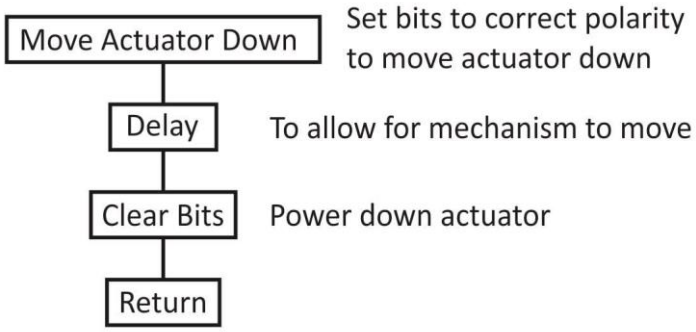

Figure 3.92, Flowchart for the movement of a single actuator. figure by author

The actuator controller

Once programming and debugging was complete the controller and the power supply were installed into an off the shelf electronics box along with the parallel port breakout board, holes were drilled into the front panel of the box for the interface buttons and plugs, all the work presented here was done by the author. To fully enable multi material deposition a second air solenoid was purchased for use with the second

syringe, with the plan for purchasing a third if the research steered into deposition with three materials.

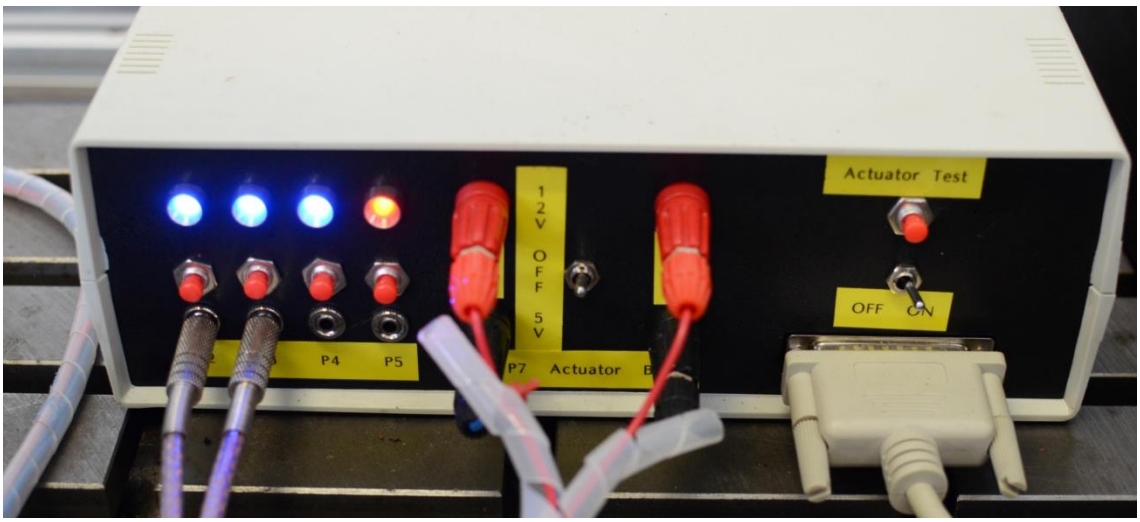

Figure 3.93, Front panel of the actuator controller. figure by author

Before these modifications the air solenoid was triggered with a relay connected to the Sherline controller. With the new setup all the connections to the air solenoid were moved to the same box as the actuator controller, a small opto-isolator board was made to protect the break-out board and the relays were connected, they were wired to 3.5mm female jack connectors installed on the outside of the actuator controller box (Figure 3.93), push to make switches were also wired to these connections to allow for easy purging of the syringes directly from the controller. Figure 3.94 shows the "birds nest" inside the actuator controller.

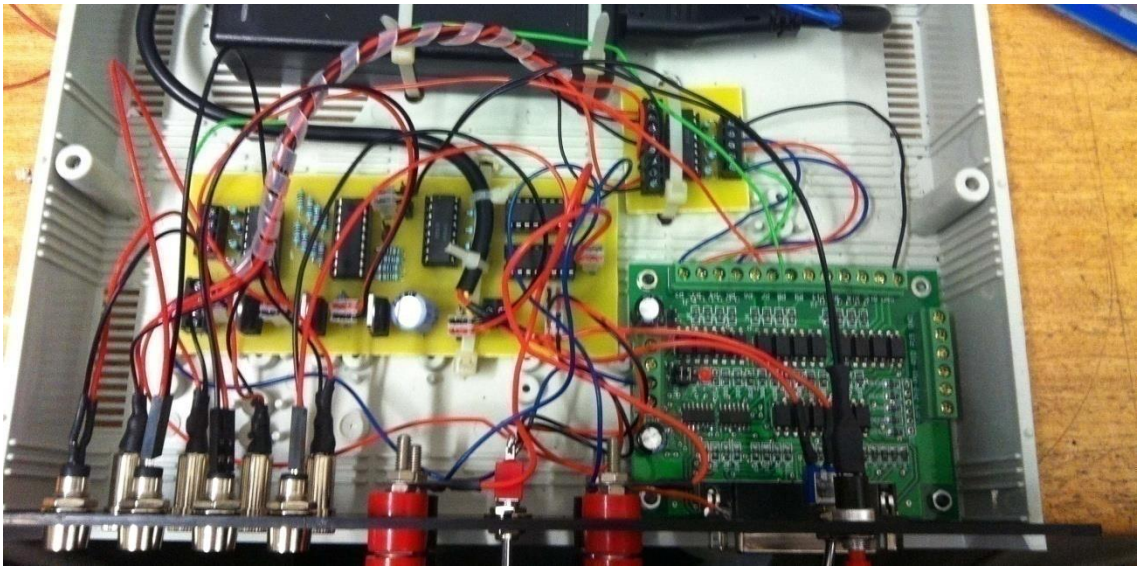

Figure 3.94, Inside of the actuator controller. figure by author

Mk3 with modifications completed

The Sherline mill used in the Mk3 had a much larger travel in the X axis than previous incarnations of the PDM equipment, however up to this point the same deposition plate as that in the Mk1 had been used, so along with the deposition head upgrades the build plate size was increased from 100 x 100mm to 230 x 100mm, the same design for the frame was used, only extended.

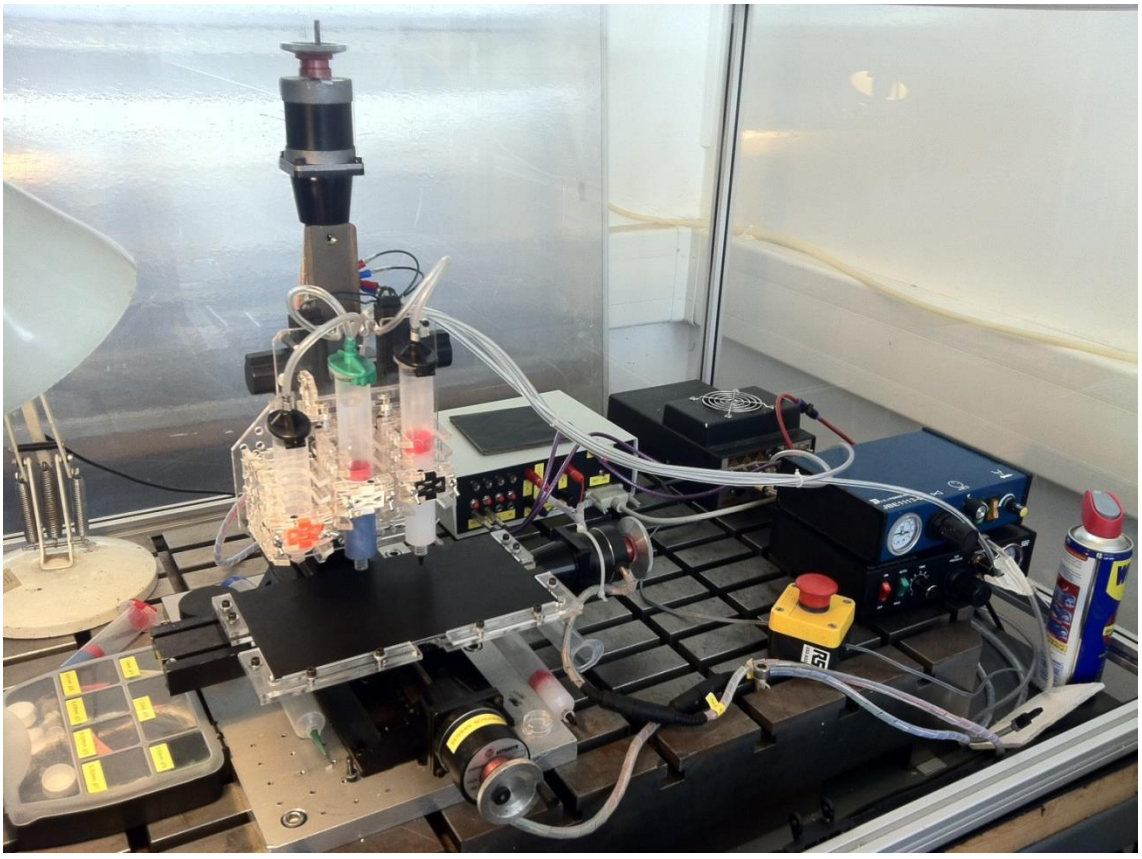

Figure 3.95, Completed modifications to Mk3, with deposition head v2 and build plate v2. figure by author

Figure 3.95 shows Mk3 with the new modifications, the triggering of the air solenoids was done with the M3 and M4 commands. Movement of the tool was controlled with M7 and M8, which are normally reserved for mist and coolant triggering in normal CNC machines, a small delay of two seconds was added to the material changing routine to account for the mechanical delay in the actuators, M9 was used to clear both the M7 and M8 commands. There were no further modifications done to the Mk3 for the remainder of the project.

3.11 Implementation of Slicers for FDM into PDM

3.11.1 Introduction

Up to this point in the research project, all tool-path generation had been done manually; this gave more control over the process and allowed for fine tuning of the tool-paths to create shapes and patterns that would otherwise be impossible if a standard slicing method had been used. However, this method limited the samples to straight walled builds as drawing individual layers was time consuming, and drawing hundreds of individual layers would not be practical or feasible. The limitation was not an issue as the exploration was more focused on the patterns and internals of the build rather than a pretty surface.

Having said that, an opportunity came up to collaborate with a researcher, Dr. Charalampos Makatsoris for the deposition of a human artery to test a mathematical model of the flow of blood inside said artery, so automated slicing would be required.

Figure 3.96, 3D model of human artery, data from scan of patient. figure by author, model provided by Dr. Makatsoris

The 3D model of the human artery was supplied (Figure 3.96), it was a direct scan from a patient. In order to test the mathematical model, the deposited artery had to be an accurate representation of the artery used in the simulation, so a more traditional approach such as glass blowing would not have been suitable as the artist would not be able to guarantee accuracy and also the glass would not be flexible like an artery. Human arteries Dr. Makatsoris mentioned, do not have a smooth surface on the inside, but rather a ridged texture, so the striation texture from the deposition process

would be desirable along with the elasticity of the silicone, the build also needed to be clear, to allow for sensors to take measurements from the outside of the artery.

3.11.2 Preliminary Testing

In order to determine if it was feasible to deposit the artery, a few tests had to be run, these were to determine the minimum number of perimeters required to create a stable hollow build, what was the maximum height that could be deposited reliably and if the resulting build would be water tight. The artery also required a wall thickness of 0.9mm +- 0.1mm.

Hollow tube build

The tests were based around the deposition of a straight walled tube with no infill, the code for this test was written using the same 2D method as pervious builds because automated slicing had not been implemented by this point. The diameter of the tube was 22mm.

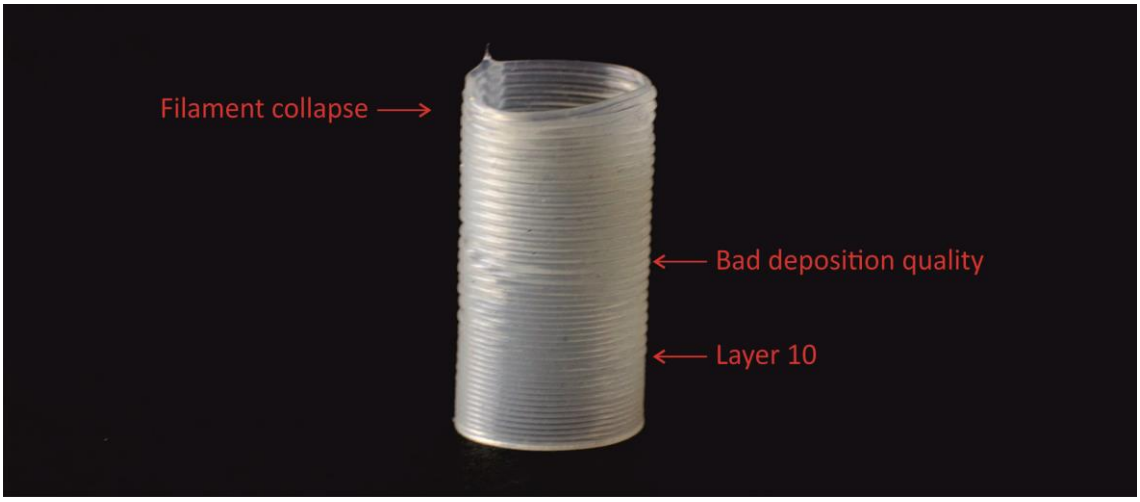

Figure 3.97, Single perimeter tube build, failure started from layer 10. figure by author

Initially the hollow tube build was tested with only one perimeter, this build was too unstable and started to collapse after 10 layers with a 0.8mm nozzle (Figure 3.97), the reason for this is that depositing with only one perimeter is inherently unstable, almost like trying to stack one bottle on top of another length wise. The diagram in Figure 3.98 illustrates the point, it also makes mention of deposition at 45°, at this angle some filaments will be deposited in mid air leading the structure to collapse, so draft angles must be kept in mind when preparing the artery for deposition.

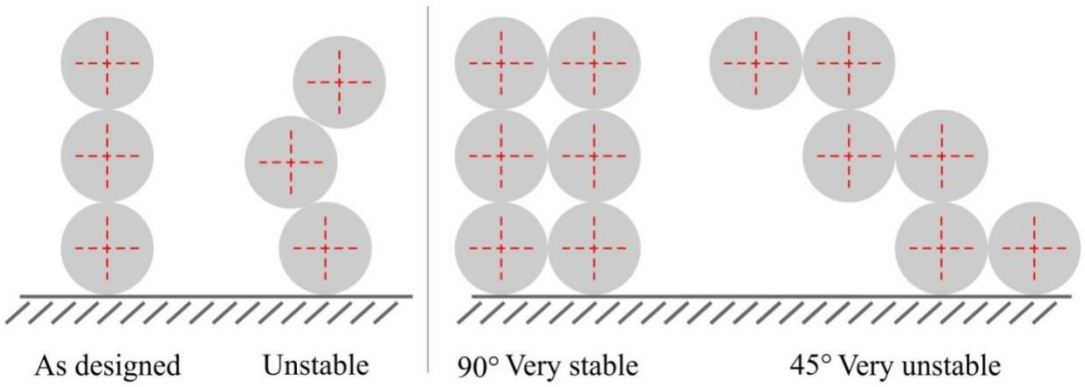

Figure 3.98, Perimeter stacking diagram. figure by author

The test was repeated but this time with two perimeters, a 0.4mm nozzle was used as this would produce a wall thickness close to the requirement of 0.9 +- 0.1mm, the diameter was changed to 17mm to match the diameter at the base of the artery.

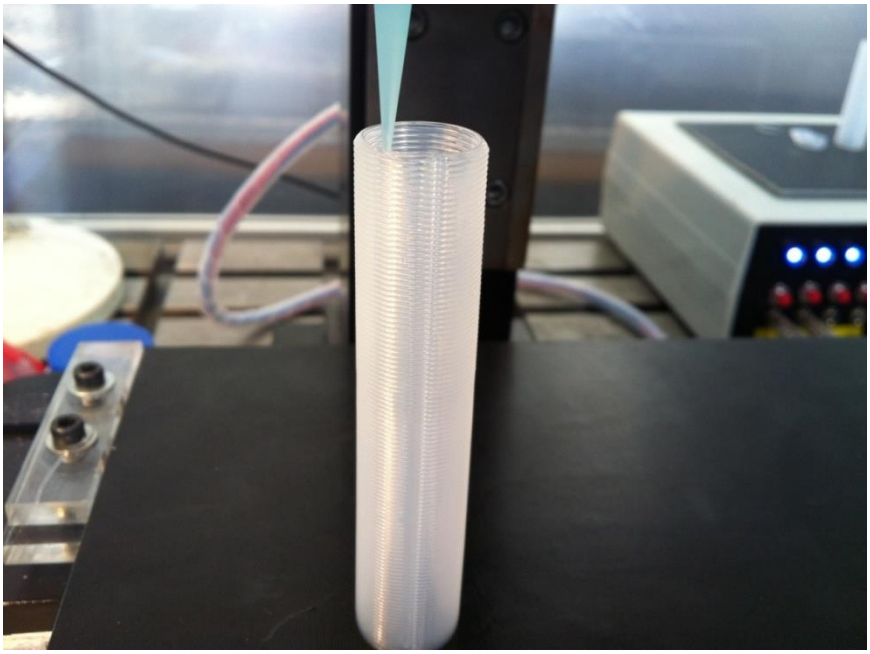

Figure 3.99, Hollow tube test with two perimeters, built to 100mm. figure by author

This test yielded better results (Figure 3.99), but it was found that as the structure reached beyond 100mm, it became unstable, swaying with the small friction from the nozzle during deposition. Beyond this point the surface quality fell, so it was determined that the maximum height was 100mm. This build was repeated several times to confirm the results and it was confirmed that the limit was in the area of 100mm, for a build of this diameter. The maximum height for narrower tubes would be lower as the stability would decrease.

Some of the tubes were tested for water tightness by crimping one end while air was blown in the other, once the tube inflated the other end was crimped to trap the air, no leaks were found during this test.

Slic3r method

The slicing program "slic3r" is a free software used to slice and generate code for FDM machines, this program also has an option for generating G-code for Mach3 (Figure 3.100), this was the program used to slice 3D models for use with the Mk3.

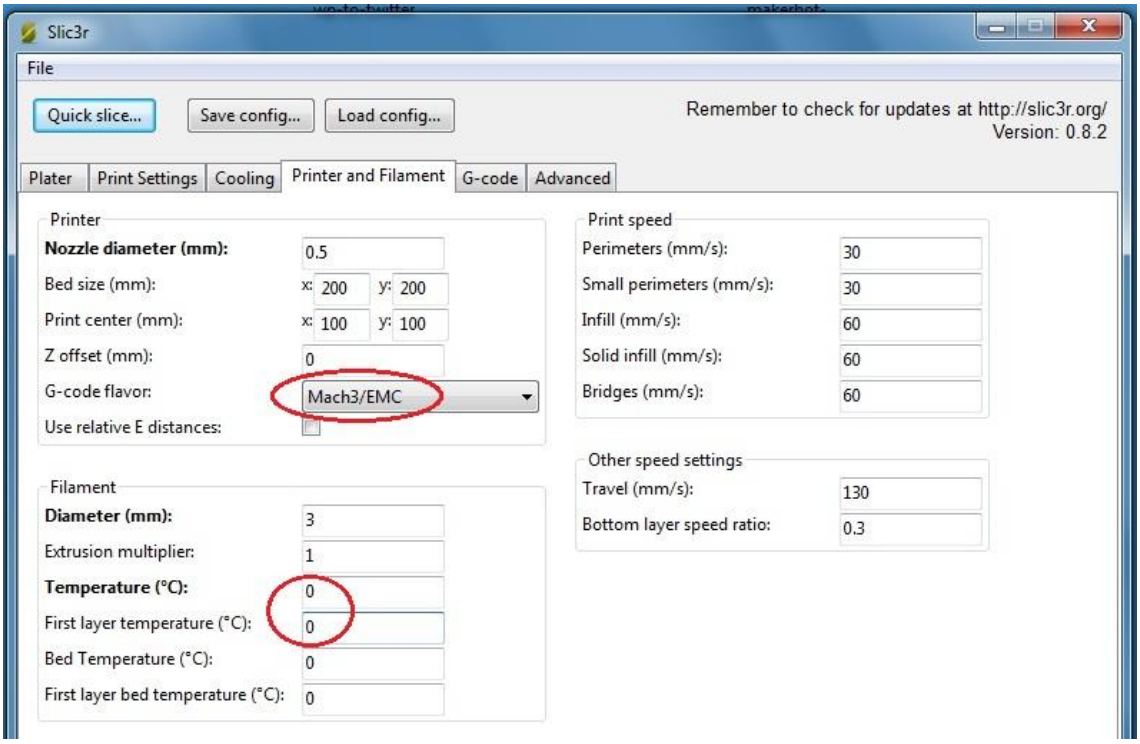

Figure 3.100, Screenshot of Slic3r software, showing configuration for use with Mach3. figure by author

However there was an issue, in FDM machines extrusion is done by a stepper motor, so instructions for this motor are added to each command in the form of travel coordinates for a fourth axis, the trouble was that deposition with the Mk3 was triggered by the M3 command, it was not feasible to add this command every time deposition had to be started or stopped to reposition the nozzle, so another solution was needed.

Mach3 has a built in function called "Brains", these can be used as macros to perform actions outside of the G-code program; it can use data from the coordinate readouts and perform other actions such as turning the spindle on and off. The plan was to setup one of these brains to look at the position of the fourth axis and start deposition

whenever there was positive movement from the axis, or stop deposition when there was negative movement. Note; the stepper motor in an FDM extruded retracts a short distance when extrusion is stopped to retract a small amount of the filament back into the nozzle.

This method did not work; there was a substantial lag in the update of the coordinate readouts which threw off the timing of the deposition. But another solution was found, as mentioned in the 'Mach3 hardware compatibility test' CNC controllers use step and direction pins to control the stepper motors in each axis, the solution was to put the output pin for the air solenoid into the direction pin-out for the fourth axis where the extruder instructions were being sent. This solution worked and G-code from slic3r could now be used in Mach3.

There are two methods that can be used when depositing hollow builds, the first is to make the 3D geometry hollow with the desired wall thickness, however if the wall thickness does not match the size of the filament it can lead to empty spaces between the perimeters. The second option is to leave the original geometry solid and set the infill in the slicer to 0%, this would then produce a hollow build with a consistent wall thickness regardless of the filament size, it would also produce solid layers are the top and bottom, these would need to be deleted from the G-code after slicing.

G-code test with the Mk3

This method was put to the test by building a tapered cone with a base diameter of 17mm, top diameter of 7mm and a draft angle of 5°. The slic3r settings were, Nozzle: 0.4mm, Layer height: 0.35, Distance between filaments: 0.35 and two perimeters. The feed-rate was corrected manually in the code as the slicer used several different speeds throughout the build; this was done with a quick find and replace operation in a text editor. The build completed successfully with a good smooth surface (Figure 3.101).

Figure 3.101, G-code cone test, 17mm diameter at the base, 0.4mm nozzle, 0.35mm layers. figure by author

Joining method

By this point it was clear that it was going to be possible to deposit the artery, but it was going to have to be done in parts as it was too long to deposit in a single build.

So a test was run to see how the individual pieces could be joined together, this test used two of the 100mm test samples, the same silicone used to deposit was used to join the tubes, silicone adheres very well to silicone, so the strength of the joint was not a concern.

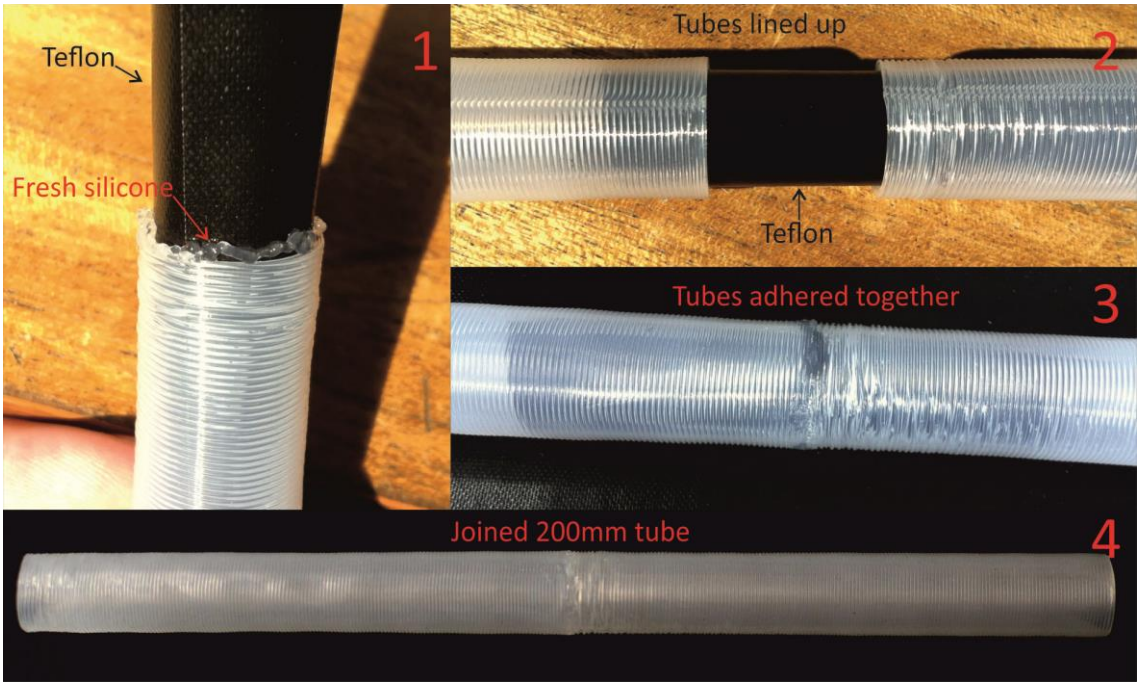

Figure 3.102, Method for joining two hollow tubes with silicone, Teflon sheet was used as a guide. figure by author

To join the tubes a Teflon off-cut from the build plate surface was used to act as a guide to help join the tubes, it also helped keep the inside of the joint smooth to the rest of the inner surface. This method worked and the tubes had a strong butt joint.

Building the artery code

The 3D model of the artery as supplied (Figure 3.96), was curved, in that state it would not have been possible to deposit without support, also the striation texture would not have been the same throughout the whole build, so the model was modified in 3D Studio Max to straighten the geometry and make deposition possible, this modification did not compromise the main features and surface deviations of the artery (Figure 3.103).

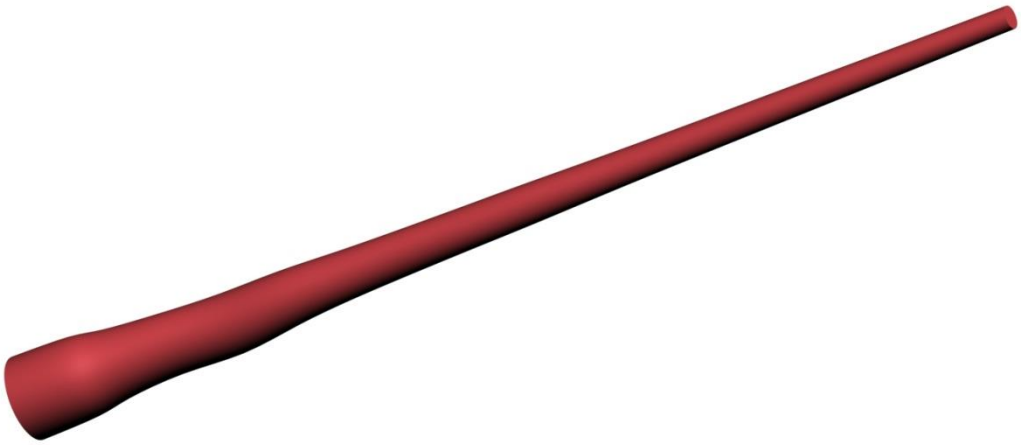

Figure 3.103, Straight artery, mesh modified in 3D Studio Max. figure by author

As mentioned in the joining method, the artery was far too long and needed to be split into parts for deposition to be possible, there were two ways this could be done, the first was to cut the 3D model into sections, this method required some guessing as it was not known how tall each section could be for reliable deposition. The second method was to convert the whole model into G-code and split the code manually, this way if any parts failed due to height limitations then only a quick adjustment would be required to re-deposit the failed part.

The method of manually editing the G-code was selected; this required some changes to how the code worked. If sections of the code were deleted, i.e. the first 30mm, then the deposition would start at a height of 30mm (in mid air) as each layer already had a height value attached to it. In Slic3r it is possible to setup the program to insert code at

the beginning of the whole G-code, the end, and at the start of every layer. So a comment (a comment is ignored by the software but the user can read it) was added at the start of every layer so it would be easy to identify when a new layer started, then every Z-height coordinate was replaced with a variable (Z#1), and using the same method to calculate layer height (#1=[#1+#2]) as that used in the 2D method made it possible to change the layer height for each layer. The code was split into sections using subroutines, if need be the routines could take up more or less of the code to change the length of each segment.

Deposition of the artery

The artery parts were deposited in sequence starting from the bottom, after every successful part was made a new routine was setup in the G-code for the next section and was deposited. This sequential method ensured that no parts were left out and the full artery was deposited. Naturally there were a few failures, it is an experimental process after all, some of the failures were caused either by depositing a segment that was too long or by motor stalls, the former became less frequent as experience was gained, Figure 3.104 shows the deposition plate with the last few segments of the build, most of the other larger segments had been removed from the plate by this point, a total of 17 segments were made for the whole artery.

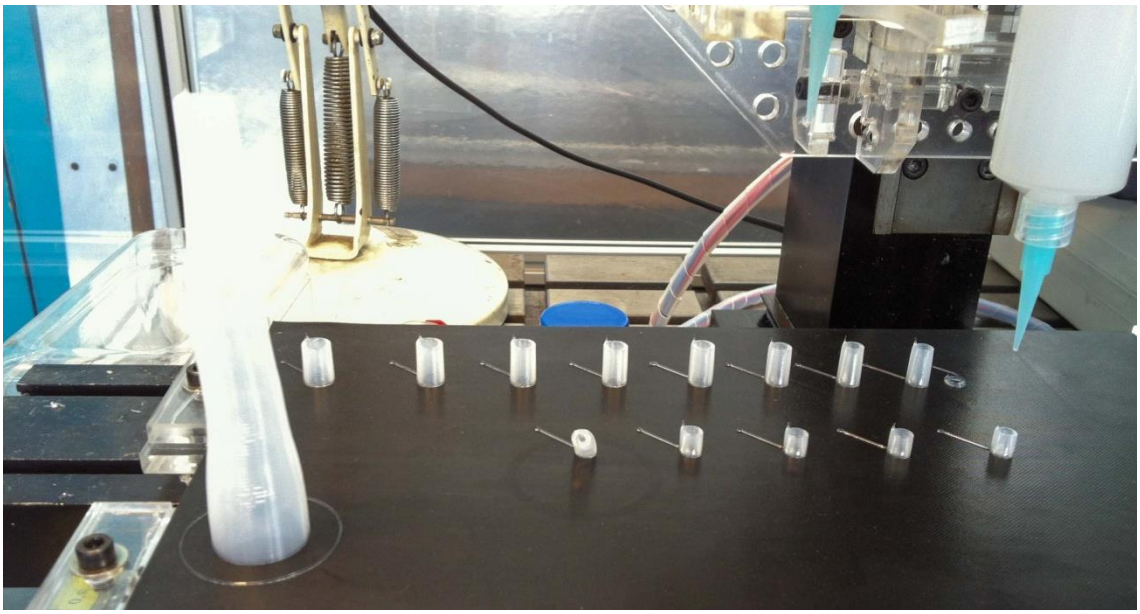

Figure 3.104, Deposition of the final segments of the artery. figure by author

The silicone normally takes a few hours or days to cure when used for its intended purpose (sealant), however the wall thickness, and surface area exposed to air reduced

this time dramatically to less than an hour, but even though the segments were touch dry by the end of the day, they were left to cure for 24 hours to reduce risk of damage as the process of gluing them together would require plenty of handling.

The method of gluing the segments together was no different from the one used in the adhesion test. All the segments were laid out in the proper order and glued in pairs to form larger segments; then when dry, the larger segments were joined together until the whole artery was complete (Figure 3.105).

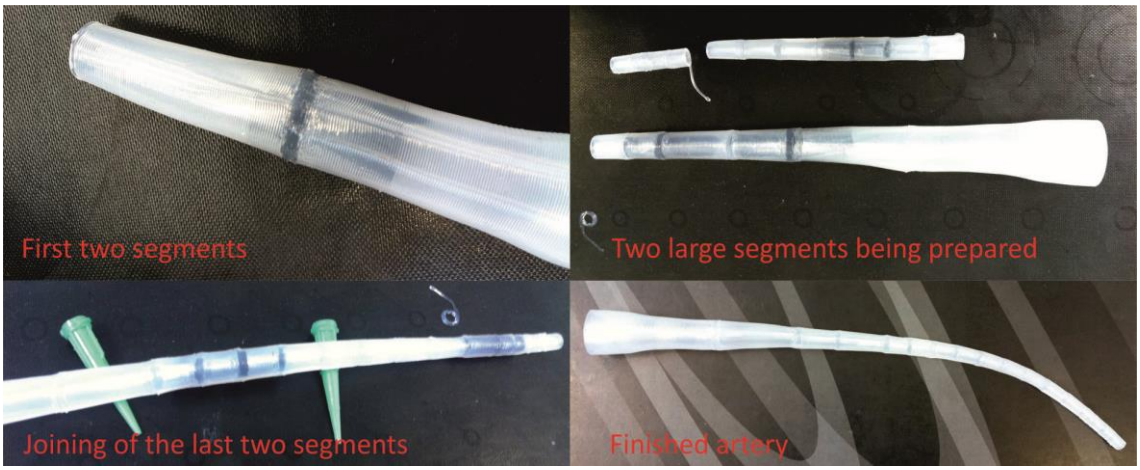

Figure 3.105, Construction of the silicone artery. figure by author

Summary of the silicone artery

This collaboration project saw the development of a new method for the generation of G-code, referred hence forth as "3D method" or "Slic3r method". Whilst the code required modification it was not as time consuming as it would have been to draw each layer individually.

With current AM methods it would have been almost impossible to make this artery, shy of casting, perhaps the only system that could have approached this would have been the Objet system with flexible materials, but the build would not have been clear or chemically resistant as the silicone used. The build produced was durable, clear and water tight.

At the time of writing, the research with the artery had not been complete, so any conclusions that could be drawn from the performance of the build are not yet available.

Further work with the 3d method

The 3D method was used to create other builds for different applications, particularly in the deposition of soft silicone moulds, this exploration can be found in Manufacture of Thin Walled Soft Moulds In Silicone section in chapter 4.

3.12 Mechanical Testing Of Silicone Parts (Collaboration)

3.12.1 Introduction

Another opportunity to collaborate arose, this time with Advanced Engineering Masters student Jonathan Oxley, his dissertation title was "Modelling and FEA analysis of flexible structures made by a novel manufacturing process" (Oxley, 2012).

The purpose of Jonathan's project was to generate a computer model capable of predicting the mechanical properties of the silicone structures deposited in this research project, It was focused on 90° linear periodic (log-pile) structures. To validate the computer model, a series of test samples were developed and deposited for the purpose of destructive tensile testing with an Instron 5967, the material used for the samples was Mapesil "SpaceBlue" acetoxy silicone manufactured by Mapei (2011).

3.12.2 Structure Modelling

The preliminary work carried out by Jonathan involved an analysis of the log-pile structure to help develop a computer model of the structure, then based on this the tensile samples would be designed and deposited for destructive testing.

A log-pile structure was produced for Jonathan to analyse, his plan was to cut the sample into thin slices so the interaction between the filaments could be modelled, however this proved to be far more difficult than anticipated, initially a cryogenic microtome was used to produce the slices, it was left to freeze overnight down to -42°C, but at that temperature the silicone was still malleable and slices could not be produced. He intended to revisit this technique but with a sample that had been flash frozen with liquid nitrogen, this however was not possible as the equipment became unavailable. Further attempts were made at cutting the sample, these involved at one instance infiltration with wax and another with polymer resin, then using a regular microtome to produce the cuts, yet these failed as well, the silicone did not cut cleanly enough to produce a useful image.

At this stage it was decided that the focus would shift toward estimating the inter-filament interactions based on observations from the samples.

Jonathan produced a computer model based on one of the large samples (Figure 3.43) deposited with the Mk2 (1.6mm nozzle) but without the perimeter filaments. When

the model was imported into the engineering simulation program (ANSYS) it was found that it was too complex for simulation, the problem was the number of filaments and the areas at the edges where the filaments turn 180° to form the structure, in view of this the model was simplified to four layers and fewer filaments and the 180° curves were omitted from the model.

3.12.3 Development of the Test Structure

The author was responsible for the development and deposition of the tool-paths for the samples used in the destructive testing.

The initial testing helped find the appropriate shape for the tensile testing sample, for the sake of brevity the tool-path design and deposition of the shapes that did not yield results will not be discussed, but rather this section will be focused on the shape that did work.

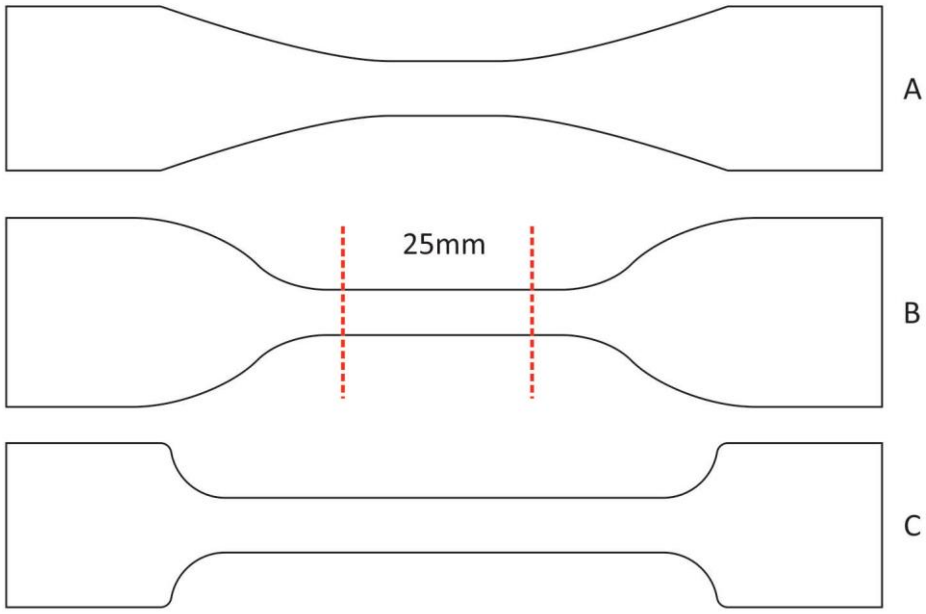

Figure 3.106, Tensile test 'dog-bones', B was based on type 1 from BS ISO 37:2011 p.5. figure by author

For a tensile test to be valid, the sample must break in the area designated by the British standard (ISO 37:2011, p.5) for the particular shape of the 'dumbbell' sample, during initial testing the shape recommended by the British standard (Figure 3.106 B) did not yield a valid test, so several other shapes were designed and tested, A and C in Figure 3.106, however these also broke outside of the testing area. To help find out what the issues were, the Masters student simulated all the proposed shapes in ANSYS

and found that the only viable shape was B, the same one recommended by the British standard.

Several designs for the tool-path based on shape B were proposed (Figure 3.107) and tested, these were made in a single batch to be tested at the same time to find the tool-path strategy that could be used in the destructive testing trials, all the samples were deposited with a 0.6mm nozzle and four layers in height.

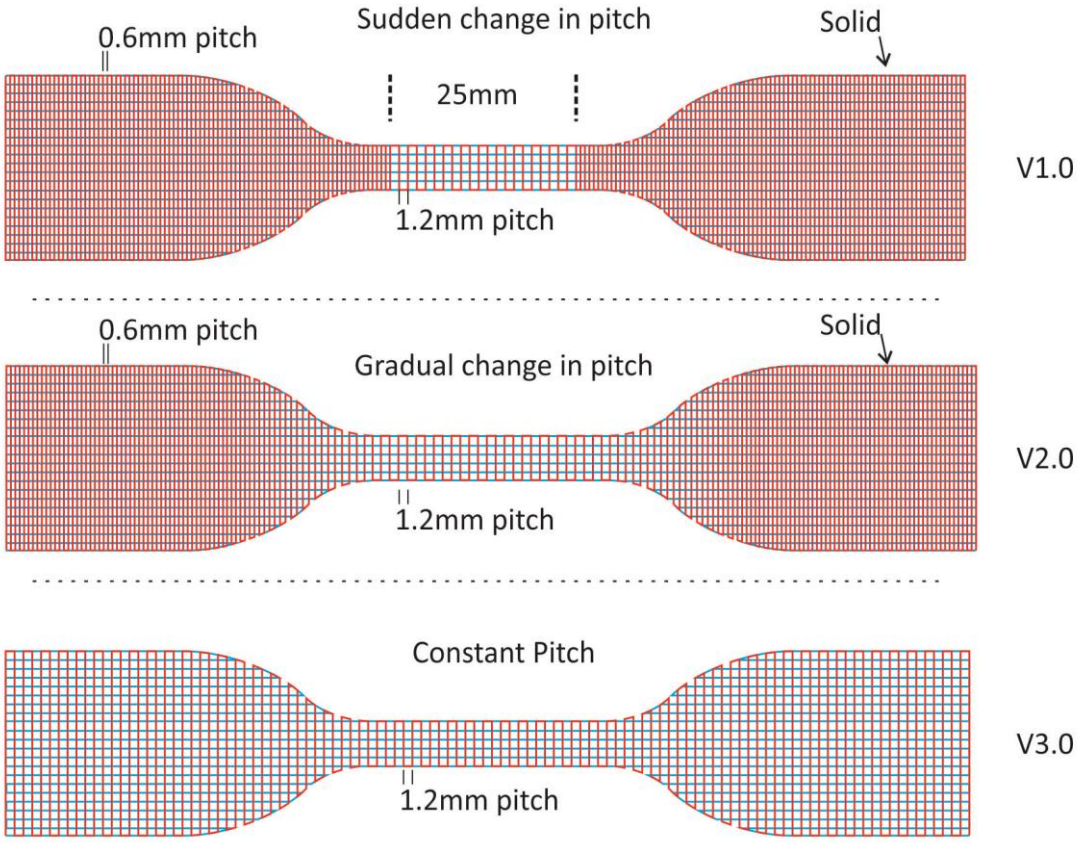

Figure 3.107, Tensile test sample B, tool-path strategies. figure by author

The design variations were named; V1.0, V2.0 and V3.0. V1.0 had solid tabs at a pitch of 0.6mm on the vertical filaments (red in Figure 3.107), the pitch was suddenly changed to 1.2mm in the 25mm testing area; this produced a loose log-pile structure as the project was aimed at the testing of log-pile structures, not solid sheets of silicone. Sample V2.0 changed the pitch of the vertical filaments gradually from the 0.6mm solid path to the loose 1.2mm pitch. Sample V3.0 had a constant pitch throughout the whole structure. The pitch for the horizontal filaments (blue in Figure 3.107) was kept the same at 1.2mm throughout the whole layer; the pitch was only changed for the vertical filaments. The tool-path of V1.0 was used in the initial testing

and was only included in this trial as a control. During initial testing this sample broke at the edge of the testing area, so V2.0 and V3.0 were developed as it was thought that the sudden change of pitch was to blame for the failed tests, Figure 3.108 shows V1.0 0.6 B being deposited.

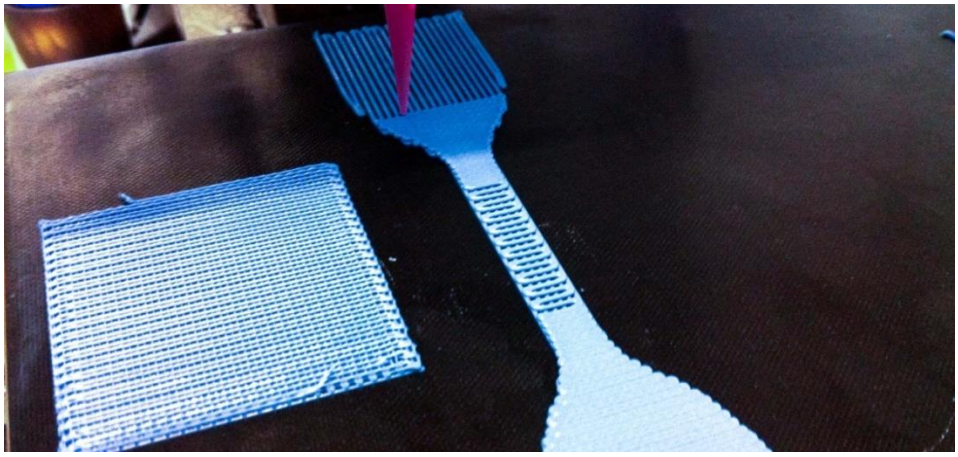

Figure 3.108, Sample v1.0 B 0.6 being deposited. figure by author

All the tests with the samples were invalid as they did not break inside the testing area; V1.0 showed the most promise as the other samples broke furthest from the target.

So V1.0 would be developed further until a valid test could be produced, all the tensile testing was filmed (on a mobile phone) so the footage could reviewed later to see if the reason for the invalid test could be found. The footage revealed that V1.0 was failing in the area where the pitch changed from 0.6 to 1.2mm, but more importantly it was failing because of the uneven distribution of the filaments (Figure 3.109).

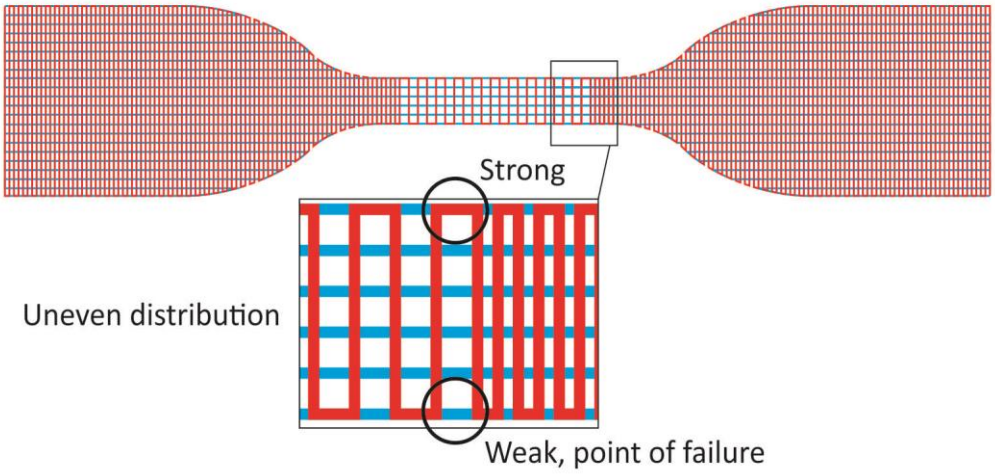

Figure 3.109, Point of failure of sample B v1.0. figure by author

The design for V1.0 was revised and two designs were proposed, in V1.1 the orientation of the second layer with the vertical filaments (red in Figure 3.109) was changed so that the weak area would be better supported by interlacing the tool-path, shown in purple in Figure 3.110. V1.1.1 had the same changes but the order of the layers was changed. In V1.0 and V1.1 the horizontal (blue) filaments were deposited first, then vertical, horizontal and finishing with vertical filaments. It was thought that because the horizontal filaments were under tension during testing that it would be better to have them as round as possible, when they were deposited first the cross-section of the first layer was not round but slightly flat at the bottom. V1.1.1 addressed this issue by making the first layer with the vertical filaments (red), thus keeping a more even cross section for the horizontal (blue) filaments which were under tension (Figure 3.110).

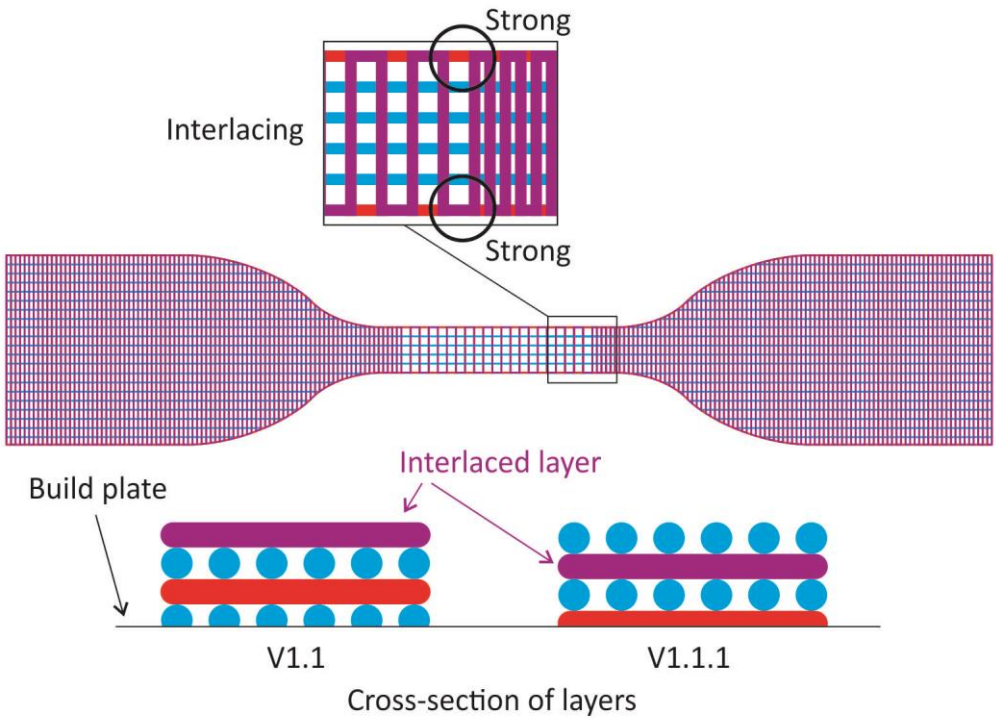

Figure 3.110, Modification done to V1.0,interlaced layer in purple and cross-section of layer order figure by author

Under testing v1.1 yielded a valid test (Figure 3.111), but v1.1.1 did not, so the tool-path strategy V1.1 was used for the destructive testing of samples.

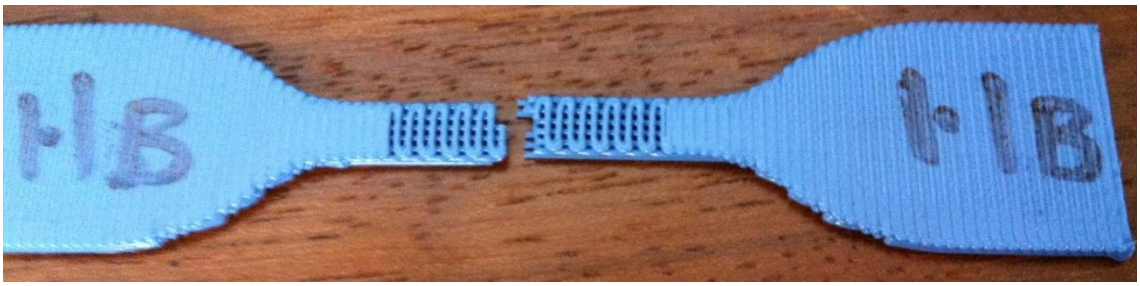

Figure 3.111, Valid test of V1.1 0.6. figure by author

3.12.4 The Test Samples

Under the testing method developed by the Masters student, the samples were produced with different nozzles sizes; 0.4mm, 0.6mm, 0.8mm and 1.2mm. The tool-paths were redrawn using the same V1.1 strategy (Figure 3.112). The original plan was to also design samples with 0.2mm and 1.6mm filaments, but due to the complexity limitations imposed by the simulation software (ANSYS) it was not possible to do this as the computer model had to match the deposited samples as closely as possible.

Deposition of the test samples for sizes 0.8 and 1.2 was straight forward once the deposition parameters were dialled in, however the samples were so large and thick that several syringes of material were used during the batch production of the samples, it was not always clear if there was enough material to produce a sample so this led to a few failed deposition due to depleted material. A total of six samples for size 0.8 were produced and four for the 1.2 as this sample was much larger and it became more difficult to deposit consistently given the volume of the syringe. Sizes 0.4 and 0.6 were a somewhat more difficult, as the build plate had to be precisely levelled, this was done by adding shims under the build plate. The build plate level played a bigger role in these builds than all others, as defects in the builds would compromise the results from the tensile testing, once the build plate was level, six samples for each size were made.

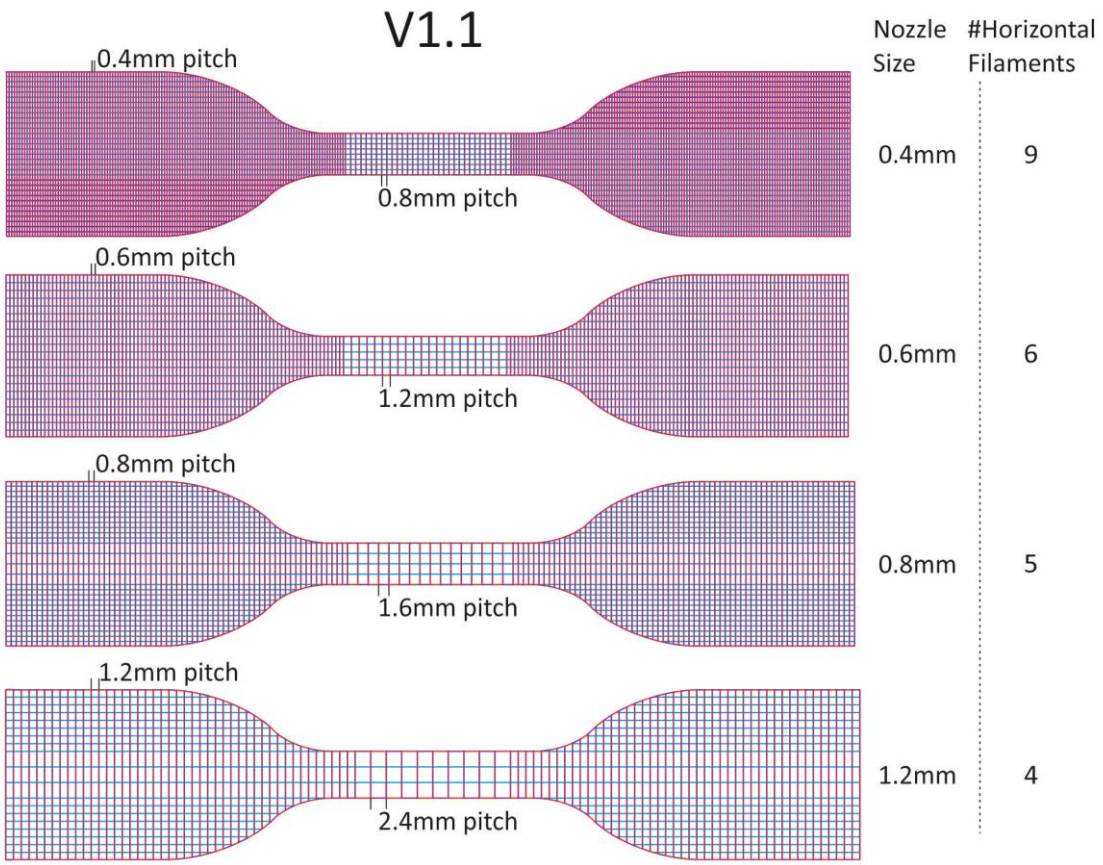

Figure 3.112, All the test samples using V1.1 tool-path strategy. figure by author

Under test conditions all the 0.8 and 1.2 samples failed to break in the test area and invalidated the results, so tests were run again with the 0.8 and 1.2 samples redrawn to the v1.0 tool-path strategy. It was found that with this strategy the 0.8 and 1.2 did break inside the testing area, so another batch of six was made for destructive testing.

3.12.5 Destructive Tensile Test

All of the V1.1 0.4 samples broke within the testing area, the results as analysed by the Masters student showed an extension of 165.07mm with a 9.14mm standard deviation, this was an extension of 106.34%, the breaking force was 3.36N with a standard deviation of 0.33N (Oxley, 2012, p.68).

Five of the six V1.1 0.6 broke within the testing area, with an extension of 175.37mm with a standard deviation of 17.21mm, the breaking force was 4.48N with a standard deviation of 0.23N (Oxley, 2012, p.69), Figure 3.113 shows the sample under testing.

In order to get a full set of data there needs to be at least three valid results, the 0.8 and 1.2 samples did not produce this requirement, all but two of the samples failed for both sizes, so the measurements were not as comprehensive as the other two sizes.

The average extension of the valid V1.0 0.8 samples was 116.2mm with a standard deviation of 5.37mm, the breaking force was 6.56N with a standard deviation of 0.05N (Oxley, 2012, p.72).

For the V1.0 1.2 the average extension was 104.37mm with a standard deviation of 2.66mm, the breaking force was 7.47N with a standard deviation of 0.05N (Oxley, 2012, p.74).

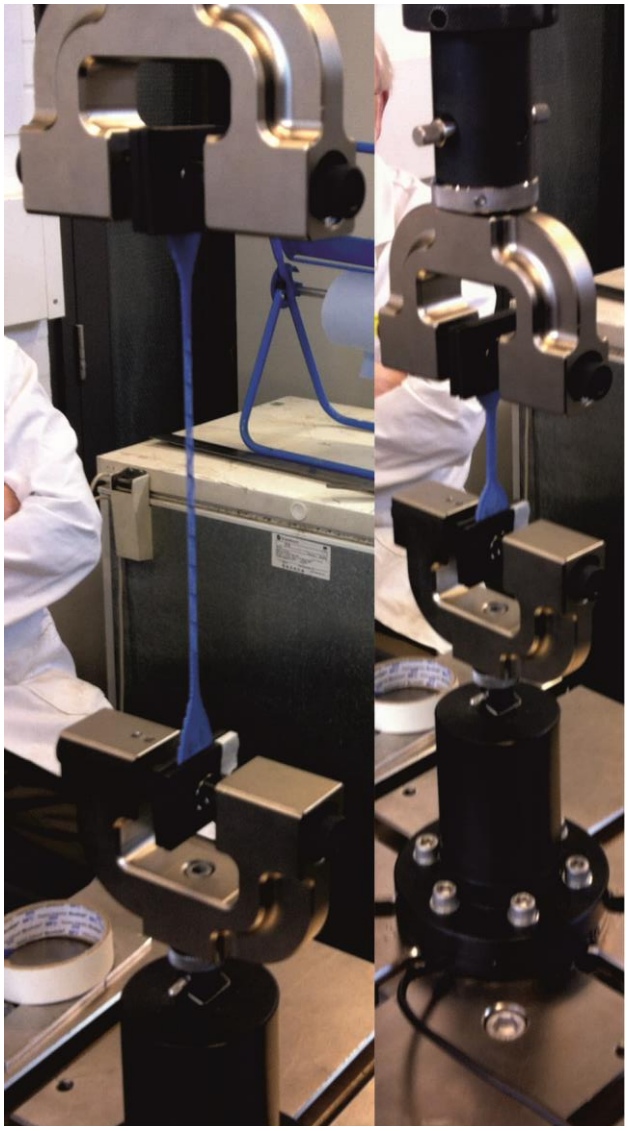

Figure 3.113, Destructive testing of V1.1 0.6, before testing and just before the sample broke. figure by author

3.12.6 Discussion

When comparing the results of the test, the Masters student concluded that the breaking force was proportional to the filament size, with thicker filaments requiring more force, however the extension was inversely proportional to the size of the filament as the extension of the 0.4 and 0.6 samples was larger than that of the thicker filaments.

It is important to note that while the crossbeams stabilise the structure, they also make it weaker when the tension is applied at 90°. This is because the cross beam filaments cause stress concentration on the tension filaments in the areas between the cross beam filaments.

Jonathan's computer model was setup to simulate with two different sets of data, one with the information from the data sheet of the material, and another with information gained by performing tensile testing with samples cast from the silicone used. The experimentally measured tensile strength was 737.5Pa, while the data sheet claimed 16MPa. However the tests with the computer model using both values showed very little difference in the predicted breaking force of the log-pile test samples, a reason for this discrepancy was not found (Oxley, 2012, p.86).

The simulated breaking forces were approximately 2.06 times larger than that measured with the destructive testing of the log-pile samples, this was attributed to the limitations in the ANSYS simulation (as the model had to be simplified to enable simulation) and to issues related to how materials were assigned for simulation (Oxley, 2012, pp.86-87).

3.12.7 Summary of the Deposition of Tensile Test Samples

The design of the tool-path went though several iterations until a suitable strategy was found; drawing of the layers was time consuming. It is evident that this could not have been done using any other method as the dimensions and density of the tabs and testing area were closely controlled in the design stage. This level of control would not have been possible using an automated solution. Keeping all the variations organised was also challenging, in the end the samples were marked in the tabs while the silicone was still soft in order to differentiate the samples.

Whilst the tool-paths were closely controlled, the deposition of material was adjusted by eye and relied on the experience of the operator. This process produced subtle differences in each sample, so they were not identical. The tolerances required pushed the 3D deposition technique to the limit of what is possible with the current equipment, to move forward a more precise deposition method would be required to guarantee that all samples are identical. However even with these inconsistencies the samples produced showed good consistency during the tests as evidenced by the standard deviation of the experimental measurements.

3.13 Development of RC Car Tyres

3.13.1 Introduction

Most of the applications developed from the research with the Mk3 were sometimes difficult to explain to people outside the field, a set of demonstrator artefacts that were fun and exciting were desired, something that could spark interest.

This is where the idea to deposit RC car tyres came from, by adjusting the tool-path parameters the performance of the tyres could be tuned, or changing the geometry of the tyres could be used to adapt a car for different terrains.

For this test the Micro-T RC car manufactured by Team Losi was selected, this was a small 1/24 scale car, it was selected because the small scale meant that the tyres would be small (22.5mm rim) and therefore quick to make.

3.13.2 G-code generation

Initially the tyres were 3D modelled in 3D Studio Max and the G-code was generated using the Slic3r method. Different parameters were tested to see if the hardness of the tyres could be changed by adjusting the number of perimeters and the density of the infill.

The concentric infill was used in slic3r, however due to the size of the tyres it became evident that this infill had a limitation, as the infill produces a series of concentric rings the perceived hardness of the tyres was not uniform, it would feel soft when pressed softly, but as the force increased the rings were pushed together and the tyre suddenly became harder. The infill pattern was changed to rectilinear, however this had a worse effect, as discussed in the early silicone tests, a 90° periodic build has anisotropic

mechanical properties, meaning that the structure behaves differently depending on the angle the force is applied, in the case of the tyres deposited with the rectilinear infill it meant that the tyres were soft when force was applied at 45° perpendicular to the perimeter but harder when the force was at 90°, a tool-path was needed that could distribute the force isotropically i.e. the same in all directions perpendicular to the perimeter of the tyre.

The tessellated tool-path would be suitable for this application, however the tyres needed to have a round profile as the RC car had a large camber in the suspension, so a straight walled cylinder would not be suitable for the car and therefore the 2D method was not suitable for this application.

3.13.3 2D+3D Programming method

To address this limitation a new method was developed, this would have the advantages of the hand drawn tool-paths but the surface geometry would not be limited to straight walls, this was called the 2D+3D method.

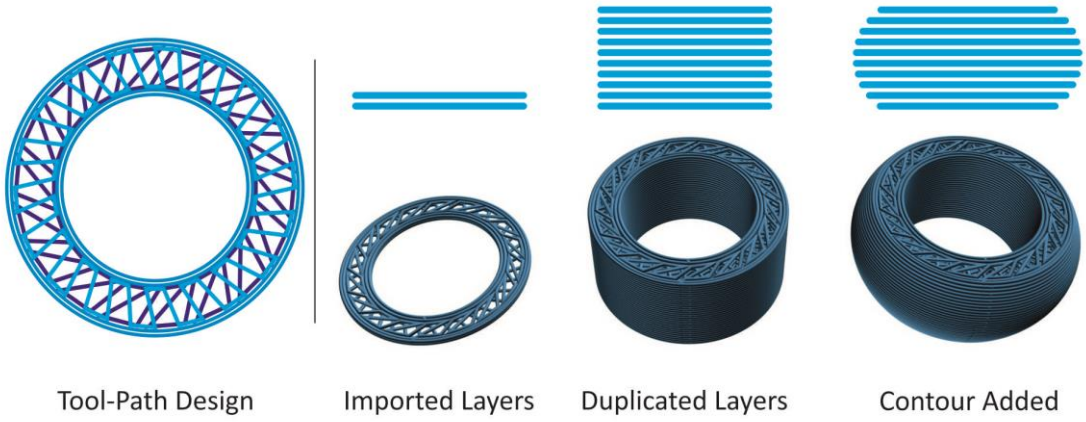

Figure 3.114, The 2D+3D method. figure by author

The layers are designed in 'Corel Draw', but only the basic shape and pattern. These are imported into 3D Studio Max, where they are duplicated to the required height. Within 3D Studio Max, the layers are collectively manipulated as if they were a 3D solid model to produce the final geometry (Figure 3.114). This method enables the possibility of creating tool paths that twist, taper and have rounded features that would otherwise be impossible just using the 2D method.

This edited group of layers is then imported as a *.dxf file into CamBam to generate the G-code. As previously mentioned in the 2D method, each layer is set as an engraving. CamBam preserves the height data as supplied by 3D Studio Max, meaning that when the G-code is generated all layers have the Z values for each layer but are offset by -0.4mm due to the engraving operation applied. The resulting G-code is then modified by replacing all the Z values with variables, this is a similar process to that used in the Slic3r method developed during the artery project, commands to start and stop deposition are also added to every layer.

3.13.4 Tessellated Car Tyre

This method was applied to the tessellated tool-path to produce the desired round profile for the tyre, the contour was only applied to the outer edges and the perimeter of the tyre, the centre was left with straight walls so that the tyre it would fit the rim of the RC car.

As this method increases the size of the original tool-path, it can reach a point where the infill pattern does not meet the perimeter and adherence is compromised. So to account for this, the 2D -tool-path was designed with the spokes of the infill closer to the perimeter than it would otherwise be necessary.

The deposition of this tool-path and the other tests with the Slic3r method are discussed in the RC Car Tyres section in Chapter 4.

3.14 Revisiting Metal Clay with The Mk3

3.14.1 Introduction

Building on the knowledge gained from the metal clay trials preformed with the Mk1, the material was revisited once enough experience had been gained with the Mk3, this time with the intention of producing more complex builds and demonstrator artefacts.

This test used some of the tool-paths already developed for some of the silicone builds, in this trial used the same BronzClay as the Mk1 trials. It was mixed to the same specifications as that used in the Mk1 trials, and the same alumina Substrate was used for deposition. The only change was the tool-paths used and by extension the positioning equipment.

Deposition

A total of three builds were made using tool-paths from the Shock resistant jar build (the bottom and the tube) and the 45° square coarse pitch build (Figure 3.115). All the builds were made using a 0.6mm nozzle, a feed-rate of 400mm/min and a pressure of 5Bar.

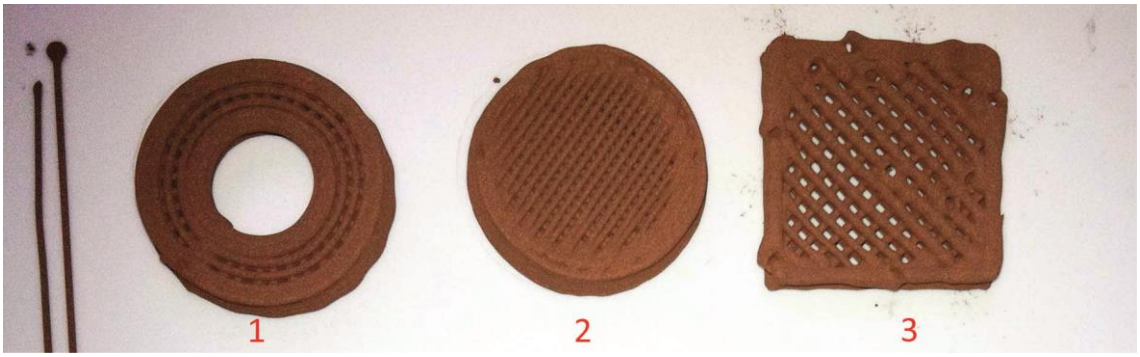

Figure 3.115, BronzClay samples, 1: Jar tube tool-path, 2: Jar bottom tool-path, 3: 45° coarse tool-path. figure by author

The deposition was uneventful for samples one and two (Figure 3.115), but sample three failed at seven layers due to air bubbles in the mixture, an attempt was made to repeat the build but the amount of material required for this test was underestimated and was near depletion by this point.

Sample two was almost solid, as this tool-path was designed for a 0.4mm nozzle the spacing between the filaments was very narrow, but a small amount of light could still be seen through the structure which indicated that the filaments did not bind into a solid mass.

Firing

The streamlined firing schedule for the BronzClay used in the Mk1 trials (Table 3.8) was further refined for the firing of these samples to reduce the firing time, the program can be found in Table 3.16.

Ramp up	*Hold time*
550°C degrees per hour to 845°C	*1 hour*

Table 3.16, Revised firing schedule for BronzClay. table by author

The samples fired well, they were buried in activated carbon to avoid oxidation of the bronze as per the method used in the Mk1 trials; Table 3.17 shows the results in terms

of shrinkage and weight loss. As the samples warped a small amount during firing the measurements shown are an average of measurements taken at several locations.

Before firing					***After firing***		
Sample #	*#layers*	*Weight (g)*	*Size (mm)*	*Height (mm)*	*Weight (g)*	*Size (mm)*	*Height (mm)*
1	*10*	*3.33*	*19,67*	*4.89*	*0.34*	*15.6*	*3.75*
2	*10*	*3.98*	*19.2*	*4.65*	*0.47*	*14.9*	*3.7*
3	*7*	*2.91*	*20.3*	*3.55*	*0.43*	*17*	*2.7*

Shrinkage after firing		
Sample #	*Shrinkage in size (%)*	*Shrinkage in height (%)*
1	*20.7*	*23.3*
2	*22.4*	*23.0*
3	*16.3*	*21.1*

Table 3.17, Firing results for samples 1, 2 and 3. table by author

The height shrinkage of samples one and two was very consistent, the diameter shrinkage was slightly different, but this can be attributed to the difference in tool-path between both samples. The lateral shrinkage of sample three was lower; this would have been due to the issues that occurred during deposition. Figure 3.116 shows the samples after firing was done, surface oxidation was cleaned using a wire brush prior to the picture.

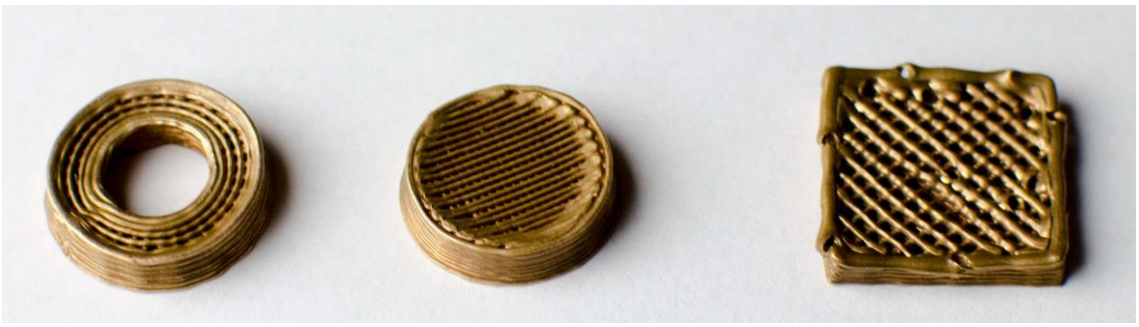

Figure 3.116, Fired test samples 1, 2 and 3. In BronzClay. figure by author

The tool-paths used for this test required no alteration apart from deposition settings. Further work was done with the Mk3 and the deposition of BronzClay and Silver PMC; the details of this investigation are in the 3D Deposition of Precious and Other Metal Clays section in Chapter 4.

3.15 Chapter summary

The work shown in this chapter has demonstrated the versatility of the Paste Deposition Modelling technique through the use of a large range of materials, structures and applications.

The programming method has evolved from the early manual coordinate control used in the Mk1 through to using automated slicers and complex user-originated tool-paths. Figure 3.117 shows a block diagram of the different G-code generation techniques developed throughout the research project.

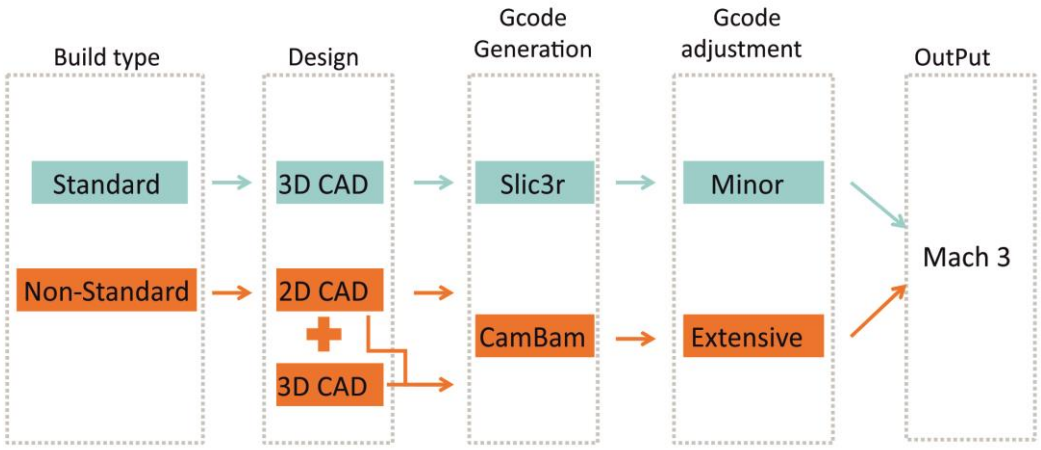

Figure 3.117, Programming methodology flow chart. figure by author

3d Deposition Process

The process of controlled and selective deposition of material is complex, and several factors determine the success or failure of a print.

The viscosity of the material cannot be readily changed without refilling the syringe with a different formulation; therefore all deposition parameters revolve around this fixed parameter.

The nozzle size is determined by the desired resolution and selected accordingly, the nozzle size then determines the layer height.
If the deposition height parameter is too low it will cause the material to be pushed to the sides of the nozzle and produce an enlarged filament, the friction then shifts and deforms previous layers rendering a very low quality print. Alternately printing too high will cause the accuracy of the rendered path to decrease due to the stochastic

nature of high viscosity liquids. It found that a layer height 0.05mm or 0.1mm smaller than the filament size yields very good results.

A good quality filament will span gaps several times its own diameter and not pull or deform previous layers, this notion was used to determine the optimal deposition pressure for a given feed-rate. This is normally a trial and error process but once determined for a particular material and nozzle size it can be used time and time again.

This thesis has a less conventional structure; due to the large body of work it was not possible to exclude results and analysis from this chapter as this would have led to very difficult reading as most decisions were done empirically based on results from the previous test. So it was decided that Chapter 4 would instead have a selection of projects that were made using the Mk3 system that could be used to validate the PDM process through applications.

Chapter 4 Case Studies

4.1 Chapter Introduction

The outcomes of this project are presented in the form of case studies since the outcomes were application based

The results and analysis were given in the methodology chapter where the relevant tests were performed and this chapter was used to discuss some of the applications that were developed during research to validate the PDM process.

Deposition of Silicone Fabric-Like Structures

Here the deposition and properties of novel silicone fabrics are discussed and potential applications are suggested.

Embedded Electronic Components and Water-Tight Structures

In this project two multi material wearable builds were developed and made in silicone, one with an embedded digital watch movement and another which is water-tight and is used to demonstrate a potential medical application.

Manufacture of Thin Walled Soft Moulds In Silicone

With the rising popularity of edible AM, this section was focused on an alternative method where bespoke soft moulds were made and used to prepare edible samples.

RC Car Tyres

This case study covers the development of silicone RC car tyres and the customisation of the deposition parameters to produce a range of tyres with different rigidity grades.

3D Deposition of Precious and Other Metal Clays

This case study covers the deposition of metal clay in the context of jewellery and craft, several benchmarking samples are presented as well as rings and a pendant, some of the builds have been exhibited in a curated online gallery and another was presented with the Goldsmiths' technological innovation award.

4.2 Deposition of Silicone Fabric-Like Structures

4.2.1 Introduction

The parametric tool-path was originally developed to deposit large square builds, using variables inside the G-code it was possible to change the size of the build and the filament pitch. These adjustments made it possible to deposit structures measuring 100mm x 100mm, the code developed only had 100 lines of code, which was necessary as at the time the trial version of Mach3 was being used, which was limited to 500 lines of code. Without the parametric code it would have been impossible to deposit structures this size at the time they were made.

The initial test with the parametric code was used to produce a silicone build 100 x 100mm five layers high (~1mm), a 0.2mm nozzle was used and the pitch was 0.4mm, leaving a gap between the filaments of 0.2mm. The resulting build had fabric like properties, it did not feel or look like the material it was made from, this development warranted further study with this code.

4.2.2 Silicone Fabric

Based on the apparent flexibility of the first fabric sample (five layers) it was decided that the tool-path would be tested with different sized nozzles to see how the layer thickness affected the structure. To emphasise the flexibility of the material only two layers were deposited per build, the pitch was changed depending on the size of the filament used and the size of 100 x 100mm remained the same for all samples.

0.2mm Build

The first silicone textile produced was made with the same parameters as the 0.2mm five layer build, but it was only made with two layers.

Figure 4.1, Silicone textile made with 0.2mm nozzle. figure by author

The 0.2mm build can be seen in Figure 4.1, It is difficult to show how impressive this build was, although the picture shows the 'drop' of the fabric and the 'sheen' of the filaments, it falls short at demonstrating the feel of the fabric. The whole structure feels like is should fall apart with the slightest bit of effort. But it does not, it is flexible and elastic, the best way to describe it is that it feels like chain mail, 0.35mm thick chain mail.

0.4mm Builds

The next nozzle size used was 0.4mm, these builds were made with coloured silicone to better show the internal structure, the pitch was 0.8mm.

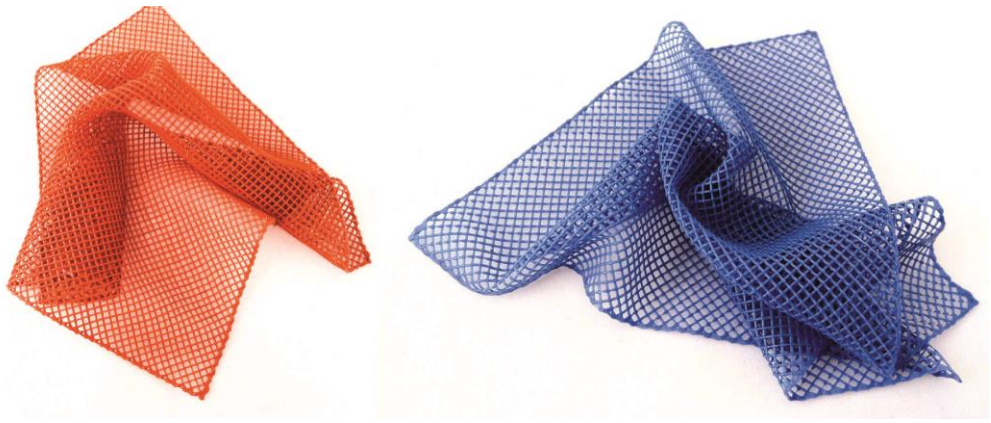

Figure 4.2, 0.4mm silicone textile builds, in red and blue silicone. figure by author

These builds felt more rigid than the 0.2mm build, this was not surprising as they were twice as thick at 0.7mm. But they still retained some of the original properties from the 0.2mm but felt more robust, where the 0.2mm build felt delicate the 0.4mm now felt like it could be stretched.

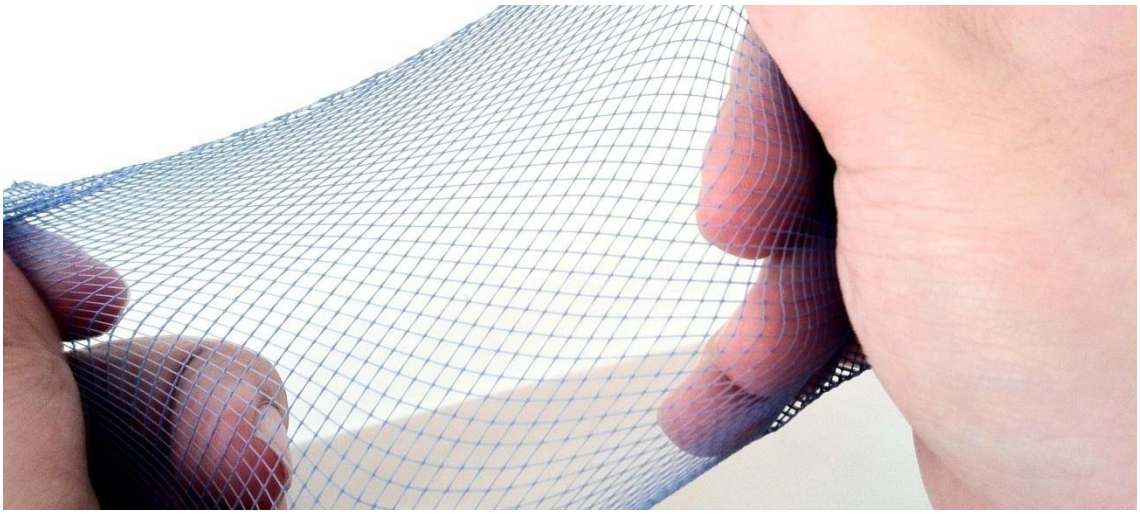

Figure 4.3, 0.4mm blue silicone fabric build, stretched to demonstrate the strength of the structure. figure by author

0.6mm Build

The tool-path was tested again but this time with a 0.6mm, the pitch was 1.2mm.

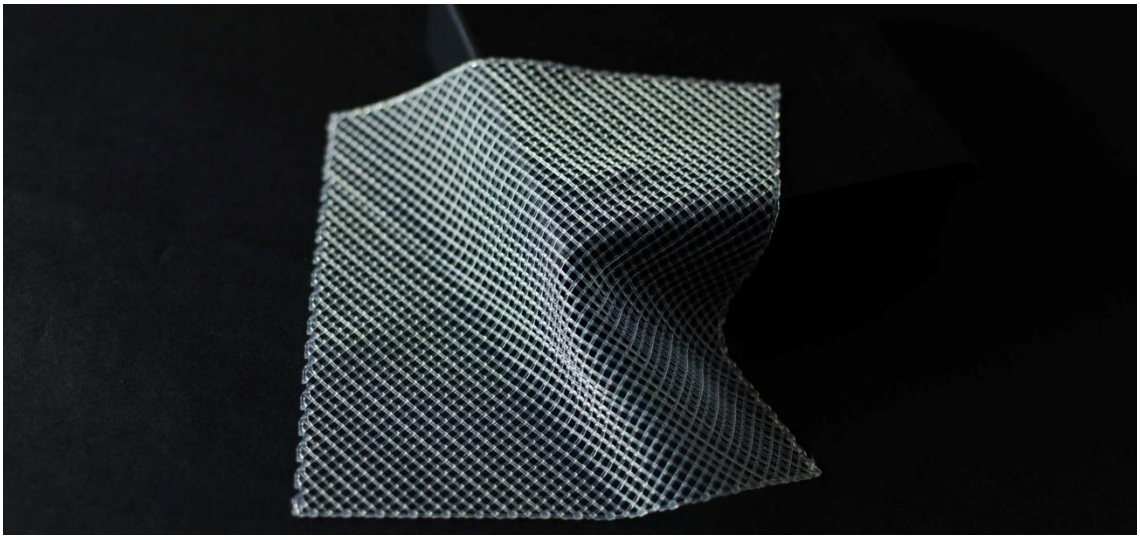

Figure 4.4, 0.6mm silicone fabric build in clear silicone. figure by author

This build was very different from the others with the smaller filaments, it did not have the smooth or delicate feel and it was far more rigid and rough.

Discussion

The silicone fabrics were demonstrated several times in conferences and lab visits throughout the research project and were handled by many. It was interesting to gage the reaction of people to the fabrics, the build with the 0.4mm filament size gave the perception that the fabric was stronger and could be handled and stretched without breaking. However when handed the 0.2mm build, the most delicate of all, it was handled carefully. As a result to this day the 0.2mm fabric sample has been the only

one to have survived unscathed, the others have rips and holes where fingers have been pushed through when stretching the fabric.

The silicone fabrics could have many uses, particularly in the medical industry where they potentially could be used in wound dressings with medical grades of silicone. The fabric would allow the skin to breathe but remain transparent for observations to be made; the elasticity also means that it could apply pressure. The clear silicone used had additives to stop the formation of fungi in humid areas; other additives could be added to the silicone to promote quicker healing.

To explore the possibility of using the silicone fabrics as medical dressings a few more tests were run, these were focused on making the fabrics stronger by embedding a material with a higher tensile strength.

4.2.3 Embedding Of Thread

Introduction

The idea of strengthening the silicone fabric required for another material to be embedded into the layers of silicone, for this test Hemp thread was selected, the large diameter of the thread would make is easier to see during deposition and still be flexible enough to be deposited from a nozzle, the multi material head v1 was used for this, with one syringe loaded with silicone and the other containing silicone and the thread, the thread would be encapsulated by the silicone as it was deposited. Due to the thickness of the thread, 0.8mm nozzles were used for both syringes; the parametric tool-path was adjusted accordingly and also made smaller (50mm).

Deposition

Several tests were conducted to embed the thread in the layers of silicone, the first idea was to feed the thread through a hole cut into the side of a nozzle, the thread would be pulled and become encapsulated by silicone deposited through the nozzle (Figure 4.5 C). This however did not work, while the thread did move quite freely while the silicone was not being deposited, upon pressurising the syringe the silicone did not pull the thread and in fact inhibited the movement of the thread.

The reason why this occurred was attributed to the side- hole arrangement, the silicone was trying to leak out through the side hole, this stalled the movement thread.

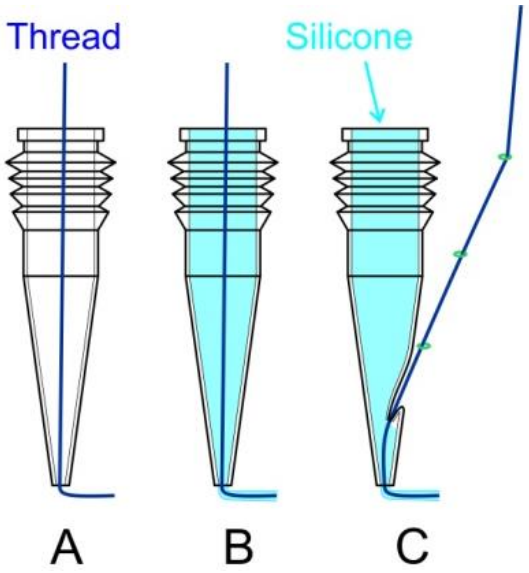

Figure 4.5, Proposed methods for thread deposition. figure by author

Another solution was attempted, this time the thread was fed from inside the syringe from a spool located inside the syringe with magnets, this time there would be no side hole on the nozzle and the thread would be fed through in the same axis as the silicone (Figure 4.5 B). This again proved futile, the silicone stalled the thread once more and simply extruded past the thread without depositing it.

The idea of encapsulating the silicone as it was deposited was abandoned and another experiment was conducted to deposit the thread onto a layer of fresh silicone, this time the syringe was loaded with thread alone, the spool was located with magnets inside the syringe and a nozzle was used to direct the thread (Figure 4.5 A).

This test was successful; the thread adhered to the layer of silicone and was pulled as the nozzle moved (Figure 4.6).

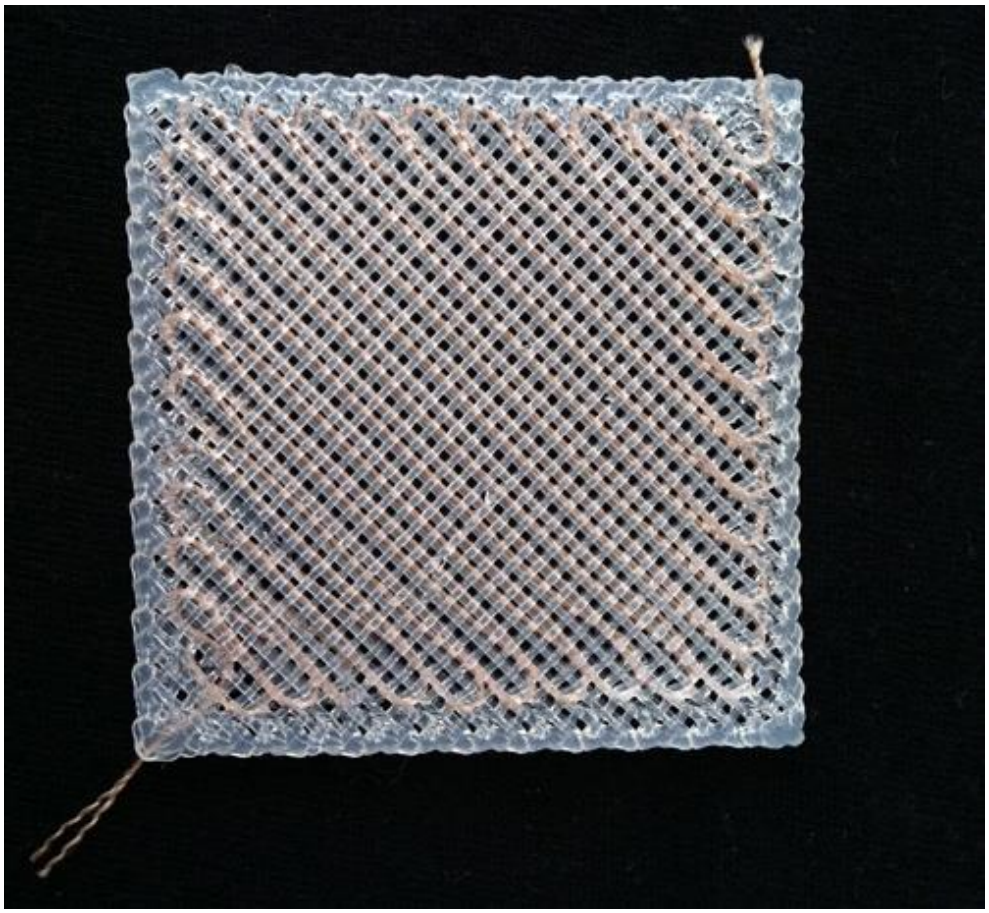

Figure 4.6, Finished Hemp reinforced silicone fabric. figure by author

The corners produced by the thread were very large, this was due to the minimum bend radius of the thread; a finer thread diameter might have produced better corners.

To ensure good thread adhesion the nozzle was set at a lower height than usual to help the thread adhere to the layer of silicone as it was deposited.

This test proved that the deposition of thread onto a silicone structure was possible, only one layer of thread was deposited between two layers of silicone, so the tensile strength of the silicone textile was only re-enforced in one direction, giving the build anisotropic properties where the textile could only be stretched in one direction.

4.3 Embedded Electronic Components and Water-Tight Structures

4.3.1 Introduction

The following products form the development of a wearable build that includes embedded electronic components and tests the potential for the structure to be water tight.

The envisioned application for these builds was in the medical device arena, where the watertight build could be used for thermal therapy, the temperature of the flowing water could be adjusted to match the patient's needs. The embedded electronics could be used to monitor the internal temperature of the water and provide other relevant telemetry.

Each of these functions was addressed as a separate demonstrator artefact; the embedding of electronics was realised here in the form of a watch. The water tight structure was designed to direct the flow of water inside the build much like a radiator.

The builds presented in this section were based on the tessellated tool-path used for multi material tube builds in Chapter 3.

4.3.2 Embedding Of Electronic Components (The AM Watch)

In this build a digital watch movement was completely encapsulated inside the build, to do this the G-code for the watch tool-path included a pause at the appropriate time for when the movement had to be inserted into the build. The silicone was allowed to rest for 30 minutes before the watch movement was inserted, after this time the deposited silicone was touch dry and the watch movement could be inserted without damaging the build or the silicone binding to the movement. After this operation the deposition was resumed to encapsulate the watch movement.

The tool-path for this build required extensive modification from the original tessellated tube tool-path strategy, it was still based on a 36 sided polygon but space had to be made inside for the watch movement. This tool-path was designed to be deposited with a 0.8mm nozzle to reduce deposition times and material use, this size filament also allowed for large gaps in the infill without collapse.

Special consideration was also taken when designing the tool-path as each layer had to be made in one continuous filament. This method ensured that there was the least amount of tool air time and reduced the chance of defective layers from the tool head lifting.

This build also used the multi material capabilities and automated tool change of the deposition head v2. The tessellated infill was deposited in "space blue" silicone, while the perimeters were deposited in the clear silicone; this formed the window for the watch movement. Figure 4.7 shows the build at the moment the watch movement was inserted into the build.

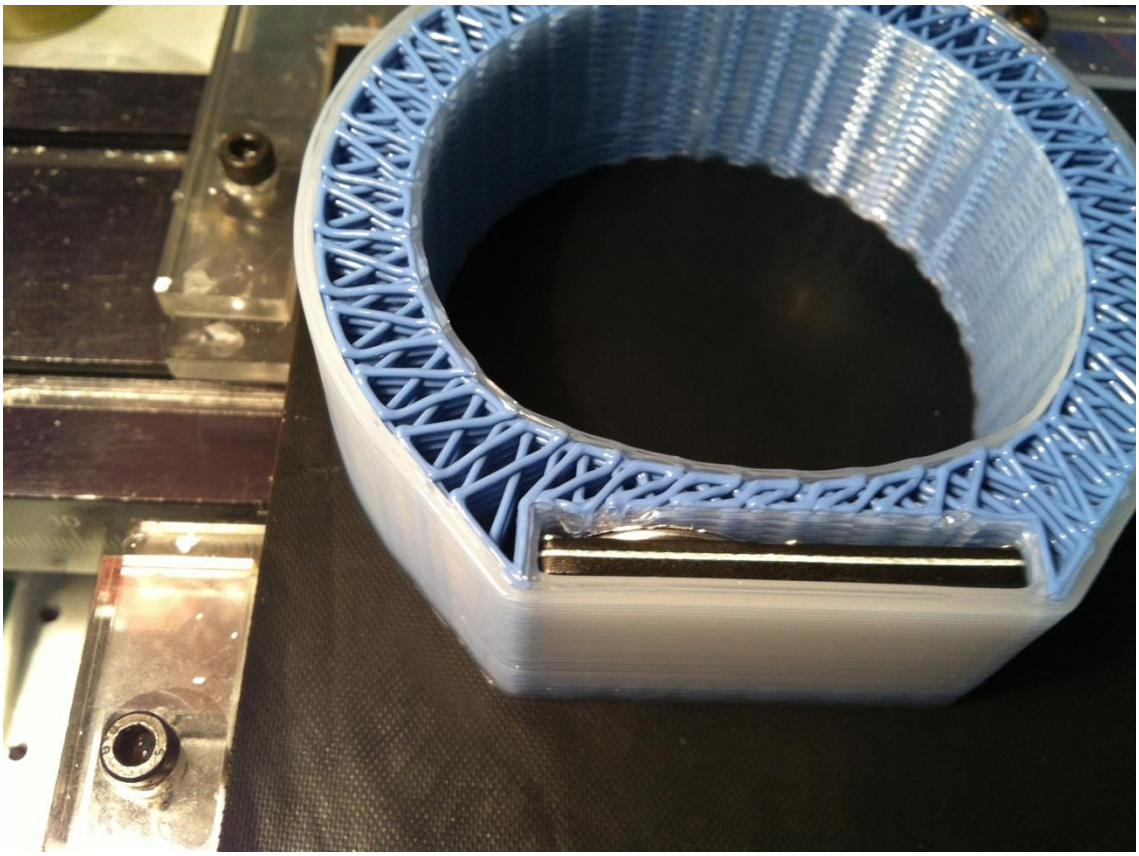

Figure 4.7, AM watch in blue and clear silicone. Build at the moment when the watch movement was inserted. figure by author

This build was successful, there were several failed attempts at this tool-path, most of the issues stemmed from the material change operation, it was difficult to calibrate the fixture offsets so that both tool-paths aligned properly.

Figure 4.8, Complete AM watch in blue and clear silicone. figure by author

Summary

This build demonstrated the multi material capabilities of the Mk3 and the method for embedding non-AM components into a build, both of which were successful in the creation of the demonstrator artefact shown.

The band was soft and comfortable when worn and the buttons on the side of the watch movement could be accessed with ease through the silicone. The clear silicone that formed the window of the watch created a lenticular effect as the light from the watch passed through it, the large 0.8mm filaments emphasised this effect as can be seen in Figure 4.8.

4.3.3 Thermal Cuff Device

The tool-path for the thermal cuff was based on the tessellated tool-path strategy, the wall thickness was 15mm and just like the AM watch it was based on a 36 sided polygon set to phase 3 to create the pattern required.

The tessellated tool-path produce a large open cell structure with gaps between the filaments and also the layers (Figure 4.9), this makes it suitable for water to pass through it as it does not block the flow.

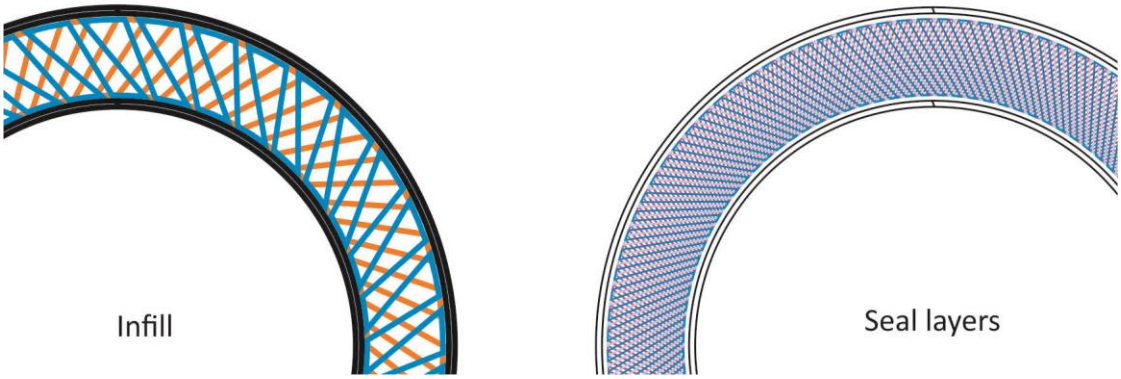

Figure 4.9, Thermal cuff tool-paths. figure by author

As the build needed to be water tight tool-paths were also designed for the top and bottom of the build that would seal the build (Figure 4.9), these were base on a 100 sided polygon to produce enough spokes to create a solid layer, the seal was made from a total of four interlaced layers, some of these were rotated about the Z axis by 5° so that the filaments would line up with the gaps from the previous layer.

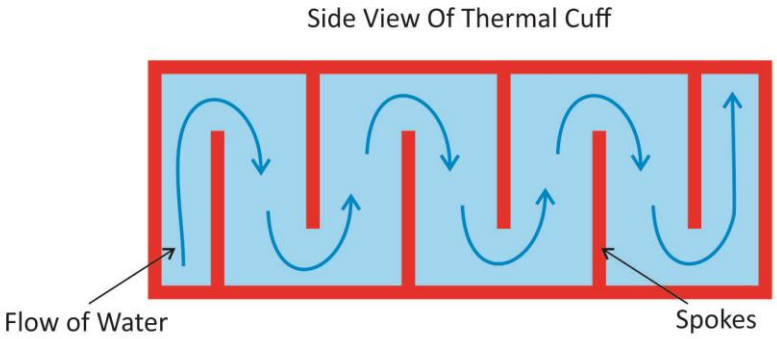

Figure 4.10, Side view of thermal cuff showing the directed flow of water. figure by author

The thermal cuff needed to direct the flow of water (Figure 4.10) and spread it evenly throughout, so internal solid spokes were added that would segment the inside of the cuff, then by strategically depositing some of the spokes the resulting structure could direct the flow of water like a radiator.

Figure 4.11, Partially completed thermal cuff showing spokes used to direct the flow of water (orange). figure by author

Figure 4.11 and Figure 4.12 show how the spokes interact with the tessellated tool-path by segmenting the structure, the spokes are separate from the infill and as such are 'over-printed' on top of the existing infill (transparent in picture), this produces some accumulation of silicone but ensures that the segment seal is good. Some spokes are deposited higher or lower than others to allow water to pass through; this creates the radiator flow required for the cuff.

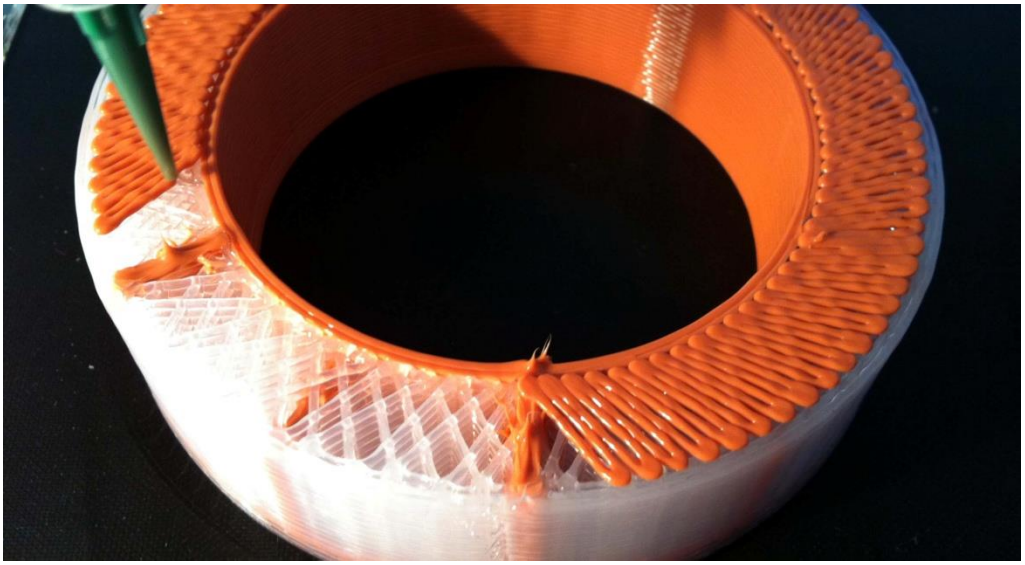

Figure 4.12, Thermal cuff being deposited. In orange is first of four seal layers. figure by author

The seal layers were tricky to deposit as the spokes open up a small amount towards the outer edges, this left small gaps between the filaments (Figure 4.12), the purpose the four seal layers was help block these gaps to ensure a good seal.

Whilst the top seal was designed to be solid, the bottom seal had two holes so that tubes could be installed to deliver liquid into the cuff, the spoke between the two holes was left solid throughout the height of the build to separate the inlet and outlet holes (Figure 4.13).

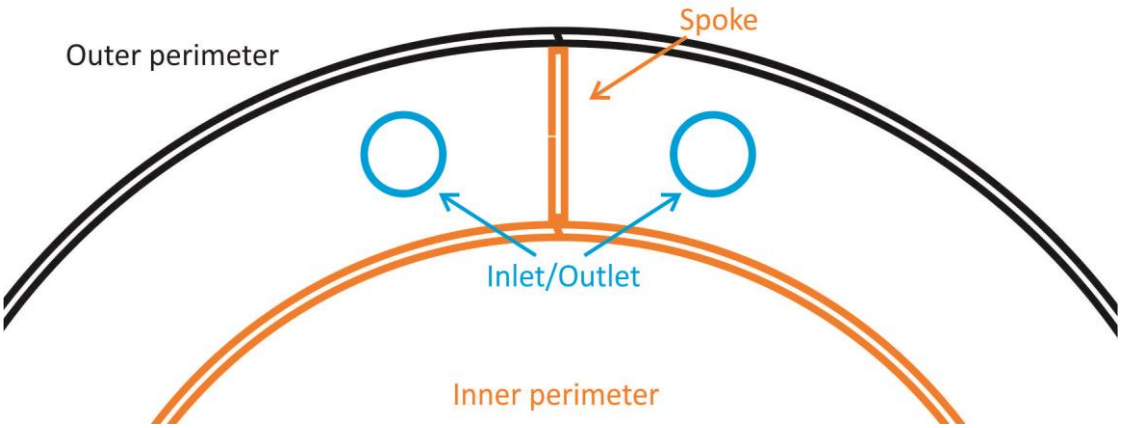

Figure 4.13, Inlet and Outlet holes of the bottom seal layer. figure by author

Once the thermal cuff was deposited, silicone tubes were installed into the holes and fresh silicone was used to adhere the tubes to the cuff, as both were made of silicone this bond was strong and permanent. The cuff was initially tested by blowing air into one of the tubes while the other was clamped shut, if the cuff was water tight then no air would escape.

Figure 4.14, Finished thermal cuff with inlet and outlet tubes installed. figure by author

This was not the case, there were several leaks around the perimeter of the top and bottom seal layers, these were sealed by applying fresh clear silicone over the seal layer, when this was done it was tested again and the leaks were gone (Figure 4.14).

The thermal cuff measured 90mm in diameter, had 15mm wall thickness and was 28mm tall. The main factor that limited how tall this build could be made was the material capacity of the syringes used; it was not possible to make this build any taller with the current equipment.

This build was revisited at a much later date with the intention of building it to a taller size, this new build also had a revised strategy for the seal layers; they were made with concentric circles instead of the tessellated path. This build was made using the Development prototype of the "Newton3D" equipment (see commercial validation Chapter 5), which although it did not have a multi material head, it was capable of depositing with the full 310ml tube of silicone, the build was completed to a height of 45mm.

Testing the thermal cuff

The original plan was to test the thermal cuff by pumping a hot or cold liquid through and recording the experiment with a thermal camera, however it was found that the resolution of the camera did not show the flow particularly well. A more suitable another method was devised to visualise the flow of liquid. The solution was to pump coloured liquid through the structure making it possible to see the flow through the clear silicone (Figure 4.15).

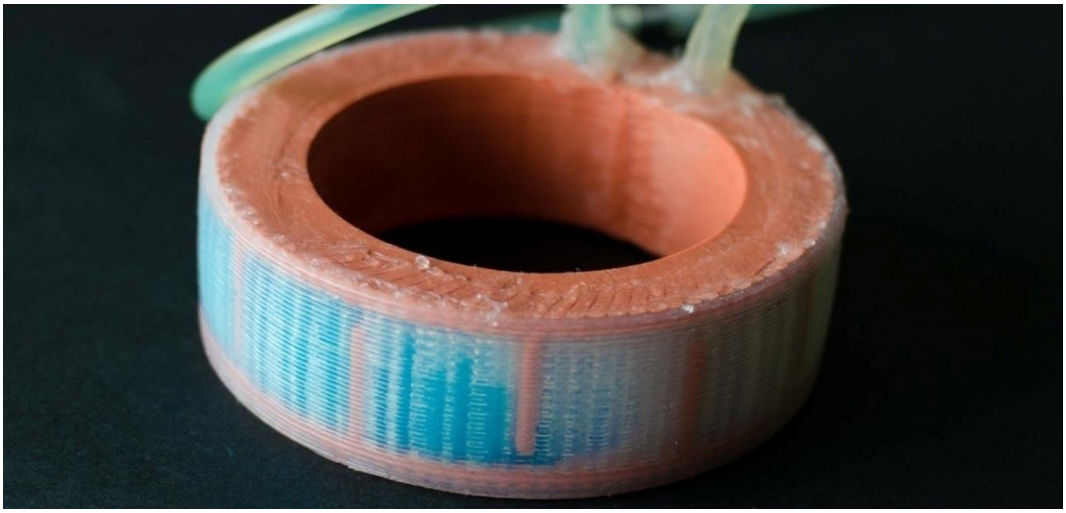

Figure 4.15, Thermal cuff with blue liquid flowing through the structure. figure by author

This test was also done with the revised thermal cuff, the larger size emphasised the flow of liquid and it could clearly be seen as it travelled through the structure (Figure 4.16).

Figure 4.16, Revised thermal cuff with blue liquid flowing through it. figure by author

The revised tool-path for the seal layers worked better and required no extra sealing post deposition.

It is evident from the images that the flow of liquid is not evenly distributed, there are large air gaps where the liquid does not flow, these are not as evident in the small thermal cuff probably due to the size, but for larger builds it might be required to increase the number of spoke segments to encourage a better flow of liquid in the pattern required.

Discussion

Both the AM watch and the thermal cuff have demonstrated that it is possible to embed electronics inside a silicone build, and that complex water tight structures are feasible, the ultimate goal would be to marry both of these into a single build.

4.4 Manufacture of Thin Walled Soft Moulds In Silicone

4.4.1 Introduction

The work presented in this section was based on the methods developed in the deposition of the artery.

AM of personalised food is becoming popular as reported in the literature review with projects such as Choc ALM and ChefJet, however for applications such as bespoke cakes and other confectionary that require batch production this method becomes less practical. For these applications it may be more suitable to produce a mould that could be reused.

To test this idea a few hollow builds were made in silicone that could be used as moulds, the silicone was designed as a bathroom sealant so it is perhaps not suitable for food, however for the purpose of testing this did not matter. In the event that the moulds be used for food consumption an alternative food safe silicone would be required. The silicone used for these tests can withstand -40°C and up to 180°C (Mapei, 2012) which means that it will survive the cooking process.

4.4.2 Geometry Benchmark

Before experimentation started with the deposition of moulds a test was run to determine if the silicone could be deposited to form concave and convex surfaces without any infill or support. To test this a model was made in 3D Studio Max featuring a group of spheres merged together (Figure 4.17), this would test for both convex and concave surfaces while at the same time exploring the limits of the deposition method.

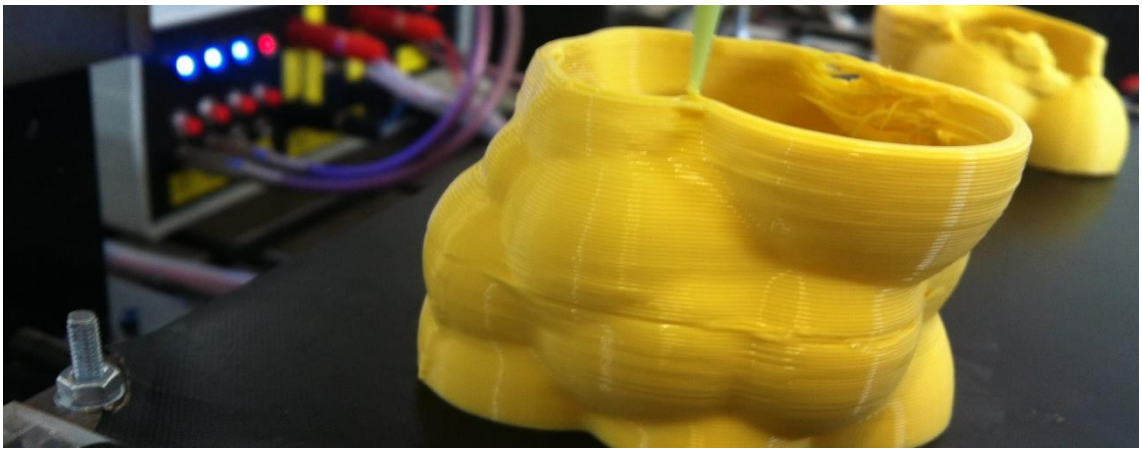

Figure 4.17, Complex surface test with silicone, Slic3r method. figure by author

This build demonstrated that while complex round surfaces were possible, when the surface angle went beyond a certain point the build started to fail as the filaments did not have enough support. This build did not complete successfully, but it was expected to fail, what was unknown was how far it could get before failure.

4.4.3 Aalto Ice Mould

The first experiment with deposited silicone moulds was aimed at testing how the structure would behave at low temperatures, so an ice mould was designed in 3D studio Max and sliced, the top layers were deleted from the G-code so the mould would have an opening, the bottom layers were left solid.

The mould was based on the famous Aalto vase (Figure 4.18), this was also made for the purpose of promoting the project at a conference as they could be given out; as such the mould was also designed for quick deposition so several could be made.

Figure 4.18, Aalto vase silicone mould, figure by author

The build was done using a 0.4mm nozzle, a layer height of 0.35mm and two perimeters. The mould worked well with no leaks, however it had the tendency of bulging in the middle when frozen with water inside as the ice expanded; this would have worked better if made with thicker walls to resist the expansion.

4.4.4 Star Cupcake Mould

The Aalto ice mould was a little too small to test anything other than ice in it as the serving size was too small, so a larger mould was designed to test the method at a

realistic size. The mould featured a large round taper and a twisted star profile, it was 50mm tall and about 65mm in diameter at the widest area (Figure 4.19), it was sliced to the same resolution as the Aalto mould but with four perimeters to increase the rigidity of the mould, this mould took around six hours to deposit.

This mould was tested at the highest recommended temperature by the manufacturer at 180°C, it was used to bake a small cake. The purpose of the twisted star shape was to see if the how much detail could be transferred to the cake as it was thought that the cake mix would expand during baking and deform the mould reducing some of the sharpness of the detail that had been deposited.

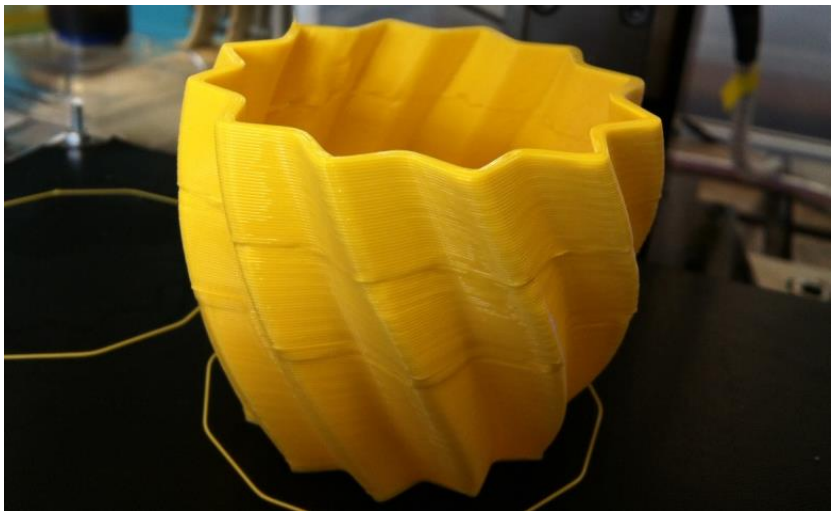

Figure 4.19, Deposited star shape cake mould in silicone. figure by author

The deposition of the mould had some defects, these were caused by the nozzle accumulating material from previous layers and causing some filaments to be damaged, however these defects were not critical and the build was completed.

The mould was tested several times in the oven, the first attempt at baking failed as the cake mix stuck to the walls of the build; it is suspected that the striation texture from the deposition had something to do with this. So the test was repeated but this time the mould was covered in flour to aid in mould release, this time the cake released successfully (Figure 4.20).

Figure 4.20, Small cake baked in star shape mould. figure by author

The silicone mould showed no signs of deterioration or discoloration from the baking tests, the elasticity did not change and the smell did not indicate that the polymer had burned. The mould did not deform during baking and the resulting cake took all of the detail from the mould with the individual layers evident on the surface.

4.4.5 Seashell Mould

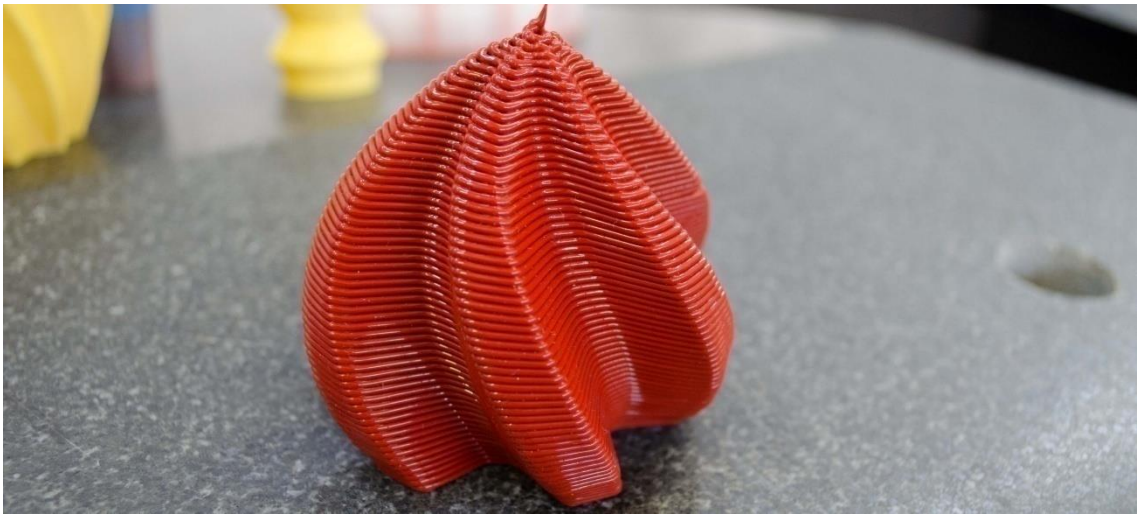

Figure 4.21, Seashell mould in red silicone. figure by author

The final mould made for this study was in a form that resembled a seashell; this mould as opposed to those made thus far was not sealed at the bottom, but was tapered to a point (Figure 4.21). This mould was designed to take into account the limits of the maximum draft angle while at the same time providing an aesthetic form. To speed up the build time this mould was made using a 0.8mm nozzle, twice the size of the one used in the previous builds, but even with these measures it still took around three hours to deposit, it had three perimeters (2.4mm wall thickness) for wall stability.

The wall thickness was ideal for the mould, it was thick enough so it did not readily deform when used but also easily inverted without tearing, this was a desirable attribute as it aids in releasing objects cast from it.

This mould was tested with a variety of materials including; glass wax which was heated before being poured in, clear polyester resin which was poured under vacuum and gelatine. The mould performed well during all these tests delivering consistent results.

The cast gelatine showed excellent surface detail with the finest features clearly visible, the gelatine was mixed to a higher concentration so it would not break when releasing from the mould (Figure 4.22).

Figure 4.22, Cast gelatine from seashell mould. figure by author

Discussion

The twisting geometry of the seashell presented an interesting notion, while there is no cutting force as one would see on a CNC machine cutting material, the friction from the filament had a small but evident effect on the filament placement. In practical terms this means that if the print direction is clockwise then the twist in the geometry must also twist clockwise, if it doesn't then the friction from deposition reduces the twist angle. This issue was encountered when depositing the seashell mould, to correct it the direction of the twist was reversed.

4.4.6 Silicone Soft Moulds Summary

Although the silicone moulds shown in this study were focused on food, the methods apply to other applications were the fast production of moulds is required.

The moulds performed very well during testing showing no signs of deterioration or tearing which bodes well for the mould life cycle, however more complex geometries with sharp undercuts would not be possible with this technique as demonstrated by the geometry benchmark test.

While the AM of moulds is not new in the field, the manufacture of moulds using durable silicone is. Normally the process of creating a silicone mould involves creating a master first, may it by subtractive or additive manufacturing, and then casting the mould from the master. With the technique demonstrated the full silicone mould would be finished by the time the master is made.

4.5RC Car Tyres

4.5.1 Introduction

One of the applications for AM in silicones is in the manufacture of bespoke RC car tyres, traditionally the hardness of RC tyres is adjusted using different grades of foam inserts inside the tyre, however this is limited to what is available in the market.

This study was focused on AM of tyres, the car selected for the test was a high performance 1/24th scale buggy manufactured by Team Losi, the scale of the car was advantageous as the size of the rim was 22.5mm, meaning that the deposition times would be short and they would fit inside the envelope of the machine.

The RC hobby is filled with customisation, with Hobbyists already designing and building their own models using AM machines, however tyres have remained outside of this scope to some extent, so the ability to build in silicone offers the opportunity to deposit tyres that suit particular applications.

The design of such applications can be manifested in the tread design as well as the rigidity of the tyre, which could be changed by way of adjusting the infill of the geometry.

4.5.2 Build Strategy

This study used a large range of design parameters to change the way the tyres behaved, most of the tyres were made using the slic3r method, but some were also made using the 2D+3D method to create a bespoke infill, this method was developed during this study. Figure 4.23 shows the range of build strategies used to create the RC car tyres, all the tyres were deposited with a 0.6mm nozzle.

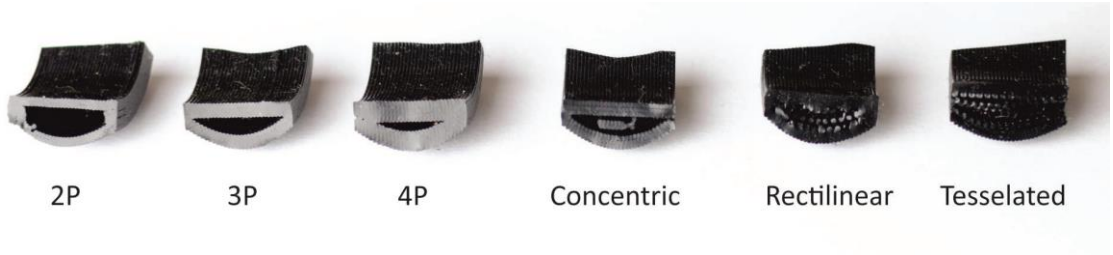

Figure 4.23, Cross-section of the tyres deposited, the P stands for perimeters. figure by author

No infill

The tyres made with this build strategy offered the most in terms of varying the harness of the tyre. They were made using the slic3r method and the hardness was adjusted by changing the number of perimeters in the slicing software, the settings tested were two (2P), three (3P) and four (4P) perimeters which produce a range of tyres from soft to hard respectively (Figure 4.23), the builds also trapped the air inside producing a pneumatic tyre.

Concentric infill

Another set of tyres were deposited using the concentric infill in slic3r, it was thought that this type of infill, having no cross members and composed solely of concentric rings would perhaps be suitable, the density for this build was set at 40%.

In practice the density of 40% was not evenly distributed along the height of the build, due to the limited space inside the tyre the slicer resolved the density to three perimeters and a narrow ring mid height of the tyre, this led to the sides of the tyre having a lower density than the middle when seen as a cross section (Figure 4.23), while this might be a desirable internal structure it was an unintended result.

Rectilinear infill

This build was made using the rectilinear infill, set at 40% and with two perimeters. This infill strategy was not ideal for this application, as demonstrated in the periodic silicone tests in chapter 3, this kind of structure tends to collapse at 45° angles and buckle at 90°; this meant that the tyres did not have an isotropic hardness.

Bespoke infill

While the tyres with no infill delivered very good results, the build strategy with the rectilinear infill was not successful. It was evident that none of the built in infill strategies could be used to produce a tyre with an isotropic hardness.

To address this issue the tessellated tool-path was used as it was capable of delivering a more consistent hardness than the rectilinear infill; it was at this point that the 2D+3D method was developed.

Several factors had to be considered while designing the 2D vector layers for this method, the distance between filaments for the outer perimeter and interaction between the infill and perimeter had to be closely controlled so that the scaling of the layers would not leave filaments either too far or too close when the contour was applied, the start and end of the layers was carefully designed so that there would be no tool air time from the end of one layer to the start of the next.

Figure 4.24, RC car tyre made with the 2D+3D method and the tessellated infill. figure by author

This test with the tessellated infill was successful, the hardness of the tyre was evenly distributed, but the start and end points of the layers left a large bump along the side of the tyre. This was alleviated in the next build by not stopping the deposition between layers, it reduced the amount of time the nozzle lingered without moving which decreased the accumulation of silicone that caused the bump in the first place, while this did not completely resolve the issue, it was greatly reduced.

Figure 4.25, RC car with silicone tyres fitted. figure by author

4.5.3 Summary of RC Car Tyres

Under testing with the RC car the silicone tyres performed far better than the stock tyres (Figure 4.25), the different hardness grades produced with no infill demonstrated a perceptible change in performance, with the two perimeter build having a noticeable larger contact patch.

In the end however this was just a hobbyist application, the highlight of this study was the development of the 2D+3D method, expanding the deposition technique toolbox. The methods developed here were applied in the production of rings in the metal deposition section (next section).

4.63D Deposition of Precious and Other Metal Clays

4.6.1 Introduction

Metal clays, by their nature, shrink on firing and this often needs consideration in the construction of craft objects. In an attempt to show control over the shrinkage, rings were considered as a suitable vehicle as they could erstwhile show the aesthetic characteristics of PDM when not considered as a strictly cast volume and using infills.

The deposited rings are then subjectively treated in view of the conventional methods of working with metal clays. Using workshop techniques the ability to deform fired rings was ascertained. This shows a bridge between the automated and the *'touched by hand'*. Considerations are given as to this hybrid nature of craft versus machine and the exploitation of PDM for its characteristics.

From initial results, a range of 3D geometries that show the limits of deposition can be developed. Finally to show how such materials, within the constraints found may be used for jewellery, a range is developed that suitably aligns the aesthetics of PDM and the possibility of self-originated infill structures with the intentions of the designer. This is subsumed within the creation of rings as they demonstrate the ability to create a product to a set size, taking into account material shrinkage during firing. It is considered that the internal structure of the part achieved by infills may also have an effect on the overall shrinkage. The investigation shows that the design exists in three domains, virtual, built as clay, and as metal and how these come together as a hybrid *AM-Craft* process.

As an aid to clarity, this case study contains some reiteration of information given in other chapters.

4.6.2 Metal clays

Metal clays consist of metal particles suspended in an organic binder which burns away upon firing; the metal particles also sinter (like DMLS) and produce a near fully dense metal part.

Precious Metal Clay (PMC) is a silver clay that emerged in the 1990s manufactured by Mitsubishi Materials; other brands such as Art Clay also exist and pre-formulated metal clays are also available in bronze and copper. Conventional techniques used with metal

clays are similar to those used in ceramic clays and pertain to craft, although the final object is commonly jewellery.

One of the fundamental issues of metal clays is that, despite manufacturer's guidelines, it is difficult to predict the shrinkage from the particles sintering. This is a relative black art, dependant on the geometry and scale of the item. It is also dependant on the specific clay formulation in terms of particle size, homogeneity, particle shape, and proportion of metal particles to binder. Some characterisation of the sintering process, relative shrinkage and the resulting material properties of the various formulations of PMC has been undertaken by (McCreight, 2010).

4.6.3 Material preparation

For BronzClay

The fresh clay is spread on a smooth surface (e.g. glass) with spatulas. Distilled water is gradually added with an atomiser. Olive oil is also added to help condition and lubricate the clay. This procedure is 'hands on' and the proportions will vary depending on the age of the clay and how long it is mixed for, but roughly the proportions are 4-6 grams of water and 0.1-0.3 grams of olive oil for every 50 grams of clay. The result is a paste with a viscosity comparable to peanut butter.

For silver PMC pro

PMC Pro is prepared in the same way as the BronzClay and to a similar consistency. The only difference being that the PMC Pro requires more water at 6-8 grams for 50 grams of clay, a little more oil is also used at 0.3-0.5 grams.

4.6.4 Deposition variables

There are three main variables to PDM: feed-rate of the X-Y table (mm/min), deposition height as in the offset of the nozzle from the layer being deposited (mm) and the flow-rate of the material. The flow-rate is determined by the material's viscosity and the air pressure. These three variables must be controlled to successfully deposit a line of material (Figure 4.26).

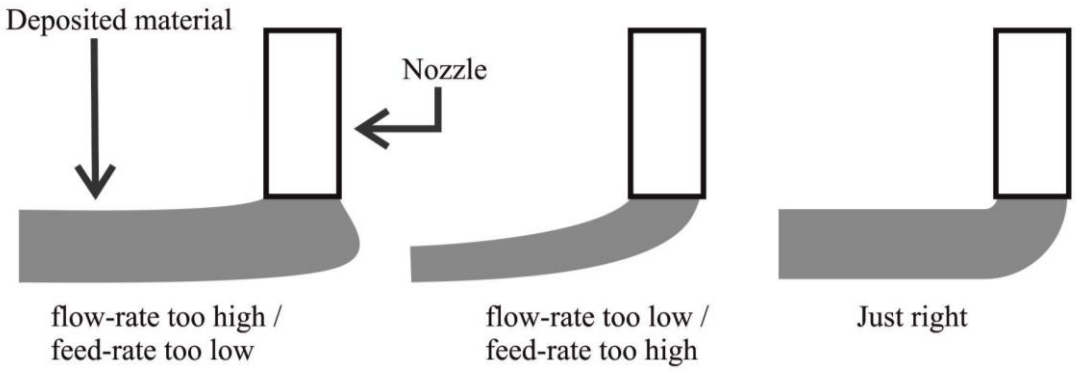

Figure 4.26, Relationship of the deposition flow-rate and feed-rate. figure by author

The feed-rate is normally 500mm/min as this is easily achievable by the Mk3. Deposition height is relative to the nozzle size being used; as a rule of thumb it is 0.1mm lower than the nozzle diameter. Using lower heights would deform the filament. If the deposition height is too high, then the filament will have the tendency to delaminate and the structure will also lack the strength to support itself. It is interesting however, that if the filament is deposited at a height of several millimetres, the material will have the tendency to coil randomly as it descends to the substrate; this stochastic property can lead to interesting structures.

Specific parameters for depositing are determined prior to the build with quick tests; this is due to variations between batches. A general working range was used as a guideline (Table 4.1).

	Nozzle diameter (mm)	*Layer height (mm)*	*Pressure (+/- 05 bar)*	*Feed-rate (mm/min)*
'BronzClay'	*0.6*	*0.5*	*5.5*	*500*
'PMC Pro'	*0.6*	*0.5*	*6.5*	*500*

Table 4.1, Table of general parameters. table by author

Depending on the geometry, for example with builds that have 90° corners, it might be necessary to use a lower feed-rate of 320mm/min. This speed produces defined corners that look better on that type of geometry. Depositing at this speed generally requires the pressure to also be lowered by 0.5-1 bar for both silver and bronze clays.

4.6.5 Determining a substrate

In previous tests with metal clays, alumina sheet was used as a substrate as it provided good adhesion when the clay was deposited, but released the sample once dry. Due to the number of samples produced during these tests an additional alternative was required to reduce deposition downtime. Square microscope glass slides were found to be an equivalent alternative.

4.6.6 Draft angle cones

These tests were undertaken to determine the maximum angle the clay could be deposited at unsupported. A filament has a round cross section, this geometry makes it very difficult for consecutive layers to stack and balance on top of each other. By adding two perimeters per layer the resulting structure is more stable and able to support the layers on top, as shown in Figure 4.27. Depositing unsupported structures with a draft angle of 45° is very difficult. This is because no matter how many perimeters the build has; at some point the filament is deposited in mid air and the stability given by several perimeters is lost.

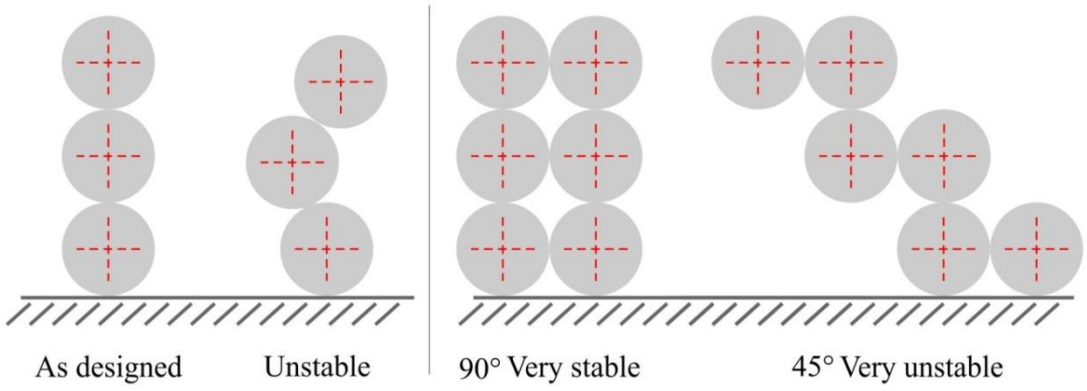

Figure 4.27, Perimeter stacking diagram. figure by author

Four variations of cones were made featuring draft angles of 30°, 35°, 40° and 45° with two perimeters. The cone specifications were that they be the same height (20mm) and have the same number of layers, in this case 40. A consequence of this is that the base diameter increases with increasing angle.

The cone geometry was created in 3D Studio Max and sliced with Slic3r.

The following parameters were set in Slic3r for the cones:

Layer height: 0.5 mm, Perimeters: 2, Solid layers: 0, Fill density: 0, Nozzle diameter: 0.6 mm, Single wall width: 0.5mm.

The single wall width is normally set to match the nozzle diameter, however with the metal clays it had been found that a wall width of 0.5mm gave better adhesion between perimeters making deposition more reliable.

The 30° and 35° cones built well, the first few layers had the tendency to slump due to the weight of the material, but as the diameter of the layer decreased the structure became more stable. This scenario, rather than producing a regular cone, results in something of a '*witch's hat*'. At 40° the inner filament struggled and became detached from the layers underneath at several points (Figure 4.28). The build completed but the surface quality was less than ideal. At 45° the deposition failed as anticipated. The filaments were unable to support the layers above which led to a flat base, this loss in height meant that consecutive layers were depositing too high, producing a randomly coiled cluster of filaments. This randomness could be a desirable feature. Only one 40° and one 45° draft angle cone were deposited as these were failures. Three 30° and two 35° cones were built to show repeatability of the findings.

Figure 4.28, 40° cone deposition defects . figure by author

BronzClay needs to be fired in an oxygen-free atmosphere for the bronze to sinter properly. This is achieved by burying the pieces in charcoal based activated carbon inside a closed stainless steel box. The hollow forms were inserted upside down with a metal mesh placed over the top. This prevents the granules getting inside the form hindering the shrinking process (Sanderson 2010, p.5). The cones are then covered with more carbon. The recommended firing schedule for BronzClay is: 'to ramp the kiln at 273°C/hr to 843°C, after which the hold time depends on the thickness of the clay and is between one to three hours (RioGrande 2011, p.9). This means a firing time of

between four and six hours depending on part thickness. From previous work with and PMC Pro, which fire successfully at a similar temperature but with the ramp at around 1000°C/hr it was reasoned that a faster more streamlined firing schedule could be possible. The recommended hold for pieces 3mm thick is two hours. The cones are about 1.2mm thick so the firing program was as follows: 550°C/hr to 845°C, hold 1:30 (h:m).

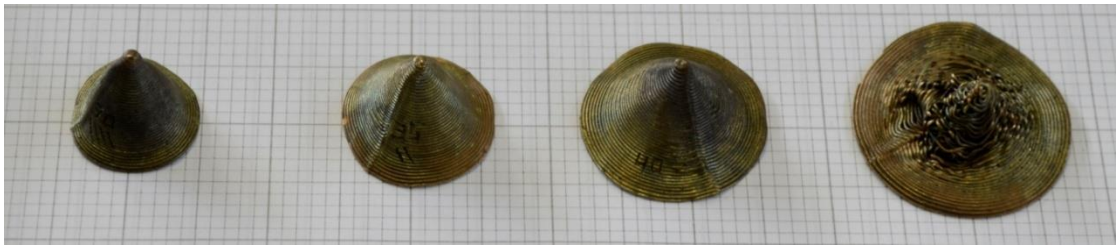

Figure 4.29, Fired cone details: from left to right, 30°, 35°, 40° and 45°, shown near 1:1 scale figure by author

The fired cones were not heavily oxidized, having just a light patina (Figure 4.29). The pieces were malleable and able to be bent without breaking suggesting the parts were fully sintered. The cones also warped a small amount, particularly at the base but this is something that is expected due shrinkage and heat distortion.

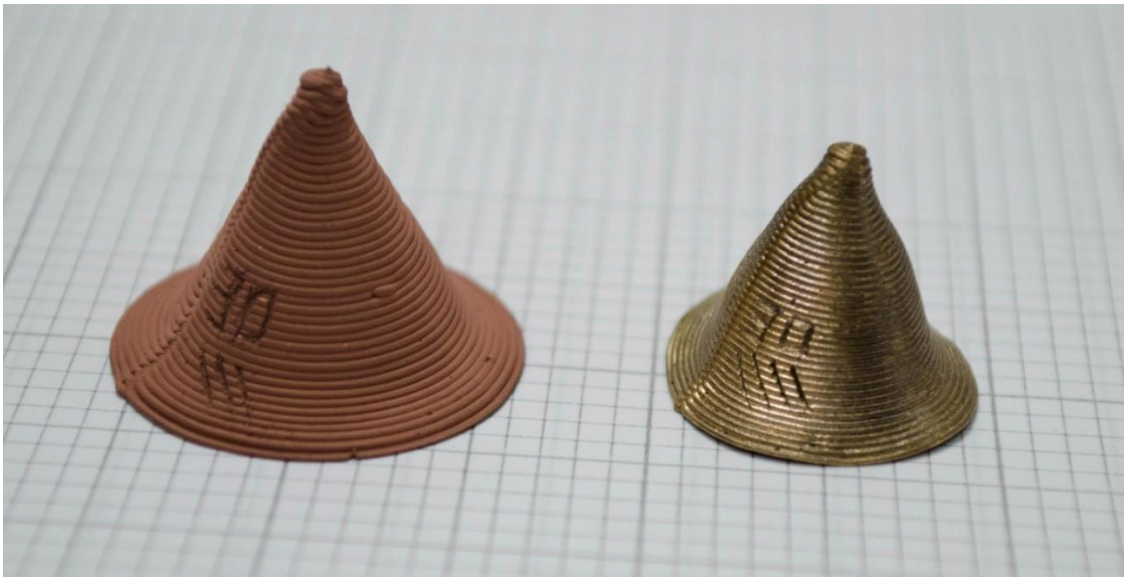

Figure 4.30, Shrinkage of the 30° cone from greenware to fired. figure by author

The shrinkage was substantial. Figure 4.30 compares the 30° cone as greenware (unfired) and fired. Table 4.2 shows the shrink percentages evident in the draft cones. Two percentages were calculated, the '*design to fired*' which shows how much the original design shrunk in total; and the *greenware to fired* illustrates the shrinkage of the material during firing. The user manual (RioGrande 2011, p.5) states that the

shrinkage should be 20 % but this is expected to be larger as the paste formulated for PDM has a higher water content, this is in line with the results, which show a maximum of 24.5 % shrinkage.

Draft angle	Design to fired height shrinkage (%)	Design to fired diameter shrinkage (%)	Greenware to fired height shrinkage (%)	Greenware to fired diameter shrinkage (%)	Greenware to fired weight change (%)
30°	*22.5*	*24.7*	*18.4*	*22.7*	*5.0*
35°	*24.0*	*25.0*	*19.2*	*24.5*	*4.7*
40°	*24.3*	*22.7*	*14.9*	*21.0*	*4.7*
45°	*31.65*	*22.0*	*21.0*	*20.0*	*5.2*

Table 4.2, Shrinkage data: design to fired and greenware to fired. table by author

4.6.7 Seashell geometry

The cones were used to underpin the development of the process towards producing sophisticated hollow builds. For this test the geometry for the Seashell mould was used as this geometry was known to be suitable for hollow builds from testing with the silicone (Figure 4.31).

This geometry was sliced with the same parameters used on the cones. While depositing in BronzClay there was an issue with the air supply which caused the pressure to constantly rise and fall. The effect was that the filament became finer as pressure fell, and as the pressure rose it became thicker. Consequently it became necessary to manually adjust the feed-rate in Mach3 on the fly. While the build was successfully completed, the surface had a wavy quality that was not part of the design. It is worth considering however, that this brings forth ideas as to how the effects of varying the flow-rate could be used for aesthetic purposes.

After firing the highest points of the geometry were filed and sanded to a fine finish, this was done to test if the BronzClay could take this sort of abrasion. Filing also revealed that the filaments were thoroughly sintered being without a trace of un-fired material. The final part can be seen in Figure 4.31.

Figure 4.31, Seashell in 'PMC Pro', 'BronzClay' and CAD geometry. figure by author

The Seashell was built in PMC Pro to compare it to the BronzClay part. PMC Pro was chosen over PMC3 as it is a stronger material (Cool Tools, n.d). As has been shown in the cone experiments the builds can, depending on geometry, be prone to some warping from drying and firing; they may subsequently need some tweaking by traditional techniques. The eventual focus of this study is to demonstrate the suitability of the process for jewellery. In a 2010 study, Sanderson demonstrated the relative strength of 'PMC Pro' by practically working the metal and sizing rings (Sanderson 2010, p.7).

The Seashell test showed that PMC Pro has a higher tendency to slump than BronzClay; this could be partially due to having higher water content. This was observed early in the build and to alleviate the slumping, air from the supply was directed at the build platform. This helped the build dry quicker as it progressed and lessened the impact of the slumping. This is analogous with fans being used in FDM systems to cool the extruded plastic filaments.

The effect of the slumping can be observed when comparing the two builds together. The BronzClay build has a steeper finish at the end, more akin to the designed geometry as opposed to the more dome-like finish of the PMC Pro build (Figure 4.31).

For PMC Pro the firing schedule is different to that of BronzClay. PMC Pro also has to be fired in activated carbon, although in coconut based carbon. There are two different firing schedules for PMC Pro, see Table 4.3 (Cool Tools n.d)

Firing option		Temperature options (°C)	***Hold time options***
1	*Bury in carbon within a stainless steel vessel*	*774* *774* *760*	*2 hours (large pieces)* *1 hour (small pieces)* *1 hour*
2	*Step 1: Burn out* *Step 2: Carbon*	*760 (on kiln shelf)* *Bury in carbon* *fire at 774 or 760*	*30 minutes* *1 hour*

Table 4.3, PMC Pro firing schedule as recommended by Cool Tools (Cool Tools n.d).

Sanderson (2010, p.3) studied the shrinkage of PMC Pro using standardised rings as a vehicle and profiled firing schedules, to determine the ideal hold time in relation to the amount of carbon used in firing. Sanderson (2010, p.10) determined that the more carbon the longer the piece should be fired for, she also stated that there is no risk in firing for longer periods.

Sanderson believed that this first phase helps reduce overall warping of the final sintered piece (2010, p.6). From both sources it was concluded that a two part firing program would be used. This program involves first firing the piece in atmosphere to burn-out the binder from the metal clay. The second phase is sintering the piece at 774°C whilst buried in activated carbon for one hour; both phases are heated at full ramp.

In firing PMC Pro, the following program was used, it was loosely based on the temperatures put forward by Cool Tools (n.d), based on Sanderson's (2010, p.6) findings the hold time was adjusted and the kiln was set at full ramp.

Phase 1: in atmosphere, full ramp to 774°C on open kiln shelf, hold for 30 min

Phase 2: in coconut carbon within stainless steel vessel, full ramp to 774°C, hold for 2 hours

The hold time was two hours as a large amount of carbon was used since the seashell is large compared to ring. This long hold time ensured the piece sintered fully. After firing was complete the seashell was left to cool in the carbon to avoid any oxidation on the surface, some fire scale was present but this cleaned off easily with a wire brush.

4.6.8 Producing rings

Tessellated pattern

Several rings were designed where the infill was the primary feature. Tool paths were created using the 2D method and the tessellated tool-path strategy. These rings were used to observe how much shrinkage occurred in the rings. The results from the draft cones showed a maximum 24.5% shrinkage. Sanderson (2010, p.4) anticipated shrinkage for PMC Pro to be around four to five ring sizes. The shrinkage for PDM with PMC Pro in terms of ring sizes would be expected to be greater due to the higher water content of the formulation.

The rings were built in BronzClay and PMC Pro to a height of eight layers (4mm). The glass substrates provided an excellent deposition surface. Once the samples were dry however, it became apparent that the layers in closer proximity to the substrate shrank less leaving walls slightly tapered. This was exacerbated in PMC Pro as it required more persuasion to release from the substrate which led to the bottom layers shrinking even less.

A further ring was deposited in BronzClay, it featured narrower walls and had a height of 16 layers; this ring emphasises the issue with the builds tapering during the drying stage (Figure 4.32).

Figure 4.32, Tessellated ring collection in BronzClay showing the taper effect. figure by author

As expected the BronzClay rings warped during firing, the geometry became elliptical and was no longer flat. The rings were strong enough however, to be hammered flat. The elliptical shape was then rounded on a ring mandrel, the rings were not stretched (Figure 4.33). In contrast the PMC Pro ring showed little warping and only required a few light taps with the mallet to make it fully flat and round. From *design to fired* all 4mm rings shrank 14.5 ring sizes from a UK 'Z+4 1/2' (23.6mm diameter) to P (17.9mm diameter) which is a linear shrinkage of 24.2 % and within the range illustrated by the draft cones. The most tapered 8mm ring shrank 13.5 sizes which considering the nature of the process does not seem unreasonable.

Figure 4.33, Tessellated ring design pictured in both its greenware state and fired state. figure by author

Hex rings

Traditionally metal clay is worked by hand. Smoothing of the surface of the clay is achieved by burnishing the piece with a wet tool and sanding once dry. To profile the shrinkage of PMC Pro, four rings were designed using the 2D+3D method, the rings feature hexagon geometry with an inner ring.

To compensate for the taper previously seen, the geometry was tapered outward by 10°. Two variations were deposited, one featuring straight walls and another twisted by 20°; two rings for each design were made. Once dry it was observed that the 10° compensation was too much, the rings were now larger at the top than the bottom; this was less noticeable in the twisted rings. In the greenware state one of the 20° twist rings was burnished to a smooth surface, this spread the clay to fill in the ridges between layers. After firing, it was polished. As fired, the rings had shrunk from the designed ring size S (19.4mm diameter) to sizes I (10 sizes, 15.1mm diameter, 22.2 % shrinkage) and J (9 sizes, 15.5mm diameter, 20.1 % shrinkage)

The taper was adjusted to 7° in the next ring and built to a larger diameter. The resulting ring was still tapered but this was barely noticeable (Figure 4.34). This large ring shrank from size Z+6 (24.4mm diameter) to ring size V (10 sizes, 20.1mm diameter, 17.6 % shrinkage). To test the strength of the ring it was annealed and stretched on a ring mandrel from its original fired size V to size W 1/2 (20.1mm to 20.8mm in diameter).

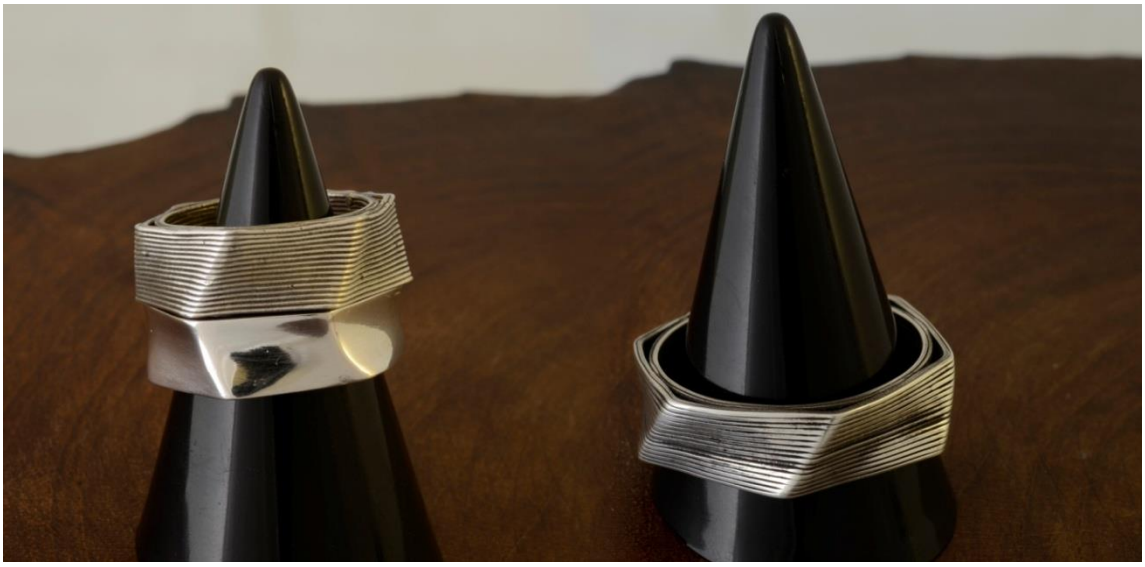

Figure 4.34, Hex rings in 'PMC Pro'. figure by author

All Hex rings shrank 9-10 ring sizes. It appears that the expressed linear shrink percentage by manufacturers would not be a good indicator for ring sizing. If you were to take the average of 21 % shrinkage shown in the previous hex tests, depositing at Z+6 would predict a ring size of S 1/2 which is far smaller than size V and a 12.5 size shrinkage rather than 10. This would suggest that depositing at around 10 ring sizes larger would yield the about correct size.

Final rings

A 'Cityscape' ring was designed with large features that could be smoothed and polished. The G-code was generated using the 2D+3D method. Figure 4.35 shows the computer generated models of both the tool path and the expected smooth outcome with respective shrinkage.

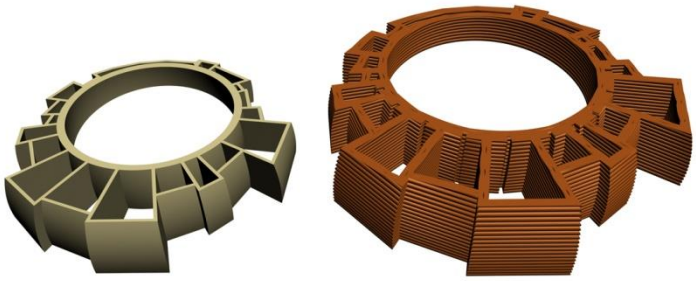

Figure 4.35, CAD models of the 'Cityscape' rings as a smoothed outcome with anticipated shrinkage and as the deposited build. figure by author

After deposition, once dry, the ring was burnished to a smooth surface. An 8° template was used to cut the build to a wedge shape. The ring cracked during firing, this happened in areas where the material was thinnest, see Figure 4.36. Warping was also evident, but it was worked by hand using the same methods as before, which made the cracks in the ring larger. These were filled with BronzClay paste and the ring was re-fired; this repaired the ring and left no evidence of the cracks. The ring shrank 13.5 ring sizes from 'Z+4 1/2' (23.6mm diameter) to Q (18.3mm diameter, 22.5 % shrinkage) and was one size off the predicted size of P.

Figure 4.36, Working the 'Cityscape' ring. figure by author

A similar design to the cityscape ring was built; this ring features a round external geometry (Figure 4.37). This Suspension ring was deposited in PMC Pro twice; to produce one version using the deposited layers as a texture, whilst the other would be smoothed by burnishing prior to firing. Both were built during the same session using the same parameters and batch of material.

Figure 4.37, Suspension and Cityscape rings. figure by author

These two rings shrank less than the expected then ring sizes (Hex ring), going down six sizes from Z (21.9mm diameter) to size T (19.5mm diameter, 11 % shrinkage) for the textured version, whilst the smooth version went down eight sizes from Z to a size R (18.7mm diameter, 14.6 % shrinkage), both presented some warping in all directions.

The shrinkage anomaly could be partly to do with the wall thickness as the burnished ring shrank more than the textured ring by two sizes, which could be due to it having thinner walls as a consequence of the burnishing procedure. The burnished ring however, still shrank two sizes less than the Hex rings.

Lower shrinkage can be attributed to under firing. This is the least likely cause, however, as the warp in the rings was alleviated by working the ring by hand on a mandrel and showed no signs of breaking.

It could also be due in part to the design's structure. This is best explored by reviewing the ring geometries within the study.

4.6.9 Process Discussion

Whilst a range of shrinkage rates have been found in the PMC Pro rings, each batch of ring designs appears to have a fairly consistent shrinkage expressed as a ring size. Observations from the geometries starting with the greatest shrinkages follow to explore potential effects of geometry.

The Tessellation rings shrank 13.5-14.5 ring sizes; they have the lowest width as a band. They feature an inner perimeter whilst the outer surface comprises an infill of a

single filament; it therefore has no strict bounding wall, which means the material is free to relax; leading to a higher shrinkage when compared with other designs.

The Hex rings shrank ten sizes, they are taller (deposited to an 8mm height). They consist of a round tube circumscribed within a hexagonal tube, so there are six points of contact through the height. Each tube has two perimeters. This presents the geometry as a thin extrusion which seems to have a balance of bounding and a relative equilibrium regarding contact, the distribution of compressive stresses and freedom of movement. The fired rings were naturally a little warped as the areas not in contact would be relatively free to move.

Comparatively the Suspension ring is much heavier (Figure 4.38), both in weight and appearance. Both the inner and outer walls have two perimeter layers. Joining the two is a stroked T-bar arrangement which is evenly spaced circumferentially. The T shape graduates from a full T at the apex of the ring to a dash at the bottom so that the inner ring is offset within the outer ring. The stroking of the T-bar infill means that a further perimeter is effectively added to the inner ring. The T-bars are holding the two rings together. Material that is unsupported by the T-bars has tried to move in towards the inner ring, perhaps because the inner ring has three perimeters. There appears to be stresses that limit the shrinkage of the part. It is exceedingly difficult to fully qualify the limited shrinkage of the Suspension rings.

Figure 4.38, : Tessellation, Hex and Suspension structure comparison in 'PMC Pro'. figure by author

What is ascertained from observations is that there are design differentials of wall thickness, external and internal wall geometry, infills and potentially build height that significantly affect the resulting size. Whilst this could be benchmarked through trial and error with personal craft enquiry; the process would also benefit from the support

of more formalised experimentation and computational modelling to predict and compensate for deformations occurring during build, and incorporate the shrinkage from design to fired part.

The latter would be pivotal if the process were commercially developed as an add-on to the software platform. For investment to be worthwhile, trust in the material preparation is needed, metal PDM clays would need to be standardised and manufactured, potentially having a common viscosity for a more consistent behaviour.

Conclusions on deposition of rings

It has been shown that metal clays can be adapted for PDM. They can be prepared with large tolerances using simple tools and dispensed through a syringe nozzle. Firing schedules were determined and it was found that BronzClay and PMC Pro sintered fully and could withstand basic wroughting. Seashell geometries demonstrated that PDM can produce sophisticated, tapered and twisted parts without support material, which bodes well for creating 3D hollow jewellery. Benchmarking the dimensional stability of metal PDM by ring size shrinkage was attempted. This was combined with developing a body of work to demonstrate some anticipated benefits of coupling the PDM characteristics with self originated infill strategies. Where consistent batches were fired more or less as built, there was good consistency within the batch but not between different designs. BronzClay was more stable irrespective of design, with a shrink range of 13.5-14.5 ring sizes from the build size. With PMC Pro the ring size shrink range was shown not to be consistent and likely to be dependent on the design features of: external and internal perimeter geometries, infill patterns, wall thicknesses and build height. PDM is in its infancy, for metal PDM of rings to be dimensionally reliable a more formalised experimental approach would be required. This would encompass process development rather than a crafts research based context. An exploration of metal PDM for craft outcomes that are not dimensionally constrained would appear an appropriate way forward.

Generating PDM programme files is a multi-step process that could be deemed complex and off-putting for many but not all. It is an approach in the open-source domain common to many types of research. Masterton (2007, p.20) created a process for intervening in the automatic generation of cutting tool paths for metal decoration

using ‘Corel Draw’. PDM similarly offers opportunities for design by control of the tool paths and infill patterns. Ideally a platform based system to develop geometries and tool paths for is needed. As such approaches become mainstream they should eventually grab the attention of software developers.

The layered PDM creates a texture which can be exploited within the product’s visual identity. PDM can deposit metal clays using a number of different sized nozzles. They could be larger or finer than the 0.6mm nozzle used here. With PDM the ability to deposit even larger filament diameters allows for further exaggeration of the texture. The ability to quickly change filament diameter makes this a re-configurable arrangement that is less directed by the constraints of the 0.1 to 0.4mm filament diameters typical of FDM. Whilst a layered texture is evident it can also be selectively blended and made smooth, according to the designer’s intention. This brings about a process that can be a hybrid in that it is RP yet regains the nature of being *‘touched by hand’*. With PDM for metal clays there isn’t a step-change and only the material required in the part is prepared, rather than a bed of powder. Combined with the desktop prototyping merits, this could be an open-source a low-cost and versatile machine for cold forming silver and which also brings aesthetic opportunities.

4.6.10 Rhodes Pendant

After the experiments with the rings were done, it was decided that an exploration was required into a jewellery piece that was not dimensionally constrained like the rings were. A pendant was made; the tool-path was based on the tessellated pattern but was heavily modified and made non-symmetrical. The aim of this design was to demonstrate the capabilities of the Mk3 at producing an aesthetically pleasing yet complex build in precious metal. as this build was to be submitted to the Goldsmith's Craft and Design Council annual jewellery competition

This build was made in PMC Pro (90% silver) using the same methods already established, the only difference here was that the pendant required a bale (a loop for the chain to link to the pendant) so that it could go on a chain. This was soldered after the pieces were fired, but with great difficulty. Although a professional jewellery torch was used and the lowest grade solder was selected, the pendant took longer than expected to reach the temperature where the solder would flow. Large silver pieces

are notoriously difficult to solder, however it is believed that the internal structure of the pendant exacerbated this issue and made soldering more difficult.

Figure 4.39, Rhodes pendant in PMC Pro. figure by author

The pendant was submitted to the competition and was Silver and Joint winner of the 3D technological Innovation award at the Goldsmiths' Craft and Design Council 2013 awards (Figure 4.39).

This was an important milestone, as the piece was judged on its merit as jewellery and not just as a technological demonstration, which bodes well for the acceptance of the PDM technique as a craft tool in the wider jewellery industry.

Figure 4.40, Copper Rhodes pendant , gold plated. figure by author

This tool-path was revisited as a later date and deposited in copper; this time bale was attached before firing so that soldering would not be an issue. The final fired piece was polished and gold plated (Figure 4.40).

Chapter 5 Commercial Validation

5.1 Chapter Introduction

It may be argued that the ultimate validation of a research project like this is that it is eventually developed into a commercial product, with this in mind this chapter briefly describes the commercialisation of the paste deposition modelling process developed in this work.

5.2 The iMakr Company

The author was approached by a company called IMakr which specialises in the sale of AM equipment and accessories. They expressed an interest in commercialising the research, in particular the deposition of metal clays. Figure 5.1 shows the company website detailing the Newton3D - this is the direct commercial development from the machine and processes created in this project.

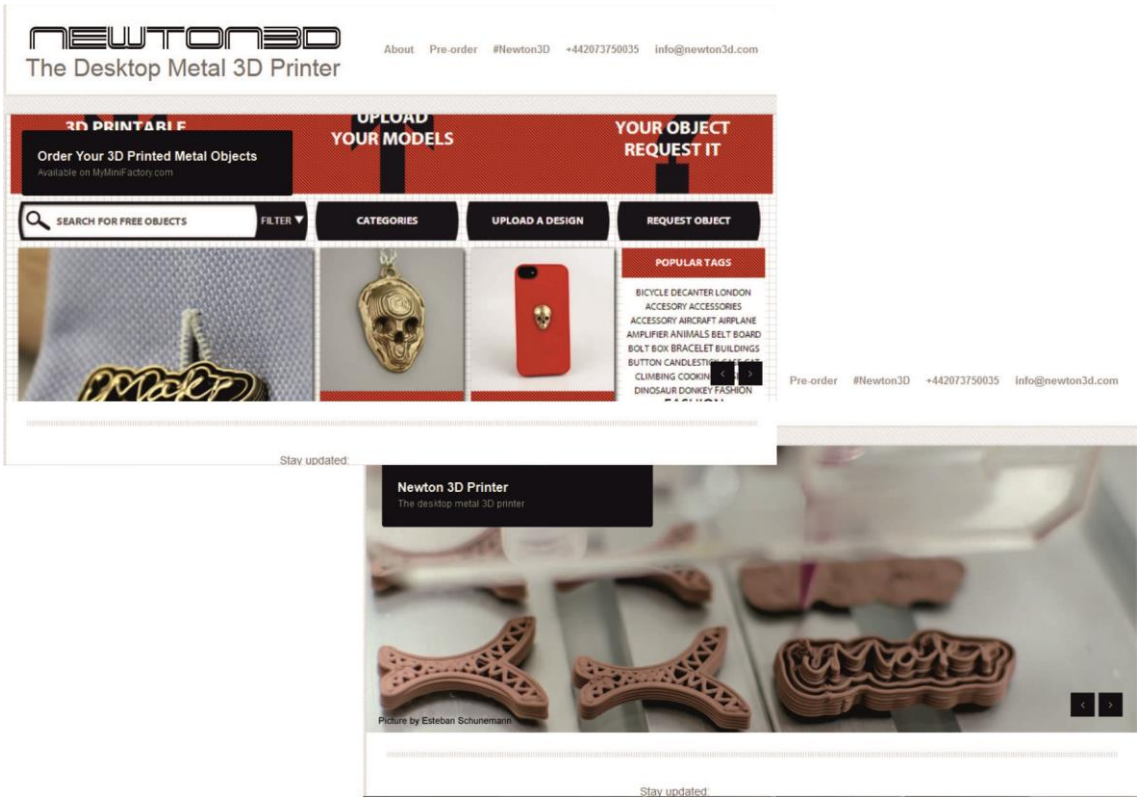

Figure 5.1, Newton 3D company website. figure by author

Part of the commercial development has been to enhance some features of the Mk3 in specific areas including increased material capacity to allow for bigger and more complex builds, Figure 5.2 shows the large 310ml capacity silicone deposition head.

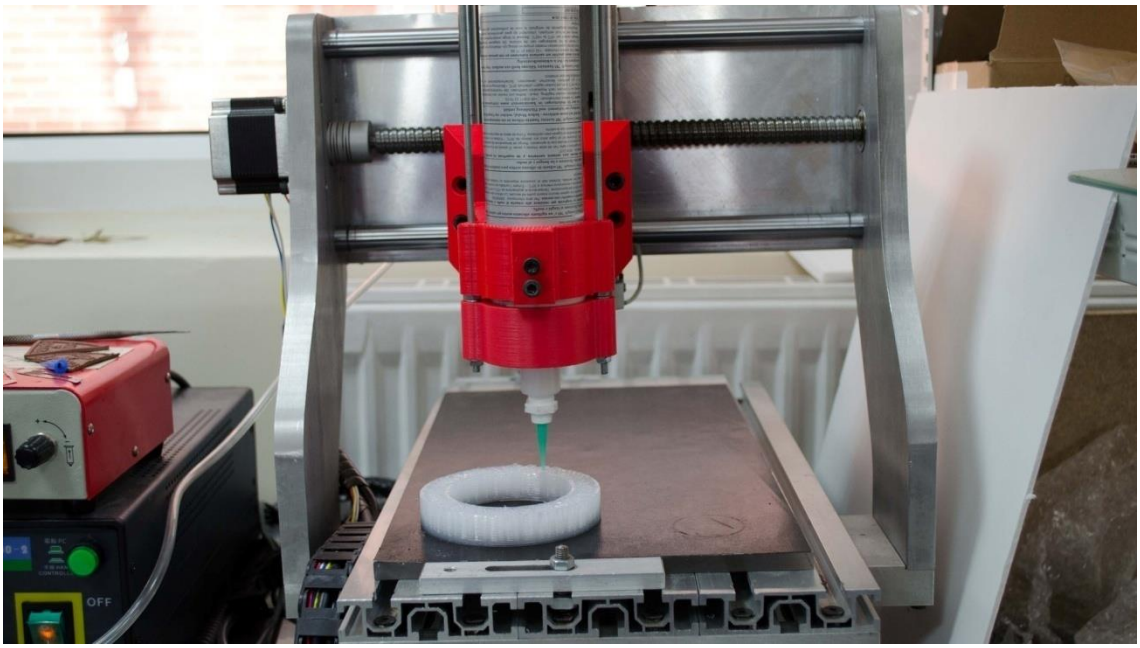

Figure 5.2, Newton3D large capacity deposition head. figure by author

A further development to the equipment was the addition of a fan to assist in the deposition of metal clay for steeper draft angles (Figure 5.3), this being based on issues encountered with the silver seashell deposition in chapter 4. The deposition heads were designed for quick release from the CNC gantry; this is a mechanism that will also be applied to future generations of the deposition head.

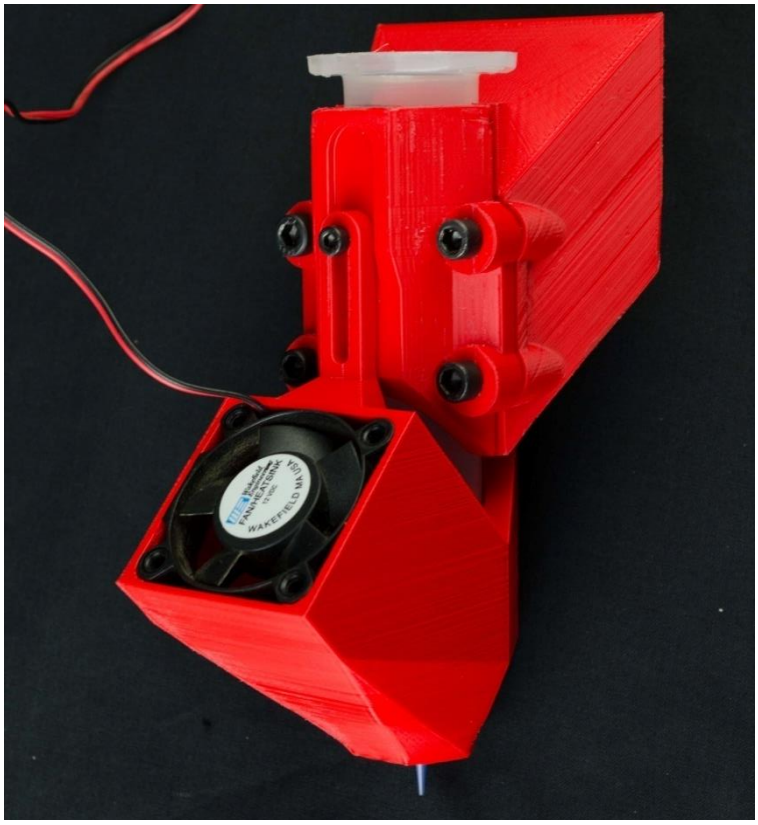

Figure 5.3, Improved metal clay deposition head with fan assist. figure by author

The new CNC gantry uses ball screws which improved the precision and speed of the deposition, movement speeds of up to 2000mm/min are now possible with 1500mm/min successfully tested in trials. Figure 5.4 shows single filament builds of a signature tool-path (Marilyn Monroe), tested with nozzle sizes down to 0.2mm.

Figure 5.4, Improved resolution demonstration, BronzClay. figure by author

Deposition of BronzClay with small nozzle sizes has also been tested with 3D sliced geometries; the Figure 5.5 shows a small head, 15mm from chin to forehead deposited at 0.17mm layers. Deposition at these layers is rather unreliable as up to this point the mixing method was still manual, but talks are taking place with the manufacturer of the BronzClay to produce a bespoke formulation to alleviate this problem.

Figure 5.5, 15mm vertical length, 0.17mm layers. BronzClay. figure by author

Figure 5.6 shows a collection of pendants made in bronze under commission from a performance group where a set of ten identical builds were made plus a larger one for

the lead performer. The tool-path was based on the original logo for the group, this builds shows a superior performance for tool-paths with sharp changes in direction.

Figure 5.6, Collection of Haus of Sequana pendants, commission work. figure by author

The post project continuation and development of this work form the core of the future work (see chapter 8).

Chapter 6 Conclusions

The overall aim of this project has been to explore additive manufacturing in an unconstraint environment through a practical and design oriented methodology, where the process is not dependant on the software/firmware developed by manufacturers.

In order to achieve this aim a number of objectives were devised including; reviewing the current literature and practitioner work to determine state of the art, investigating the constraints in existing systems and developing a solution for unconstraint AM, creating a system to develop and explore the process, and finally validating the process through a series of case studies and demonstrator artefacts. This project has successfully achieved all these targets aims and objectives.

A series of case studies were conducted, each with a particular theme, medical, food industry and jewellery the outcomes and products produced serving as strong validations of the significance of the paste deposition modelling process.

A further step in demonstrating the validity of the process and its capabilities was demonstrated by the commercial collaboration with the AM company (iMakr).

The commercial development of the experimental system is soon to be launched under the brand name Newton3D.

Some interesting new directions were discovered along the way which showed great potential i.e. silicone fabrics, these have generated great interest whenever they have been shown.

6.1 Contribution to Knowledge

The contribution to knowledge lies in several places;

Original output of the research has been demonstrated by the development of an additive manufacturing process with increased design freedom necessary for craft practitioners to engage with this technology in the manner of a craft enquiry. The advantage of the simplistic unconstrained approach has been clearly demonstrated in the case studies in chapter 4.

The contribution to knowledge is particularly evident in the four following areas;

6.2 Silicone

6.2.1 Additive Manufacturing of Bespoke Moulds

While some work has been done on direct deposition of silicone, there is little to no research published in the field suggesting no-one has explored AM with silicone in any great depth. It is thought this is because of the constraints of slicing software; this software is designed for the deposition of thermoplastics and not specifically silicone. Therefore there is no standardised solution for this material and as such it is largely ignored. While AM of moulds is not new, it has been done before with several systems, the novelty here lies in the direct production of soft moulds. Before to produce a soft silicone mould from a 3D printed part; the first step would be to print the desired part, then submerging it in silicone RTV, cutting the mould to release the part and finally casting. This process would also require the addition of pouring sprues and air release ducts into the mould, the end result would be a large block of silicone with a negative void of the part inside.

The originality is in direct deposition of soft silicone moulds, by this digital manufacturing process, not only does it reduce the three or four step process of producing soft silicone moulds down to one but it also allows for the production of a series of individually bespoke moulds (each can be the same or completely different to each other) without the need for a mould pattern, 3D printed or otherwise for different permutation. The soft moulds demonstrated are unique in that they are thin walled, reducing the amount of silicone required and improving mould release due to the thickness of the material.

6.2.2 AM of textiles

It would be hard to argue that the work in this project on silicone textiles is not in need of substantial further work however, the properties and behaviour of the textile are so unexpected and exciting that it is obvious the silicone textiles created by the PDM process clearly show great potential for a wide variety of applications. As it stands it would be impossible to manufacture the textiles any other way, there might be similar meshes made by either casting or die cutting but they will not feature the 3D mesh demonstrated, which can be tuned to suit an application without retooling.

Given the layer wise nature of the process the possibility also exists to create 3D textiles and also embed varying kinds of threads for re-enforcing or for functional purposes e.g. embedded electronics.

The works done in this project in silicone textiles only represents the bare beginnings of this area but nonetheless it is a novel finding un-reported anywhere else.

6.2.3 Tube builds

Up to this point there is no built in solution in slicers to produce a tube with an even distribution throughout the whole geometry, the solution developed by the author goes a long way towards solving this issue. The tool-path strategy and subsequently the tool-path itself was originally developed for the AM watch and the thermal cuff and has been demonstrated in several of the case studies to be capable of handling both narrow and wide wall thicknesses, as well as asymmetric as in the Rhodes pendant. The method by which this tool-path is produced allows for modification as required, the straight elements of the path mean that spanning large gaps is easier, this tool-path being particularly useful in the thermal cuff where the large gaps allowed for the flow of liquids through the internal structure. The novelty here is in the tool-path strategy for producing round builds with straight lines that create an isotropic structure.

6.3 Deposition of Metals

This area of the research has received the most external attention with two conference papers, an award, two articles in a book and a commercialization opportunity.

The AM of metals is not new SLM has been around for a number of decades. However AM in precious metals only came into the market with the release of the EOS and Concept laser systems in recent years however such systems are unattainable to the general public, PDM in precious metals provides a more accessible solution. The lack of published research suggests that the system developed was the first one to create parts in precious metals using paste deposition, particularly in jewellery.

The Rhodes pendant with its filament structure would have been challenging to make with DMLS due to the long span between filaments; it is a structure that would have only been possible with the PDM process.

The advantages of using metal clays also give novelty to the project, the fact that they are water soluble means that complex objects that require several parts can be joined using traditional clay working techniques, surfaces can also be treated with similar regard. Practitioners who are accustomed to working by hand would find such attributes desirable. These attributes are truly unique to this process.

Chapter 7
Recommendations/Future Work

7.1 Immediate Future

The immediate future work from this project will be focused on the commercial development of the PDM process through my partnership with iMakr, the initial stages of this mentioned in Chapter 5 Commercial validation.

The programming process for PDM can be laborious and off-putting for some users. Further work will need carried out to simplify (possibly with iMakr) the process of creating user-generated infill strategies and structures through more inclusive software.

A second promising avenue for future work has arisen via an approach through academic contacts from a Senior Lecturer at UCL Centre for Nanotechnology and Regenerative Medicine. The intention here is to develop and build a bio printer based on the deposition techniques developed during this research project, with the aim of creating bio implants. This may be funded by an E.U project.

7.2 Other Areas Worthy of Further research

Based on the work done in the case studies there are some areas that are definitely worthy of further research.

Design and make a machine capable of producing the textile tool-path at a real world scale.

Perform standard tests on the silicone textiles to test their suitability as an actual textile.

The embedding of threads in the silicone textiles could be explored further with conductive threads and elastic conductive threads for the development of wearable technology.

The embedding of electronic components as seen the AM watch in Chapter 4 could be developed further with automated pick and place implementation such as that used in the electronics manufacturing industry to increase the precision and complexity feasible in a single component AM part. This method of stopping a build to add

internal components is widely discussed in the academic field but it is as yet to be implemented into a commercial system.

X. References

3ders, (2013) *3ders.org - Rotary 3D printers under development| 3D Printer News & 3D Printing News*. [Online]. 2013. Available from: http://www.3ders.org/articles/20131227-rotary-3d-printers-under-development.html [Accessed: 8 February 2014].

3ders., (2012). *LAYWOO-D3*. [online] Available at: http://www.3ders.org/articles/20120920-laywoo-d3-new-fdm-filament-can-print-wood-with-tree-rings.html [Accessed 15 Nov. 2012].

3DPrinter4U, (2013) *NEW: 3D Printer Color mixing with Builder 3D Printer*. [Online]. 2013. Available from: http://3dprinter4u.com/color-mixing-2/ [Accessed: 19 November 2013].

3dprintsexpress.com, (2013). *3D Refiner*. [online] Available at: http://3dprintsexpress.com/faq.html [Accessed 9 Jun. 2013].

3DSystems A, (2014). *ProJet x60 Brochure*. [online] Available at: http://www.3dsystems.com/sites/www.3dsystems.com/files/projet_x60_series_us_0514_web.pdf [Accessed 9 May. 2014].

3DSystems B, (2014). *ColorBond SDS*. [online] Available at: http://www.3dsystems.com/sites/www.3dsystems.com/files/22-83104-s12-02-a-sds-ghs-english-colorbond-and-zbond-90.pdf [Accessed 21 Jul. 2014].

3DSystems C, (2013). *Projet x60pro user guide*. [online] Available at: https://3dscentral.3dsystems.com/attachments/2239_22-95048%203D%20Print%20User%20Guide.pdf [Accessed 6 Nov. 2013].

3DSystems, (2003). *SLA 500 system*. [online] Available at: http://www.3dsystems.com/products/datafiles/sla5000/datasheets/sla5000_uk_aktualisiert.qxd.pdf [Accessed 8 May. 2012].

3DSystems, (2013). *30 Years of Innovation*. [online] Available at: http://www.3dsystems.com/30-years-innovation [Accessed 5 May. 2013].

3Dsystems, (2014) C. *ProJet 5500X*. [online] Available at: http://www.3dsystems.com/sites/www.3dsystems.com/files/projet-5500x-0714-usen-web.pdf [Accessed 18 Jul. 2014].

3Dsystems, (n.d.). *SLS Material Properties*. [online] Available at: http://www.3dsystems.com/quickparts/prototyping-pre-production/selective-laser-sintering-sls/materials [Accessed 11 Nov. 2013].

3Dsystems, A, (2013). *VisiJet PXL core SDS*. [online] Available at: http://www.3dsystems.com/sites/www.3dsystems.com/files/22-83100-S12-00-A-SDS-GHS-English-VisiJet-PXL-Core.pdf [Accessed 19 Jan. 2014].

3DSystems, B, (2013). *VisiJet PXL SDS*. [online] Available at: http://www.3dsystems.com/sites/www.3dsystems.com/files/22-83101-S12-00-A-SDS-GHS-English-VisiJet-PXL-Colors.pdf [Accessed 3 Jul. 2014].

Adhesivedispensing, (2005, A). *Spool Valves*. [online] Available at: http://www.adhesivedispensing.co.uk/spool.htm [Accessed 25 October 2010].

Adhesivedispensing, (2005, B). *Diaphragm Valves*. [online] Available at: http://www.adhesivedispensing.co.uk/diaphragm.htm [Accessed 25 October 2010].

Adhesivedispensing, (2005, C). *Needle Valve10s*. [online] Available at: http://www.adhesivedispensing.co.uk/needle.htm [Accessed 25 October 2010].

Adhesivedispensing, (2005, D). *Motor Drive Auger Dispensing Valves*. [online] Available at: http://www.adhesivedispensing.co.uk/auger.htm [Accessed 25 October 2010].

Adhesivedispensing, (2005, F) *30cc Adapter Assembly 3ft long*. [Online].Available from: http://www.adhesivedispensing.co.uk/73003RHB.htm [Accessed: 21 October 2013].

Adhesivedispensing, (2005, G) *30cc Syringe Barrel Clear 7300LL1NPK Adhesive Dispensing*. [Online]. 2005. Available from: http://www.adhesivedispensing.co.uk/7300LL1NPK.htm [Accessed: 21 October 2013].

Adhesivedispensing, (2005, H) *30cc Straight Wall Pistons*. [Online]. Available from: http://www.adhesivedispensing.co.uk/7300006RPK.htm [Accessed: 21 October 2013].

Adhesivedispensing, (2005, I) *30cc and 55cc Wiper Pistons for syringe barrels 7300009WPK*. [Online]. 2005. Available from: http://www.adhesivedispensing.co.uk/7300009WPK.htm [Accessed: 21 October 2013].

Adhesivedispensing, (2005, J) *20 gauge dispensing tip 1/2" TE720050PK*. [Online]. Available from: http://www.adhesivedispensing.co.uk/TE720050PK.htm [Accessed: 21 May 2010].

Adhesivedispensing, (2005, L) *Syringe Filling Systems*. [Online]. Available from: http://www.adhesivedispensing.co.uk/barrelfillers.htm [Accessed: 24 May 2010].

Adhesivedispensing, (2005, M) *Techcon Systems TS941/TS934 TS941A/TS934A Spool Valve*. [Online]. Available from: http://www.adhesivedispensers.co.uk/Datasheets/TS941M.pdf [Accessed: 26 July 2012].

Adhevisedispensing, (2005, K) *Female to female luer lock fitting*. [Online]. Available from: http://www.adhesivedispensers.co.uk/TSD931-28.htm [Accessed: 21 October 2013].

Ahn, B., Shoji, D., Hansen, C. & Hong, E. et al. (2010) Printed origami structures. *Advanced Materials*. 22 (20), 2251--2254.

Americanart, (n.d.) *Coiled Pot by Louise Goodman / American Art*. [Online]. Available from: http://americanart.si.edu/collections/search/artwork/?id=36246 [Accessed: 21 July 2014].

Arnold, D. (2011) *Fantastic Stochastic Masa: Finally a Good 3-D Food Printing Application*. [Online]. 2011. Cookingissues.com. Available from: http://www.cookingissues.com/2011/01/24/fantastic-stochasic-masa-finally-a-good-3-d-food-printing-application/ [Accessed: 17 November 2011].

Asiga, (2014). *The Freeform Pico - Products - Asiga*. [online] Available at: https://www.asiga.com/products/printers/pico/ [Accessed 3 Mar. 2014].

Bass, C. (2013) *An Insider's View of the Myths and Truths of the 3-D Printing 'Phenomenon' | WIRED*. [Online]. 2013. Available from: http://www.wired.com/2013/05/an-insiders-view-of-the-hype-and-realities-of-3-d-printing/ [Accessed: 12 September 2013].

Bechmann, F. (2010). *Developer of Selective Laser Melting Looks toward New Applications for the Generative Manufacturing Process*. [online] concept-laser.de. Available at: http://www.concept-laser.de/uploads/tx_j2press/presse_uk_201005.pdf [Accessed 4 Jul. 2015].

Bibus, (2007). *Zprinter 450 user manual*. [online] Available at: http://www.bibus.hu/fileadmin/editors/countries/bihun/product_data/zcorp/documents/zcorp_series_zprinter_450_hardware_manual_en.pdf [Accessed 3 Jun. 2012].

Brown, R. (2012) *Pulling back from open source hardware, MakerBot angers some adherents - CNET*. [Online]. 2012. CNET. Available from: http://www.cnet.com/uk/news/pulling-back-from-open-source-hardware-makerbot-angers-some-adherents/ [Accessed: 16 October 2012].

Bryan, R. (2012). Lost-PLA Aluminum Casting. [Blog] *The Boulder HackerSpace*. Available at: http://boulderhackerspace.com/2012/08/18/lost-pla-aluminum-casting/ [Accessed 24 Nov. 2013].

Bujis, K. and Leewen, V. (2005). *Lasercusing Will it make removing metal by machine and casting a thing of the past?*. [ebook] Stainless-steel-world.com. Available at: http://innomet.nl/docs/LaserCusing.pdf [Accessed 8 Jul. 2013].

Campanelli, S., Contuzzi, N., Angelastro, A. and Ludovico, A. (2010). Capabilities and performances of the selective laser melting process. *New Trends in Technologies: Devices, Computer, Communication and Industrial Systems*, pp.233--252.

Campbell, J.R., New craft future voices conference, Dundee, Scotland, 2007.

Cater, C. (2013). *Student case studies, esTechnology,* Jewellery Industry Innovation Centre. [email].

Cesarano III, J., King, B. and Denham, H. (1998). Recent Development in Robocasting of Ceramics and Miltimaterial Deposition. In: *SFF Symposium*. Austin Texas: University of Texas, pp.697-704.

Cesaretti, G., Dini, E., De Kestelier, X., Colla, V. and Pambaguian, L. (2014). Building components for an outpost on the Lunar soil by means of a novel 3D printing technology. *Acta Astronautica*, 93, pp.430--450.

Chen, Y., Zhou, C. and Lao, J. (2011). A layerless additive manufacturing process based on CNC accumulation. *Rapid Prototyping Journal*, 17(3), pp.218--227.

Colorfabb.com, (n.d.). *ColorFabb - bronzeFill*. [online] Available at: http://colorfabb.com/bronzefill#.U96aBWOTDC8 [Accessed 26 May. 2014].

Continuumfashion, (2011) *Continuum Fashion : N12 bikini*. [Online]. 2011. Available from: http://www.continuumfashion.com/N12.php [Accessed: 23 October 2012].

Cool Tools. (n.d). PMC PRO Silver Metal Clay High Strength. Available: http://www.cooltools.us/PMC-PRO-Metal-Clay-High-Strength-50-gram-pak-p/pmc-605.htm. Accessed 17th November 2012.

Cooper, E. (1981). *A history of world pottery*. 2nd ed. London: Batsford, p.15.

Copeland, M. (2013) *DIY Market Slows Dramatically as 3-D Printing Hits Its Industrial Stride | WIRED*. [Online]. 2013. WIRED. Available from: http://www.wired.com/2013/05/3d-printing-hits-its-industrial-stride-while-the-diy-market-slows-dramatically/ [Accessed: 12 September 2013].

CPM, EOS, (n.d.). *CPM Direct Metal Laser Sintering Design Guidelines [PDF]*. [online] Available at: http://www.cooksongold-emanufacturing.com/ [Accessed 20 Nov. 2013].

Creativetools, (n.d.) *Roland DG - MDX 20*. [Online]. Available from: http://www.creativetools.se/roland-dg-mdx-20 [Accessed: 13 September 2012].

Crump ,S. (1994) *Modeling apparatus for three-dimensional objects*, US patent 5340433 A

Custompartnet, (2009). *Laminated Object Manufacturing (LOM)*. [online] Available at: http://www.custompartnet.com/wu/laminated-object-manufacturing [Accessed 8 May. 2012].

Damienideas. (2013) Episode 2 : Form1 calibration strikes back. [Blog] *Explore Ideas Daily*. Available at: http://exploreideasdaily.wordpress.com/2013/07/12/episode-2-form1-calibration-strikes-back/ [Accessed 3 Nov. 2013].

Davis, L. (n.d.). *Plugins - Newfangled Solutions*. [online] Machsupport.com. Available at: http://www.machsupport.com/software/plugins/ [Accessed 12 Aug. 2011].

Dean, L. (2013) FutureFactories: Practice - Based Research in the Creative Use of Digital Design and Manufacturing Technologies. In: *Praxis and Poetics*. 2013 Northumbira University. pp. 63-66.

Designplaygrounds, (n.d.) *designplaygrounds.com » Archive » l'Artisan Electronique by UNFOLD Studio*. [Online]. Available from: http://designplaygrounds.com/deviants/lartisan-electronique-by-unfold-studio/ [Accessed: 12 February 2012].

Dewidar, M., Dalgarno, K. et al., (2008). A comparison between direct and indirect laser sintering of metals., 24(2)

Dickens, C. (2012) *Carrie Dickens | Tactile Neckpiece 2012*. [Online]. 2012. Carriedickens. Available from: http://www.carriedickens.co.uk/gallery/tactile_neckpiece.html [Accessed: 24 July 2013].

Doctorow, C. (2011) *3D printed food-sculptures*. [Online]. 2011. Boingboing.net. Available from: http://boingboing.net/2011/03/02/3d-printed-food-scul.html [Accessed: 17 November 2011].

Dormer, P.,(1997) `Craft and the Turing test for Practical thinking` in Dormer ,P. (ed.) the culture of craft, Manchester University Press

D-shape, (n.d.). *Sand evaluation*. [image] Available at: http://press.d-shape.com/index.php?flag=2.1&id=85 [Accessed 7 May. 2013].

DWS LAB, (2014). *DWS LAB - XFAB*. [online] Available at: http://dwslab.com/xfab/ [Accessed 9 Mar. 2014].

DWSSYSTEMS, (n.d.). *DWS Systems - Jewelry & Fashion*. [online] Available at: http://dwssystems.com/printers/jewelry-fashion [Accessed 4 Jun. 2013].

Efunda, (n.d.). *Rapid Prototyping: LOM*. [online] Available at: http://www.efunda.com/processes/rapid_prototyping/lom.cfm [Accessed 11 May. 2012].

EMC2, (n.d.) *LinuxCNC.org*. [Online]. Available from: http://www.linuxcnc.org/ [Accessed: 11 February 2012].

Exone, (2012). *What Is Digital Part Materialization? | ExOne*. [online] Available at: http://www.exone.com/en/materialization/what-digital-part-materialization [Accessed 5 May. 2013].

Faberdashery.co.uk, (n.d.). *Shop - faberdashery*. [online] Available at: http://www.faberdashery.co.uk/products-page/ [Accessed 16 Oct. 2013].

Fisnar, (2009) *B1113- LF AND JBE1113- LF AUTOMATIC LIQUID DISPENSERS*. [Online]. 2009. Available from: http://www.fisnar.com.cn/pdfs/JB1113-LF.pdf [Accessed: 20 May 2010].

Formfutura, (n.d.). *1.75mm Water Soluble filament - PVA*. [online] Available at: http://www.formfutura.com/175mm-water-soluble-filament-pva.html [Accessed 4 Mar. 2014].

Formlabs, (2014). *Buy Materials — Formlabs*. [online] Available at: http://formlabs.com/store/eu/buy-materials/ [Accessed 4 Jun. 2014].

Formlabs, (n.d.). *Formlabs Form 1*. [online] Available at: http://formlabs.com/ [Accessed 6 Feb. 2013].

Fourthaxis, (2009). *Tilt Motor Axis Tutorial for Roland MDX-15 and MDX-20*. [online] Available at: http://www.fourthaxis.com/tilt-motor-axis-tutorial/ [Accessed 8 Jul. 2011].

Gilkin, I., Hamel, M. & Mraz, S. (2009) *A Critical Look at Acme, Ball, and Roller Screws for Linear Motion | Motion Control content from Machine Design*. [Online]. 2009. Machinedesign.com. Available from: http://machinedesign.com/motion-control/critical-look-acme-ball-and-roller-screws-linear-motion [Accessed: 7 September 2011].

Gratson, G., Xu, M. & Lewis, J. (2004) Microperiodic structures: Direct writing of three-dimensional webs. *Nature*. [Online] 428 (6981), 386-386. Available from: doi:10.1038/428386a [Accessed: 20 March 2011].

Greenlees. R. (n.d). what is craft. Available: http://www.vam.ac.uk/content/articles/w/what-is-craft/. Last accessed 10th May 2013.

Groover, M. (2011) *Principles of modern manufacturing SI version*. 4th edition. Hoboken, N.J., J. Wiley & Sons.

Hao, L., Mellor, S., Seaman, O. & Henderson, J. et al. (2010) Material characterisation and process development for chocolate additive layer manufacturing. *Virtual and Physical Prototyping*. 5 (2), 57-64.

Hodgson, G. (n.d.) *Slic3r Manual - Infill Patterns and Density*. [Online]. Available from: http://manual.slic3r.org/expert-mode/infill#fnref1 [Accessed: 13 June 2013].

Honagas, (2013). *Digital metal for manufacturing of complex metal parts*. [online] Available at:http://hoganas.com/Documents/Segmentbrochures/Digital%20Metal/Digital_Metal_For_Rapid_Manufacturing_of_Complex_Parts_Nov_2013_0629HOG.pdf.pdf [Accessed 9 Jan. 2014].

iMakr. (2014). *Conversation with system operator.* [Personal correspondence]

Ipmd, (2013). *Höganäs Digital Metal produces highly complex and intricate designs with 3D printing*. [online] Available at: http://www.ipmd.net/articles/002466.html [Accessed 9 Jan. 2014].

Jacobson, D. and Bennett, G. (2006). PRACTICAL ISSUES IN THE APPLICATION OF DIRECT METAL LASER SINTERING. *SFF Symposium procedings*. [online] Available at: http://utwired.engr.utexas.edu/lff/symposium/proceedingsArchive/pubs/Manuscripts/2006/2006-63-Jacobson.pdf [Accessed 20 Nov. 2013].

JUSTPRINT3D, (2014). *3D Printer calibration Basic 2: Extrusion width/layer height value*. [online] Available at: http://www.justprint3d.com/3d-printer-calibration-basic-2-extrusion-widthlayer-height-value/ [Accessed 28 Apr. 2014].

Kennedy, G. (2011) *Dirk vander Kooij at DMY - Design.nl*. [Online]. 2011. Design.nl. Available from: http://design.nl/item/dirk_vander_kooij_at_dmy [Accessed: 16 August 2012].

Khoshnevis, B. (2004). Automated construction by contour crafting—related robotics and information technologies. *Automation in construction*, 13(1), pp.5--19.

Lacock, J. (2013). *Lost PLA Casting with Jeshua Lacock - 3D Printing Industry*. [online] Available at: http://3dprintingindustry.com/2013/11/09/lost-pla-casting-jeshua-lacock/ [Accessed 29 Nov. 2013].

Lewis, J. & Gratson, G. (2004) Direct writing in three dimensions. *Materials today*. 7 (7), 32--39.

Lim, S., Buswell, R., Le, T., Austin, S., Gibb, A. and Thorpe, T. (2012). Developments in construction-scale additive manufacturing processes. *Automation in construction*, 21, pp.262--268.

Lim, S., Buswell, R., Le, T., Wackrow, R., Austin, S., Gibb, A. and Thorpe, T. (2011). Development of a viable concrete printing process.

Lu, X., Lee, Y., Yang, S. & Hao, Y. et al. (2009) Fine lattice structures fabricated by extrusion freeforming: Process variables. *Journal of Materials Processing Technology*. 209 (10), 4654--4661.

Machmotion, (n.d.) *CNC Mach3 G-Codes*. [Online]. Available from: http://machmotion.com/cnc-info/g-code.html [Accessed: 17 February 2011].

Machsupport, (2008). *Mach3 CNC Controller Software Installation and Configuration*. [online] Available at: http://www.machsupport.com/wp-content/uploads/2013/02/Mach3Mill_Install_Config.pdf [Accessed 3 Aug. 2011].

Makerjuice, (2014). *SubSF for Form 1 | MakerJuice Labs*. [online] Available at: http://makerjuice.com/product/subsf-form1/ [Accessed 9 May. 2014].

Malone, E. & Lipson, H. (2007) Fab@Home: The Personal Desktop Fabricator Kit. *Rapid Prototyping Journal*. 13 (4), 245-255.

Mapei, (2011). *Mapesil AC and primer FD*. [online] Available at: http://www.mapei.com/public/COM/products/401_mapesil%20ac_gb.pdf [Accessed 14 Jan. 2012].

Mason, M., Huang, T., Landers, R. & Leu, M. et al. (2009) Aqueous-based extrusion of high solids loading ceramic pastes: process modeling and control. *Journal of materials processing technology*. 209 (6), 2946--2957.

Masterton, D., H., (2007), 'Deconstructing the digital', Proceedings of the New Craft Future Voices Conference, pp. 7-24

MaxNc, (n.d.). *MAXNC SOFTWARE PIN ASSIGNMENT FILES - LEGACY AND CU*. [online] Available at: http://www.maxnc.net/v/vspfiles/downloadables/PINASS_TABLE.pdf [Accessed 6 Aug. 2011].

McCreight, T., (2010), 'PMC: The clay that just might change jewelry', *Proceedings of the 24th Santa fe Symposium on Jewelry Manufacturing Technology*, pp.1-28

Microfabricator, (2014). *WASP VERY LARGE VOLUME CLAY PRINTING DELTA FROM ITALY on microfabricator.com*. [online] Available at: http://microfabricator.com/articles/view/id/53114d959aad9d5477000005/wasp-very-large-volume-clay-printing-delta-from-italy [Accessed 5 May. 2014].

MiiCraft, (2012). *Products*. [online] Available at: http://www.miicraft.com/products/ [Accessed 4 Sep. 2013].

Mmc, (n.d.) *Precious Metal Clay -- Mitsubishi Materials --*. [Online]. Available from: https://www.mmc.co.jp/pmc/english/pmc/product.html [Accessed: 20 July 2010].

Mnl, (n.d.). *Finishing Touches*. [online] Available at: http://www.mnl.co.uk/Finishing-Touches-id10327.aspx [Accessed 16 Apr. 2013].

Moyer, I. E. (2012) *CoreXY | Cartesian Motion Platform*. [Online]. 2012. Available from: http://corexy.com/theory.html [Accessed: 15 March 2013].

Newfangled, (n.d.) *Mach3 - Newfangled Solutions*. [Online]. Available from: http://www.machsupport.com/software/mach3/ [Accessed: 20 January 2011].

NinjaFlex, (2014) *Flexible 3D Printing with Strong Flexible Filament | NinjaFlex*. [Online]. 2014. Available from: http://www.ninjaflex3d.com/ [Accessed: 16 February 2014].

Owen_W. (2012). [Blog] *ZBrushCentral*. Available at: http://Bronze Casting Sculpture from RP Mould [Accessed 21 Mar. 2013].

Oxley, J. (2012). *Modelling and FEA analysis of flexible structures made by a novel manufacturing process*. Master of Science in Advanced Engineering Design. Brunel University.

Passmark, (n.d.). *PassMark Software - Serial (RS232) and Parallel Loopback Plugs*. [online] Available at: http://www.passmark.com/products/loopback.htm [Accessed 26 Jul. 2011].

Peters, B. (n.d.) *Fabrication – Building Bytes*. [Online]. Buildingbytes.info. Available from: http://buildingbytes.info/fabrication/ [Accessed: 14 February 2014].

Physikinstrumente, (2008) *MP 35E User Manual*. [Online]. 2008. Available from: http://www.physikinstrumente.com/index.php?id=543&eID=dam_frontend_push&docID=4690 [Accessed: 28 October 2010].

Poggenpohl, S. and Sato, K. (2003). Models of Dissertation Research in Design. In: *3rd Doctoral Education in Design Research Conference*.

Pye, D. (1995) *The nature and art of workmanship*. 2nd edition. London, Herbert Press.

Rahaman, M. (2003). *Ceramic Processing and Sintering*. 2nd ed. Hoboken: Marcel Dekker Inc.

RapidToday, (n.d.). *STL 2.0 May Replace Old, Limited File Format*. [online] Available at: http://www.rapidtoday.com/stl-file-format.html [Accessed 14 Mar. 2012].

Realizeinc, (n.d.). *Multi-Jet Modeling (MJM) | Rapid Prototyping, Rapid Prototypes, Stereolithography – RealizeInc*. [online] Available at: http://www.realizeinc.com/multi-jet-modeling/ [Accessed 4 Oct. 2013].

Reeves, P. (2008). “Rapid Manufacturing for the Production of Ceramic Components,” CERAM 2008, Econolyst.

Reprap, (2012) *RepRap Family Tree - RepRapWiki*. [Online]. 2012. Available from: http://reprap.org/wiki/RepRap_Family_Tree [Accessed: 22 November 2013].

Reprap.org, (n.d.) *Fused filament fabrication - RepRapWiki*. [Online]. Available from: http://reprap.org/wiki/Fused_filament_fabrication [Accessed: 12 November 2011].

Reprappro.com, (2011) *About | RepRapPro*. [Online]. 2011. Available from: https://reprappro.com/about/ [Accessed: 19 February 2012].

Riogrande, (2008) *Welcome to Bronzclay*. [Online]. 2008. Available from: http://www.metalclayacademy.com/pdfs/2008WelcometoBronzClay.pdf [Accessed: 23 October 2012].

RioGrande, (2011), WelcometoBronzClay. Available: http://www.bronzclay.com/2011WelcometoBronzClay.pdf. Last accessed 23rd October 2012.

Riogrande, (n.d.) *BRONZclay, 100g*. [Online]. Available from: http://www.riogrande.com/Product/BRONZclay/101007?Pos=1 [Accessed: 17 July 2010].

Robocasting, (n.d.) A. *Robocasting Enterprises*. [online] Available at: http://www.robocasting.net/robocasting_original/filtration.html [Accessed 6 Apr. 2011].

Robocasting, (n.d.) B. *Robocasting Enterprises materials*. [online] Available at: http://www.robocasting.net/robocasting_original/materials.html [Accessed 6 Apr. 2012].

Sanderson, H. (2010). PMC PRO Ring Tests. Available: http://www.metalclayguru.com/storage/pdfs/PMC-PRO-Ring-Tests-Hattie-Sanderson.pdf. Accessed 17th November 2012.

Shapeways, (n.d.) *Shapeways - 3D Printing Service and Marketplace*. [Online]. Available from: http://www.shapeways.com/ [Accessed: 18 August 2013].

Sherline, (n.d.). *Sherline 5400/5410 Mills*. [online] Available at: http://www.sherline.com/5400pg.htm [Accessed 7 Jun. 2011].

Shillito, A. (2013). *Digital crafts*. 1st ed. London: Bloombury.

Singh, R. (2011) Process capability study of polyjet printing for plastic components. Journal of mechanical science and technology. 25 (4), 1011--1015.

Sinirlioglu, M. (2009). Rapid Manufacturing of Dental and Medical Parts via LaserCUSING Technology using Titanium and CoCr Powder Materials.

SlashGear, (2013). *3D Systems ProJet 5500X multi-material composites 3D printer unveiled*. [online] Available at: http://www.slashgear.com/3d-systems-projet-5500x-multi-material-composites-3d-printer-unveiled-02307296/ [Accessed 5 Jan. 2014].

Smay, J., Cesarano, J. & Lewis, J. (2002) Colloidal inks for directed assembly of 3-D periodic structures. *Langmuir*. 18 (14), 5429--5437.

Smith, D. (2006). *PIC in practice: A Project-Based Approach*. Oxford: Newnes.

Smyth, C. (2013). *Functional design for 3D printing*. 1st ed.

Solid-scape, (2014). *Solidscape datatsheet*. [online] Available at: http://www.solid-scape.com/sites/default/files/products/pdf/usa_paper_size_max2_data_sheet_5-1-2014.pdf [Accessed 12 Jun. 2014].

Sollmann, K., Jouaneh, M. & Lavender, D. (2010) Dynamic modeling of a two-axis, parallel, H-frame-type XY positioning system. *Mechatronics, IEEE/ASME Transactions on*. 15 (2), 280--290.

Stenerson, J. & Curran, K. (2007) *Computer numerical control*. 3rd edition. Upper Saddle River, N.J., Pearson Prentice Hall.

Stratasys, (2014) B. *PolyJte Color Materials*. [online] Available at: http://www.stratasys.com/~/media/Main/Secure/Material%20Specs%20MS/PolyJet-Material-Specs/PolyJet_Color_Spec_Sheet_06-14_web.pdf [Accessed 10 Jul. 2014].

Stratasys, (n.d.) A. *Objet500 Connex3 - High Resolution 3D Printing | Stratasys*. [online] Available at: http://www.stratasys.com/3d-printers/design-series/precision/objet500-connex3 [Accessed 16 Jul. 2014].

Stratoconception, (n.d.). *Stratoconception, Fabrication Additive (Prototypage Rapide, Outillage Rapide, Impression 3D) - Galerie - Pièces*. [online] Available at: http://www.stratoconception.com/procede [Accessed 5 May. 2013].

Symes, M., Kitson, P., Yan, J. & Richmond, C. et al. (2012) Integrated 3D-printed reactionware for chemical synthesis and analysis. *Nature Chemistry*. 4 (5), 349--354.

The British Standards Institution. Rubber, vulcanized or thermoplastic — Determination of tensile stress-strain properties. s.l. : BSI Standards, 2011. BS ISO 37:2011.

The sugar lab, (2014) *chefJet gallery*. [Online]. 2014. Available from: http://the-sugar-lab.com/gallery [Accessed: 5 March 2014].

Thepmcstudio, (n.d.) *PMC3 Syringe 10g Fine Silver | The PMC Studio UK*. [Online]. Available from: http://www.thepmcstudio.com/collections/metal-clay/products/pmc3-syringe-10g [Accessed: 18 February 2011].

Thingiverse.com, (2011). *Yoda by bmoshe - Thingiverse*. [online] Available at: http://www.thingiverse.com/thing:10650 [Accessed 7 May. 2012].

Ultimaker.com, (n.d.). *Ultimaker 2*. [online] Available at: https://www.ultimaker.com/pages/our-printers/ultimaker-2 [Accessed 7 Nov. 2013].

Underwood, N. (2013). Vapor Treating ABS RP parts. [Blog] *RepRap: Blog*. Available at: http://blog.reprap.org/2013/02/vapor-treating-abs-rp-parts.html [Accessed 12 Mar. 2013].

unfoldfab. (2012). [Blog] *Print, Print, Print...*. Available at: http://unfoldfab.blogspot.co.uk/ [Accessed 4 Jan. 2013].

Vaezi, M., Chianrabutra, S., Mellor, B. & Yang, S. (2013) Multiple material additive manufacturing--Part 1: a review. *Virtual and Physical Prototyping*. 8 (1), 19--50.

Von Busch, O., (2010), 'Exploring net Political craft: From Collective to Connective', *Craft Research* 1,pp. 113–124, doi: 10.1386/crre.1.113_7

VoxelJet, (2010). *VoxelJet services*. [online] Available at: http://www.aida-sl.com/PDF/Voxeljet_Services.pdf [Accessed 9 Oct. 2013].

VoxelJet, (2013). *VoxelJet system brochure*. [online] Available at: http://www.voxeljet.de/fileadmin/Voxeljet/Systems/Gesamtbroschuere_SYSTEMS_en_2013.pdf [Accessed 7 Oct. 2013].

VoxelJet, (2013, B). *Continuous 3D printer VXC800 for sand moulds and plastic parts*. [video] Available at: http://www.voxeljet.de/en/systems/3d-druckervxc800/ [Accessed 7 Nov. 2013].

Warnier, C., Verbruggen, D., Ehmann, S. & Klanten, R. (2014) *Printing Things Visions and Essentials for 3D Printing*. 1st edition. Berlin, Gestalten.

Weisensel L., Travitzky N. and Greil P., (2004). *Advanced Laminated Object Manufacturing (LOM) of Si SiC Ceramics*. [online] Available at: http://utwired.engr.utexas.edu/lff/symposium/proceedingsArchive/pubs/Manuscripts/2004/2004-26-Weisensel.pdf [Accessed 8 Mar. 2012].

Wenman, C. (2013). 3D Scanning, 3D Printing, Bronze Casting, and the Art of the Living Dead. [Blog] *CosmoWenman*. Available at: http://cosmowenman.wordpress.com/2013/10/24/3d-scanning-3d-printed-lost-pla-bronze-casting-and-the-art-of-the-living-dead/ [Accessed 7th Nov. 2013].

Wenman, C., (2013, B). Colossal bust of Ramesses II / Ozymandias. [Blog] *CosmoWenman*. Available at: http://cosmowenman.wordpress.com/2013/06/15/colossal-bust-of-ramesses-ii-ozymandias/ [Accessed 7th Nov. 2013].

Yang, S., Yang, H., Chi, X. & Evans, J. et al. (2008) Rapid prototyping of ceramic lattices for hard tissue scaffolds. *Materials \& Design*. 29 (9), 1802--1809.

Zhang, J. & Khoshnevis, B. (2013) Optimal machine operation planning for construction by Contour Crafting. *Automation in Construction*. 29, 50--67.

Zsolutions, (n.d.). *Z Solutions - Materials*. [online] Available at: http://www.zsolutions.eu.com/3d_printing_materials_uk.htm [Accessed 11 May. 2014].

XI. Appendices

List of appendices

A Nozzle dispensing medium

PRODUCT NO.:JM0001

Johnson Matthey
Colour Technologies

SAFETY DATA SHEET
Nozzle Dispensing Medium

1 IDENTIFICATION OF THE SUBSTANCE/PREPARATION AND OF THE COMPANY/UNDERTAKING

PRODUCT NAME	Nozzle Dispensing Medium
PRODUCT NO.	JM0001
APPLICATION	Printing ink.
SUPPLIER	Johnson Matthey Colour Technologies Unit 26 Blythe Park Business Base Cresswell Stoke on Trent ST11 9RD 01782 384100 sdsrequest@matthey.com
EMERGENCY TELEPHONE	+44 (0) 7890 276 580

2 HAZARDS IDENTIFICATION

Not regarded as a health or environmental hazard under current legislation.

ENVIRONMENT

The product is not expected to be hazardous to the environment.

HUMAN HEALTH

May cause minor irritation on eye contact. May cause minor irritation on skin contact. Frequent inhalation of vapour/spray over a long period of time increases the risk of developing lung diseases.

3 COMPOSITION/INFORMATION ON INGREDIENTS

Name	EC No.	CAS-No.	Content	Classification (67/548)
Tetrahydro-1,3,4,6-tetrakis(hydrooxymethyl)midazo(4,5-d)midazole-2,5(1H,3H)-dione	226-408-0	5395-50-6	< 1%	R43.
2,2'-OXYBISETHANOL	203-872-2	111-46-6	< 1%	Xn;R22

The Full Text for all R-Phrases are Displayed in Section 16

COMPOSITION COMMENTS

Not regarded as a health or environmental hazard under current legislation.

4 FIRST-AID MEASURES

INHALATION

Move the exposed person to fresh air at once. Get medical attention if any discomfort continues.

INGESTION

Do not induce vomiting. Immediately give a couple of glasses of water or milk, provided the victim is fully conscious. Get medical attention if any discomfort continues.

SKIN CONTACT

Wash skin thoroughly with soap and water. Get medical attention if irritation persists after washing.

EYE CONTACT

Make sure to remove any contact lenses from the eyes before rinsing. Immediately rinse with water for several minutes. Get medical attention if any discomfort continues.

5 FIRE-FIGHTING MEASURES

EXTINGUISHING MEDIA

Use fire-extinguishing media appropriate for surrounding materials.

SPECIAL FIRE FIGHTING PROCEDURES

No specific fire fighting procedure given.

UNUSUAL FIRE & EXPLOSION HAZARDS

No unusual fire or explosion hazards noted.

SPECIFIC HAZARDS

When heated and in case of fire, harmful vapours/gases may be formed.

PROTECTIVE MEASURES IN FIRE

Use air-supplied respirator, gloves and protective goggles.

6 ACCIDENTAL RELEASE MEASURES

PERSONAL PRECAUTIONS

Wear protective clothing as described in Section 8 of this safety data sheet.

ENVIRONMENTAL PRECAUTIONS

Do not discharge into drains, water courses or onto the ground.

SPILL CLEAN UP METHODS

Dam and absorb spillage with sand, sawdust or other absorbent.

7 HANDLING AND STORAGE

USAGE PRECAUTIONS

Do not eat, drink or smoke when using the product. Good personal hygiene is necessary. Wash hands and contaminated areas with water and soap before leaving the work site. Do not use in confined spaces without adequate ventilation and/or respirator.

STORAGE PRECAUTIONS

Store in tightly closed original container in a dry and cool place.

8 EXPOSURE CONTROLS/PERSONAL PROTECTION

Name	Std	TWA - 8 hrs		STEL - 15 min		Notes
2,2'-OXYBISETHANOL	OES	23 ppm	101 mg/m3			

INGREDIENT COMMENTS

No exposure limits noted for ingredient(s).

PROTECTIVE EQUIPMENT

ENGINEERING MEASURES

Provide adequate ventilation, including appropriate local extraction, to ensure that the defined occupational exposure limit is not exceeded.

RESPIRATORY EQUIPMENT

No specific recommendation made, but respiratory protection must be used if the general level exceeds the recommended occupational exposure limit.

HAND PROTECTION

For prolonged or repeated skin contact use suitable protective gloves.

EYE PROTECTION

If risk of splashing, wear safety goggles or face shield.

HYGIENE MEASURES

Wash at the end of each work shift and before eating, smoking and using the toilet. When using do not eat, drink or smoke.

9 PHYSICAL AND CHEMICAL PROPERTIES

APPEARANCE	Coloured gel		
COLOUR	White / off-white		
ODOUR	Odourless		
RELATIVE DENSITY	1 - 2	pH-VALUE, CONC. SOLUTION	7
FLASH POINT (°C)	>65		

10 STABILITY AND REACTIVITY

STABILITY

Stable under normal temperature conditions and recommended use.

CONDITIONS TO AVOID

Not known.

HAZARDOUS POLYMERISATION

Not relevant.

MATERIALS TO AVOID

No incompatible groups noted.

HAZARDOUS DECOMPOSITION PRODUCTS

Not known.

11 TOXICOLOGICAL INFORMATION

TOXICOLOGICAL INFORMATION

No data recorded.

GENERAL INFORMATION

No specific health warnings noted.

12 ECOLOGICAL INFORMATION

ECOTOXICITY

The product components are not classified as environmentally hazardous. However, this does not exclude the possibility that large or frequent spills can have a harmful or damaging effect on the environment.

13 DISPOSAL CONSIDERATIONS

GENERAL INFORMATION

When handling waste, consideration should be made to the safety precautions applying to handling of the product.

DISPOSAL METHODS

Dispose of waste and residues in accordance with local authority requirements.

14 TRANSPORT INFORMATION

GENERAL	The product is not covered by international regulation on the transport of dangerous goods (IMDG, IATA, ADR/RID).

15 REGULATORY INFORMATION

RISK PHRASES

NC	Not classified.

SAFETY PHRASES

P14	Contains Tetrahydro-1,3,4,6-tetrakis(hydrooxymethyl)midazo(4,5-d)midazole-2,5(1H,3H)-dione. May produce an allergic reaction.

UK REGULATORY REFERENCES

Health and Safety at Work Act 1974.

EU DIRECTIVES

Dangerous Substance Directive 67/548/EEC. Dangerous Preparations Directive 1999/45/EC. Regulation (EC) No 1907/2006 of the European Parliament and of the Council of 18 December 2006 concerning the Registration, Evaluation, Authorisation and Restriction of Chemicals (REACH), establishing a European Chemicals Agency, amending Directive 1999/45/EC and repealing Council Regulation (EEC) No 793/93 and Commission Regulation (EC) No 1488/94 as well as Council Directive 76/769/EEC and Commission Directives 91/155/EEC, 93/67/EEC, 93/105/EC and 2000/21/EC, including amendments.

STATUTORY INSTRUMENTS

Chemicals (Hazard Information and Packaging) Regulations.

APPROVED CODE OF PRACTICE

Safety Data Sheets for Substances and Preparations. Classification and Labelling of Substances and Preparations Dangerous for Supply.

16 OTHER INFORMATION

ISSUED BY

Development

SDS NO.	45273

SAFETY DATA SHEET STATUS

Approved.

DATE	08.08.2010

RISK PHRASES IN FULL	
R22	Harmful if swallowed.
R43	May cause sensitisation by skin contact.

B Deposition Head V1

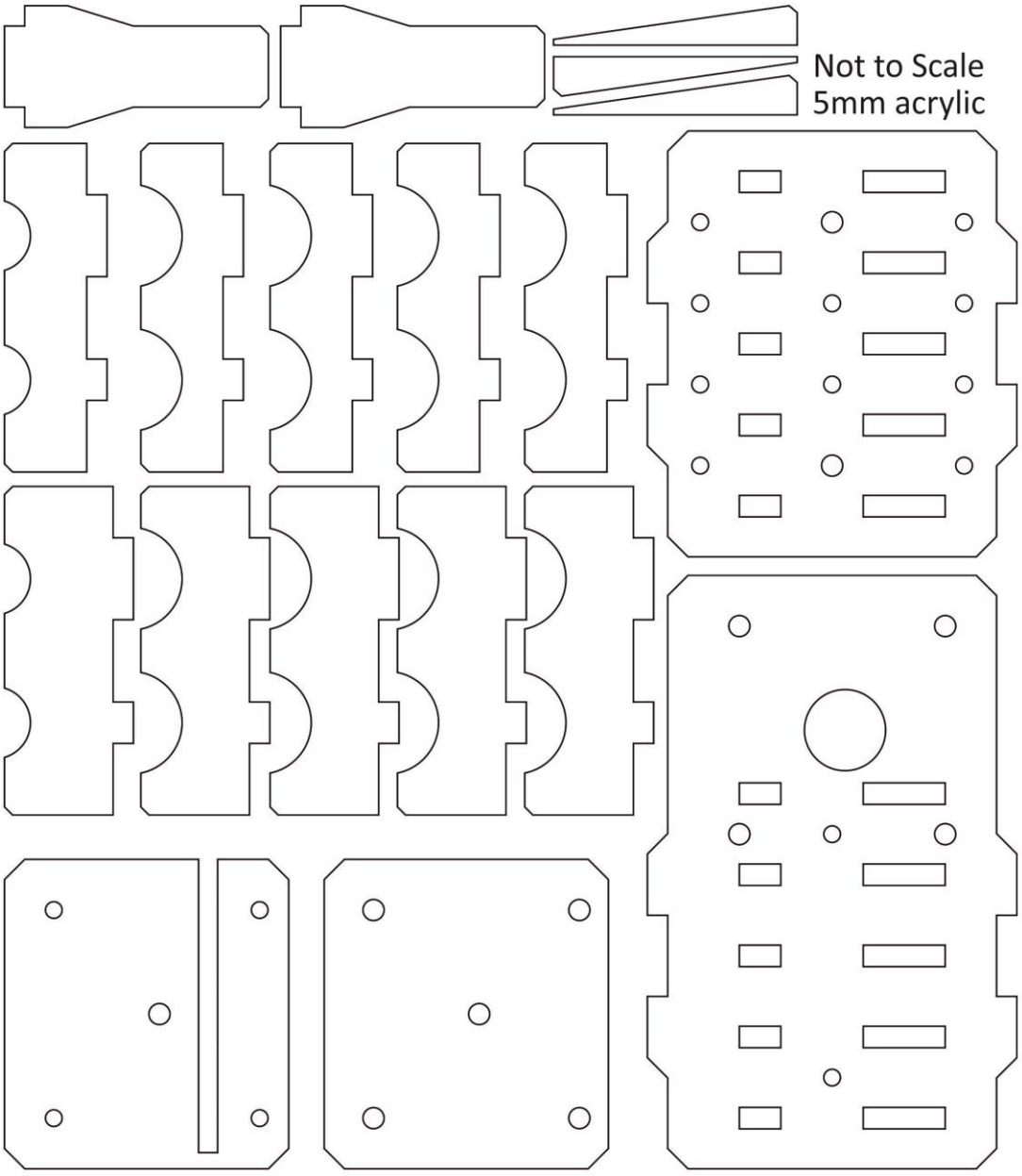

C Parametric Tool-Path

```
(Parametric Tool-Path G-code )
G21 G90 G61 G40 G54
G0 Z5.0
G17

#1 = 0.6 (Z HEIGHT)           (0.20, 0.60, 0.40, 0.40)
#2 = 0.5 (LAYER HEIGHT)     (0.15, 0.50, 0.40, 0.30)
#3 = 3   (HEAD RETRACTION VALUE)
G1 F700.00
#12 = 34 (dimension)
#8 = 1.2 (pitch)
#9 = 0 (used to return to origin)
#11 = [[#12/#8]/2] (used to calculate repetitions)
#10 = [[FIX[#11]]*[#8*2]] (fix rounds down to the nearest integer)
M98 P7 L2 (L defines how many layers to build, 2= 4 layers)
G0 Z[#1 + 50] (move the depo head up 50mm over build at the end of build)

M30 (PROGRAM END)

O7
M98 P5 (pattern for first layer)
M98 P6 (pattern for second layer)
M99

O5(PATTERN 1 START)
#4 = #9 (start x value)
#5 = #9 (x value reg)
#6 = #10 (start Y value)
#7 = #10 (y value reg)
G0 X#4 Y[#6 - #8] (MOVE TO START)
G1 Z#1
M3
G1 X#4 Y#6
M98 P1 L#11 (PATTERN 1A)
#4 = #5 (VAR SET)
#5 = #9
#6 = #7
#7 = #10

M98 P2 L#11 (PATTERN 1B)
G1 X#5 Y[#7 + #8]
M5
G1 Z[#1 + #3]
#1 = [#2 + #1]
M99 (PATTERN 1 END)

O6 (PATTERN 2 START)
#4 = #9 (VAR SET)
#5 = #9
#6 = #9
#7 = #9
G0 X#4 Y[#6 + #8]
G1 Z#1
M3
G1 X#4 Y#6
M98 P3 L#11 (PATTERN 2A)
```

```
#4 = #5 (VAR SET)
#5 = #9
#6 = #7
#7 = #9
M98 P4 L#11 (PATTERN 2B)
G1 X#5 Y[#7 - #8]
M5
G1 Z[#1 + #3]
#1 = [#2 + #1]
M99 (PATTERN 2 END)

O1 (PATTERN 1A)
#5 = [#5 + #8]
G1 X#5 Y#6
#7 = [#7 - #8]
G1 X#4 Y#7
#7 = [#7 - #8]
G1 X#4 Y#7
#5 = [#5 + #8]
G1 X#5 Y#6
M99

O2 (PATTERN 1B)
#7 = [#7 - #8]
G1 X#4 Y#7
#5 = [#5 + #8]
G1 X#5 Y#6
#5 = [#5 + #8]
G1 X#5 Y#6
#7 = [#7 - #8]
G1 X#4 Y#7
M99

O3 (PATTERN 2A)
#5 = [#5 + #8]
G1 X#5 Y#6
#7 = [#7 + #8]
G1 X#4 Y#7
#7 = [#7 + #8]
G1 X#4 Y#7
#5 = [#5 + #8]
G1 X#5 Y#6
M99

O4 (PATTERN 2B)
#7 = [#7 + #8]
G1 X#4 Y#7
#5 = [#5 + #8]
G1 X#5 Y#6
#5 = [#5 + #8]
G1 X#5 Y#6
#7 = [#7 + #8]
G1 X#4 Y#7
M99
```

(end of parametric code, rest of the page was left blank)

D Deposition Head v2

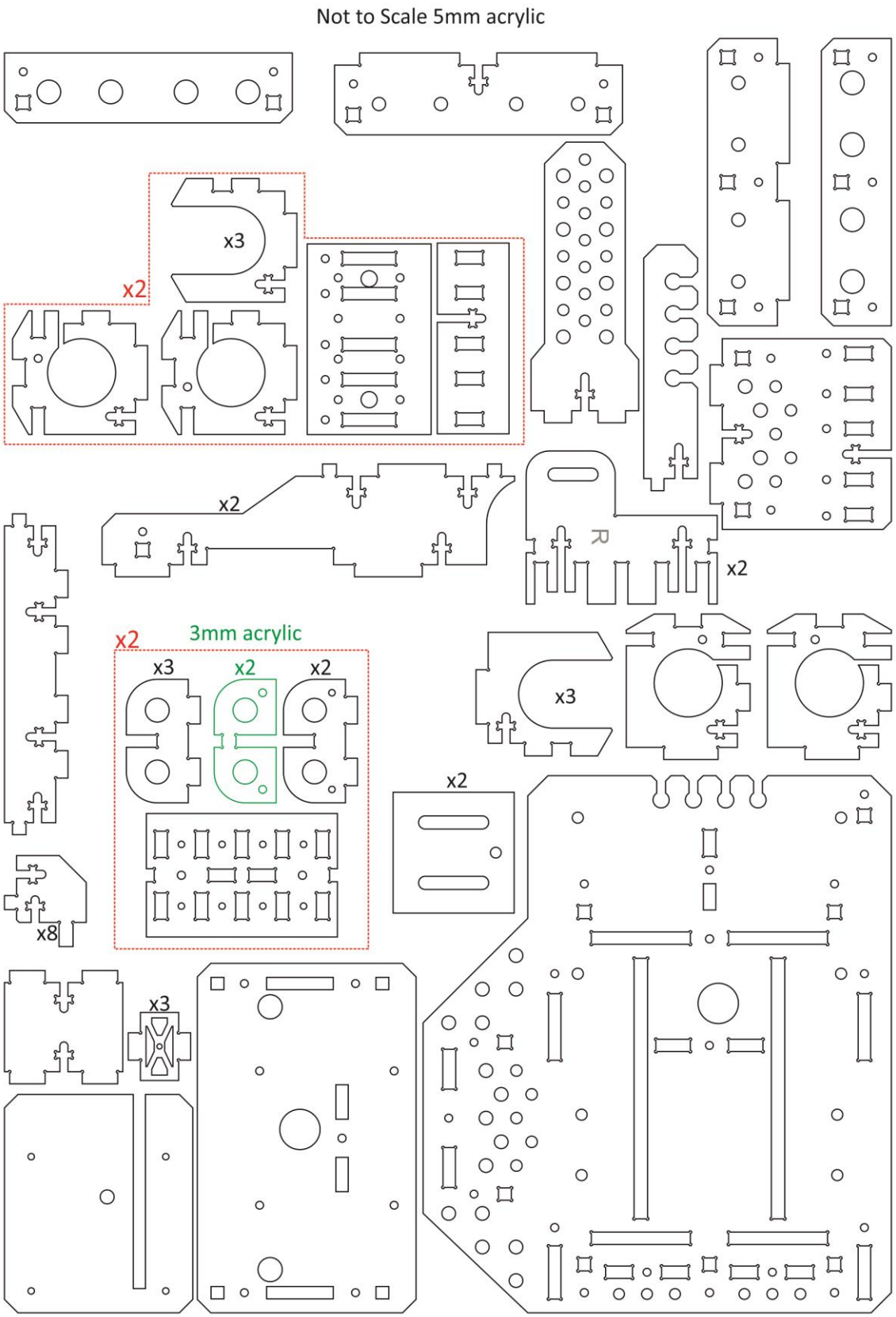

E Actuator Controller PCB Artwork

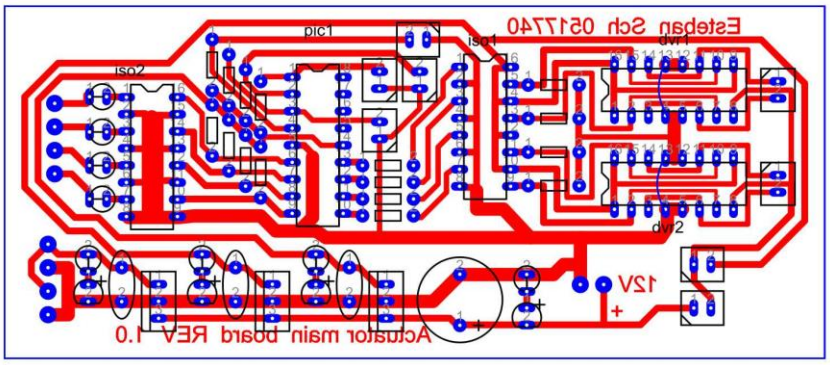

Main Board

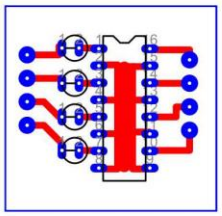

Opto-isolator